2010

Vacuolar trafficking and vesicle fusion machineries at the Arabidopsis

Sang-jin Kim
Iowa State University

Vacuolar trafficking and vesicle fusion machineries at the Arabidopsis *trans*-Golgi network

By

Sang-Jin Kim

A dissertation submitted to the graduate faculty

in partial fulfillment of the requirement for the degree of

DOCTOR OF PHILOSOPHY

Major : Genetics

Program of study committee:
Diane C. Bassham, Major Professor
Martin H. Spalding
Adam J. Bogdanove
M Heather West Greenlee
Yanhai Yin

Iowa State University

Ames, Iowa

2010

DEDICATION

This dissertation is dedicated to my parents, parents-in law, brother and my beloved daughters. Without their extreme support I would not be able to achieve this accomplishment. Lastly, my dearest wife Jaeun Kim, without her, I would not be here today.

TABLE OF CONTENTS

ABSTRACT

Endomembrane trafficking is required for maintaining diverse cellular processes. Disruption of endomembrane trafficking affects cell viability, stress responses, development and other processes. The Arabidopsis *trans*-Golgi network (TGN) in the endomembrane system is an important organelle where several sorting events take place. The SYP41 complex, a protein complex at the *Arabidopsis* TGN, is involved in vacuolar trafficking. SYP41 interacts with AtVPS45, SYP61 and VTI12, which are proteins that are involved in vesicle transport to the vacuole. A previously uncharacterized protein was identified as a SYP41-interacting protein by co-immunoprecipitation, and was named TNO1 (TGN-localized SYP41-interacting protein). TNO1 localizes to the TGN and is involved in salt tolerance and vacuolar trafficking. TNO1 is important for the localization of SYP61, suggesting that TNO1 may assist recruitment of SYP61 to the SYP41 complex. Application of the trafficking inhibitor Brefeldin A indicated that TNO1 may be also involved in membrane fusion and in maintaining TGN structure. These results suggest that membrane fusion and stability of the TGN are important for salt tolerance and vacuolar trafficking in *Arabidopsis*.

Vesicle fusion is an essential process for maintaining the structure and function of the endomembrane system. The SYP41 complex consists of an SM protein, SNAREs, and TNO1. A role for the SYP41 complex in membrane fusion has been shown previously using *in vitro* fusion assays. In Arabidopsis, there are three SYP4 and four VTI1 family proteins. Here we used a proteoliposome fusion assay to demonstrate that other proteins in the SYP4 family and two members of the VTI1 family (VTI11 and VTI12) are also able to drive vesicle fusion. The results indicate that all members of the SYP4 family can also function

with VTI12 in membrane fusion, and that VTI11 can substitute for VTI12 in this reaction.

In addition, we have demonstrated that AtVPS45 interacts with SYP4 protein complexes via direct binding to SYP4 family proteins *in vitro*. Addition of AtVPS45 reduces the efficiency of membrane fusion between vesicles containing SYP4 and VTI1 family proteins, suggesting that strong binding of AtVPS45 to SYP4 family proteins may inhibit membrane fusion between these vesicles. These results demonstrate that functional redundancy of VTI11 with VTI12 and regulation of vesicle fusion by VPS45 are mediated by interaction with SYP4 family SNAREs.

CHAPTER 1. INTRODUCTION

Introduction to vesicle trafficking

Transport vesicles are small, intracellular, membrane-enclosed sacs that store or transport substances within a cell. Vesicles deliver membrane lipids and proteins to the endomembrane system or plasma membrane and polysaccharides to the cell wall. Transport vesicles bud from donor organelles and fuse with target organelles where they deliver their cargos. Thus, vesicle formation at the donor organelle and fusion with the target membrane are essential processes in vesicle trafficking. For a vesicle to bud from the donor organelle, coat proteins are required to deform the membrane and capture cargo. There are three major well-characterized types of vesicle coats: COPI (coat protein complex I), COPII (coat protein complex II) and clathrin (Barlowe et al., 1994; Kirsch et al., 1994). Precise recruitment of cargo proteins, cargo receptor proteins and SNAREs (soluble *N*-ethylmaleimide-sensitive fusion protein attachment protein receptors) are also required for vesicle budding (Hwang and Robinson, 2009). Vesicles bud from the donor organelle and move along a cytoskeletal filament (either microtubules or actin filaments) to their target organelle (Hamm-Alvarez, 1998; DePina and Langford, 1999; Kahn et al., 2005). When they are close to the target membrane, vesicles are uncoated and are ready to fuse (Newmyer et al., 2003). During vesicle fusion, correct recognition of the target membrane via SNAREs, SM (Sec1/Munc18) proteins and tethering factors is critical (Weber et al., 1998; Shorter and Warren, 1999). This cognate SNARE interaction drives membrane fusion, and cargos are released into the lumen

of the target organelle. Vesicle budding and fusion are tightly regulated in the cell and maintain homeostasis of the endomembrane system.

Plant vacuoles

The vacuole is typically the biggest organelle in plant cells and takes part in cell expansion. In addition, the vacuole has diverse roles such as the maintenance of turgor, the degradation of cellular components, the compartmentalization of ions and secondary metabolites such as pigments and toxic compounds and the accumulation of proteins. Vacuoles not only have multiple functions, but there are two major types of vacuoles, lytic and storage (Wink, 1993), and three major trafficking pathways lead to the vacuole (Marty, 1999).

Lytic Vacuole. The lytic vacuole has an acidic pH and contains hydrolytic enzymes and functionally is similar to the mammalian lysosome. Lytic vacuoles are usually found throughout the plant, and the large central vacuole in most cells is a lytic vacuole. The lytic vacuole is identified by the presence of γ−tonoplast intrinsic protein (TIP) in the vacuolar membrane (Hofte et al., 1992; Paris et al., 1996), and the cys-protease aleurain is in the lumen (Holwerda et al., 1992). In some cell types, defense or signal compounds are stored in the vacuole, particularly within specialized cells.

Storage Vacuole. Seeds and fruits contain storage vacuoles in which storage proteins are stored for later use during seedling growth. Storage vacuoles contain the marker α-TIP (Hofte et al., 1992; Paris et al., 1996). Seed storage proteins are found in storage vacuoles and can be used as markers to investigate trafficking pathways to these vacuoles. In

some cases, storage vacuoles are also found in vegetative cells in response to wounding and to developmental changes (Staswick, 1990).

Other vacuoles. Other specialized types of vacuole, with some characteristics in common with the lytic vacuole, are also present in plant cells at certain developmental stages. During leaf senescence, senescence-associated vacuoles (SAVs), which have high cys-protease activity and a lower pH than lytic vacuoles, are formed. The lytic vacuole marker ɣ-TIP is not detected in the tonoplast of SAVs, suggesting SAVs are distinct from lytic vacuoles (Otegui et al., 2005). In addition, small vacuoles containing the vacuolar Ca^{2+} pump ACA4 (Arabidopsis Ca^{2+} ATPase 4) on the membrane were identified in Arabidopsis protoplasts (Geisler et al., 2000). In tobacco mesophyll protoplasts, small peripheral vacuoles labeled with GFP-fused chitinase were identified and they were found to fuse with the lytic vacuole after complete regeneration of the lytic vacuole in evacuolated protoplasts (Di Sansebastiano et al., 2001).

Vacuolar trafficking pathways

For maintaining the function of vacuoles, proteins and lipids are transported to the vacuole through biosynthetic, endocytic and autophagic pathways. These three pathways originate in different places, with the biosynthetic and endocytic pathways merging in the *trans*-Golgi network (TGN) or in the pre-vacuolar compartment (PVC) (Tse et al., 2004; Dettmer et al., 2006; Viotti et al., 2010). An overview of vacuolar trafficking pathways in plants is shown in Fig 1.

Biosynthetic pathway. The biosynthetic pathway maintains vacuolar function via transport of newly synthesized proteins. Through this pathway, enzymes including proteases, storage proteins or lipids are transported to the vacuole. Vacuolar proteins are synthesized at the surface of the ER and are transported co-translationally into the ER lumen. In the ER, proteins are folded with the help of chaperones and undergo glycosylation. From the ER, they are transported to the *cis*-Golgi via COPII vesicles which contain the coat protein complex required for vesicle budding from the ER (Barlowe et al., 1994; Tormakangas et al., 2001) and are then transported through the Golgi to the *trans*-Golgi Network. In the TGN, proteins are sorted according to their targeting signal. Proteins without a targeting signal are secreted to the plasma membrane, while proteins with vacuolar sorting determinants are transported to the vacuole by vacuolar sorting receptors.

To date two major types of vacuolar sorting determinant (VSD) have been characterized, sequence specific VSDs (ssVSD) and C-terminal VSDs (ctVSD) (Hofte et al., 1992). The ssVSD (previously called NTPP) is an N-terminal sorting signal and the amino acid sequence NPIR is within this signal and important for its function. An ssVSD is found in sweet potato sporamin, aleurain and lytic vacuole cargo proteins, and this sequence alone is able to transport a chimeric protein to the vacuole (Holwerda et al., 1992; Nakamura et al., 1993). The ctVSD does not have a specific sequence, but hydrophobic amino acids are located at the C-terminus of the protein. This ctVSD was also found to be necessary and sufficient for vacuolar targeting (Bednarek and Raikhel, 1991; Matsuoka et al., 1995). Interestingly, a ctVSD is mostly found in vacuolar storage proteins, which are sorted in the Golgi and transported to the storage vacuole. However, soybean ß-conglycinin has both a ctVSD and a ssVSD at its C-terminus, each of which is also sufficient for targeting to the

storage vacuole (Nishizawa et al., 2006). Arabidopsis Aleurain has a ctVSD and an ssVSD at its N-terminus, both of which were found to be important for vacuolar targeting (Hinz et al., 2007). Chimeric proteins such as GFP fused to ctVSD or ssVSD are transported to the vacuole, suggesting that VSDs are more important for transport than the structural properties of the proteins.

Extensive investigation of vacuolar targeting led to the discovery of specific vacuolar sorting receptors that bind to the VSDs of proteins and are involved in packing of cargo. In *Arabidopsis*, two families of vacuolar sorting receptors have been characterized. The vacuolar sorting receptor (VSR) family consists of seven members in *Arabidopsis* (Shimada et al., 2003b), and the receptor homology-transmembrane-ring H2 domain (RMR) family consists of six members (Jiang et al., 2000; Park et al., 2005). VSR1 is thought to be involved in recognition of lytic cargo by binding ssVSDs. However, mis-sorting of storage proteins in a *vsr1* mutant showed that VSR1 is also important for transport of storage cargo (Shimada et al., 2003b). The RMR family is not fully investigated, but RMR1 is thought to recruit storage proteins as RMRs co-localize with storage proteins in the *cis*-Golgi (Park et al., 2005). Investigation of the localization of VSRs and RMRs showed that RMRs co-localize with cruciferins in cisternal rims at the *cis*-Golgi, while VSRs mostly localize to the *trans* side of the Golgi, dense vesicles (DV) and PVC with storage proteins. These results suggest that in the initial sorting step, RMRs function in compartmentalization of storage cargo to the rims at the Golgi, and VSRs cooperate at a later sorting step to load storage cargo into DVs at the *trans*-Golgi.

Unlike other vacuolar proteins, some storage proteins are packaged into electron-dense vesicles that directly bud from the ER and deliver cargo to the vacuole (Fukasawa et

al., 1988; Hara-Nishimura et al., 1998). These proteins lack vacuolar targeting signals commonly found in other vacuolar proteins. Some proteases are also transported to the vacuole from the ER (Hayashi et al., 2001; Rojo et al., 2003b; Yamada et al., 2008). During seed development or when plants are under stress, vesicles derived from the ER (ER bodies) that contain proteases involved in defense responses fuse with the storage vacuole or central vacuole and release the proteases for the degradation of storage proteins or to trigger a stress response.

Autophagy is a vacuolar trafficking pathway for protein degradation. This pathway is different from the biosynthetic pathway described above in a number of ways. Firstly, cargos of the autophagy pathway are proteins, starch and lipids for recycling during nutrient starvation, and damaged or toxic material to be removed from the cytoplasm (Journet et al., 1986; Toyooka et al., 2001; Xiong et al., 2007; Liu et al., 2009). Secondly, autophagy occurs at a low level for house-keeping purposes, but is extensively induced under stress conditions such as nutrient, salt, osmotic or oxidative stress (Aubert et al., 1996; Xiong et al., 2007; Liu et al., 2009). Lastly, autophagosomes, vesicles induced during autophagy, are not formed by budding from a specific organelle. The mechanism of autophagosome formation is not yet clear, but it is thought that pre-autophagosomes are formed in the cytosol and enclose cargo for degradation, finally forming double-membrane autophagosomes which fuse with the vacuole (Noda et al., 2002). Although the autophagic pathway has different vesicles and cargos, it shares some common components with the biosynthetic pathway. VTI12 is a SNARE protein that is important for the biosynthetic vacuolar pathway. However, a *vti12* mutant showed an early senescence phenotype under starvation conditions, suggesting a defect in the autophagy pathway (Surpin et al., 2003). Although the role of VTI12 in

autophagy is not yet understood, autophagosomes need SNARE proteins for fusion with the tonoplast. VTI12 may therefore function in fusion between autophagosomes and the tonoplast. We hypothesize that autophagy could use the same fusion machinery as the biosynthetic pathway for the delivery of cargo to the vacuole.

Endocytosis is the pathway delivering proteins and lipids from the plasma membrane to the vacuole. Proteins and lipids required at the plasma membrane are transported there by the secretory pathway. Increase in the plasma membrane surface area by continuous secretion must be counter-balanced by endocytosis (Battey et al., 1999). Clathrin-coated vesicles originated from the plasma membrane initially deliver materials to endosomes. Endosomes containing cargo destined for degradation mature into late endosomes, which are equivalent to the pre-vacuolar compartment. Finally, cargo in the endosome is transported to the vacuole for degradation (Neumann et al., 2003; Samaj et al., 2005).

Some metal transporters are tightly regulated by the endosome-to-vacuole degradation pathway. AtBOR1 is present at the plasma membrane in normal conditions, but excessive amounts of boron cause AtBOR1 internalization, compartmentalizing boron with AtBOR1 into the vacuole to avoid accumulation of toxic levels of boron (Takano et al., 2005). The endocytic pathway is also important for delivering gravity signals. Polar auxin transport is caused by polar distribution of PIN (pin-formed) proteins involved in auxin efflux, and is required for gravity sensing (Galweiler et al., 1998; Abas et al., 2006). During gravi-stimulation, endocytosis of the PIN2 auxin efflux carrier is increased in the auxin-accumulating cells at the upper and lower side of the root. This causes asymmetric distribution of PIN2 proteins in the root. In addition, increased endocytosis leads to increased

degradation of PIN2, probably through ubiquitin-mediated sorting to the vacuole, and non-degradable PIN2 caused defects in auxin distribution and gravitropic response due to its high stability and abundant distribution (Abas et al., 2006). This suggests that endocytosis regulates redistribution of auxin.

Vesicle fusion

Vacuolar proteins are synthesized at the surface of the ER and pass through the endomembrane system, consisting of distinct membrane-bound organelles, to reach the vacuole. Trafficking between organelles is mediated by different types of vesicles. For example, COPII vesicles are responsible for ER- to -Golgi trafficking, and clathrin-coated vesicles mediate TGN- to -PVC trafficking (Kirsch et al., 1994; Barlowe, 2002). Likewise, several different types of vesicles function in the transport of proteins to the vacuole or plasma membrane. Vesicle trafficking consists of three important steps, budding from the donor organelle, movement along cytoskeletal filaments and fusion with the target organelle. Docking and fusion of vesicles at the target membrane requires SNAREs, an SM protein, a tethering factor and a Rab GTPase, which are responsible for target recognition and providing energy to drive membrane fusion.

SNAREs. SNAREs (soluble *N*-ethylmaleimide-sensitive fusion protein attachment protein receptors) were originally identified by their ability to bind to NSF (*N*-ethylmaleimide-sensitive fusion protein) and SNAP (soluble *N*-ethylmaleimide-sensitive factor attachment protein) (Sollner et al., 1993). NSF and SNAP are proteins required for efficient SNARE-mediated membrane fusion through freeing SNAREs from SNARE

complexes after membrane fusion (Woodman, 1997; Matveeva and Whiteheart, 1998; Weber et al., 1998). SNAREs are core proteins for vesicle fusion and can be categorized into two types; SNAREs on the vesicle are called v-SNAREs, while SNAREs on the target membrane are called t-SNAREs. When a vesicle comes close to its target membrane, the v-SNARE on the vesicle assembles with three t-SNAREs on the target membrane, forming a tetrameric *trans*-SNARE complex which pulls the two membranes closer to each other and drives membrane fusion (Fig 2; McNew et al., 2000).

During vesicle fusion, the specificity of SNARE interactions seems to be a major factor in determining patterns of membrane recognition and vesicle targeting (McNew et al., 2000; Paumet et al., 2004), and SNAREs confer energy to overcome the hydration forces to merge two lipid bilayers in an aqueous environment (Rand and Parsegian, 1989). Before vesicle fusion, SNAREs on the target membrane pre-exist as a *cis*-SNARE complex which consists of four α-helices of the SNARE core complex from a previous fusion event. The core region of a SNARE has hydrophobic heptad repeats with a core amino acid of either a glutamine residue (Qa, Qb and Qc domains) or an arginine residue (R domain). In mammalian cells, Qa- (syntaxin 1 like), Qb- (N-terminal half of SNAP25 like) and Qc- (C-terminal half of SNAP25 like) SNAREs typically form a complex on the target membrane and the R-SNARE is present on the vesicle (Bock et al., 2001). In *Arabidopsis*, there are 19 syntaxin-like Qa-SNAREs, 11 Qb-SNAREs, 12 Qc-SNAREs and 18 R-SNAREs, and SNARE complexes in *Arabidopsis* are thought to form in the same combination as in mammalian cells (Sutter et al., 2006a). However, in some cases, proteins of the VTI1 family (Qb-SNAREs) are thought to function as a v-SNARE in *Arabidopsis*, due to their similarity to the yeast v-SNARE Vti1p (Zheng et al., 1999).

Although SNAREs are fundamentally involved in vesicle fusion, some SNAREs have been found to have additional functions. Distribution and traffic of the K^+ channel KAT1 is mediated by SYP121, a t-SNARE on the plasma membrane, through its traditional SNARE function upon ABA signaling (Sutter et al., 2006). Recently, SYP121 was also reported to regulate the inward-rectifying K^+ channel AKT1 by interacting with a regulatory K^+ channel subunit KC1 (Honsbein et al., 2009). NtSyp121 is a AtSYP121 homolog in tobacco that was also found to regulate Ca^{2+} channel gating in tobacco guard cells (Sokolovski et al., 2008).

In *Arabidopsis*, the role of SNAREs in vacuolar trafficking, gravitropism, defense responses and development has been investigated. The SYP41 SNARE complex is thought to be involved in vacuolar trafficking. SYP41 is a Qa-SNARE and a T-DNA insertion knockout mutant exhibited a gametophyte lethal phenotype, suggesting it is an essential protein in development (Sanderfoot et al., 2001). The VTI1 family proteins are Qb-SNAREs, presumably serving as v-SNAREs. Mutant analysis of the VTI1 family showed that VTI11, which interacts with SNAREs at the PVC, is involved in vesicle trafficking to the lytic vacuole, whereas VTI12, a component of the SYP41 complex, is involved in vesicle trafficking to the storage vacuole (Sanmartin et al., 2007). Another interesting feature of SNAREs is their involvement in gravitropism. SYP22 and VTI11 are SNAREs on the membrane of the PVC. *syp22* and *vti11* mutants showed abnormal shoot gravitropism and abnormal distribution of amyloplasts in endodermal cells (Yano et al., 2003). This gravitropism defect is thought to be caused by defects in amyloplast movement (Saito et al., 2005; Ebine et al., 2008). The role of SNAREs during salt stress was also investigated. SYP61 is a Qc-SNARE in the SYP41 complex at the TGN. A *syp61* mutant showed a salt

and osmotic stress-sensitive phenotype and defects in stomatal control (Zhu et al., 2002). The molecular basis for the defects is not clear, but SYP61 is thought to affect salt tolerance indirectly. The VAMP7C (vesicle-associated membrane protein) family is involved in vesicle fusion with the tonoplast and salt tolerance. Reduced expression of VAMP711 increased tolerance and vacuolar function under salt stress conditions by inhibiting fusion of H_2O_2 containing vesicles with the vacuole, helping the vacuole to maintain its ΔpH for normal function (Leshem et al., 2006).

SNAREs at the Arabidopsis plasma membrane are involved in defense responses. SYP121 is involved in distribution and traffic of the K^+ channel KAT1 and is also important to confer resistance against barley (*Hordeum vulgare*) powdery mildew. Arabidopsis is not a host plant for this pathogen, but a mutation in SYP121 increased susceptibility of Arabidopsis to the barley powdery mildew (Collins et al., 2003). However, mutants in SYP122, the closest homolog of SYP121, do not have defects in non-host resistance (Assaad et al., 2004). Single *syp121* or *syp122* mutants did not show any growth defects, but a *syp121* and *syp122* double mutant showed a dwarfed and necrotic phenotype, suggesting that these two proteins have distinct functions in defense responses and partially redundant functions in development. Although only SYP121 is important to resist non-host pathogen infection, SYP121 and SYP122 are also negative regulators of salicylic acid and jasmonic acid, which are important hormones in plant defense pathways (Zhang et al., 2007). In addition, SYP121 forms SNARE complexes with AtSNAP33, an Arabidopsis homolog of the t-SNARE SNAP25, and either VAMP721 or VAMP722, and these SNARE complexes are responsible for disease resistance (Kwon et al., 2008). The exact role of these proteins during non-host infection is not known; it is hypothesized that they may be involved in exocytosis, which

mediates transport of anti-fungal molecules to the site of infection (Assaad et al., 2004; Kwon et al., 2008)

The role of cytokinesis-specific SNAREs during development is well characterized. KNOLLE (SYP111) and AtSNAP33 are highly expressed during cytokinesis, and individual *knolle* and *atsnap33* mutants have multinucleate cells with incomplete cross walls and are dwarfed with incomplete cell wall formation, respectively. This suggests that they are essential for the formation of the cell plate (Lukowitz et al., 1996; Lauber et al., 1997; Heese et al., 2001). Therefore, research on SNAREs has demonstrated that SNAREs are important for maintaining cellular function as well as vesicle fusion.

SM proteins. SNAREs are core proteins involved in membrane fusion. However, a number of proteins are required for the formation of SNARE complexes, vesicle docking and fusion *in vivo* (Malsam et al., 2008). Sec1/Munc18 proteins (SM proteins) play an important role in vesicle trafficking**.** SM proteins have been extensively studied in yeast and mammalian cells and shown to be essential factors in vesicle fusion via binding to a syntaxin-type SNARE or to a SNARE complex.

Studies on the role of SM proteins in vesicle fusion suggested three different modes of binding to SNAREs. The first mode is binding to the closed conformation. Munc18 is a mammalian SM protein involved in neurotransmitter release that binds to a closed form of the t-SNARE syntaxin 1 (Kee et al., 1995; Yang et al., 2000). The closed form of syntaxin 1 is generated by an N-terminal three-helix bundle (Habc domain) masking the SNARE motif, preventing interaction between SNAREs (Dulubova et al., 1999; Misura et al., 2000; Furgason et al., 2009). In this binding mode, Munc18 is thought to be a negative regulator to stabilize the closed form of the SNARE, which is then unable to form a SNARE complex

due to the inaccessible SNARE motif. The second mode is binding to the SNARE complex. Sec1p in yeast was shown to interact only with the SNARE complex, not with the single SNARE protein Sso1 as described in the first mode (Carr et al., 1999; Scott et al., 2004; Togneri et al., 2006). Munc18 is also able to bind to SNARE complexes (Dulubova et al., 2007). Binding of Munc18 to the SNARE complex was found to facilitate vesicle priming, suggesting Munc18 regulates both SNARE complex formation and vesicle fusion (Deak et al., 2009). The third mode is similar to the first mode, but the SNARE does not need to be in a closed form. This binding mode is found for VPS45 in yeast. VPS45 binds to the N-terminal domain (N-peptide) of the t-SNARE Tlg2p beyond the Habc domain regardless of the conformation of Tlg2p (Bryant and James, 2001; Dulubova et al., 2002). In this mode, VPS45 seems to positively regulate the formation of SNARE complexes. This type of binding mode is also found in Munc18c as shown in a crystal structure of Munc18c in complex with the Syntaxin 4 N-peptide (Hu et al., 2007). These three modes suggest a role for SM proteins as chaperones in formation of SNARE complexes.

SM proteins also regulate the cellular level of their interacting SNARE protein. Mutation of the interacting domain of VPS45 in yeast and reduced expression of AtVPS45 in Arabidopsis resulted in a decreased cellular level of Tlg2p in yeast and the Arabidopsis homolog SYP41 (Carpp et al., 2007; Zouhar et al., 2009).

The specific function of SM proteins in docking and fusion is not clear. However, study of the VPS33, an SM protein in yeast, showed a role for the SM protein in facilitating homotypic vesicle fusion *in vitro* (Mima et al., 2008). In this homotypic vesicle fusion, SNAP and NSF as well as VPS33 are required to make an active SNARE complex. Arabidopsis VPS33 localizes to the PVC and tonoplast and is proposed to function in

membrane fusion at these organelles (Rojo et al., 2003a). The role of AtVPS33 is not yet fully understood, but its interacting protein, VCL1 (vacuoleless 1) is involved in vacuole biogenesis (Rojo et al., 2001; Hicks et al., 2004). Thus, AtVPS33 may be involved in vacuole generation by mediating membrane fusion.

Lack of vesicle fusion in SM protein mutants inhibits diverse cellular processes. Null mutants of VPS45 in yeast and AtVPS45 RNAi transgenic plants showed inhibition of vacuolar trafficking (Cowles et al., 1994; Zouhar et al., 2009). Munc18c in adipose tissue was found to regulate glucose transporter (GLUT4) translocation to the plasma membrane by exocytosis (Thurmond et al., 2000). KEULE, a Sec1 like protein in the SM family, interacts with KNOLLE and drives membrane fusion (Assaad et al., 2001). Both *keule* and *knolle* single mutants showed defects in the formation of cell plates, suggesting they are essential during cell division (Lukowitz et al., 1996; Assaad et al., 2001). In summary, SM proteins are essential for SNARE complex formation and vesicle fusion, which are essential processes in cellular trafficking.

Tethering Factors. Tethering factors facilitate membrane recognition before vesicle fusion. There are two types of tethering factor, proteins containing extensive coiled-coil domains and large multisubunit complexes.

Proteins with long coiled-coil domains have a rod shape structure and tether as dimers. Well-documented examples are USO1 in yeast and GM130 in mammalian cells. USO1 is involved in ER-Golgi trafficking and a *uso1* temperature sensitive mutant has inhibition of transport of yeast invertase to the Golgi at the restrictive temperature (Nakajima et al., 1991). An *in vitro* fusion assay demonstrated that USO1 was required to tether COPII vesicles to the Golgi (Barlowe, 1997). GM130 is a peripheral membrane protein that is

bound to the Golgi via the Golgi reassembly stacking protein of 65kDa (GRASP65). GM130 is an extended rod-like protein with 6 coiled-coil domains (Nakamura et al., 1995). Like USO1, the role of GM130 in tethering was investigated by an *in vitro* fusion assay. GM130 interacts with activated Rab1-GTP, a member of the Rab family of small GTPases, and is required for COPII vesicle targeting/fusion with the *cis*-Golgi (Moyer et al., 2001). The tethering of COPII vesicles to the Golgi is proposed to be mediated by binding of p115 on COPII vesicles to GM130 on the Golgi.

In addition to coiled-coil proteins, multisubunit complexes have been shown to regulate membrane trafficking. Like coiled-coil tethering factors, all of the multisubunit tethering factors interact with SNAREs and small GTPases. Several different multi-subunit complexes have been identified to date. The homotypic fusion and vacuolar protein sorting (HOPS) complex is a well-studied multisubunit complex involved in vacuolar trafficking in yeast. The HOPS complex consists of six polypeptides and interacts with the vacuolar Rab GTPase Ypt7p, resulting in vacuolar SNARE complex assembly, homotypic fusion of yeast vacuoles and the fusion of transport vesicles with the vacuole (Mayer and Wickner, 1997; Price et al., 2000; Seals et al., 2000). In addition to the interaction with Ypt7p, the HOPS complex also interacts with the vacuolar SNARE protein Vam7p to support HOPS complex association with the vacuole (Stroupe et al., 2006). Mutations in each protein of the HOPS complex caused defects in sorting of proteins to the vacuole (Raymond et al., 1992). Therefore, the HOPS complex is thought to be involved in vacuolar trafficking by mediating membrane fusion.

Tethering factors often have other functions in addition to their tethering function. The coiled-coil domain of p115 is similar to a SNARE motif and stimulates SNARE

assembly (Shorter et al., 2002). During apoptosis, tethering factors including golgin-160, p115 and GM130 are targets of caspases (Mancini et al., 2000; Chin et al., 2002). In particular, golgin-160 is important in apoptotic signal transduction which is induced by fragmentation of golgin-160. Caspase-resistant golgin-160 delayed apoptosis compared with the wild-type protein (Maag et al., 2005). Golgins, large proteins with long coiled-coil domains for tethering vesicles in mammalian cells, are not affected by treatment with the trafficking inhibitor BFA and remain at the Golgi apparatus (Seemann et al., 2000). Thus, these proteins are regarded as Golgi matrix proteins, involved in tethering membranes, linking cisternae during Golgi stack formation and maintaining Golgi structure (Slusarewicz et al., 1994; Sonnichsen et al., 1998; Shorter and Warren, 1999).

In *Arabidopsis*, two putative tethering factors containing extensive coiled-coil domains have been identified. AtCASP (CCAAT-displacement protein), a homolog of human CASP, has a long N-terminal coiled-coil and a C-terminal transmembrane domain for Golgi localization (Renna et al., 2005). A mutation in the transmembrane domain of the CASP homolog in yeast, COY1 was able to restore normal growth in cells lacking the yeast SNARE Gos1p (Gillingham et al., 2002). The exact role of CASP needs to be further investigated. The other identified tethering factor is AtGRIP (Gilson et al., 2004). GRIP-domain proteins have extensive coiled-coil regions and a 40-amino-acid C-terminal domain called the GRIP domain. AtGRIP was found to interact with ADP-ribosylation factor 1 (ARF1) and be involved in coat-free vesicle trafficking at the Golgi (Stefano et al., 2006; Matheson et al., 2007). Although the function of AtCASP and AtGRIP in tethering has not yet been studied, they are suggested to be tethering factors due to their sequence similarity to mammalian tethering factors at the Golgi (Gilson et al., 2004; Renna et al., 2005). The

HOPS complex in Arabidopsis was also identified and components of the yeast HOPS complex are well conserved in Arabidopsis (Rojo et al., 2003a). The Arabidopsis HOPS complex also localizes to the PVC and tonoplast similar to the yeast complex, suggesting that the function of the HOPS complex in Arabidopsis could also be conserved (Rojo et al., 2003a).

Trafficking inhibitors

Vacuolar and secretory proteins are transported through the endomembrane system by vesicle trafficking before they reach their destination. To study vesicle trafficking, organelle marker proteins fused with fluorescence tags have been used extensively (Chalfie et al., 1994). With these marker proteins, application of trafficking inhibitors has further identified and confirmed trafficking events in the cell. Trafficking inhibitors specifically inhibit proteins that regulate vesicle trafficking, resulting in complete inhibition of the trafficking step. Several trafficking inhibitors are commonly used to inhibit endocytosis, ER-Golgi trafficking or post-Golgi trafficking.

Brefeldin A. The fungal toxin brefeldin A (BFA) has been widely used to study protein trafficking and for organelle identification. BFA has been extensively studied in mammalian cells where it inhibits the Sec7-type GTP exchange factor (GEF), which is required to activate the Arf1-GTPase involved in recruiting COPI coat protein (Jackson and Casanova, 2000). Inhibition of COPI vesicle formation for internal Golgi trafficking or retrograde trafficking to the ER is hypothesized to expose the v-SNARE required for COPI

vesicle fusion on the Golgi, resulting in fusion with the ER and the formation of ER-Golgi hybrid structures (Jackson and Casanova, 2000; Nebenfuhr et al., 2002).

In Arabidopsis, BFA targets GNOM, the Arf GEF, BFA-sensitive Sec7-like protein at the Arabidopsis endosome (Steinmann et al., 1999). Inhibition of GNOM by BFA blocks anterograde trafficking from endosomes to the plasma membrane, resulting in endosomal aggregates (BFA compartment; Geldner et al., 2003). GNOM is involved in recycling of PIN1, an auxin transporter with a polar distribution in the plasma membrane (Galweiler et al., 1998; Geldner et al., 2003). Upon BFA treatment, PIN1 was detected in the BFA compartment, while PIN1 still showed polar distribution in BFA-resistant GNOM transgenic plants. This recycling of PIN1 is a good example showing the usefulness of BFA in investigation of cellular trafficking. When roots perceive gravi-stimulation, PIN1 is re-localized to maintain its polar distribution for auxin efflux (Geldner et al., 2003). Therefore, recycling of PIN1 via GNOM-positive endosomes rapidly redistributes PIN1 according to the direction of gravity.

Vacuolar H^+ATPase (VHAa1), SYP61 and Secretory Carrier Membrane Protein 1 (SCAMP1) localize to the TGN and early endosome, and they are found in the BFA compartment (Dettmer et al., 2006; Lam et al., 2009). Application of the endosomal trafficking inhibitor Tyrphostin A23 prevents formation of the BFA compartment, suggesting that the BFA compartment may be formed by fusion between early endosomes and TGN (Lam et al., 2009). Application of BFA in plants produces several distinct structures depending on cell type. BFA application to tobacco BY-2 suspension cells produces a Golgi-PVC hybrid structure. This structure is distinct from the BFA compartment induced by fusion between early endosomes and TGN, although the PVC is considered a late

endosome (Tse et al., 2006). In tobacco, BFA causes redistribution of proteins in the Golgi to the ER. Differently from tobacco and mammalian cells, proteins in the Golgi of Arabidopsis roots are not redistributed to the ER by BFA treatment due to the presence of a BFA-resistant GNOM-LIKE 1 protein (GNL1; Richter et al., 2007; Teh and Moore, 2007). Although BFA appears to target a SEC7-type GEF in all eukaryotic cells, susceptibility of specific SEC7-type GEFs upon BFA treatment determines the sensitivity of a particular trafficking pathway to BFA.

Wortmannin is an inhibitor of phosphatidyl inositol 3-kinase. The effect of wortmannin is well studied in yeast. Wortmannin inhibits yeast VPS34, the phosphatidylinositol 3-kinase responsible for the synthesis of phosphatidylinositol 3-phosphate (PI-3P), resulting in depletion of a key component of the endosomal membrane and in defects in signal transduction and cell proliferation (Simonsen and Stenmark, 2001; Burda et al., 2002; Lee et al., 2008). VPS5p and VPS17p, components of the yeast retromer complex required for recycling of trafficking components, have Phox domains that interact with PI-3P and are involved in vacuolar trafficking. This suggests that wortmannin inhibits retromer complex-mediated receptor recycling to the TGN, causing enlargement of the PVC (Seaman, 2005). Yeast VPS35 is a component of the retromer complex and is involved in sorting of vacuolar proteins (Nothwehr et al., 1999; Nothwehr et al., 2000; Restrepo et al., 2007). AtVPS35, a yeast VPS35 homolog is also required for vacuolar protein sorting, forms a retromer complex with AtVPS5 and is sensitive to wortmannin treatment (Oliviusson et al., 2006; Yamazaki et al., 2008). This result shows that function of retromer complex is well conserved in eukaryotic cells.

In plants, wortmannin produces swelling of the PVC to produce a ring shaped structure seen by confocal microscopy. This ring structure is formed by fusion between the TGN/ endosomes and PVCs in BY-2 cells (Wang et al., 2009), resulting in enlargement of the PVC.

Although the BFA compartment and wortmannin-induced ring structures are formed by fusion between TGN/ endosomes and between TGN/ endosomes and PVCs, respectively, they are distinct structures. AtSNX1 in *Arabidopsis* is a protein involved in PIN2 recycling. Upon BFA treatment, AtSNX1 co-localizes with GNOM in the BFA compartment, while AtSNX1 and GNOM do not co-localize after wortmannin treatment (Jaillais et al., 2006). This result suggests that there is a different endosomal pool for PIN1 and PIN2 recycling, and PIN1-positive endosomes may be resistant to wortmannin.

Perspectives

Improving crop quality is one way to increase its economic value. Storage vacuoles in crop plants are responsible for determining protein quantity due to the deposition of storage proteins, the composition of which determines protein quality. Thus, the content of essential amino acids, i.e. those which cannot be synthesized by humans or animals, has been a primary target to improve crop nutritional quality (Dijkstra et al., 2003; Williams, 2003). Therefore, genetic engineering to increase essential amino acid content has been performed using a number of approaches such as expressing foreign storage proteins with a high content of essential amino acids in heterologous systems and expressing enzymes involved in synthesis of the essential amino acids (Altenbach et al., 1992; Avraham et al., 2005). In

addition, production of pharmaceutical proteins in plants has been widely investigated (Deckers et al., 1999; Ma et al., 2003; Vitale and Pedrazzini, 2005). Protein bodies, the ER and storage vacuoles in seeds are primary targets for the storage of foreign proteins. For the efficient trafficking of overexpressed or foreign proteins, components involved in vesicle transport may also need to be overexpressed to meet the requirement for efficient transport. Thus, further investigation of endomembrane trafficking pathways and vesicle transport will help in improving crop quality and producing pharmaceutical products.

Dissertation Outline

The primary goal of this dissertation is investigation of the role of TNO1 (TGN-localized SYP41 interacting protein) in vacuolar trafficking in *Arabidopsis* and investigation of membrane fusion mediated by TGN-localized SNAREs. Two chapters will present the results of this study. In Chapter 2, the localization of TNO1 and its role in vacuolar trafficking, salt and osmotic stress tolerance and putative function in vesicle fusion will be addressed. Chapter 3 will analyze vesicle fusion driven by SYP4 family proteins, VTI1 family proteins and AtVPS45 at the TGN using an *in vitro* liposome fusion assay. The final chapter in this dissertation will be a general discussion and future directions to determine a more detailed role for TNO1 in trafficking and vesicle fusion at TGN. For chapter 2 and 3, I am responsible for all of the experiments, figures and manuscripts. Two appendices (published manuscripts) will be presented at the end of the thesis. Appendix A is titled 'Transcriptome profiling of the response of Arabidopsis suspension culture cells to Suc starvation.' I am responsible for figure 9 and the corresponding results and discussion.

Appendix B is titled ‘Overexpression of *Arabidopsis* sorting nexin AtSNX2b inhibits endocytic trafficking to the vacuole.’ I am responsible for generating figures 1 and 9, and the corresponding results and discussion.

References

Abas L, Benjamins R, Malenica N, Paciorek T, Wirniewska J, Moulinier-Anzola JC, Sieberer T, Friml J, Luschnig C (2006) Intracellular trafficking and proteolysis of the Arabidopsis auxin-efflux facilitator PIN2 are involved in root gravitropism. Nature Cell Biology **8:** 249-256

Altenbach SB, Kuo CC, Staraci LC, Pearson KW, Wainwright C, Georgescu A, Townsend J (1992) Accumulation of a Brazil Nut Albumin in Seeds of Transgenic Canola Results in Enhanced Levels of Seed Protein Methionine. Plant Molecular Biology **18:** 235-245

Assaad FF, Huet Y, Mayer U, Jurgens G (2001) The cytokinesis gene KEULE encodes a Sec1 protein that binds the syntaxin KNOLLE. Journal of Cell Biology **152:** 531-543

Assaad FF, Qiu JL, Youngs H, Ehrhardt D, Zimmerli L, Kalde M, Wanner G, Peck SC, Edwards H, Ramonell K, Somerville CR, Thordal-Christensen H (2004) The PEN1 syntaxin defines a novel cellular compartment upon fungal attack and is required for the timely assembly of papillae\. Molecular Biology of the Cell **15:** 5118-5129

Aubert S, Gout E, Bligny R, MartyMazars D, Barrieu F, Alabouvette J, Marty F, Douce R (1996) Ultrastructural and biochemical characterization of autophagy in higher plant cells subjected to carbon deprivation: Control by the supply of mitochondria with respiratory substrates. Journal of Cell Biology **133:** 1251-1263

Avraham T, Badani H, Galili S, Amir R (2005) Enhanced levels of methionine and cysteine in transgenic alfalfa (Medicago sativa L.) plants over-expressing the Arabidopsis cystathionine gamma-synthase gene. Plant Biotechnology Journal **3:** 71-79

Barlowe C (1997) Coupled ER to Golgi transport reconstituted with purified cytosolic proteins. Journal of Cell Biology **139:** 1097-1108

Barlowe C (2002) COPII-dependent transport from the endoplasmic reticulum. Current Opinion in Cell Biology **14:** 417-422

Barlowe C, Orci L, Yeung T, Hosobuchi M, Hamamoto S, Salama N, Rexach MF, Ravazzola M, Amherdt M, Schekman R (1994) Copii - a Membrane Coat Formed by Sec Proteins That Drive Vesicle Budding from the Endoplasmic-Reticulum. Cell **77:** 895-907

Battey NH, James NC, Greenland AJ, Brownlee C (1999) Exocytosis and endocytosis. Plant Cell **11:** 643-659

Bednarek SY, Raikhel NV (1991) The Barley Lectin Carboxyl-Terminal Propeptide Is a Vacuolar Protein Sorting Determinant in Plants. Plant Cell **3:** 1195-1206

Bock JB, Matern HT, Peden AA, Scheller RH (2001) A genomic perspective on membrane compartment organization. Nature **409:** 839-841

Bryant NJ, James DE (2001) Vps45p stabilizes the syntaxin homologue Tlg2p and positively regulates SNARE complex formation. Embo Journal **20:** 3380-3388

Burda P, Padilla SM, Sarkar S, Emr SD (2002) Retromer function in endosome-to-Golgi retrograde transport is regulated by the yeast Vps34 PtdIns 3-kinase. Journal of Cell Science **115:** 3889-3900

Carpp LN, Shanks SG, Struthers MS, Bryant NJ (2007) Cellular levels of the syntaxin Tlg2p are regulated by a single mode of binding to Vps45p. Biochemical and Biophysical Research Communications **363:** 857-860

Carr CM, Grote E, Munson M, Hughson FM, Novick PJ (1999) Sec1p binds to SNARE complexes and concentrates at sites of secretion. Journal of Cell Biology **146:** 333-344

Chalfie M, Tu Y, Euskirchen G, Ward WW, Prasher DC (1994) Green Fluorescent Protein as a Marker for Gene-Expression. Science **263:** 802-805

Chin R, Novikov L, Mukherjee S, Shields D (2002) A caspase cleavage fragment of p115 induces fragmentation of the Golgi apparatus and apoptosis. Journal of Cell Biology **159:** 637-648

Collins NC, Thordal-Christensen H, Lipka V, Bau S, Kombrink E, Qiu JL, Huckelhoven R, Stein M, Freialdenhoven A, Somerville SC, Schulze-Lefert P

(2003) SNARE-protein-mediated disease resistance at the plant cell wall. Nature **425:** 973-977

Cowles CR, Emr SD, Horazdovsky BF (1994) Mutations in the Vps45 Gene, a Sec1 Homolog, Result in Vacuolar Protein Sorting Defects and Accumulation of Membrane-Vesicles. Journal of Cell Science **107:** 3449-3459

Deak F, Xu Y, Chang WP, Dulubova I, Khvotchev M, Liu X, Sudhof TC, Rizo J (2009) Munc18-1 binding to the neuronal SNARE complex controls synaptic vesicle priming. J Cell Biol **184:** 751-764

Deckers H, Moloney M, Baum A (1999) The case for recombinant production of pharmaceutical proteins in plants. Annual Reports in Medicinal Chemistry, Vol 34 **34:** 237-245

DePina AS, Langford GM (1999) Vesicle transport: The role of actin filaments and myosin motors. Microscopy Research and Technique **47:** 93-106

Dettmer J, Hong-Hermesdorf A, Stierhof YD, Schumacher K (2006) Vacuolar H+-ATPase activity is required for Endocytic and secretory trafficking in Arabidopsis. Plant Cell **18:** 715-730

Di Sansebastiano GP, Paris N, Marc-Martin S, Neuhaus JM (2001) Regeneration of a lytic central vacuole and of neutral peripheral vacuoles can be visualized by green fluorescent proteins targeted to either type of vacuoles. Plant Physiol **126:** 78-86

Dijkstra DS, Linnemann AR, van Boekel TAJS (2003) Towards sustainable production of protein-rich foods: Appraisal of eight crops for Western Europe. PART II: Analysis of the technological aspects of the production chain. Critical Reviews in Food Science and Nutrition **43:** 481-506

Dulubova I, Khvotchev M, Liu S, Huryeva I, Sudhof TC, Rizo J (2007) Munc18-1 binds directly to the neuronal SNARE complex. Proc Natl Acad Sci U S A **104:** 2697-2702

Dulubova I, Sugita S, Hill S, Hosaka M, Fernandez I, Sudhof TC, Rizo J (1999) A conformational switch in syntaxin during exocytosis: role of munc18. Embo Journal **18:** 4372-4382

Dulubova I, Yamaguchi T, Gao Y, Min SW, Huryeva I, Sudhof TC, Rizo J (2002) How Tlg2p/syntaxin 16 'snares' Vps45. Embo Journal **21:** 3620-3631

Ebine K, Okatani Y, Uemura T, Goh T, Shoda K, Niihama M, Morita MT, Spitzer C, Otegui MS, Nakano A, Ueda T (2008) A SNARE Complex Unique to Seed Plants Is Required for Protein Storage Vacuole Biogenesis and Seed Development of Arabidopsis thaliana. Plant Cell **20:** 3006-3021

Fukasawa T, Haranishimura I, Nishimura M (1988) Biosynthesis, Intracellular-Transport and Invitro Processing of 11S Globulin Precursor Proteins of Developing Castor Bean Endosperm. Plant and Cell Physiology **29:** 339-345

Furgason ML, MacDonald C, Shanks SG, Ryder SP, Bryant NJ, Munson M (2009) The N-terminal peptide of the syntaxin Tlg2p modulates binding of its closed conformation to Vps45p. Proc Natl Acad Sci U S A **106:** 14303-14308

Galweiler L, Guan CH, Muller A, Wisman E, Mendgen K, Yephremov A, Palme K (1998) Regulation of polar auxin transport by AtPIN1 in Arabidopsis vascular tissue. Science **282:** 2226-2230

Geisler M, Frangne N, Gomes E, Martinoia E, Palmgren MG (2000) The ACA4 gene of Arabidopsis encodes a vacuolar membrane calcium pump that improves salt tolerance in yeast. Plant Physiol **124:** 1814-1827

Geldner N, Anders N, Wolters H, Keicher J, Kornberger W, Muller P, Delbarre A, Ueda T, Nakano A, Jurgens G (2003) The Arabidopsis GNOM ARF-GEF mediates endosomal recycling, auxin transport, and auxin-dependent plant growth. Cell **112:** 219-230

Gillingham AK, Pfeifer AC, Munro S (2002) CASP, the alternatively spliced product of the gene encoding the CCAAT-displacement protein transcription factor, is a Golgi membrane protein related to giantin. Molecular Biology of the Cell **13:** 3761-3774

Gilson PR, Vergara CE, Kjer-Nielsen L, Teasdale RD, Bacic A, Gleeson PA (2004) Identification of a Golgi-localised GRIP domain protein from Arabidopsis thaliana. Planta **219:** 1050-1056

Hamm-Alvarez SF (1998) Molecular motors and their role in membrane traffic. Advanced Drug Delivery Reviews **29:** 229-242

Hara-Nishimura I, Shimada T, Hatano K, Takeuchi Y, Nishimura M (1998) Transport of storage proteins to protein storage vacuoles is mediated by large precursor-accumulating vesicles. Plant Cell **10:** 825-836

Hayashi Y, Yamada K, Shimada T, Matsushima R, Nishizawa NK, Nishimura M, Hara-Nishimura I (2001) A proteinase-storing body that prepares for cell death or stresses in the epidermal cells of Arabidopsis. Plant and Cell Physiology **42:** 894-899

Heese M, Gansel X, Sticher L, Wick P, Grebe M, Granier F, Jurgens G (2001) Functional characterization of the KNOLLE-interacting t-SNARE AtSNAP33 and its role in plant cytokinesis. Journal of Cell Biology **155:** 239-249

Hicks GR, Rojo E, Hong SH, Carter DG, Raikhel NV (2004) Geminating pollen has tubular vacuoles, displays highly dynamic vacuole biogenesis, and requires VACUOLESS1 for proper function. Plant Physiology **134:** 1227-1239

Hinz G, Colanesi S, Hillmer S, Rogers JC, Robinson DG (2007) Localization of vacuolar transport receptors and cargo proteins in the Golgi apparatus of developing Arabidopsis embryos. Traffic **8:** 1452-1464

Hofte H, Hubbard L, Reizer J, Ludevid D, Herman EM, Chrispeels MJ (1992) Vegetative and Seed-Specific Forms of Tonoplast Intrinsic Protein in the Vacuolar Membrane of Arabidopsis-Thaliana. Plant Physiology **99:** 561-570

Hofte H, Hubbard L, Reizer J, Ludevid D, Herman EM, Chrispeels MJ (1992) Vegetative and Seed-Specific Forms of Tonoplast Intrinsic Protein in the Vacuolar Membrane of Arabidopsis thaliana. Plant Physiol **99:** 561-570

Holwerda BC, Padgett HS, Rogers JC (1992) Proaleurain Vacuolar Targeting Is Mediated by Short Contiguous Peptide Interactions. Plant Cell **4:** 307-318

Honsbein A, Sokolovski S, Grefen C, Campanoni P, Pratelli R, Paneque M, Chen ZH, Johansson I, Blatt MR (2009) A Tripartite SNARE-K+ Channel Complex Mediates in Channel-Dependent K+ Nutrition in Arabidopsis. Plant Cell **21:** 2859-2877

Hu SH, Latham CF, Gee CL, James DE, Martin JL (2007) Structure of the Munc18c/Syntaxin4 N-peptide complex defines universal features of the N-peptide binding mode of Sec1/Munc18 proteins. Proceedings of the National Academy of Sciences of the United States of America **104:** 8773-8778

Hwang I, Robinson DG (2009) Transport vesicle formation in plant cells. Current Opinion in Plant Biology **12:** 660-669

Jackson CL, Casanova JE (2000) Turning on ARF: the Sec7 family of guanine-nucleotide-exchange factors. Trends in Cell Biology **10:** 60-67

Jaillais Y, Fobis-Loisy I, Miege C, Rollin C, Gaude T (2006) AtSNX1 defines an endosome for auxin-carrier trafficking in Arabidopsis. Nature **443:** 106-109

Jiang LW, Phillips TE, Rogers SW, Rogers JC (2000) Biogenesis of the protein storage vacuole crystalloid. Journal of Cell Biology **150:** 755-769

Journet EP, Bligny R, Douce R (1986) Biochemical-Changes during Sucrose Deprivation in Higher-Plant Cells. Journal of Biological Chemistry **261:** 3193-3199

Kahn RA, Volpicelli-Daley L, Bowzard B, Shrivastava-Ranjan P, Li Y, Zhou C, Cunningham L (2005) Arf family GTPases: roles in membrane traffic and microtubule dynamics. Biochemical Society Transactions **33:** 1269-1272

Kee Y, Lin RC, Hsu SC, Scheller RH (1995) Distinct Domains of Syntaxin Are Required for Synaptic Vesicle Fusion Complex-Formation and Dissociation. Neuron **14:** 991-998

Kirsch T, Paris N, Butler JM, Beevers L, Rogers JC (1994) Purification and Initial Characterization of a Potential Plant Vacuolar Targeting Receptor. Proceedings of the National Academy of Sciences of the United States of America **91:** 3403-3407

Kwon C, Neu C, Pajonk S, Yun HS, Lipka U, Humphry M, Bau S, Straus M, Kwaaitaal M, Rampelt H, El Kasmi F, Jurgens G, Parker J, Panstruga R, Lipka V, Schulze-Lefert P (2008) Co-option of a default secretory pathway for plant immune responses. Nature **451:** 835-840

Lam SK, Cai Y, Tse YC, Wang J, Law AHY, Pimpl P, Chan HYE, Xia J, Jiang LW (2009) BFA-induced compartments from the Golgi apparatus and trans-Golgi network/early endosome are distinct in plant cells. Plant Journal **60:** 865-881

Lauber MH, Waizenegger I, Steinmann T, Schwarz H, Mayer U, Hwang I, Lukowitz W, Jurgens G (1997) The Arabidopsis KNOLLE protein is a cytokinesis-specific syntaxin. Journal of Cell Biology **139:** 1485-1493

Lee Y, Bak G, Choi Y, Chuang WI, Cho HT, Lee Y (2008) Roles of phosphatidylinositol 3-kinase in root hair growth. Plant Physiol **147:** 624-635

Leshem Y, Melamed-Book N, Cagnac O, Ronen G, Nishri Y, Solomon M, Cohen G, Levine A (2006) Suppression of Arabidopsis vesicle-SNARE expression inhibited fusion of H2O2 containing vesicles with tonoplast and increased salt tolerance.

Proceedings of the National Academy of Sciences of the United States of America **103:** 18008-18013

Liu YM, Xiong Y, Bassham DC (2009) Autophagy is required for tolerance of drought and salt stress in plants. Autophagy **5:** 954-963

Lukowitz W, Mayer U, Jurgens G (1996) Cytokinesis in the Arabidopsis embryo involves the syntaxin-related KNOLLE gene product. Cell **84:** 61-71

Ma JKC, Drake PMW, Christou P (2003) The production of recombinant pharmaceutical proteins in plants. Nature Reviews Genetics **4:** 794-805

Maag RS, Mancini M, Rosen A, Machamer CE (2005) Caspase-resistant golgin-160 by secretory pathway stress disrupts apoptosis induced and ligation of death receptors. Molecular Biology of the Cell **16:** 3019-3027

Malsam J, Kreye S, Sollner TH (2008) Membrane fusion: SNAREs and regulation. Cellular and Molecular Life Sciences **65:** 2814-2832

Mancini M, Machamer CE, Roy S, Nicholson DW, Thornberry NA, Casciola-Rosen LA, Rosen A (2000) Caspase-2 is localized at the Golgi complex and cleaves golgin-160 during apoptosis. Journal of Cell Biology **149:** 603-612

Marty F (1999) Plant vacuoles. Plant Cell **11:** 587-599

Matheson LA, Hanton SL, Rossi M, Latijnhouwers M, Stefano G, Renna L, Brandizzi F (2007) Multiple roles of ADP-ribosylation factor 1 in plant cells include spatially regulated recruitment of coatomer and elements of the golgi matrix. Plant Physiology **143:** 1615-1627

Matsuoka K, Bassham DC, Raikhel NV, Nakamura K (1995) Different Sensitivity to Wortmannin of 2 Vacuolar Sorting Signals Indicates the Presence of Distinct Sorting Machineries in Tobacco Cells. Journal of Cell Biology **130:** 1307-1318

Matveeva E, Whiteheart SW (1998) The effects of SNAP/SNARE complexes on the ATPase of NSF. Febs Letters **435:** 211-214

Mayer A, Wickner W (1997) Docking of yeast vacuoles is catalyzed by the Ras-like GTPase Ypt7p after symmetric priming by Sec18p (NSF). Journal of Cell Biology **136:** 307-317

McNew JA, Parlati F, Fukuda R, Johnston RJ, Paz K, Paumet F, Sollner TH, Rothman JE (2000) Compartmental specificity of cellular membrane fusion encoded in SNARE proteins. Nature **407:** 153-159

Mima J, Hickey CM, Xu H, Jun Y, Wickner W (2008) Reconstituted membrane fusion requires regulatory lipids, SNAREs and synergistic SNARE chaperones. Embo Journal **27:** 2031-2042

Misura KMS, Scheller RH, Weis WI (2000) Three-dimensional structure of the neuronal-Sec1-syntaxin 1a complex. Nature **404:** 355-362

Moyer BD, Allan BB, Balch WE (2001) Rab1 interaction with a GM130 effector complex regulates COPII vesicle cis-Golgi tethering. Traffic **2:** 268-276

Nakajima H, Hirata A, Ogawa Y, Yonehara T, Yoda K, Yamasaki M (1991) A Cytoskeleton-Related Gene, Uso1, Is Required for Intracellular Protein-Transport in Saccharomyces-Cerevisiae. Journal of Cell Biology **113:** 245-260

Nakamura K, Matsuoka K, Mukumoto F, Watanabe N (1993) Processing and Transport to the Vacuole of a Precursor to Sweet-Potato Sporamin in Transformed Tobacco Cell Line-by-2. Journal of Experimental Botany **44:** 331-338

Nakamura N, Rabouille C, Watson R, Nilsson T, Hui N, Slusarewicz P, Kreis TE, Warren G (1995) Characterization of a cis-Golgi matrix protein, GM130. Journal of Cell Biology **131:** 1715-1726

Nebenfuhr A, Ritzenthaler C, Robinson DG (2002) Brefeldin A: Deciphering an enigmatic inhibitor of secretion. Plant Physiology **130:** 1102-1108

Neumann U, Brandizzi F, Hawes C (2003) Protein transport in plant cells: In and out of the Golgi. Annals of Botany **92:** 167-180

Newmyer SL, Christensen A, Sever S (2003) Auxilin-dynamin interactions link the uncoating ATPase chaperone machinery with vesicle formation. Developmental Cell **4:** 929-940

Nishizawa K, Maruyama N, Utsumi S (2006) The C-terminal region of alpha ' subunit of soybean beta-conglycinin contains two types of vacuolar sorting determinants. Plant Molecular Biology **62:** 111-125

Noda T, Suzuki K, Ohsumi Y (2002) Yeast autophagosomes: de novo formation of a membrane structure. Trends in Cell Biology **12:** 231-235

Nothwehr SF, Bruinsma P, Strawn LA (1999) Distinct domains within Vps35p mediate the retrieval of two different cargo proteins from the yeast prevacuolar/endosomal compartment. Molecular Biology of the Cell **10:** 875-890

Nothwehr SF, Ha SA, Bruinsma P (2000) Sorting of yeast membrane proteins into an endosome-to-Golgi pathway involves direct interaction of their cytosolic domains with Vps35p. Journal of Cell Biology **151:** 297-309

Oliviusson P, Heinzerling O, Hillmer S, Hinz G, Tse YC, Jiang LW, Robinson DG (2006) Plant retromer, localized to the prevacuolar compartment and microvesicles in Arabidopsis, may interact with vacuolar sorting receptors. Plant Cell **18:** 1239-1252

Otegui MS, Noh YS, Martinez DE, Vila Petroff MG, Andrew Staehelin L, Amasino RM, Guiamet JJ (2005) Senescence-associated vacuoles with intense proteolytic activity develop in leaves of Arabidopsis and soybean. Plant Journal **41:** 831-844

Paris N, Stanley CM, Jones RL, Rogers JC (1996) Plant cells contain two functionally distinct vacuolar compartments. Cell **85:** 563-572

Park M, Lee D, Lee GJ, Hwang I (2005) AtRMR1 functions as a cargo receptor for protein trafficking to the protein storage vacuole. Journal of Cell Biology **170:** 757-767

Paumet F, Rahimian V, Rothman JE (2004) The specificity of SNARE-dependent fusion is encoded in the SNARE motif. Proceedings of the National Academy of Sciences of the United States of America **101:** 3376-3380

Price A, Wickner W, Ungermann C (2000) Proteins needed for vesicle budding from the golgi complex are also required for the docking step of homotypic vacuole fusion. Journal of Cell Biology **148:** 1223-1229

Rand RP, Parsegian VA (1989) Hydration Forces between Phospholipid-Bilayers. Biochimica Et Biophysica Acta **988:** 351-376

Raymond CK, Howaldstevenson I, Vater CA, Stevens TH (1992) Morphological Classification of the Yeast Vacuolar Protein Sorting Mutants - Evidence for a Prevacuolar Compartment in Class-E Vps Mutants. Molecular Biology of the Cell **3:** 1389-1402

Renna L, Hanton SL, Stefano G, Bortolotti L, Misra V, Brandizzi F (2005) Identification and characterization of AtCASP, a plant transmembrane Golgi matrix protein. Plant Molecular Biology **58:** 109-122

Restrepo R, Zhao X, Peter H, Zhang BY, Arvan P, Nothwehr SF (2007) Structural features of Vps35p involved in interaction with other subunits of the retromer complex. Traffic **8:** 1841-1853

Richter S, Geldner N, Schrader J, Wolters H, Stierhof YD, Rios G, Koncz C, Robinson DG, Jurgens G (2007) Functional diversification of closely related ARF-GEFs in protein secretion and recycling. Nature **448:** 488-U410

Rojo E, Gillmor CS, Kovaleva V, Somerville CR, Raikhel NV (2001) VACUOLELESS1 is an essential gene required for vacuole formation and morphogenesis in Arabidopsis. Developmental Cell **1:** 303-310

Rojo E, Zouhar J, Carter C, Kovaleva V, Raikhel NV (2003b) A unique mechanism for protein processing and degradation in Arabidopsis thaliana. Proceedings of the National Academy of Sciences of the United States of America **100:** 7389-7394

Rojo E, Zouhar J, Kovaleva V, Hong S, Raikhel NV (2003a) The AtC-VPS protein complex is localized to the tonoplast and the prevacuolar compartment in Arabidopsis. Molecular Biology of the Cell **14:** 361-369

Saito C, Morita MT, Kato T, Tasaka M (2005) Amyloplasts and vacuolar membrane dynamics in the living graviperceptive cell of the Arabidopsis inflorescence stem. Plant Cell **17:** 548-558

Samaj J, Read ND, Volkmann D, Menzel D, Baluska F (2005) The endocytic network in plants. Trends in Cell Biology **15:** 425-433

Sanderfoot AA, Pilgrim M, Adam L, Raikhel NV (2001) Disruption of individual members of arabidopsis syntaxin gene families indicates each has essential functions. Plant Cell **13:** 659-666

Sanmartin M, Ordonez A, Sohn EJ, Robert S, Sanchez-Serrano JJ, Surpin MA, Raikhel NV, Rojo E (2007) Divergent functions of VTI12 and VTI11 in trafficking to storage and lytic vacuoles in Arabidopsis. Proceedings of the National Academy of Sciences of the United States of America **104:** 3645-3650

Scott BL, Van Komen JS, Irshad H, Liu S, Wilson KA, McNew JA (2004) Sec1p directly stimulates SNARE-mediated membrane fusion in vitro. J Cell Biol **167:** 75-85

Seals DF, Eitzen G, Margolis N, Wickner WT, Price A (2000) A Ypt/Rab effector complex containing the Sec1 homolog Vps33p is required for homotypic vacuole

fusion. Proceedings of the National Academy of Sciences of the United States of America **97:** 9402-9407

Seaman MNJ (2005) Recycle your receptors with retromer. Trends in Cell Biology **15:** 68-75

Seemann J, Jokitalo E, Pypaert M, Warren G (2000) Matrix proteins can generate the higher order architecture of the Golgi apparatus. Nature **407:** 1022-1026

Shimada T, Fuji K, Tamura K, Kondo M, Nishimura M, Hara-Nishimura I (2003b) Vacuolar sorting receptor for seed storage proteins in Arabidopsis thaliana. Proceedings of the National Academy of Sciences of the United States of America **100:** 16095-16100

Shorter J, Beard MB, Seemann J, Dirac-Svejstrup AB, Warren G (2002) Sequential tethering of Golgins and catalysis of SNAREpin assembly by the vesicle-tethering protein p115. Journal of Cell Biology **157:** 45-62

Shorter J, Warren G (1999) A role for the vesicle tethering protein, p115, in the post-mitotic stacking of reassembling Golgi cisternae in a cell-free system. Journal of Cell Biology **146:** 57-70

Simonsen A, Stenmark H (2001) PX domains: attracted by phosphoinositides. Nat Cell Biol **3:** E179-182

Slusarewicz P, Nilsson T, Hui N, Watson R, Warren G (1994) Isolation of a Matrix That Binds Medial Golgi Enzymes. Journal of Cell Biology **124:** 405-413

Sokolovski S, Hills A, Gay RA, Blatt MR (2008) Functional interaction of the SNARE protein NtSyp121 in Ca2+ channel gating, Ca2+ transients and ABA signalling of stomatal guard cells. Molecular Plant **1:** 347-358

Sollner T, Whitehart SW, Brunner M, Erdjumentbromage H, Geromanos S, Tempst P, Rothman JE (1993) Snap Receptors Implicated in Vesicle Targeting and Fusion. Nature **362:** 318-324

Sonnichsen B, Lowe M, Levine T, Jamsa E, Dirac-Svejstrup B, Warren G (1998) Role for giantin in docking COPI vesicles to Golgi membranes. Journal of Cell Biology **140:** 1013-1021

Staswick PE (1990) Novel Regulation of Vegetative Storage Protein Genes. Plant Cell **2:** 1-6

Stefano G, Renna L, Hanton SL, Chatre L, Haas TA, Brandizzi F (2006) ARL1 plays a role in the binding of the GRIP domain of a peripheral matrix protein to the Golgi apparatus in plant cells. Plant Molecular Biology **61:** 431-449

Steinmann T, Geldner N, Grebe M, Mangold S, Jackson CL, Paris S, Galweiler L, Palme K, Jurgens G (1999) Coordinated polar localization of auxin efflux carrier PIN1 by GNOM ARF GEF. Science **286:** 316-318

Stroupe C, Collins KM, Fratti RA, Wickner W (2006) Purification of active HOPS complex reveals its affinities for phosphoinositides and the SNARE Vam7p. Embo Journal **25:** 1579-1589

Surpin M, Zheng HJ, Morita MT, Saito C, Avila E, Blakeslee JJ, Bandyopadhyay A, Kovaleva V, Carter D, Murphy A, Tasaka M, Raikhel N (2003) The VTI family of SNARE proteins is necessary for plant viability and mediates different protein transport pathways. Plant Cell **15:** 2885-2899

Sutter JU, Campanoni P, Blatt MR, Paneque M (2006a) Setting SNAREs in a different wood. Traffic **7:** 627-638

Sutter JU, Campanoni P, Tyrrell M, Blatt MR (2006) Selective mobility and sensitivity to SNAREs is exhibited by the Arabidopsis KAT1 K+ channel at the plasma membrane. Plant Cell **18:** 935-954

Takano J, Miwa K, Yuan LX, von Wiren N, Fujiwara T (2005) Endocytosis and degradation of BOR1, a boron transporter of Arabidopsis thaliana, regulated by boron availability. Proceedings of the National Academy of Sciences of the United States of America **102:** 12276-12281

Teh OK, Moore I (2007) An ARF-GEF acting at the Golgi and in selective endocytosis in polarized plant cells. Nature **448:** 493-496

Thurmond DC, Kanzaki M, Khan AH, Pessin JE (2000) Munc18e function is required for insulin-stimulated plasma membrane fusion of GLUT4 and insulin-responsive amino peptidase storage vesicles. Molecular and Cellular Biology **20:** 379-388

Togneri J, Cheng YS, Munson M, Hughson FM, Carr CM (2006) Specific SNARE complex binding mode of the Sec1/Munc-18 protein, Sec1p. Proc Natl Acad Sci U S A **103:** 17730-17735

Tormakangas K, Hadlington JL, Pimpl P, Hillmer S, Brandizzi F, Teeri TH, Denecke J (2001) A vacuolar sorting domain may also influence the way in which proteins leave the endoplasmic reticulum. Plant Cell **13:** 2021-2032

Toyooka K, Okamoto T, Minamikawa T (2001) Cotyledon cells of Vigna mungo seedlings use at least two distinct autophagic machineries for degradation of starch granules and cellular components. J Cell Biol **154:** 973-982

Tse YC, Lo SW, Hillmer S, Dupree P, Jiang LW (2006) Dynamic response of prevacuolar compartments to brefeldin A in plant cells. Plant Physiology **142:** 1442-1459

Tse YC, Mo BX, Hillmer S, Zhao M, Lo SW, Robinson DG, Jiang LW (2004) Identification of multivesicular bodies as prevacuolar compartments in Nicotiana tabacum BY-2 cells. Plant Cell **16:** 672-693

Viotti C, Bubeck J, Stierhof YD, Krebs M, Langhans M, van den Berg W, van Dongen W, Richter S, Geldner N, Takano J, Jurgens G, de Vries SC, Robinson DG, Schumacher K (2010) Endocytic and Secretory Traffic in Arabidopsis Merge in the Trans-Golgi Network/Early Endosome, an Independent and Highly Dynamic Organelle. Plant Cell

Vitale A, Pedrazzini E (2005) Recombinant pharmaceuticals from plants: The plant endomembrane system as bioreactor. Molecular Interventions **5:** 216-225

Wang JQ, Cai Y, Miao YS, Lam SK, Jiang LW (2009) Wortmannin induces homotypic fusion of plant prevacuolar compartments*. Journal of Experimental Botany **60:** 3075-3083

Weber T, Zemelman BV, McNew JA, Westermann B, Gmachl M, Parlati F, Sollner TH, Rothman JE (1998) SNAREpins: Minimal machinery for membrane fusion. Cell **92:** 759-772

Williams PEV (2003) Engineering plants for animal feed for improved nutritional value. Proceedings of the Nutrition Society **62:** 301-309

Wink M (1993) The Plant Vacuole - a Multifunctional Compartment. Journal of Experimental Botany **44:** 231-246

Woodman PG (1997) The roles of NSF, SNAPs and SNAREs during membrane fusion. Biochimica Et Biophysica Acta-Molecular Cell Research **1357:** 155-172

Xiong Y, Contento AL, Nguyen PQ, Bassham DC (2007) Degradation of oxidized proteins by autophagy during oxidative stress in Arabidopsis. Plant Physiology **143:** 291-299

Yamada K, Nagano AJ, Nishina M, Hara-Nishimura I, Nishimura M (2008) NAI2 is an endoplasmic reticulum body component that enables ER body formation in Arabidopsis thaliana. Plant Cell **20:** 2529-2540

Yamazaki M, Shimada T, Takahashi H, Tamura K, Kondo M, Nishimura M, Hara-Nishimura I (2008) Arabidopsis VPS35, a retromer component, is required for vacuolar protein sorting and involved in plant growth and leaf senescence. Plant Cell Physiol **49:** 142-156

Yang B, Steegmaier M, Gonzalez LC, Jr., Scheller RH (2000) nSec1 binds a closed conformation of syntaxin1A. J Cell Biol **148:** 247-252

Yano D, Sato M, Saito C, Sato MH, Morita MT, Tasaka M (2003) A SNARE complex containing SGR3/AtVAM3 and ZIG/VTI11 in gravity-sensing cells is important for Arabidopsis shoot gravitropism. Proceedings of the National Academy of Sciences of the United States of America **100:** 8589-8594

Zhang Z, Feechan A, Pedersen C, Newman MA, Qiu JL, Olesen KL, Thordal-Christensen H (2007) A SNARE-protein has opposing functions in penetration resistance and defence signalling pathways. Plant J **49:** 302-312

Zheng HY, von Mollard GF, Kovaleva V, Stevens TH, Raikhel NV (1999) The plant vesicle-associated SNARE AtVTI1a likely mediates vesicle transport from the trans-Golgi network to the prevacuolar compartment. Molecular Biology of the Cell **10:** 2251-2264

Zhu JH, Gong ZZ, Zhang CQ, Song CP, Damsz B, Inan G, Koiwa H, Zhu JK, Hasegawa PM, Bressan RA (2002) OSM1/SYP61: A syntaxin protein in Arabidopsis controls abscisic acid-mediated and non-abscisic acid-mediated responses to abiotic stress. Plant Cell **14:** 3009-3028

Zouhar J, Rojo E, Bassham DC (2009) AtVPS45 Is a Positive Regulator of the SYP41/SYP61/VTI12 SNARE Complex Involved in Trafficking of Vacuolar Cargo. Plant Physiology **149:** 1668-1678

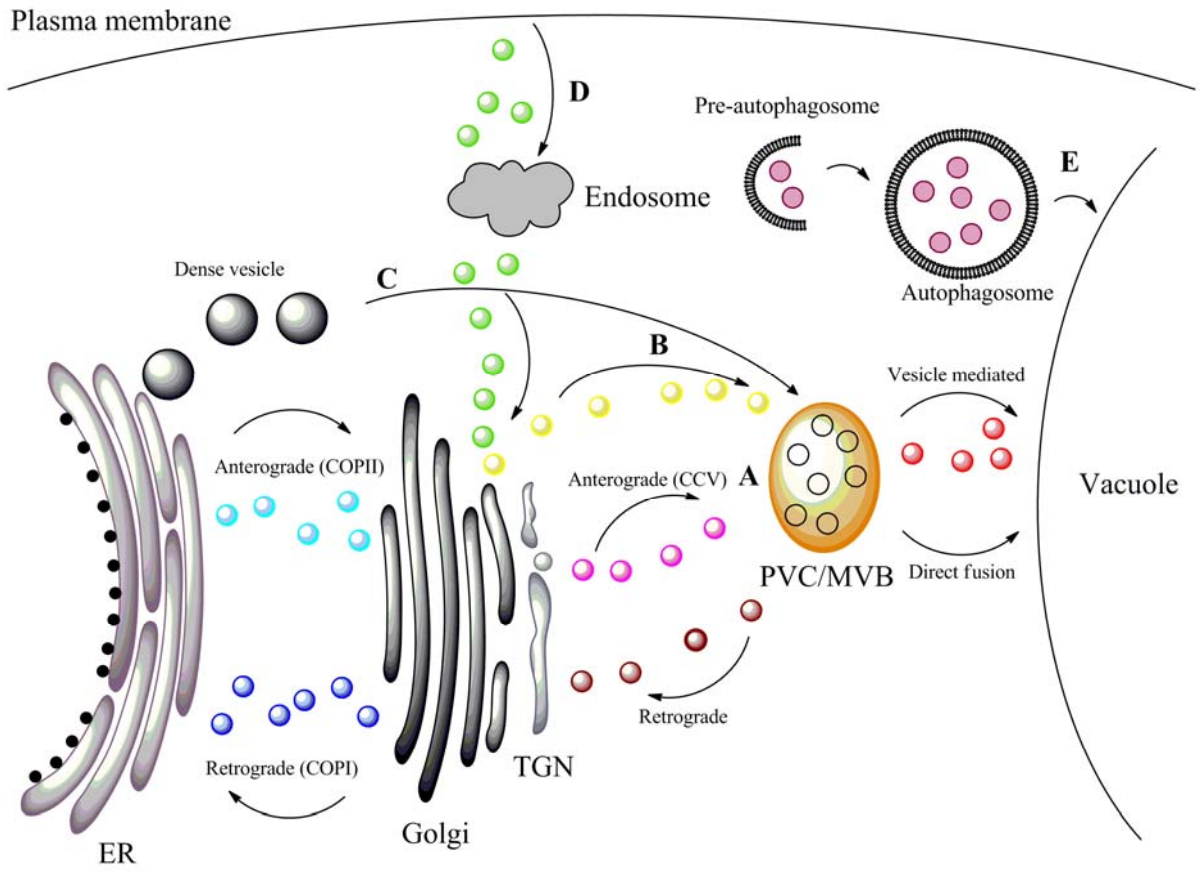

Figure 1. Overview of vacuolar trafficking pathways in plants.

A-C. Biosynthetic vacuolar trafficking pathway; Lytic cargo (A), storage proteins (B and C). D. Endocytic pathway E. Autophagy pathway. Abbreviations: ER – endoplasmic reticulum; TGN – *trans*-Golgi network; PVC - prevacuolar compartment; MVB - multivesicular bodies.

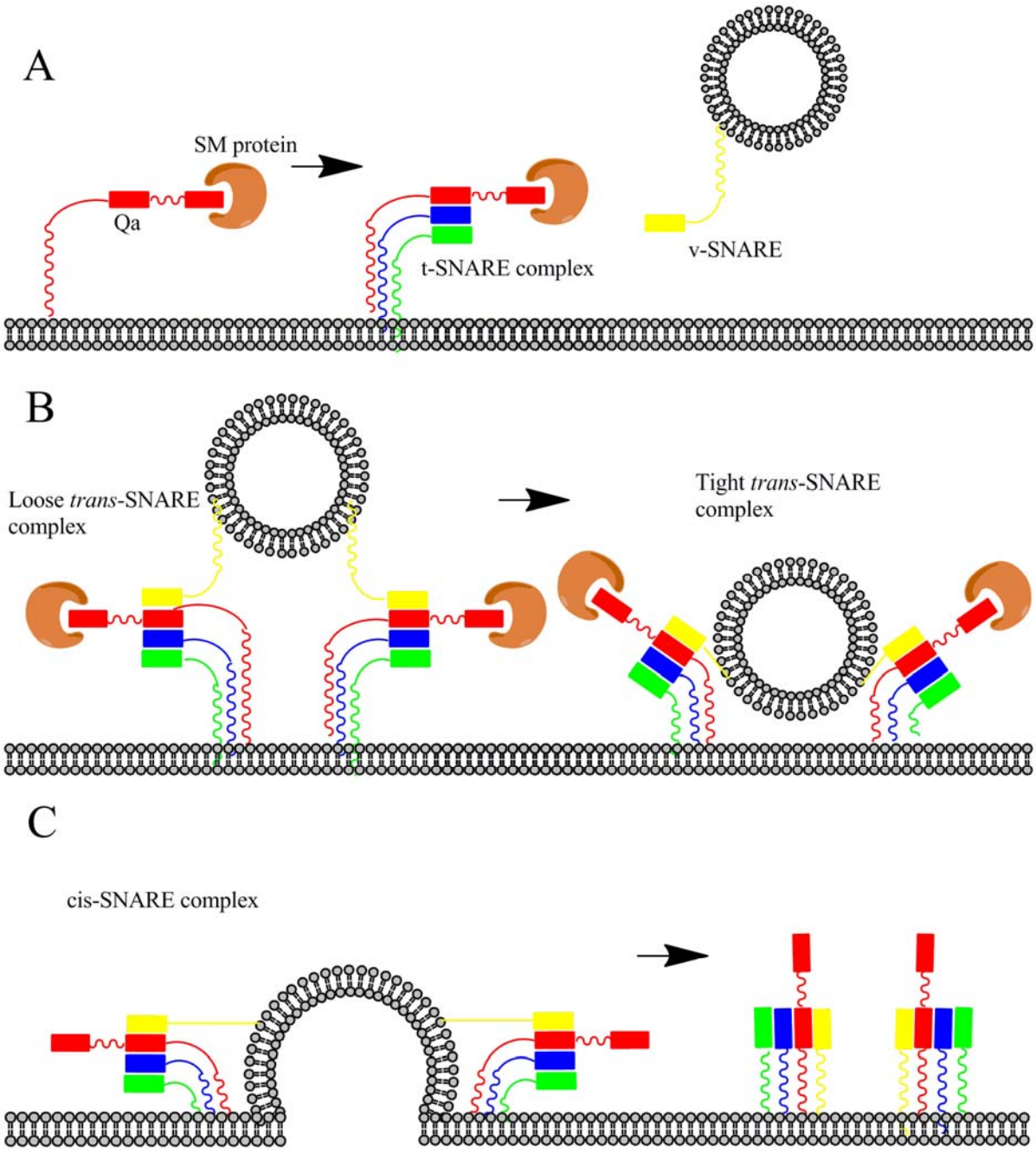

Figure 2. Mechanism of vesicle fusion.

An SM protein binds to a Qa SNARE to expose the SNARE motif, and a t-SNARE complex forms on the target membrane (A). A three helix SNARE bundle interacts with a v-SNARE on the vesicle membrane and forms a *trans*-SNARE complex, driving membrane fusion (B

and C). After completion of vesicle fusion, a cis-SNARE complex is formed on the target membrane (C). SNARE components are indicated: Red – Qa SNARE; yellow – R SNARE; blue and green – Qb and Qc SNARE.

CHAPTER 2. TNO1 IS INVOLVED IN SALT TOLERANCE AND VACUOLAR TRAFFICKING IN *ARABIDOPSIS*

A paper to be submitted to Journal of Cell Science

Sang-Jin Kim[1,2] and Diane C Bassham[1,2,3]

[1]Department of Genetics, Development and Cell Biology, [2]Interdepartmental Genetics Program and [3]Plant Sciences Institute, Iowa State University, Ames, IA 50011, USA

Abstract

The *Arabidopsis* t-SNARE SYP41 is involved in vesicle fusion at the *trans*-Golgi network. SYP41 interacts with AtVPS45, SYP61 and VTI12, which are proteins involved in protein transport to the vacuole. Mutant analysis of each protein in the SYP41 complex showed these proteins are also involved in diverse cellular processes. A previously uncharacterized protein was identified as a SYP41-interacting protein by co-immunoprecipitation, and was named TNO1 (TGN-localized SYP41 Interacting protein). TNO1 has a predicted C-terminal transmembrane domain and was found to localize to the TGN by immunofluorescence microscopy. A *tno1* knockout (KO) mutant showed increased sensitivity to high concentrations of NaCl, KCl and LiCl, and also to mannitol-induced osmotic stress. Localization of SYP61, which is involved in the salt stress response, was disrupted in the *tno1* mutant. Secretion of vacuolar proteins to the apoplast in the *tno1* mutant suggests that TNO1 is required for efficient vesicle trafficking to the vacuole. The *tno1* mutant had a delayed formation of the Brefeldin A (BFA) compartment in the peripheral region of cotyledons upon application of BFA, suggesting less efficient membrane

fusion processes in the mutant. Unlike most TGN proteins, TNO1 does not relocate to the BFA compartment upon BFA treatment, suggesting a possible role for TNO1 in maintaining TGN structure. These data demonstrate that TNO1 is involved in vacuolar trafficking and salt tolerance, presumably via a role in vesicle fusion and maintaining TGN structure.

Introduction

The vacuole is a versatile organelle in plants that has important functions including maintaining turgor, ion homeostasis, compartmentalizing toxic material, accumulating defense compounds and storing and degrading proteins. There are two major types of vacuoles which are specialized for either lytic or storage functions and sometimes these two types can co-exist within a single cell (Wink, 1993; Paris et al., 1996). To maintain these functions, correct transport of proteins to the vacuole is required. Vacuolar proteins are synthesized at the surface of the ER, and are transported co-translationally into the ER lumen. From the ER, they are transported to the *cis*-Golgi via COPII vesicles (Tormakangas et al., 2001), and then transported through the Golgi to the *trans*-Golgi Network (TGN). In the TGN, vacuolar proteins with sequence specific vacuolar sorting determinants (ssVSDs) are recognized by vacuolar sorting receptors (VSRs; Ahmed et al., 2000; daSilva et al., 2005). Storage proteins with C-terminal sorting sequences (ctVSDs) are also bound by VSRs or by a second putative sorting receptor, receptor homology region transmembrane domain ring H2 motif protein (RMR; Jiang et al., 2000; Shimada et al., 2003a; Park et al., 2005; RMR; Park et al., 2007). After the receptors recognize their cargo, vacuolar proteins are transported to the vacuole via the pre-vacuolar compartment (PVC). In an alternative pathway, storage proteins in pumpkin seed and castor bean are aggregated in the ER and transported to the

storage vacuole via precursor accumulating vesicles (Fukasawa et al., 1988; Hara-Nishimura et al., 1998). In pea cotyledons, the storage protein legumin was found in dense vesicles which lack the vacuolar sorting receptor BP-80 and clathrin coats, suggesting the existence of an alternative vacuolar trafficking pathway (Hinz et al., 1999).

The cargo receptor VSR1 has been suggested to be involved in transport of vacuolar proteins with ssVSDs or ctVSDs to the vacuole. In the TGN, VSR1 interacts with clathrin, clathrin adapter-1, EPSIN1 and VTI11, which suggests that vacuolar cargo bound to VSR1 is transported in clathrin-coated vesicles (Sanderfoot et al., 1998; Song et al., 2006). In mammalian cells, cargo receptors are recycled from their destination to the site of cargo binding (Seaman, 2005). VSR1 was found to localize to the TGN and the PVC (Paris et al., 1997; Sanderfoot et al., 1998); thus, VSR1 was also suggested to cycle between these organelles.

SNAREs are integral membrane proteins required for the fusion of vesicles with their target membrane. There are two types of SNAREs: v (vesicle) -SNAREs are localized to the vesicle membrane and t (target) -SNAREs are localized to the target membrane (Rothman, 1994; Sogaard et al., 1994). Generally, one v-SNARE on the vesicle and three t-SNAREs on the target membrane form a *trans*-SNARE complex, bringing the two membranes closer to each other and driving membrane fusion (McNew et al., 2000). Clathrin-coated vesicles containing VSR1 contain the v-SNARE VTI11, which makes a SNARE complex with SYP5, SYP2 and VAMP727 in the PVC, indicating anterograde trafficking from the TGN to the PVC (Kirsch et al., 1994; Sanderfoot et al., 2001a; Ebine et al., 2008). However, the mechanism of recycling of VSR1 from the PVC to the TGN is not yet fully understood. A complex containing the SNAREs SYP41, SYP61 and VTI12 and the SM (Sec1/ Munc18-

like) protein AtVPS45 is found at the TGN in *Arabidopsis* (Bassham et al., 2000). SNAREs in the SYP41 complex along with another SNARE YKT61/62 were found to be sufficient for vesicle fusion *in vitro* (Chen et al., 2005). AtVPS45 belongs to the SM protein family which is thought to regulate vesicle fusion (Dulubova et al., 2002; Bryant and James, 2003). Thus, AtVPS45 is hypothesized to regulate the SYP41 complex. Recently, AtVPS45 was suggested to be involved in recycling VSR1, as RNAi knockdown of AtVPS45 expression causes mis-localization of VSR1 (Zouhar et al., 2009).

SYP41 and SYP42 are highly homologous t-SNAREs with 62% amino acid sequence similarity. However, they are not functionally redundant, and they form separate complexes with AtVPS45 in different subdomains of the TGN (Bassham et al., 2000). Individual *syp41* and *syp42* knockout mutants are gametophytic lethal (Sanderfoot et al., 2001b). Therefore, they are essential genes and have specific functions in the different AtVPS45 complexes. A mutation in SYP61, another t-SNARE in the SYP41 complex, was generated by T-DNA insertion (Zhu et al., 2002). From characterization of the *osm1/syp61* mutant phenotype, SYP61 is thought to have important roles in osmotic stress tolerance and ABA regulation of stomatal responses. VTI12, a v-SNARE that interacts with SYP41, is involved in trafficking of storage proteins (Sanmartin et al., 2007), and a *vti12* T-DNA insertion mutant showed an early senescence phenotype under starvation conditions, suggesting VTI12 is also involved in the autophagy pathway for the degradation of cellular contents (Surpin et al., 2003). Components of the AtVPS45 complex function together in vesicle fusion, but each protein appears to be also involved in other specific processes, suggesting they may also function in additional SNARE complexes.

The fungal toxin brefeldin A (BFA) has been widely used to study protein trafficking and for organelle identification. BFA has been well-studied in mammalian cells where it inhibits a Sec7-type GTP exchange factor (GEF), which is required to activate Arf1-GTPase, leading to the formation of an ER-Golgi hybrid structure (Jackson and Casanova, 2000). In *Arabidopsis*, BFA targets the Arf-GEF GNOM, which is involved in recycling of the auxin efflux transporter PIN1, and induces the formation of BFA compartments which are regarded as early endosomal aggregates (Geldner et al., 2001). Interestingly, these BFA compartments also contains TGN markers, suggesting that they may be formed by fusion between early endosomes and the TGN, presumably mediated by SNAREs (Lam et al., 2009).

In this study, we identified an additional novel SYP41-interacting protein we named TNO1 (TGN-localized SYP41 interacting protein). TNO1 was found to be a membrane protein at the TGN and involved in vacuolar trafficking, consistent with the hypothesis that it functions together with the SYP41 SNARE complex. A *tno1* knockout mutant has a salt and osmotic stress-sensitive phenotype, and the vacuolar proteins aleurain and RD21 were partially secreted in the *tno1* knockout mutant. A BFA-treated *tno1* knockout mutant showed a delayed formation of the BFA compartment in cotyledons and shorter root growth on MS plates containing BFA, indicating that TNO1 could be important in fusion events during BFA treatment. We propose that TNO1 is involved in vacuolar trafficking and salt stress resistance by facilitating the vesicle fusion process.

Materials and Methods

cDNA cloning and sequencing

RNA was extracted from *Arabidopsis* siliques and treated with DNase I, followed by reverse transcription using an oligo dT primer. cDNAs were amplified using Herculase long and accurate polymerase mix (Agilent Technologies, Wilmington, DE) and *TNO1* cDNA forward (FP) and reverse (RP) primers (Table 1) according to the manufacturer's protocol. The amplification product was inserted into pGEM T-easy vector (Invitrogen, Carlsbad, CA), and DNA sequencing was performed at the W.M. Keck Foundation (Yale University, New Haven, CT).

Plant materials and growth conditions

Arabidopsis thaliana (ecotype Col-0) seeds were surface sterilized and grown on soil or MS (Murashige–Skoog Vitamin and Salt Mixture (Caisson Lab, Inc., North Logan, UT)) solid medium containing 1% (w/v) sucrose. A *tno1* knockout (KO) mutant line (Salk_112503) which has a T-DNA insertion in the third exon was obtained from the *Arabidopsis* Biological Resource Center (ABRC). A homozygous *tno1* KO mutant was identified by PCR using primers *TNO1* internal FP/ RP primers and T-DNA left border-a1 (Table 1), and immunoblot using affinity-purified TNO1 antibody.

Generation of transgenic plants

GFP-fused vacuolar H^+ATPase (GFP-VHAa1) plasmid (Dettmer et al., 2006) was introduced into *Agrobacterium tumefaciens* strain GV2260, which was used to transform *tno1* KO mutant plants by the floral dipping method (Clough and Bent, 1998). The resulting VHAa1-GFP transformed *tno1* plants were selected on MS solid medium containing 50 μg/ml kanamycin.

For *tno1* KO mutant complementation, the full length *TNO1* gene and its promoter were amplified by PCR separately with *TNO1* promoter primers and genomic *TNO1* primers with corresponding restriction sites (Table 1). The *TNO1* promoter fragment was digested using *Sal*I and *Not*I, and the *TNO1* genomic fragment was digested using *Not*I and *Kpn*I. The digested *TNO1* promoter and genomic DNA were ligated into the binary vector pCAMBIA1300MCS1 digested using *Sal*I and *Kpn*I (Sanderfoot et al., 2001a). The resulting plasmid was introduced into *Agrobacterium tumefaciens* strain GV2260, which was used to transform *tno1* KO mutant plants. The transgenic *tno1* KO mutant plants were identified by resistance to 50 μg/ml hygromycin, and expression of *TNO1* was confirmed by immunoblotting with affinity purified TNO1 antibody.

Identification of TNO1

Protein extracts were made essentially as in Bassham et al. (2000) and Sanderfoot et al. (2001). *Arabidopsis* suspension cells were ground in extraction buffer (phosphate buffered saline (PBS), 1 mM EDTA, 0.1 mM phenylmethylsulfonyl fluoride (PMSF) and 1% (v/v) Triton X-100), and solubilized for 2 h at 4^{o}C. Solubilized total proteins were added to a column containing immobilized SYP41 antibodies or SYP41 pre-immune serum, and incubated for 2 h at 4^{o}C. The columns were washed 5 times with extraction buffer, and the bound proteins were eluted using 0.2 M glycine pH 2.5. Immunoprecipitates from SYP41 and pre-immune antibody were separated by SDS-PAGE, and proteins were visualized using silver staining.

Protein bands migrating at MW of a 200, 67, 35 and 15 kDa were excised and analyzed at the Protein Microsequencing and Proteomic Mass Spectroscopy Lab at the

University of Massachusetts Medical School (Worchester, MA). Proteins were digested in the gel using trypsin, and the peptides after digestion were applied to a Finnigan Electrospray LCQ Deca ion trap mass spectrometer, and the resulting peptide masses were used to identify potential matches within the *Arabidopsis* proteome. Identities of immunoprecipitated proteins were further confirmed by immunoblotting using SYP41 and TNO1 antibodies.

RT-PCR analysis of *TNO1, SYP41* and salt/ osmotic stress responsive genes

Total RNA was extracted from *Arabidopsis* organs using the TRIzol RNA isolation method (http://www.*Arabidopsis*.org/portals/masc/AFGC/RevisedAFGC/site2RnaL.htm#isolation). Roots were harvested from 4-week old *Arabidopsis* plants grown in liquid culture (MS plus 1% (w/v) sucrose), and stem, rosette leaves, cauline leaves, flower and siliques were harvested from 7-week old *Arabidopsis* plants grown in soil. Extracted RNA was treated with DNase I, followed by reverse transcription using an oligo dT primer. cDNAs were amplified for 25 cycles using *TNO1* internal FP and RP primers or *SYP41* FP and RP primers (Table 1).

One week old wild-type and *tno1* KO mutant seedlings were treated with 300 mM NaCl, 40 mM LiCl, 300 mM KCl or 600 mM mannitol for 5 h. Total RNA was extracted from the seedlings as described above. Expression of salt-overly sensitive 1 (*SOS1),* DRE binding protein (*DREB2A*)*, RD29, TNO1* and *SYP61* was analyzed by RT-PCR using gene specific primers (Table1; Yamaguchi-Shinozaki and Shinozaki, 1993; Liu et al., 1998; Shi et al., 2000; Zhu et al., 2002).

Antibody Production and Purification

A 1.7kb C-terminal fragment of the *TNO1* cDNA was cloned into pET28b(+) expression vector (Novagen, Madison, WI) to produce a 6x His-partial TNO1 fusion construct. The fusion protein construct was introduced into *Escherichia coli* BL21 (DE3) and selected on LB plates containing 50 μg/ml kanamycin. Expression and purification of partial TNO1 was as described in Bassham et al. (2000). The partial TNO1 was purified using Ni-NTA agarose and used to immunize rabbits at Cocalico Biologicals (Reamstown, PA) after gel purification.

For purification of TNO1-specific antibodies, purified His-tagged TNO1 protein was separated by SDS-PAGE, transferred to nitrocellulose membrane followed by staining with Ponceau S, and the strip containing the fusion protein was cut out. The strip was blocked in 3% (w/v) dried nonfat milk in PBS, and crude rabbit serum was incubated with the strip for 2 hrs at 4°C. The strip was washed 5 times with PBS, antibodies were eluted using 0.1 M glycine pH 2.2 and neutralized with 2 M Tris-HCl pH 8.0.

Intercellular fluid (ICF) extraction

ICF was extracted as described (Neuhaus et al., 1991). One gram of *Arabidopsis* leaves were infiltrated under vacuum in 50 mM sodium citrate pH 5.5. After infiltration, buffer on the leaves was removed by blotting with filter paper. Surface dried leaves were rolled with filter paper and inserted into a 10 ml syringe. The syringe was inserted into a 50 ml conical tube, which was centrifuged at 1000 x g for 10 min at 10°C. ICF was collected in the bottom of the tube, and ICF depleted leaves after centrifugation were ground in 50 mM sodium citrate for the control. ICF and ICF-depleted leaf extracts were analyzed by

immunoblotting with aleurain (AALP; Ahmed et al., 2000)), RD21 (Hayashi et al., 2001) and invertase (Rojo et al., 2003) antibodies.

Preparation of vacuoles

Leaf protoplasts were generated as described (Sheen, 2002). Two grams of leaves were digested for 2 h in enzyme solution (1% (w/v) cellulose, 0.4% (w/v) macerozyme; (Yakult Pharmaceutical, Osaka, Japan), 0.4 M mannitol, 0.2 M KCl, 0.2 M MES pH 5.7 and 10 mM $CaCl_2$). Digested protoplasts were passed through 70 ηm nylon mesh and washed twice with washing solution (0.4 M mannitol and 10 mM MES pH 5.6). Vacuole isolation was performed as described (Sanmartin et al., 2007). After adding 6 ml of pre-warmed lysis buffer (0.2 M mannitol, 10% (w/v) ficoll, 1 mM EDTA and 5 mM Na phosphate pH 8.0) at 42°C, lysed protoplasts were transferred to clear tubes for a SW41 swinging bucket rotor and overlayed with 3 ml of 4% (w/v) ficoll (by mixing lysis and vacuole buffer) and 1 ml of vacuole buffer (0.45 M mannitol, 2 mM EDTA and 5 mM Na phosphate pH 7.5) followed by centrifugation at 20,000 rpm for 50 min at 10°C. Vacuoles were recovered from the interface between 4% (w/v) ficoll and vacuole buffer.

Differential centrifugation

Arabidopsis plants were homogenized in 0.3 M sucrose, 100 mM Tris-HCl pH 7.5, 1 mM EDTA, 0.1 mM PMSF. The homogenate was centrifuged at 1,000 x *g* for 10 min at 4°C to remove cell debris. The supernatant was centrifuged at 20,000 x g, the supernatant removed and further centrifuged at 100,000 x g. The TCA-precipitated supernatant after

centrifugation at 100,000 x g and pellets after centrifugation at 20,000 x g and 100,000 x g were analyzed by immunoblot with TNO1 and SYP41 antibodies.

Extraction of TNO1 from membranes

Total membrane fractions were isolated from 2 week old seedlings by centrifugation at 125,000 x g and treated with 1% (v/v) Triton X-100, 2 M urea, 1 M NaCl or 0.1 M Na_2CO_3, followed by pelleting of non-solubilized proteins at 125,000 x g (Phan et al., 2008). Supernatants were precipitated using TCA followed by washing twice with 100% acetone. Pellets and the TCA-precipitated supernatants were analyzed by immunoblotting with TNO1 and SYP41 antibodies (Bassham et al., 2000).

Sucrose Gradients

Four week old wild-type and *tno1* mutant plants were ground in HKE buffer (50 mM Hepes-KOH, pH 7.5, 10 mM potassium acetate, 1 mM EDTA) containing 0.4 M sucrose, 1 mM dithiothreitol and 0.1 mM PMSF and centrifuged at 1,000 x *g* for 10 min at 4°C. The supernatant was passed through 2 layers of cheesecloth and loaded onto the top of a sucrose step gradient (54%, 40%, 33%, 24% and 15%). After centrifuging at 150,000 x *g* in a swinging-bucket rotor at 4°C for 18 h, the gradients were fractionated from the top into 12 x 1 ml fractions. 20 µl of each fraction was analyzed by immunoblotting. Antibodies used were anti-γTIP (1:2000; Hofte et al., 1992), anti-FUM1 (fumarase; 1:500; Behal and Oliver, 1997), anti-SYP61 (1:1000; Sanderfoot et al., 2001a), anti-TNO1 (1:200), anti-VSR1 (1:1000; Ahmed et al., 2000), anti-carboxypeptidase Y (CPY; 1:1000; Rojo et al., 2003) and anti-VPS45 (1:500; Bassham and Raikhel, 1998)

Immunofluorescence

Three or four day old *Arabidopsis* seedlings grown on MS solid medium were immunolabeled with a protocol slightly modified from Phan et al., (2008). Seedlings were transferred to MTSB buffer (50 mM PIPES-KOH pH 6.9, 5 mM EGTA and 5 mM $MgSO_4$) with 5% (v/v) dimethyl sulfoxide (DMSO) for 15 min at room temperature and fixed in 4% (w/v) paraformaldehyde in MTSB with 10% (v/v) DMSO for 1 h after 10 min under vacuum. Seedlings were washed twice with MTSB and mounted onto slides. Seedlings were treated with 2% drieselase in MTSB for 30 min to digest cell walls and permeabilized in 0.5% (v/v) NP40, 10% (v/v) DMSO in MTSB for 1 h. After washing seedlings with MTSB 3 times, seedlings were blocked in 3% (w/v) bovine serum albumin (BSA) in MTSB for 2 h. Slides were treated with the primary antibody in 3% (w/v) BSA in MTSB in a moist chamber overnight at 4°C, washed 3 times with MTSB and treated with Alexa Fluor® 594-conjugated secondary anti-rabbit IgG antibody (1:250; Molecular Probes, Eugene, OR) in 3% (w/v) BSA in MTSB for 45 min. Slides were washed 5 times with MTSB, mounted with a coverslip in 50% (v/v) glycerol in PBS and sealed using nail polish. Seedlings used for immunofluorescence were ST-GFP transgenic plants (Wee et al., 1998), VHAa1-GFP transgenic plants (Dettmer et al., 2006) and YFP-RHA1 transgenic plants (Preuss et al., 2004) to label Golgi, TGN and PVC, respectively.

For protoplast immunofluorescence, protoplasts were fixed in 3% (w/v) paraformaldehyde in MTSB with 0.4 M sorbitol for 30 min and washed twice with MTSB with 0.4 M sorbitol. Fixed protoplasts were mounted onto slides and dried for 1 h. Protoplasts were permeabilized using permeabilization buffer (0.5% (v/v) NP40, 10% (v/v)

DMSO in MTSB) for 30 min in a moist chamber followed by washing 3 times using MTSB. Protoplasts were blocked in 3% BSA in MTSB for 2 h, and primary antibodies in 3% (w/v) BSA in MTSB were added. After 3 h incubation, protoplasts were washed 3 times using MTSB and treated with conjugated secondary antibody in 3% (w/v) BSA in MTSB for 50 min followed by washing 5 times with MTSB. Anti-TNO1 (1:25), anti-SYP41 (1:50) and anti-SYP61 (1:50) were used as primary antibodies. Alexa Fluor® 594-conjugated goat anti-rabbit IgG (1:250) was used as secondary antibody.

Fluorescent signals were viewed with a confocal laser scanning microscope (Leica SP5, Leica Microsystems, Exton, PA, USA). Excitation and emission wavelengths of GFP were 488/500 ηm and those of Alexa Fluor® 594 were 590/600 ηm.

Salt, ionic and osmotic stress, and drug treatment

For salt, ionic and osmotic stress response analysis, seedlings were grown on MS solid medium for 5 days and transferred to MS solid medium containing 130 mM NaCl, 17 mM LiCl, 140 mM KCl or 300 mM mannitol, followed by growth for an additional 10 days (Zhu et al., 2002).

For BFA treatment, seedlings were grown on MS solid medium for 4 day and transferred to MS liquid medium containing 50 μM BFA or DMSO as the carrier control for 5 h. BFA-treated seedlings were washed twice with MS liquid medium and incubated in MS liquid medium for recovery. BFA treatment of protoplasts was performed as described above for 2 h with the same concentration of BFA. 2.5 μM BFA in solid MS medium was used to observe the effect of BFA on root growth from germination as described (Teh and Moore, 2007).

Results

Identification of TNO1

SYP41 is a t-SNARE at the TGN that is required for vesicle fusion (Bassham and Raikhel, 2000; Chen et al., 2005). SYP41 was shown to form a complex with VTI12, SYP61 and AtVPS45. To identify additional SYP41-interacting proteins, SYP41 antibody was used for immunoprecipitation with detergent-solubilized membrane extracts of *Arabidopsis* suspension cells. Proteins that co-immunoprecipitated with SYP41, or with pre-immune antibody as a control, were separated by SDS-PAGE and visualized by silver staining. Four bands corresponding to proteins migrating at approximately 200, 67, 35 and 15 kDa were found only in the SYP41 precipitate and were not present in the SYP41 pre-immune precipitate, suggesting that they specifically interacted with SYP41 (Fig 1A).

The 200, 67, 35 and 15 kDa bands were cut out of the gel, subjected to in-gel digestion with trypsin and the proteins were analyzed by tandom mass spectrometry, comparing the fragmentation patterns with the National Center for Biotechnology Information (NCBI) *Arabidopsis* database. The 67 and 15 kDa bands were identified as AtVPS45 and a degradation product of SYP61, respectively. The 35 kDa band contained SYP41, SYP42 and SYP43, which is an additional protein in the SYP4 family that has not yet been characterized. Nine peptides from the 200 kDa band (Supplementary Fig 1) could be matched to the predicted protein encoded by At1g24460, corresponding to 5.2% amino acid coverage, and the protein was named TNO1 (TGN-localized SYP41 interacting protein). RT-PCR was performed to obtain cDNA from ORF of *TNO1*. When we compared our *TNO1* sequence with the sequence in The *Arabidopsis* Information Resource (TAIR), a deletion of

63 nt from 4190 to 4252 was found in TAIR sequence, suggesting the presence of an extra exon in our *TNO1* sequence and that the predicted sequence in TAIR has incorrectly predicted splice sites (Supplementary Fig 1). TNO1 (At1g24460) is a previously uncharacterized protein of predicted MW 209 kDa, consistent with its migration on SDS-PAGE. It was predicted to have 6 coiled-coil domains in the arabi-coil database (Rose et al., 2004) and one transmembrane domain at the extreme C-terminus by TopPred-transmembrane prediction (Supplementary Fig 2; von Heijne, 1992; Claros and von Heijne, 1994). TNO1 antibodies (see below) were used to probe a SYP41 immunoprecipitate to confirm that the approximately 200 kDa band in the SYP41 precipitate corresponds to TNO1. Immunoprecipitation was performed from detergent-solubilized membrane extracts of *Arabidopsis* suspension cells using antibodies against SYP41 or pre-immune serum. Immunoprecipitates were analyzed by immunoblotting using antibodies against SYP41 or TNO1. TNO1 was detected in the SYP41 precipitate, but not in the pre-immune precipitate, confirming the correct identification of the 200 kDa band co-immunoprecipitated with SYP41 (Fig 1B).

To investigate the expression pattern of *TNO1*, RNA was extracted from different *Arabidopsis* plant organs. The mRNA level of *TNO1* was determined by RT-PCR using *TNO1*-specific primers with *SYP41* and 18S RNA primers used as controls. *TNO1* was ubiquitously expressed in roots, rosette leaves, cauline leaves and flowers, with lower expression in stems. *SYP41* also showed highest expression in flower and lowest expression in stem (Fig 1C). Expression of *TNO1* in *Arabidopsis* plant organs and through developmental process was also analyzed using GENEVESTIGATOR, a database and Web-browser data mining interface for Affymetrix GeneChip data (Hruz et al., 2008) and showed

the similar expression pattern consistent with our RT-PCR result, and *TNO1* is highly expressed during germination, flower development and siliques maturation (Supplementary Fig 3). This expression pattern suggests that *TNO1* may have an important role throughout the plant during reproductive stages.

TNO1 is a TGN-localized membrane protein

To study the function of TNO1, an antibody was raised against a 66 kDa fragment from the C-terminus of TNO1. This partial TNO1 protein was synthesized in *E. coli* with an N-terminal His tag for purification. The recombinant protein was injected into rabbits to produce antiserum, followed by affinity purification against the recombinant protein. The specificity of purified TNO1 antibody was tested by immunoblotting against total *Arabidopsis* cell extract, total *Arabidopsis* membrane and total *Arabidopsis* soluble proteins from 2 week old *Arabidopsis* seedlings. Purified TNO1 antibody specifically recognized a band of approximately 200 kDa in *Arabidopsis* extracts (Fig 2A), which was not detected by the pre-immune serum (Fig 2B).

To investigate the potential membrane association of TNO1, the presence of TNO1 in membrane fractions was analyzed. TNO1 was detected in the pellet fraction from *Arabidopsis* extracts after centrifugation at 100,000 x g, consistent with the prediction of having a transmembrane domain at its C-terminus (Fig 2A), suggesting TNO1 is a membrane-bound protein. Differential centrifugation was performed to determine the fractionation pattern of TNO1. *Arabidopsis* suspension cell extract was centrifuged sequentially at 20,000 x g and 100,000 x g, producing three different fractions, P20 (pellet at 20,000 x g), P100 (pellet at 100,000 x g) and S (supernatant from 100,000 x g). These

fractions and total protein were analyzed by immunoblotting using TNO1 and SYP61 antibodies. The integral membrane protein SYP61 was detected strongly in all membrane fractions and was not present in the soluble fraction. TNO1 was also present in all the membrane fractions, but not in the soluble fraction, suggesting TNO1 is associated with membranes (Fig 2C).

To determine how TNO1 associates with membranes, total membrane fractions were isolated from 2 week old seedlings by centrifugation at 125,000 x g and treated with 1% (v/v) Triton X-100, 2 M urea, 1 M NaCl or 0.1 M Na_2CO_3 to solubilize proteins from the membrane, followed by re-pelleting of non-solubilized proteins. The pellet and soluble fractions after treatment were analyzed by immunoblotting using TNO1 antibody. SYP41, an integral membrane protein control, was solubilized by 1% Triton X-100. TNO1 was solubilized by 1% (v/v) Triton X-100 and partially by 2 M urea (Fig 2D), but not by 1 M NaCl or 0.1 M Na_2CO_3, suggesting that TNO1 is a membrane-integrated protein consistent with the transmembrane domain prediction of a C-terminal membrane anchor.

As an initial approach to determine the subcellular localization of TNO1, a sucrose density gradient was performed to compare the fractionation pattern of TNO1 with that of known organelle markers. Four week old *Arabidopsis* plants grown in MS liquid medium were homogenized, layered on the top of a discontinuous sucrose gradient (13%~55%) and centrifuged at 100,000 x g for 18 h. Twelve fractions were collected and analyzed by immunoblotting using antibodies against TNO1, AtVPS45 to label the TGN, SYP61 for the TGN and PVC, γ-tonoplast intrinsic protein (γTIP) for the vacuolar membrane, carboxypeptidase Y (CPY) for the vacuolar lumen, fumerase (FUM1) for mitochondria, and vacuolar cargo receptor (VSR1) for the PVC. The TNO1 fractionation pattern was identical

to that of AtVPS45 (Fig 2E). Therefore, it is possible that TNO1 localizes to the TGN or to organelles with similar density.

To analyze TNO1 localization more conclusively, immunofluorescence microscopy was performed and TNO1 labeling compared with that of known markers. Cotyledons of WT and *tno1* KO mutant seedlings were immunolabeled using purified TNO1 antibody and Alexa Fluor® 594-conjugated goat anti-rabbit IgG to confirm the specificity of TNO1 labeling. In WT seedlings, TNO1 antibody labeled endogenous TNO1 in punctuate structures, while no specific signal was observed in the cotyledons of *tno1* KO mutant seedlings (Fig 3A). After confirming the specificity of TNO1 antibody, purified TNO1 antibody was used to label endogenous TNO1 in VHAa1-GFP transgenic *Arabidopsis* seedlings (Dettmer et al., 2006), ST-GFP transgenic *Arabidopsis* seedlings (Wee et al., 1998) and RHA1-YFP transgenic *Arabidopsis* seedlings (Preuss et al., 2004), which were used to label TGN, Golgi and PVC, respectively. VHAa1-GFP, RHA1-YFP and ST-GFP exhibited a dot-like pattern in cotyledons and TNO1-labeled structures completely overlapped with VHAa1-labeled structures, but were distinct from those labeled with ST-GFP or RHA1-YFP (Fig 3B-3D). This result suggests that TNO1 localizes to the TGN.

Omission of the first antibody, second antibody and both first and second antibody were tested as controls for non-specific staining or cross-talk between different fluorescence channels. No specific fluorescence was observed in any of the controls (data not shown).

Identification of a *tno1* knockout (KO) mutant

To analyze the function of TNO1, we obtained a knockout (KO) mutant (salk_112503) containing a T-DNA insertion in the *TNO1* gene from the *Arabidopsis*

Biological Resource Center (ABRC). A homozygous *tno1* KO mutant was identified by PCR using *TNO1* specific primers and T-DNA left border primer (LBa1) in three combinations (*TNO1* internal FP (shown LP in Fig 4B) + *TNO1* internal RP (shown RP in Fig 4B), LP + LBa1 and RP + LBa1; Fig 4B). A 900 bp fragment from the genomic DNA could only be amplified from genomic DNA of the wild-type plants using LP and RP primers. The 900 bp band was not seen in the *tno1* KO mutant due to disruption by T-DNA. PCR using LBa1 and LP/RP primers generated 450 bp bands, showing the existence of T-DNA insertion in the *tno1* KO mutant. Thus, PCR indicated that the *tno1* KO mutant has a complex insertion in its third exon (Fig 4A and 4B). Lack of TNO1 protein expression was confirmed by immunoblotting of total *Arabidopsis* protein extracts from WT and *tno1* KO mutant using affinity purified TNO1 antibody (Fig 4C). No difference in overall morphology or development was seen between *tno1* KO mutant and WT plants grown in MS medium or soil.

TNO1 knockout mutant plants are sensitive to salt and osmotic stress

SYP61/ OSM1, a t-SNARE in the SYP41 complex, has been reported to be involved in general salt/ osmotic stress responses (Zhu et al., 2002). Under salt/ osmotic stresses, an *osm1/syp61* mutant had more branched and shorter roots than those of wild type plants. As TNO1 also interacts with SYP41, we hypothesized TNO1 could be involved in the same stress response. Sensitivity of homozygous *tno1* mutant plants to salt, ionic and osmotic stress was tested. WT and *tno1* mutant seedlings were grown on MS solid medium for 1 week and transferred to MS solid medium containing 130 mM NaCl (Fig 5A and 5E), 140 mM KCl (Fig 5B and 5F), 17 mM LiCl (Fig 5C and 5G) or 300 mM Mannitol (Fig 5D and 5H) and root length was measured after 4 and 8 days. *tno1* mutant seedlings exhibited

shorter root and earlier leaf chlorosis than wild-type seedlings under Na^+, K^+, Li^+ and non-ionic osmotic stress. This result shows that lack of TNO1 causes sensitivity to salt and osmotic stresses.

To confirm that the observed phenotype of the *tno1* mutant is due to disruption of *TNO1* gene, a genomic fragment of the *TNO1* including the native promoter was introduced into the *tno1* mutant. TNO1 expression was restored in the complemented lines as determined by immunoblotting using TNO1 antibody. The expression level of TNO1 in the *tno1*/*TNO1* promoter::*TNO1* line is similar to that in WT plants (Fig 4D), and complemented the salt, ionic and osmotic sensitive phenotype of the *tno1* mutant (Fig 5).

To test whether expression of salt or osmotic stress-responsive genes was altered in the *tno1* mutant, expression of *TNO1, SYP61* and salt (*SOS1*) or osmotic (*RD29 and DREB2A*) stress responsive genes were analyzed by RT-PCR using gene specific primers. *TNO1* was expressed at a basal level in the non-treated condition, and its mRNA level increased slightly during NaCl and KCl treatment, while no expression of *TNO1* was detected in *tno1* KO mutant as expected (Fig 6A). Interestingly, an increase in the transcript level of *SYP61* was observed in both WT and *tno1* mutant in all stress conditions, suggesting *SYP61* could be directly involved in response to these stress conditions. The salt/ osmotic stress responsive genes (*SOS1, DREB2A and RD29*) increased as expected (Yamaguchishinozaki and Shinozaki, 1993; Liu et al., 1998; Qiu et al., 2004), and no visible difference between WT and *tno1* mutant was observed (Fig 6). Although overall intensity of *DREB2A* appears different between WT and *tno1* mutant, multiple experiments showed that they were not different significantly. This result suggests that the phenotype of the *tno1*

mutant is not caused by disruption of expression of genes involved in salt or osmotic stress responses.

The increase of *SYP61* transcript during salt and osmotic stress led us to test whether loss of TNO1 affects SYP61. Thus, we investigated localization of SYP61 and SYP41 in WT and *tno1* mutant protoplasts. Previously, SYP61 has been reported to co-localize with VHAa1-GFP (Dettmer et al., 2006). To investigate localization of SYP61 in the *tno1* mutant, VHAa1-GFP transgenic *tno1* mutant was generated using Agrobacterium mediated transformation. We performed immunofluorescence analysis using protoplasts generated from VHAa1-GFP transgenic wild-type and *tno1* KO mutant plants, and percentage of co-localization was calculated (dots SYP61 overlapping with VHAa1/ total SYP61 labeled dots). In wild type protoplast, 70% of SYP61 co-localized with VHAa1-GFP, while 47% of SYP61 was found to co-localize with VHAa1-GFP in the *tno1* KO mutant protoplasts. This difference was significant by statistical analysis (*t*-test, p=0.00038; n=15 repeated 3 times). When co-localization of SYP41 with VHAa1-GFP was compared between WT and *tno1* mutant, no difference was observed (Fig 7A and 7B), suggesting that loss of TNO1 specifically affects localization of SYP61 and not SYP41.

Lack of TNO1 causes secretion of vacuolar proteins

For correct transport of vacuolar proteins, vacuolar sorting receptors that recognize the VSDs are necessary, and without them vacuolar proteins are secreted out of the cell by a default pathway (Shimada et al., 1997; Shimada et al., 2003a). Previously, disruption of AtVPS45 or VTI12 has been shown to cause secretion of aleurain and a marker consisting of CLAVATA 3 (CLV3) fused to the vacuolar sorting signal from the storage protein barley

lectin (Sanmartin et al., 2007; Zouhar et al., 2009). Therefore, we hypothesized that lack of TNO1 may also cause secretion of vacuolar proteins.

To test the potential involvement of TNO1 in vacuolar trafficking, we compared the amount of the vacuolar proteins *Arabidopsis* aleurain-like protein (AALP), RD21 and invertase in vacuoles between WT and *tno1* mutant. Vacuoles were isolated from WT plants and *tno1* mutants and analyzed by immunoblotting using AALP, RD21 and invertase antibodies. No significant differences were seen in the between WT and *tno1* mutant plants, suggesting that overall vacuolar trafficking is not inhibited in the *tno1* mutant (Fig 8A).

Although the *tno1* mutant does not appear to have a general block in vacuolar trafficking, this does not preclude a mild or partial disruption in this pathway as seen in a *vti12* mutant (Sanmartin et al., 2007). Thus, intercellular wash fluid (ICF) was collected from leaves of wild-type and *tno1* mutant plants to determine whether any vacuolar proteins were partially secreted (Neuhaus et al., 1991). Proteins in the ICF were analyzed by immunoblotting using antibodies against the vacuolar proteins AALP, RD21 and invertase. AALP, RD21 and invertase bands in the ICF-depleted leaf extract showed no difference between wild-type and *tno1* mutant. However, the *tno1* mutant had stronger AALP and RD21 bands in the ICF than wild-type plants, suggesting that lack of TNO1 caused some secretion of AALP and RD21 (Fig 8B). However, no secretion of vacuolar invertase was observed, although vacuolar invertase was suggested previously to be transported to the vacuole by a similar pathway to RD21 (Rojo et al., 2003). Secretion of RD21 may suggest that it has an alternative or additional transport pathway to the vacuole. TNO1 is therefore hypothesized to be required for efficient trafficking of vacuolar proteins.

Involvement of TNO1 in vesicle fusion

The fungal toxin brefeldin A (BFA) is a useful tool to investigate protein trafficking. VHAa1-GFP was found to relocate to a BFA induced compartment in *Arabidopsis* (Dettmer et al., 2006) and SYP61 and the endosomal protein secretory carrier membrane protein 1 (SCAMP1) were also found in the BFA compartment in living BY-2 cells (Lam et al., 2009), suggesting that the BFA compartment may be formed by fusion between TGN and endosomes. Therefore, SNAREs at the TGN may function in this fusion event upon BFA treatment. We showed that loss of TNO1 affected localization of SYP61, and TNO1 interacts with SYP41. Thus, we hypothesized that TNO1 could be involved in membrane fusion upon BFA treatment as a component in the SYP41 complex at the TGN.

To test this hypothesis, formation of the BFA compartment in VHAa1-GFP transgenic WT and *tno1* mutant seedlings was investigated. VHAa1-GFP transgenic WT and *tno1* mutant seedlings were grown for 4 days on MS solid medium, the seedlings were transferred to MS liquid medium and treated with 50 μM BFA for up to 5 h. Without BFA treatment, there was no difference in the appearance of VHAa1-GFP positive structures in roots and cotyledons between WT and *tno1* mutant seedlings (Fig 9A-D). After 1 h BFA treatment, VHAa1-GFP accumulated in the BFA compartments in roots of WT seedlings as reported previously and in *tno1* mutant seedlings (Fig 8E and 8F; Dettmer et al., 2006). In WT cotyledons, the BFA compartments were seen in the peripheral region. By contrast, VHAa1-GFP in the peripheral region of *tno1* mutant cotyledons did not accumulate in BFA compartments after 1 h BFA treatment (Fig 8G and 8H). VHAa1-GFP labeled BFA compartments in cotyledons of the *tno1* mutant could be seen only after 5 h of BFA

treatment in the peripheral region (Fig 9K). No difference was seen in recovery from BFA treatment between WT and *tno1* mutant (Fig 9I and 9J).

The response of TNO1 to BFA treatment was also investigated. The mammalian golgin GM130 is a tethering factor during vesicle fusion and a Golgi matrix protein required for the integrity of the Golgi structure. After BFA treatment, GM130 remains in a Golgi remnant, while Golgi luminal proteins are transported back to the ER, indicating that GM130 is involved in maintaining Golgi structure (Seemann et al., 2000). VHAa1-GFP transgenic seedlings were treated in MS liquid medium supplemented with 50 μM BFA for 2 h, followed by fixing and immunolabeling using TNO1 antibody. TNO1 was not found in the VHAa1-GFP-labeled BFA compartment, although TNO1 still co-localized with the remaining small VHAa1-GFP-labeled structures (Fig 9L-O), indicating that TNO1 reacted in a similar way to GM130.

Root growth of the *tno1* mutant on MS solid medium containing 2.5 μM BFA was compared with wild-type. *tno1* mutant seedlings showed reduced root growth compared with WT seedlings (Fig 10), suggesting that the *tno1* mutant is more sensitive to BFA treatment, although no visible difference in the formation of BFA compartments in roots of WT and *tno1* mutant was seen from microscopy (Fig 9I and 9J).

Together, these results suggest that lack of TNO1 delays homotypic fusion between TGN or fusion between TGN and endosomes in cotyledons. Therefore, the BFA compartment forms more slowly in the *tno1* mutant presumably due to delayed fusion. TNO1 may also function in maintaining TGN structure.

Discussion

Identity of TNO1

TNO1 was identified as a novel protein that co-immunoprecipitates with SYP41. As SYP41 is a t-SNARE residing at the TGN, we hypothesize that TNO1 may also be involved in vesicle fusion. Here, we demonstrate that TNO1 is involved in salt and osmotic stress responses and vacuolar trafficking. Based on the effects of BFA treatment, TNO1 is proposed to be involved in the formation of the BFA compartment and may function in maintaining TGN structure.

As a first step to understanding the function of TNO1, we analyzed potential domain structure of TNO1. From coiled-coil and transmembrane domain predictions, TNO1 was found to have 6 coiled-coil domains occupying a large part of the protein and one putative transmembrane domain at the extreme C-terminus. The Conserved Domain Architecture Retrieval Tool (CDART) identified that TNO1 has two previously characterized domains, SMC_prok_B and SMC_N (Geer et al., 2002). These domains are characteristic of structural maintenance of chromosomes (SMC) proteins which are involved in chromatin and DNA dynamics (Castano et al., 1996; Losada et al., 1998). Previously SMC_prok_B and SMC_N domains have been reported to have long coiled-coil regions for protein interaction. (Akhmedov et al., 1998). Although SMC domains are commonly found in SMC proteins, they are also found in other proteins with multiple coiled-coil domains such as vesicular tethering factors and cytoskeleton binding proteins. A search of homologous proteins using the BLAST algorithm against swiss prot database with TNO1 amino acid sequence found myosin related proteins, ATPase and tethering factors including USO1 in yeast, tgolgin-1 in mouse and gigantin in human with high significance (Altschul et al., 1998; Altschul et al., 2005).

USO1, which has 20% amino acid sequence identity and 39% amino acid similarity to TNO1, is a tethering factor involved in ER to Golgi trafficking by tethering COPII vesicles at *cis*-Golgi (Cao et al., 1998). There are two general types of tethering factors, extended rod shaped proteins containing long coiled-coil domains and multimeric protein complexes. Tethering factors, which have been extensively studied in mammalian cells, have been reported to be involved in vesicle fusion by interacting with their tethering partner to pull vesicles to their target (Cao et al., 1998). Some are also involved in maintaining organelle structure and assisting formation of SNARE complexes via direct interaction with a SNARE (Shorter et al., 2002; Vasile et al., 2003). Thus, the presence of multiple predicted coiled-coil domains and the similarity to USO1 suggest that TNO1 could be a tethering factor at the TGN.

Phenotype of *tno1* KO mutant

To determine the function of TNO1, a *tno1* KO mutant was isolated and four major phenotypes were identified – sensitivity to high salt and osmotic stress, secretion of some vacuolar proteins, mis-localization of SYP61, and delayed BFA compartment formation. Opposite effects on salt tolerance have been seen for mutations in different trafficking proteins. Previously, a role for SNARE proteins in salt stress responses has been demonstrated. Knockdown of AtVAMP7C, a v-SNARE involved in vesicle fusion with the vacuole, was found to confer salt tolerance by preventing H_2O_2 containing vesicles from fusing with the vacuolar membrane (Leshem et al., 2006). Knockout of SYP22, a t-SNARE in the PVC and tonoplast, also increased salt tolerance in shoots, and a decreased level of Na^+ in shoots was observed (Hamaji et al., 2009). Thus, salt tolerance in these SNARE

knockout mutants implies that vesicle fusion directly or indirectly affects salt tolerance at the PVC and tonoplast. By contrast, the *tno1* mutant and a mutation in *SYP61*, a t-SNARE in the SYP41 complex, showed a salt sensitive phenotype. TNO1 and SYP61 co-localize to the TGN and are likely to exist in the same protein complex. They are probably involved in trafficking from the PVC to TGN or in endocytosis from plasma membrane to the TGN. TNO1 may have a salt sensitive phenotype due to its effect on SYP61 (Fig 7). In a *tno1* mutant, less SYP61 co-localized with VHAa1-GFP-labeled TGN compared with in WT plants, leading to possible reduced SYP61 function in salt stress. Although some phenotypes of the SYP61 mutant such as defects in stomata control and increased water loss were not observed in the *tno1* mutant (data not shown). The *tno1* mutant may show salt sensitive phenotype by affecting recruitment of SYP61 to the complex, and the same factor causing salt sensitivity in *syp61* mutant could apply to *tno1* mutant for salt sensitivity. It was hypothesized that a cation transporter in the *osm1/syp61* mutant may not function correctly, affecting guard cell turgor and salt sensitivity (Zhu et al., 2002). Extensive investigations of cation transporters in yeast, plants and mammalian cells have shown that cation/ H^+ antiporters in the Golgi, TGN, endosome and the PVC regulate the pH and cation concentration in these organelle, affecting vesicle trafficking (Brett et al., 2002; Brett et al., 2005; Nakamura et al., 2005; Pardo et al., 2006; Fuji et al., 2007). Thus, we hypothesize that this salt sensitive phenotype in *tno1* mutant and *osm1/syp61* mutant could be caused by defects in the transport of cation/H^+ antiporters or in the function of cation/H^+ antiporters at the *Arabidopsis* TGN.

Another noticeable phenotype is the secretion of normally vacuolar proteins in the *tno1* mutant. Analysis of ICF from the *tno1* mutant demonstrated partial secretion of AALP

in common with the vesicle trafficking mutants *vps45*-RNAi and *vti12* (Sanmartin et al., 2007; Zouhar et al., 2009). AALP has dual vacuolar targeting signals and is a cargo for VSR1 (Watanabe et al., 2004; Hinz et al., 2007). TNO1, AtVPS45 and VTI12 may therefore cooperate in VSR1-mediated vacuolar trafficking, via recycling of VSR1 from PVC to TGN. RD21 is another protein that is partially secreted in the *tno1* mutant. RD21 is a cys-protease like AALP, but is probably transported via a VSR1- independent pathway. Interestingly, RD21 and invertase are transported to the vacuole by ER bodies rather than by the VSR1-mediated transport pathway (Hayashi et al., 2001; Rojo et al., 2003); however, invertase was not secreted in the *tno1* mutant. Secretion of RD21 may suggest that it has another transport pathway to the vacuole. Protein profiles from isolated vacuoles of wild-type and *tno1* mutant leaf protoplasts were compared by 2D gel electrophoresis. However, no significant differences were observed between wild type and *tno1* mutant plants (data not shown). This may be only a small fraction of proteins is secreted, with most proteins still being correctly transported to the vacuole. We hypothesize that the partial secretion of vacuolar proteins may be an indirect effect of the loss of TNO1.

Although salt sensitivity and secretion of some vacuolar proteins in the *tno1* mutant may appear to be independent phenotypes, these two phenotypes are closely related. Recently, a connection between salt sensitivity and vacuolar trafficking has been well established. In yeast and mammalian cells, post Golgi organelles involved in vacuolar trafficking were shown to be targets for salt stress, resulting in inefficient vacuolar trafficking (Bachert et al., 2001; Pardo et al., 2006; Hernandez et al., 2009). In *Arabidopsis*, the endocytic pathway to the vacuole has also been shown to be important for salt tolerance

(Leshem et al., 2006; Leshem et al., 2007). Thus, our result also provides evidence that vacuolar trafficking is important for salt tolerance.

BFA treatment

BFA, a well known trafficking inhibitor, has been widely used to investigate vesicle trafficking pathways. In *Arabidopsis*, BFA targets the Arf-GEF (guanine-nucleotide exchange factor for ADP-ribosylation factor) GNOM and causes the formation of BFA compartments, which are regarded as endosomal aggregates (Geldner et al., 2001). VHAa1-GFP-labeled TGN forms a large aggregate in *Arabidopsis* roots upon BFA treatment (Dettmer et al., 2006).

In this study, we used BFA to investigate the involvement of TNO1 in fusion events upon BFA treatment, because TNO1 is a member of a protein complex predicted to be required for vesicle fusion at the TGN, and BFA treatment causes the formation of BFA compartments by fusion between TGN and endosomes. As expected, VHAa1-GFP transgenic plants formed BFA compartments after 1 h BFA treatment, but VHAa1-GFP transgenic *tno1* mutant plants showed formation of BFA compartment only after 5 h BFA treatment. This result implies that TNO1 could be involved in homotypic fusion of the TGN upon BFA treatment. Loss of co-localization between TNO1 and VHAa1-GFP was observed upon BFA treatment, indicating that TNO1 does not enter BFA compartments (Fig 9). A similar effect was also observed for the mammalian golgin GM130, which unlike most Golgi protein, does not relocate to the ER (Seemann et al., 2000). GM130 also interacts with SNAREs and functions as a tethering factor and Golgi matrix protein (Diao et al., 2008). Although there is no sequence homology between TNO1 and GM130, based on the

properties of TNO1, it is possible that TNO1 also functions as a tethering factor and is involved in maintaining TGN structure. *In vitro* fusion assays using recombinant TNO1 and SNAREs at the TGN may provide insight into the role of TNO1 in this vesicle fusion event.

Acknowledgements

We thank Drs Karin Schumacher, Chris Hawes, Erik Nielsen, David Oliver, Natasha Raikhel and Tony Sanderfoot for providing constructs, antibodies and transgenic lines, Margie Carter (ISU Confocal Microscopy and Image Analysis Facility) for valuable assistance and expertise in microscopy, John Leszyk (Protein Microsequencing and Proteomic Mass Spectroscopy Lab at the University of Massachusetts Medical School) for tandem mass spectrometry.

References

Ahmed SU, Rojo E, Kovaleva V, Venkataraman S, Dombrowski JE, Matsuoka K, Raikhel NV (2000) The plant vacuolar sorting receptor AtELP is involved in transport of NH2-terminal propeptide-containing vacuolar proteins in Arabidopsis thaliana. Journal of Cell Biology **149:** 1335-1344

Akhmedov AT, Frei C, Tsai-Pflugfelder M, Kemper B, Gasser SM, Jessberger R (1998) Structural maintenance of chromosomes protein C-terminal domains bind preferentially to DNA with secondary structure. Journal of Biological Chemistry **273:** 24088-24094

Altschul S, Madden T, Schaffer A, Zhang JH, Zhang Z, Miller W, Lipman D (1998) Gapped BLAST and PSI-BLAST: A new generation of protein database search programs. Faseb Journal **12:** A1326-a1326

Altschul SF, Wootton JC, Gertz EM, Agarwala R, Morgulis A, Schaffer AA, Yu YK (2005) Protein database searches using compositionally adjusted substitution matrices. Febs Journal **272:** 5101-5109

Bachert C, Lee TH, Linstedt AD (2001) Lumenal endosomal and Golgi-retrieval determinants involved in pH-sensitive targeting of an early Golgi protein. Mol Biol Cell **12:** 3152-3160

Bassham DC, Raikhel NV (1998) An Arabidopsis VPS45p homolog implicated in protein transport to the vacuole. Plant Physiology **117:** 407-415

Bassham DC, Raikhel NV (2000) Unique features of the plant vacuolar sorting machinery. Current Opinion in Cell Biology **12:** 491-495

Bassham DC, Sanderfoot AA, Kovaleva V, Zheng HY, Raikhel NV (2000) AtVPS45 complex formation at the trans-Golgi network. Molecular Biology of the Cell **11:** 2251-2265

Behal RH, Oliver DJ (1997) Biochemical and molecular characterization of fumarase from plants: Purification and characterization of the enzyme - Cloning, sequencing, and expression of the gene. Archives of Biochemistry and Biophysics **348:** 65-74

Brett CL, Tukaye DN, Mukherjee S, Rao RJ (2005) The yeast endosomal Na+(K+)/H+ exchanger Nhx1 regulates cellular pH to control vesicle trafficking. Molecular Biology of the Cell **16:** 1396-1405

Brett CL, Wei Y, Donowitz M, Rao R (2002) Human Na+/H+ exchanger isoform 6 is found in recycling endosomes of cells, not in mitochondria. American Journal of Physiology-Cell Physiology **282:** C1031-C1041

Bryant NJ, James DE (2003) The Sec1p/Munc18 (SM) protein, Vps45p, cycles on and off membranes during vesicle transport. Journal of Cell Biology **161:** 691-696

Cao XC, Ballew N, Barlowe C (1998) Initial docking of ER-derived vesicles requires Uso1p and Ypt1p but is independent of SNARE proteins. Embo Journal **17:** 2156-2165

Castano IB, Brzoska PM, Sadoff BU, Chen HY, Christman MF (1996) Mitotic chromosome condensation in the rDNA requires TRF4 and DNA topoisomerase I in Saccharomyces cerevisiae. Genes & Development **10:** 2564-2576

Chen Y, Shin YK, Bassham DC (2005) YKT6 is a core constituent of membrane fusion machineries at the Arabidopsis trans-Golgi network. Journal of Molecular Biology **350:** 92-101

Claros MG, von Heijne G (1994) TopPred II: an improved software for membrane protein structure predictions. Comput Appl Biosci **10:** 685-686

Clough SJ, Bent AF (1998) Floral dip: a simplified method for Agrobacterium-mediated transformation of Arabidopsis thaliana. Plant Journal **16:** 735-743

daSilva LLP, Taylor JP, Hadlington JL, Hanton SL, Snowden CJ, Fox SJ, Foresti O, Brandizzi F, Denecke J (2005) Receptor salvage from the prevacuolar compartment is essential for efficient vacuolar protein targeting. Plant Cell **17:** 132-148

Dettmer J, Hong-Hermesdorf A, Stierhof YD, Schumacher K (2006) Vacuolar H+-ATPase activity is required for Endocytic and secretory trafficking in Arabidopsis. Plant Cell **18:** 715-730

Diao A, Frost L, Morohashi Y, Lowe M (2008) Coordination of golgin tethering and SNARE assembly - GM130 binds syntaxin 5 in a p115-regulated manner. Journal of Biological Chemistry **283:** 6957-6967

Dulubova I, Yamaguchi T, Gao Y, Min SW, Huryeva I, Sudhof TC, Rizo J (2002) How Tlg2p/syntaxin 16 'snares' Vps45. Embo Journal **21:** 3620-3631

Ebine K, Okatani Y, Uemura T, Goh T, Shoda K, Niihama M, Morita MT, Spitzer C, Otegui MS, Nakano A, Ueda T (2008) A SNARE Complex Unique to Seed Plants Is Required for Protein Storage Vacuole Biogenesis and Seed Development of Arabidopsis thaliana. Plant Cell **20:** 3006-3021

Fuji K, Shimada T, Takahashi H, Tamura K, Koumoto Y, Utsumi S, Nishizawa K, Maruyama N, Hara-Nishimura I (2007) Arabidopsis vacuolar sorting mutants (green fluorescent seed) can be identified efficiently by secretion of vacuole-targeted green fluorescent protein in their seeds. Plant Cell **19:** 597-609

Fukasawa T, Haranishimura I, Nishimura M (1988) Biosynthesis, Intracellular-Transport and Invitro Processing of 11S Globulin Precursor Proteins of Developing Castor Bean Endosperm. Plant and Cell Physiology **29:** 339-345

Geer LY, Domrachev M, Lipman DJ, Bryant SH (2002) CDART: Protein homology by domain architecture. Genome Research **12:** 1619-1623

Geldner N, Friml J, Stierhof YD, Jurgens G, Palme K (2001) Auxin transport inhibitors block PIN1 cycling and vesicle traficking. Nature **413:** 425-428

Hamaji K, Nagira M, Yoshida K, Ohnishi M, Oda Y, Uemura T, Goh T, Sato MH, Morita MT, Tasaka M, Hasezawa S, Nakano A, Hara-Nishimura I, Maeshima M, Fukaki H, Mimura T (2009) Dynamic Aspects of Ion Accumulation by Vesicle Traffic Under Salt Stress in Arabidopsis. Plant and Cell Physiology **50:** 2023-2033

Hara-Nishimura I, Shimada T, Hatano K, Takeuchi Y, Nishimura M (1998) Transport of storage proteins to protein storage vacuoles is mediated by large precursor-accumulating vesicles. Plant Cell **10:** 825-836

Hayashi Y, Yamada K, Shimada T, Matsushima R, Nishizawa NK, Nishimura M, Hara-Nishimura I (2001) A proteinase-storing body that prepares for cell death or stresses in the epidermal cells of Arabidopsis. Plant and Cell Physiology **42:** 894-899

Hernandez A, Jiang XY, Cubero B, Nieto PM, Bressan RA, Hasegawa PM, Pardo JM (2009) Mutants of the Arabidopsis thaliana Cation/H+ Antiporter AtNHX1 Conferring Increased Salt Tolerance in Yeast THE ENDOSOME/PREVACUOLAR COMPARTMENT IS A TARGET FOR SALT TOXICITY. Journal of Biological Chemistry **284:** 14276-14285

Hinz G, Hillmer S, Baumer M, Hohl I (1999) Vacuolar storage proteins and the putative vacuolar sorting receptor BP-80 exit the Golgi apparatus of developing pea cotyledons in different transport vesicles. Plant Cell **11:** 1509-1524

Hofte H, Hubbard L, Reizer J, Ludevid D, Herman EM, Chrispeels MJ (1992) Vegetative and Seed-Specific Forms of Tonoplast Intrinsic Protein in the Vacuolar Membrane of Arabidopsis thaliana. Plant Physiol **99:** 561-570

Hruz T, Laule O, Szabo G, Wessendorp F, Bleuler S, Oertle L, Widmayer P, Gruissem W, Zimmermann P (2008) Genevestigator v3: a reference expression database for the meta-analysis of transcriptomes. Adv Bioinformatics **2008:** 420747

Jackson CL, Casanova JE (2000) Turning on ARF: the Sec7 family of guanine-nucleotide-exchange factors. Trends in Cell Biology **10:** 60-67

Jiang LW, Phillips TE, Rogers SW, Rogers JC (2000) Biogenesis of the protein storage vacuole crystalloid. Journal of Cell Biology **150:** 755-769

Kirsch T, Paris N, Butler JM, Beevers L, Rogers JC (1994) Purification and Initial Characterization of a Potential Plant Vacuolar Targeting Receptor. Proceedings of the National Academy of Sciences of the United States of America **91:** 3403-3407

Lam SK, Cai Y, Tse YC, Wang J, Law AHY, Pimpl P, Chan HYE, Xia J, Jiang LW (2009) BFA-induced compartments from the Golgi apparatus and trans-Golgi network/early endosome are distinct in plant cells. Plant Journal **60:** 865-881

Leshem Y, Melamed-Book N, Cagnac O, Ronen G, Nishri Y, Solomon M, Cohen G, Levine A (2006) Suppression of Arabidopsis vesicle-SNARE expression inhibited fusion of H2O2 containing vesicles with tonoplast and increased salt tolerance. Proceedings of the National Academy of Sciences of the United States of America **103:** 18008-18013

Leshem Y, Seri L, Levine A (2007) Induction of phosphatidylinositol 3-kinase-mediated endocytosis by salt stress leads to intracellular production of reactive oxygen species and salt tolerance. Plant Journal **51:** 185-197

Liu Q, Kasuga M, Sakuma Y, Abe H, Miura S, Yamaguchi-Shinozaki K, Shinozaki K (1998) Two transcription factors, DREB1 and DREB2, with an EREBP/AP2 DNA binding domain separate two cellular signal transduction pathways in drought- and low-temperature-responsive gene expression, respectively, in Arabidopsis. Plant Cell **10:** 1391-1406

Losada A, Hirano M, Hirano T (1998) Identification of Xenopus SMC protein complexes required for sister chromatid cohesion. Genes & Development **12:** 1986-1997

McNew JA, Parlati F, Fukuda R, Johnston RJ, Paz K, Paumet F, Sollner TH, Rothman JE (2000) Compartmental specificity of cellular membrane fusion encoded in SNARE proteins. Nature **407:** 153-159

Nakamura N, Tanaka S, Teko Y, Mitsui K, Kanazawa H (2005) Four Na+/H+ exchanger isoforms are distributed to Golgi and post-Golgi compartments and are involved in organelle pH regulation. Journal of Biological Chemistry **280:** 1561-1572

Neuhaus JM, Ahlgoy P, Hinz U, Flores S, Meins F (1991) High-Level Expression of a Tobacco Chitinase Gene in Nicotiana-Sylvestris - Susceptibility of Transgenic Plants to Cercospora-Nicotianae Infection. Plant Molecular Biology **16:** 141-151

Pardo JM, Cubero B, Leidi EO, Quintero FJ (2006) Alkali cation exchangers: roles in cellular homeostasis and stress tolerance. Journal of Experimental Botany **57:** 1181-1199

Paris N, Rogers SW, Jiang LW, Kirsch T, Beevers L, Phillips TE, Rogers JC (1997) Molecular cloning and further characterization of a probable plant vacuolar sorting receptor. Plant Physiology **115:** 29-39

Paris N, Stanley CM, Jones RL, Rogers JC (1996) Plant cells contain two functionally distinct vacuolar compartments. Cell **85:** 563-572

Park JH, Oufattole M, Rogers JC (2007) Golgi-mediated vacuolar sorting in plant cells: RMR proteins are sorting receptors for the protein aggregation/membrane internalization pathway. Plant Science **172:** 728-745

Park M, Lee D, Lee GJ, Hwang I (2005) AtRMR1 functions as a cargo receptor for protein trafficking to the protein storage vacuole. Journal of Cell Biology **170:** 757-767

Phan NQ, Kima SJ, Bassham DC (2008) Overexpression of Arabidopsis Sorting Nexin AtSNX2b Inhibits Endocytic Trafficking to the Vacuole. Molecular Plant **1:** 961-976

Preuss ML, Serna J, Falbel TG, Bednarek SY, Nielsen E (2004) The Arabidopsis Rab GTPase RabA4b localizes to the tips of growing root hair cells. Plant Cell **16:** 1589-1603

Qiu QS, Guo Y, Quintero FJ, Pardo JM, Schumaker KS, Zhu JK (2004) Regulation of vacuolar Na+/H+ exchange in Arabidopsis thaliana by the salt-overly-sensitive (SOS) pathway. Journal of Biological Chemistry **279:** 207-215

Rojo E, Zouhar J, Carter C, Kovaleva V, Raikhel NV (2003) A unique mechanism for protein processing and degradation in Arabidopsis thaliana. Proceedings of the National Academy of Sciences of the United States of America **100:** 7389-7394

Rose A, Manikantan S, Schraegle SJ, Maloy MA, Stahlberg EA, Meier I (2004) Genome-wide identification of arabidopsis coiled-coil proteins and establishment of the ARABI-COIL database. Plant Physiology **134:** 927-939

Rothman JE (1994) Mechanism of Intracellular Protein-Transport. Nature **372:** 55-63

Sanderfoot AA, Ahmed SU, Marty-Mazars D, Rapoport I, Kirchhausen T, Marty F, Raikhel NV (1998) A putative vacuolar cargo receptor partially colocalizes with

AtPEP12p on a prevacuolar compartment in Arabidopsis roots. Proceedings of the National Academy of Sciences of the United States of America **95:** 9920-9925

Sanderfoot AA, Kovaleva V, Bassham DC, Raikhel NV (2001a) Interactions between syntaxins identify at least five SNARE complexes within the golgi/prevacuolar system of the arabidopsis cell. Molecular Biology of the Cell **12:** 3733-3743

Sanderfoot AA, Pilgrim M, Adam L, Raikhel NV (2001b) Disruption of individual members of arabidopsis syntaxin gene families indicates each has essential functions. Plant Cell **13:** 659-666

Sanmartin M, Ordonez A, Sohn EJ, Robert S, Sanchez-Serrano JJ, Surpin MA, Raikhel NV, Rojo E (2007) Divergent functions of VTI12 and VTI11 in trafficking to storage and lytic vacuoles in Arabidopsis. Proceedings of the National Academy of Sciences of the United States of America **104:** 3645-3650

Seaman MNJ (2005) Recycle your receptors with retromer. Trends in Cell Biology **15:** 68-75

Seemann J, Jokitalo E, Pypaert M, Warren G (2000) Matrix proteins can generate the higher order architecture of the Golgi apparatus. Nature **407:** 1022-1026

Sheen J (2002) A transient expression assay using Arabidopsis mesophyll protoplasts. Available online at http://genetics.mgh.harvard.edu/sheenweb/.

Shi H, Ishitani M, Kim C, Zhu JK (2000) The Arabidopsis thaliana salt tolerance gene SOS1 encodes a putative Na+/H+ antiporter. Proc Natl Acad Sci U S A **97:** 6896-6901

Shimada T, Fuji K, Tamura K, Kondo M, Nishimura M, Hara-Nishimura I (2003a) Vacuolar sorting receptor for seed storage proteins in Arabidopsis thaliana. Proceedings of the National Academy of Sciences of the United States of America **100:** 16095-16100

Shimada T, Kuroyanagi M, Nishimura M, Hara-Nishimura I (1997) A pumpkin 72-kDa membrane protein of precursor-accumulating vesicles has characteristics of a vacuolar sorting receptor. Plant Cell Physiol **38:** 1414-1420

Shorter J, Beard MB, Seemann J, Dirac-Svejstrup AB, Warren G (2002) Sequential tethering of Golgins and catalysis of SNAREpin assembly by the vesicle-tethering protein p115. Journal of Cell Biology **157:** 45-62

Sogaard M, Tani K, Ye RR, Geromanos S, Tempst P, Kirchhausen T, Rothman JE, Sollner T (1994) A Rab Protein Is Required for the Assembly of Snare Complexes in the Docking of Transport Vesicles. Cell **78:** 937-948

Song J, Lee MH, Lee GJ, Yoo CM, Hwang I (2006) Arabidopsis EPSIN1 plays an important role in vacuolar trafficking of soluble cargo proteins in plant cells via interactions with clathrin, AP-1, VTI11, and VSR1. Plant Cell **18:** 2258-2274

Surpin M, Zheng HJ, Morita MT, Saito C, Avila E, Blakeslee JJ, Bandyopadhyay A, Kovaleva V, Carter D, Murphy A, Tasaka M, Raikhel N (2003) The VTI family of SNARE proteins is necessary for plant viability and mediates different protein transport pathways. Plant Cell **15:** 2885-2899

Teh OK, Moore I (2007) An ARF-GEF acting at the Golgi and in selective endocytosis in polarized plant cells. Nature **448:** 493-496

Tormakangas K, Hadlington JL, Pimpl P, Hillmer S, Brandizzi F, Teeri TH, Denecke J (2001) A vacuolar sorting domain may also influence the way in which proteins leave the endoplasmic reticulum. Plant Cell **13:** 2021-2032

Vasile E, Perez T, Nakamura N, Krieger M (2003) Structural integrity of the Golgi is temperature sensitive in conditional-lethal mutants with no detectable GM130. Traffic **4:** 254-272

von Heijne G (1992) Membrane protein structure prediction. Hydrophobicity analysis and the positive-inside rule. J Mol Biol **225:** 487-494

Wee EGT, Sherrier DJ, Prime TA, Dupree P (1998) Targeting of active sialyltransferase to the plant Golgi apparatus. Plant Cell **10:** 1759-1768

Wink M (1993) The Plant Vacuole - a Multifunctional Compartment. Journal of Experimental Botany **44:** 231-246

Yamaguchi-Shinozaki K, Shinozaki K (1993) Arabidopsis DNA encoding two desiccation-responsive rd29 genes. Plant Physiol **101:** 1119-1120

Yamaguchishinozaki K, Shinozaki K (1993) Characterization of the Expression of a Desiccation-Responsive Rd29 Gene of Arabidopsis-Thaliana and Analysis of Its Promoter in Transgenic Plants. Molecular & General Genetics **236:** 331-340

Zhu JH, Gong ZZ, Zhang CQ, Song CP, Damsz B, Inan G, Koiwa H, Zhu JK, Hasegawa PM, Bressan RA (2002) OSM1/SYP61: A syntaxin protein in

Arabidopsis controls abscisic acid-mediated and non-abscisic acid-mediated responses to abiotic stress. Plant Cell **14:** 3009-3028

Zouhar J, Rojo E, Bassham DC (2009) AtVPS45 Is a Positive Regulator of the SYP41/SYP61/VTI12 SNARE Complex Involved in Trafficking of Vacuolar Cargo. Plant Physiology **149:** 1668-1678

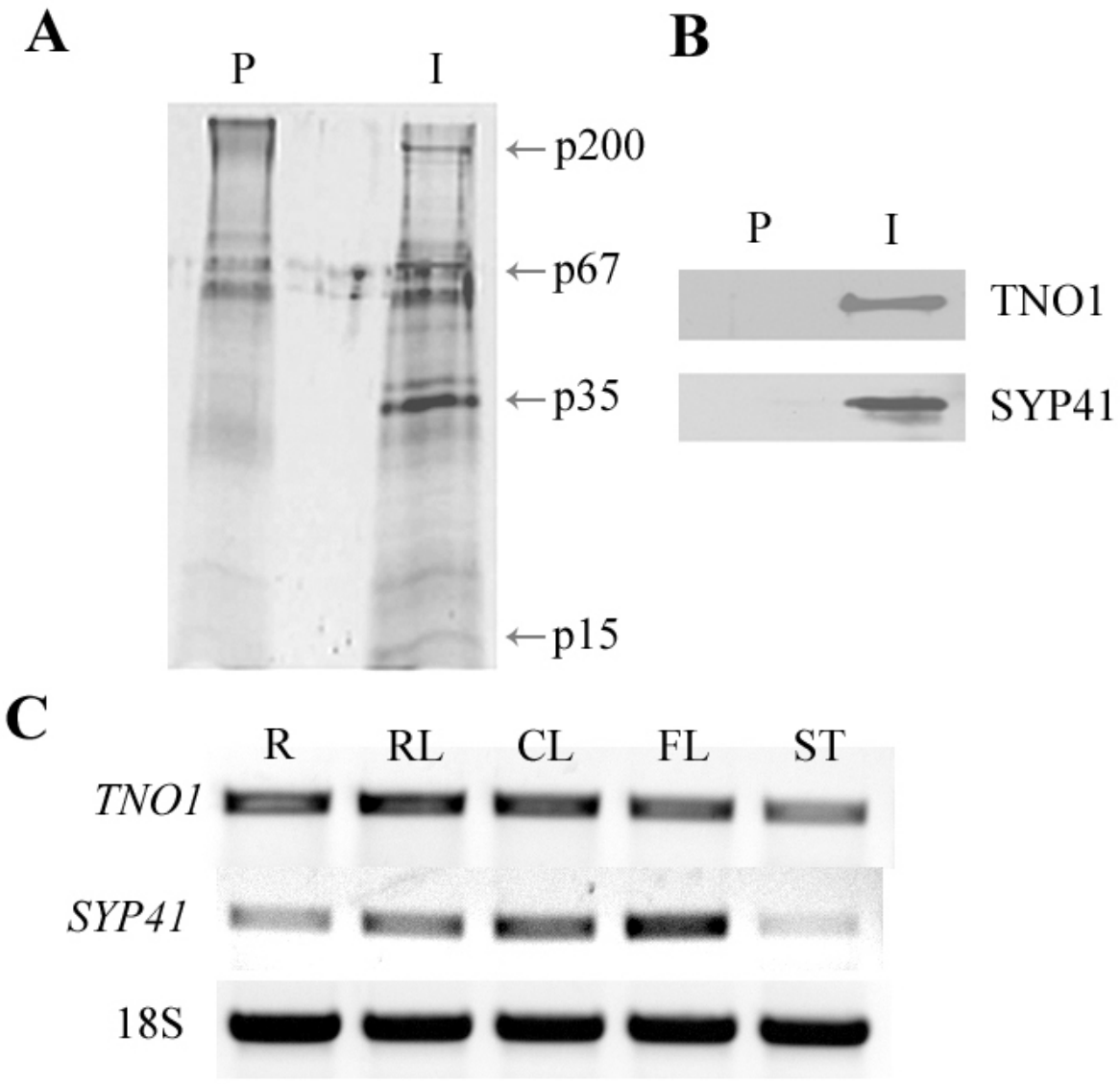

Figure 1. Identification of TNO1

A. Detection of TNO1 in SYP41 immunoprecipitate

Detergent-solubilized *Arabidopsis* suspension cell extracts were applied to a column containing resin cross-linked to either immobilized SYP41 antibodies (I) or SYP41 pre-immune serum (P). The eluates from each column were analyzed by SDS-PAGE and silver

staining. p200, p67, p35 and p15 indicate the mobility of protein bands, when compared with molecular weight marker.

B. Co-immunoprecipitation of TNO1 with SYP41

Immunoprecipitations were performed from detergent-solubilized *Arabidopsis* membrane extracts using SYP41 antibodies (I) and pre-immune serum (P). Immunoprecipitates were analyzed by immunoblotting with antibodies against SYP41 or TNO1.

C. Expression of TNO1 mRNA in *Arabidopsis*

RT-PCR was performed using cDNA from different tissues of *Arabidopsis* using *TNO1*- and *SYP41*- specific primers. 18S RNA was used as a control. (R; root, RL; rosette leaves, CL; cauline leaves, FL; flower, ST; stem).

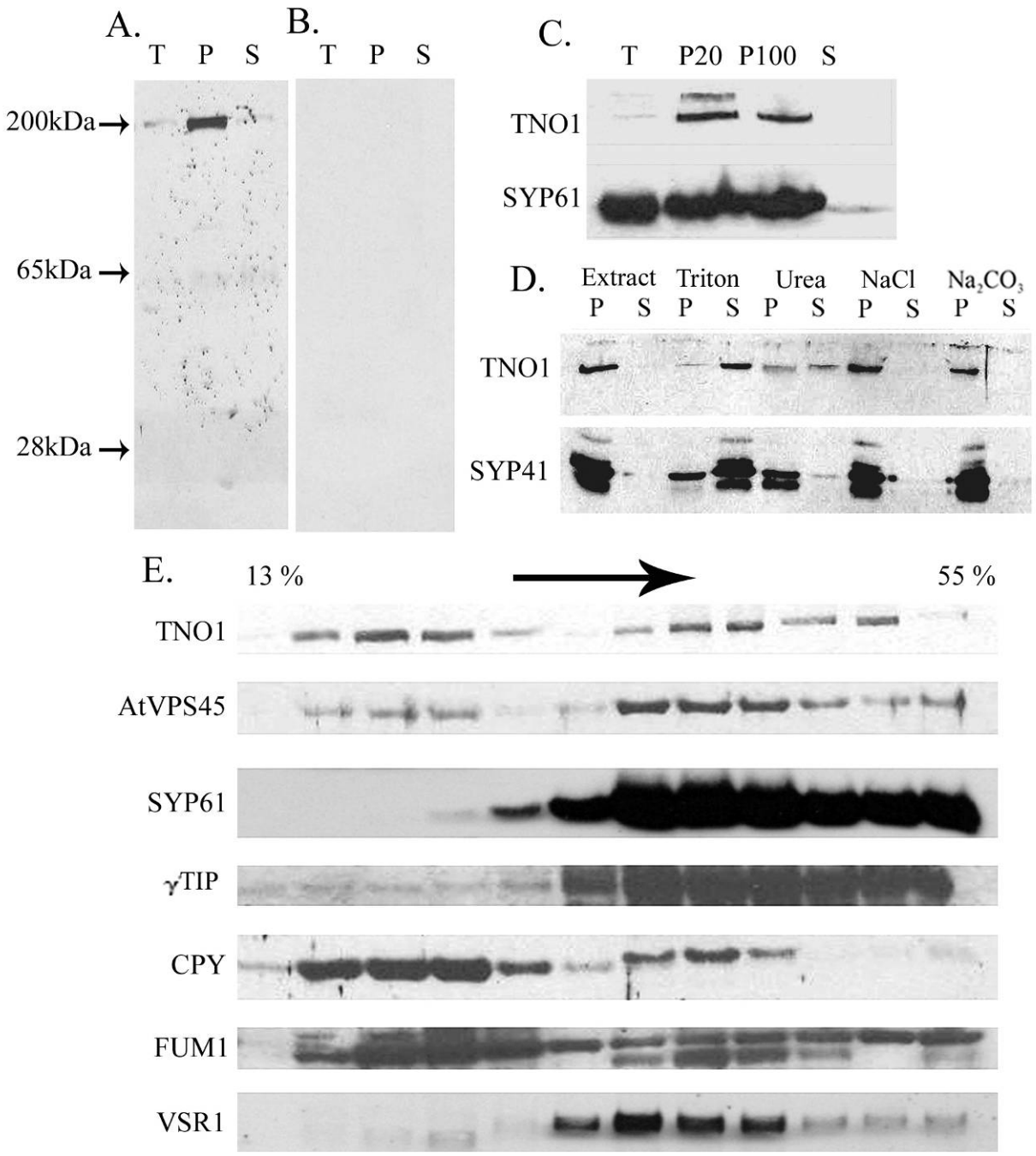

Figure 2. Membrane association of TNO1

A-B. Detection of TNO1 using TNO1 antibody

Total protein extract (T), membrane extract (P), and soluble proteins (S) from *Arabidopsis* seedlings were separated by SDS-PAGE and analyzed by immunoblotting using affinity-purified TNO1 antibody (A) and TNO1 pre-immune serum (B). Position of molecular markers is shown at left.

C. Differential centrifugation

Total *Arabidopsis* extracts (T) from 2 week old seedlings were centrifuged sequentially at 20,000 x g and 100,000 x g, resulting in a 20,000g pellet (P20) and 100,000g pellet (P100) and soluble fractions (S), followed by immunoblotting using TNO1 and SYP61 antibodies

D. Membrane association test

Total membrane pellets from *Arabidopsis* seedlings were resuspended in 1% (v/v) Triton X-100, 2 M urea, 1 M NaCl or 0.1 M Na_2CO_3. Suspensions were re-centrifuged at 125,000 x g to separate solubilized fractions (S) and insoluble fractions (P), which were analyzed by immunoblotting using TNO1 and SYP41 antibodies.

E. Sucrose gradient fractionation

Arabidopsis extracts from a 4 week old root culture were fractionated on a sucrose density gradient (13% - 55%). Equal volumes of each fraction were analyzed by immunoblotting using antibodies against TNO1, AtVPS45, SYP61, γ-tonoplast intrinsic protein (γTIP), carboxypeptidase Y (CPY), fumarase (FUM1), and VSR1.

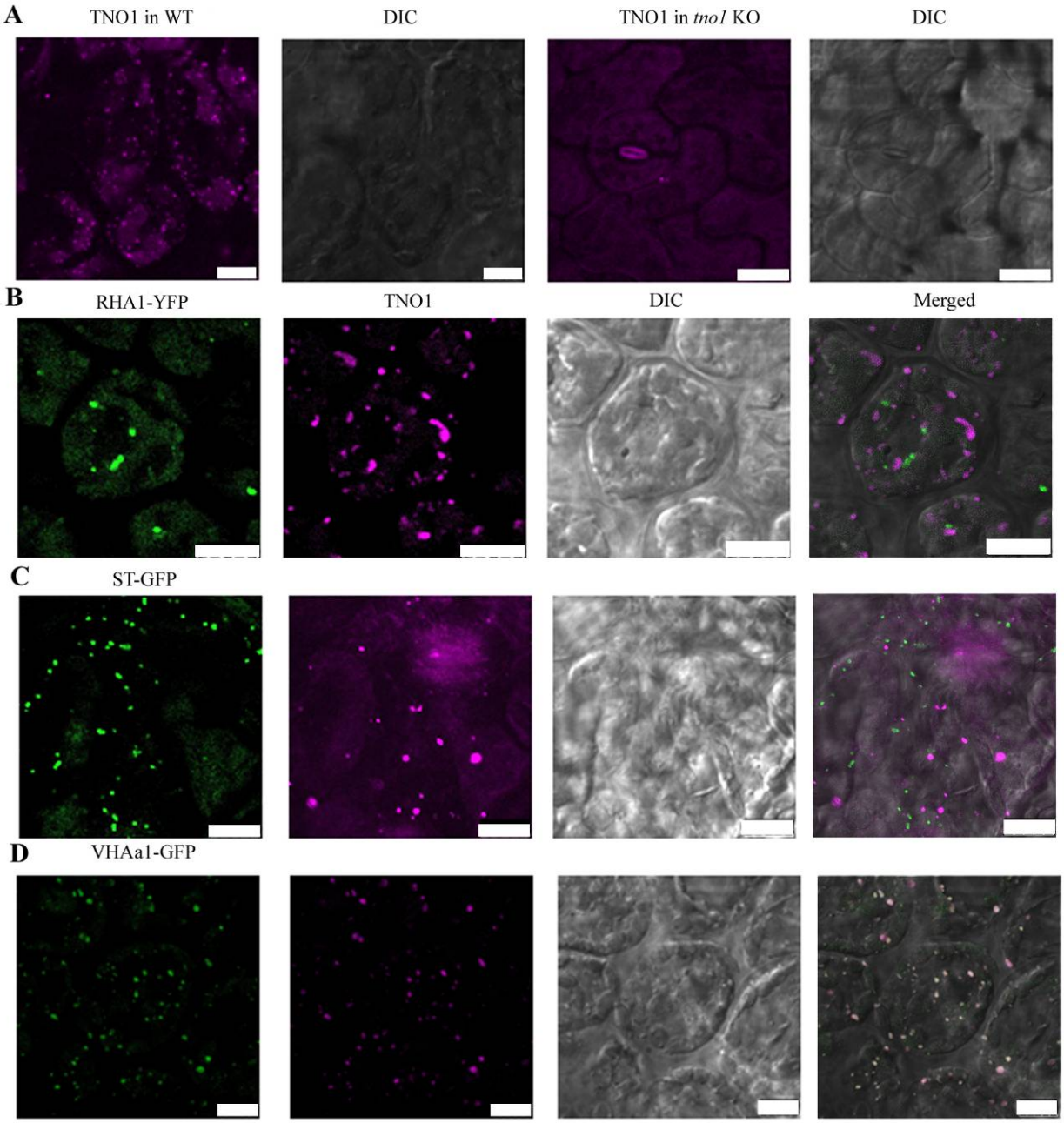

Figure 3. TNO1 is localized to the TGN

A. TNO1 antibodies specifically label punctuate structures

4 day old wild type and *tno1* mutant seedlings were fixed and processed for immunofluorescence using TNO1 antibody and DIC images.

B-D. TNO1 co-localizes with VHAa1 at the TGN

4 day old RHA1-YFP (PVC; B), ST-GFP (Golgi; C), and VHAa1-GFP (TGN; D) transgenic *Arabidopsis* seedlings were fixed and immunolabeled using TNO1 antibody. Scale bars represent 10 μm.

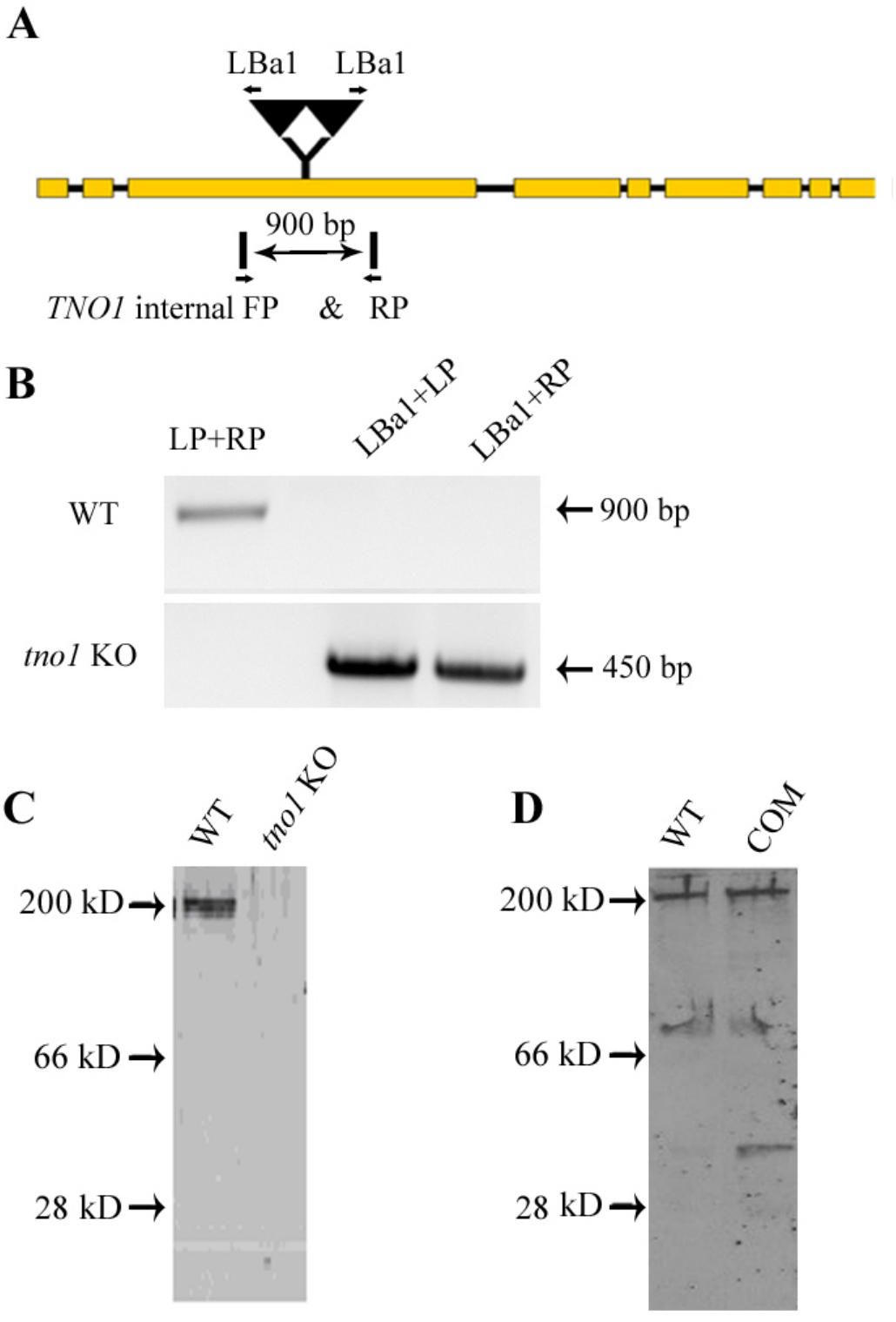

Figure 4. Identification of a homozygous *tno1* knockout mutant

A. T-DNA insertion site in *tno1* knockout mutant

tno1 KO mutant has a complex T-DNA insertion in its third exon. LB1, *TNO1* internal LP and RP primers are used to identify *tno1* knockout mutant in Figure 4B. Arrow indicates the direction of each primer. Yellow box and lines indicates exon and intron, respectively.

B. Identification of homozygous *tno1* knockout mutant

PCR from wild-type and *tno1* KO mutant genomic DNA was performed using LP (*TNO1* internal forward)/ RP (*TNO1* internal reverse) primers and LB1 primer from the T-DNA, and produced a 900 bp band from LP and RP primers and a 450 bp band from LBa1 and either LP or RP primers.

C. Lack of TNO1 in *tno1* KO mutant

Membrane extracts from wild-type (WT) and *tno1* mutant plants were analyzed by SDS-PAGE and immunoblotting using TNO1 antibody. Position of molecular markers is shown at left.

D. Expression of TNO1 in TNO1 complemented line

Membrane extracts from wild-type (WT) and *tno1*/*TNO1* promoter::*TNO1* plants (COM) were analyzed by SDS-PAGE and immunoblotting using TNO1 antibody.

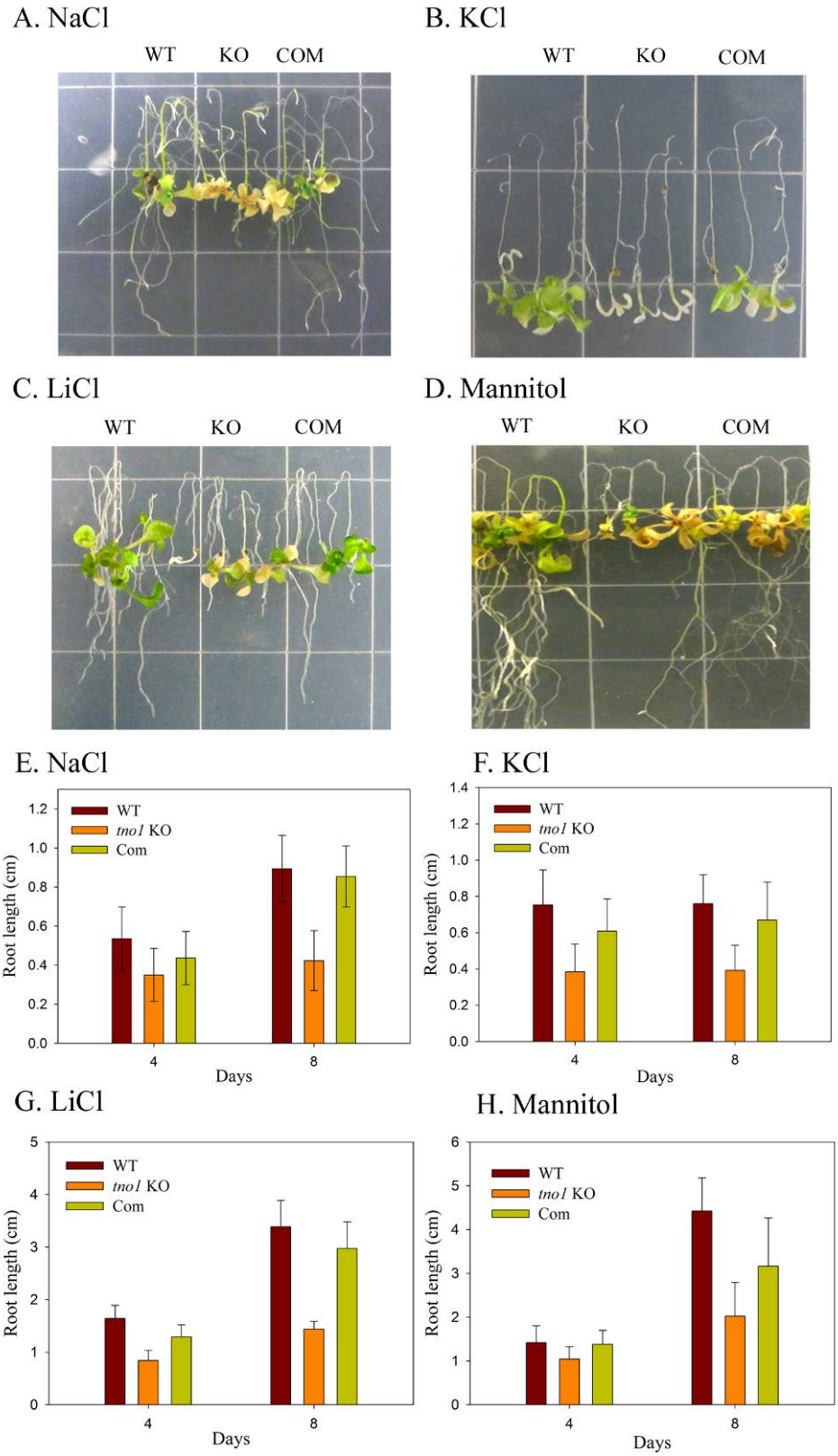
A. NaCl
WT
KO
COM
B. KCl
WT
KO
COM
C. LiCl
WT
KO
COM
D. Mannitol
WT
KO
COM
E. NaCl
F. KCl
G. LiCl
H. Mannitol
WT
tno1 KO
Com
Root length (cm)
Days
4
8

Figure 5. *tno1* mutant is sensitive to salt, ionic and osmotic stresses

A-D. Wild-type, *tno1* mutant and TNO1 complemented seedlings were grown vertically on MS solid medium for 4 days and transferred to MS plates containing 130 mM NaCl (A), 140 mM KCl (B), 17mM LiCl (C) or 300 mM mannitol (D) and grown inverted. Images were taken after 1 week. WT, Wild type; KO, *tno1* KO mutant; COM, *tno1*/*TNO1* promoter::*TNO1*.

E-H. Root growth under salt, ionic and osmotic stress conditions.

Seeds were germinated on MS plates containing 130 mM NaCl (E), 140 mM KCl (F), 17 mM LiCl (G) or 300 mM mannitol (H) and the root length was measured at four and eight days after germination. Error bars represent standard deviation (n = 18 for each genotype). WT, Wild type; KO, *tno1* KO mutant; COM, *tno1*/*TNO1* promoter::*TNO1*.

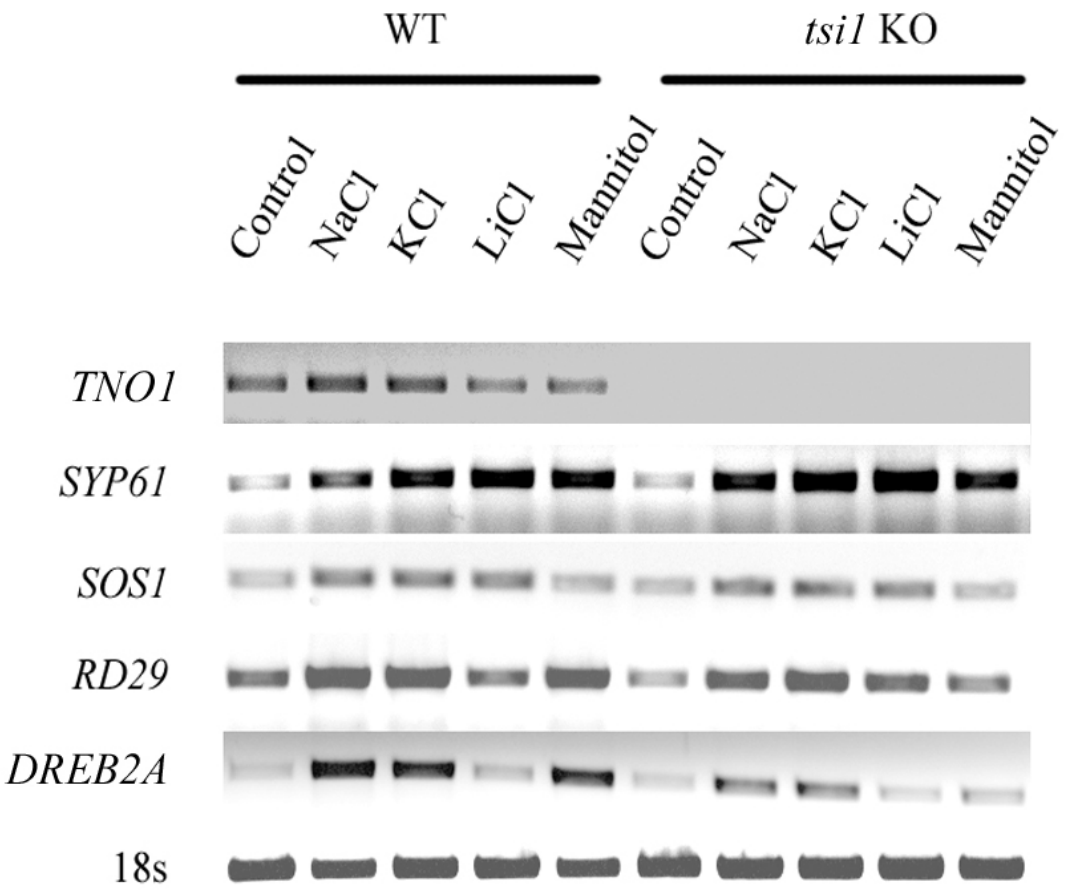

Figure 6. Salt/ osmotic responsive gene expression in wild-type and *tno1* mutant

RT-PCR was performed using RNA extracted from wild-type and *tno1* mutant seedlings after the indicated treatments with TNO1, SYP61, SOS1, DREB2A and RD29-specific primers. Treatments were as follows: control (no treatment), NaCl (300 mM NaCl), KCl (300 mM), LiCl (40 mM LiCl), Mannitol (600 mM).

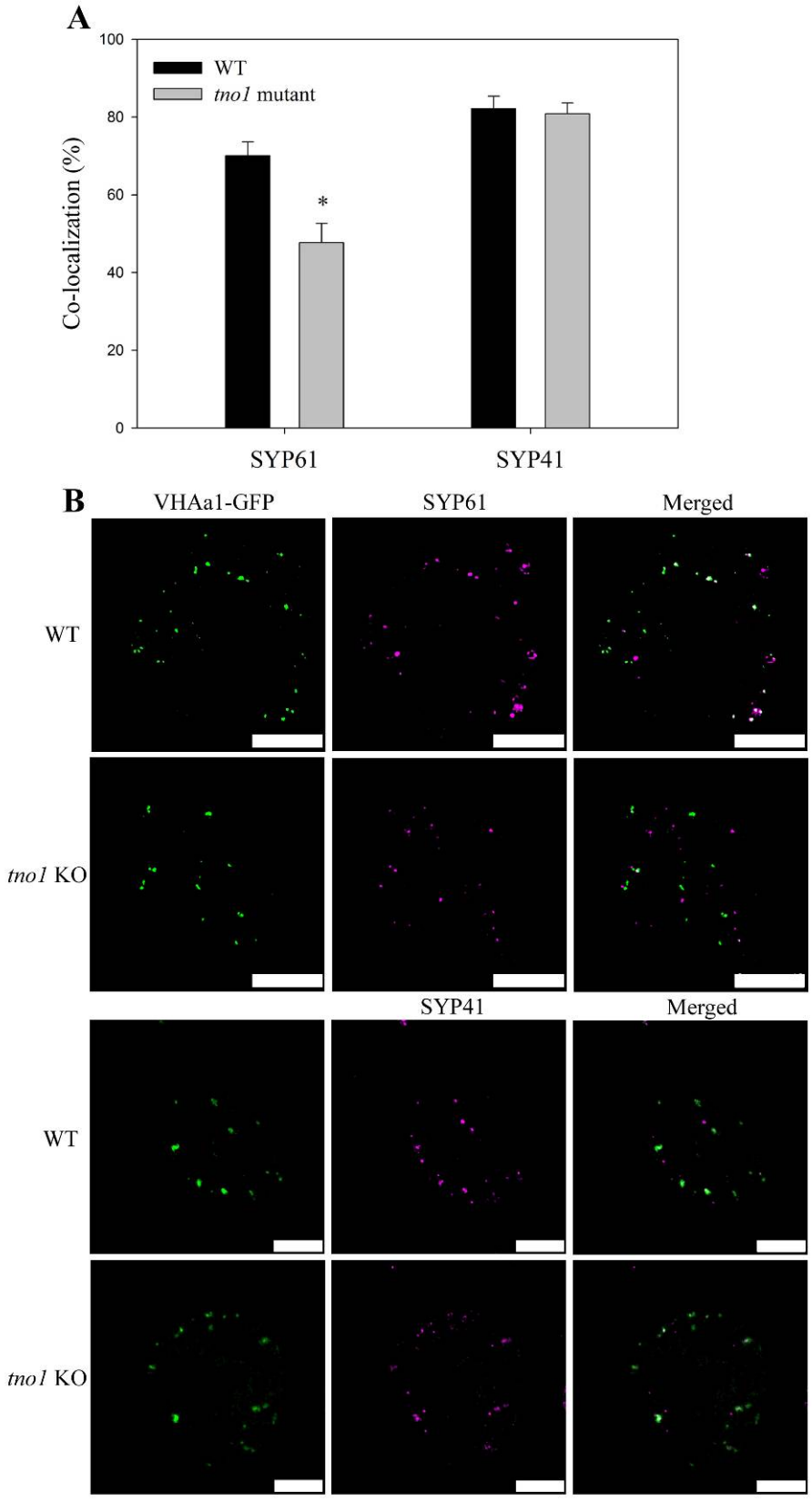
A
100
80
60
40
20
0
Co-localization (%)
WT
tno1 mutant
*
SYP61
SYP41
B
VHAa1-GFP
SYP61
Merged
WT
tno1 KO
SYP41
Merged
WT
tno1 KO

Figure 7. Mis-localization of SYP61 in *tno1* mutant

A. Co-localization of SYP61 or SYP41 with VHAa1-GFP in wild-type and *tno1* mutant

Protoplasts were isolated from leaves of VHAa1-GFP transgenic wild-type plants and VHAa1-GFP transgenic *tno1* mutants and fixed, followed by immunofluorescence labeling using SYP61 or SYP41 antibodies. Scale bars represent 10 μm.

B. Quantification of co-localization of SYP61 and SYP41 with VHAa1-GFP in wild-type and *tno1* mutant

Percentage of co-localization of SYP61 or SYP41 with VHAa1 in Fig B was measured. Error bars represent standard error. Results shown are an average of three independent experiments. The asterisk shows statistically significant difference between wild-type and *tno1* mutant (*t*-test, $p = 0.00038$)

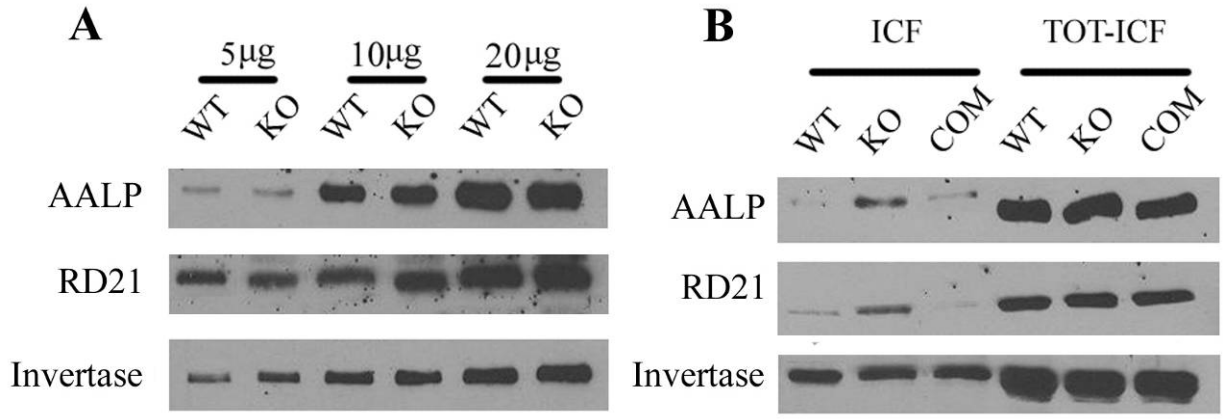

Figure 8. Secretion of vacuolar proteins in the *tno1* mutant

A. Comparison of the amount of vacuolar proteins in wild-type and *tno1* mutant

Vacuoles were isolated from leaves of WT and *tno1* mutant and analyzed by immunoblotting using AALP, RD21, and invertase antibodies. Amount of vacuolar proteins loaded is shown on the top.

B. Secretion of vacuolar proteins in *tno1* mutant

Intercellular wash fluids were harvested from wild type (WT), *tno1* mutant (KO), and TNO1 complemented line (COM) and analyzed by SDS-PAGE and immunoblotting using AALP, RD21, and invertase antibodies. ICF (intercellular wash fluid), TOT-ICF (*Arabidopsis* extract after collection of ICF).

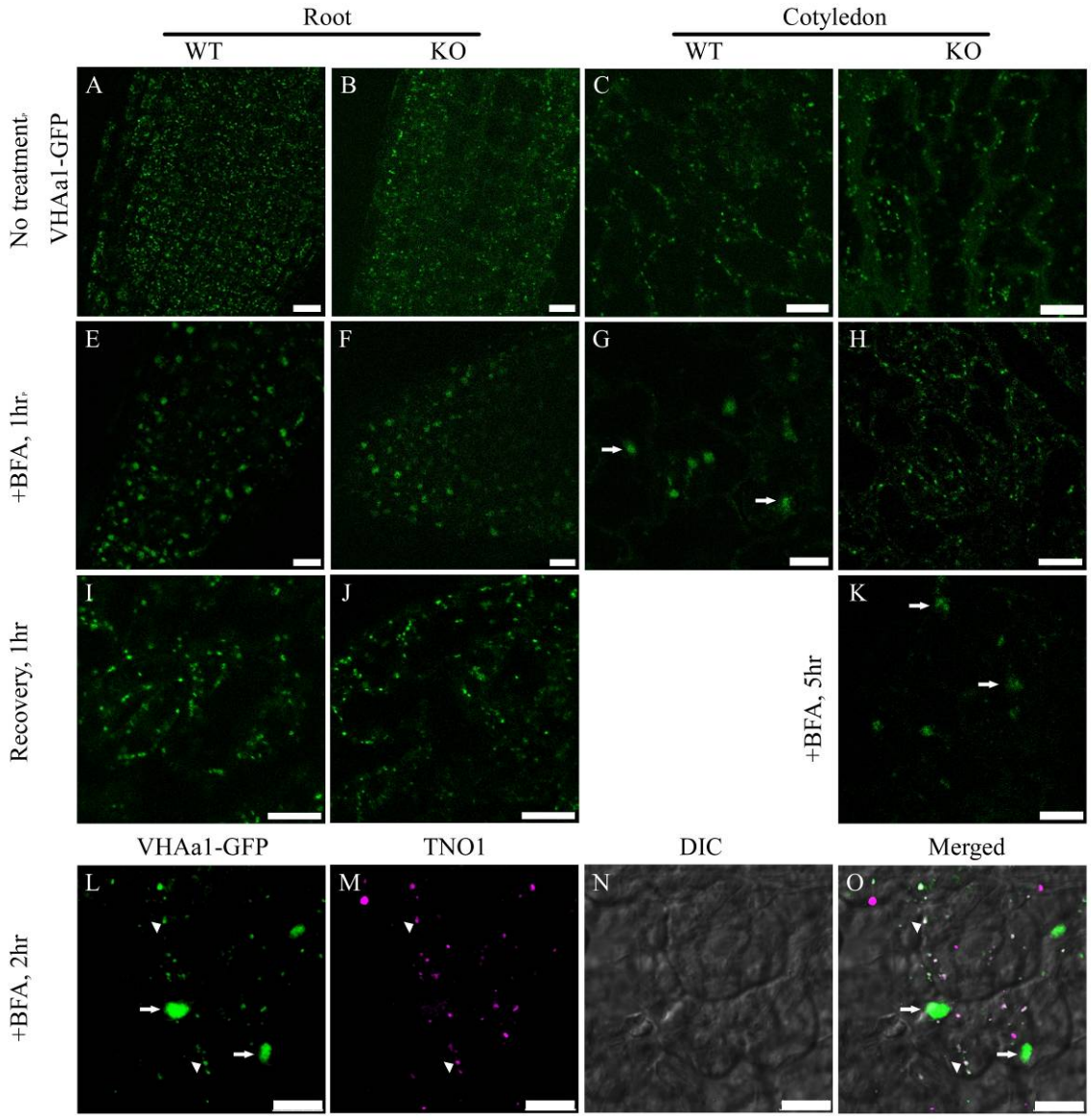

Figure 9. Delayed formation of a BFA compartment in *tno1* mutant and localization of TNO1 upon BFA treatment

A-D. The VHAa1-GFP in wild-type and *tno1* mutant without BFA treatment

TGN is labeled with VHAa1-GFP in roots of wild-type (A) and *tno1* mutant (B), and in the cotyledons of wild-type (C) and *tno1* mutant (D).

E-K. The formation of BFA compartment in wild-type and *tno1* mutant

Wild-type and *tno1* mutant seedlings were treated with 50 µg/ml BFA in half strength MS liquid medium for either 1 h (E-H) or 5 hr (K). For the recovery, BFA treated seedlings were washed twice with the same incubation medium and incubated for 1 h (I and J). Formation of the BFA compartments in roots of wild type (E) and *tno1* mutant (F), and in cotyledons of wild-type (G) was observed after 1 h BFA treatment. Formation of BFA compartment in cotyledons of *tno1* mutant was not observed after 1 h BFA treatment (H). Recovery from BFA treatment in cotyledons of wild-type (I) and *tno1* KO mutant (J) was observed. Formation of BFA compartments in cotyledons of *tno1* KO mutant (K) was observed after 5 hr BFA treatment.

L-O. Localization of TNO1 after BFA treatment

VHAa1-GFP transgenic seedlings were treated with 50 µg/ml of BFA in half strength MS liquid medium for 2 hr and fixed, followed by immunofluorescence using TNO1 antibody. Arrows indicate the BFA compartment and arrow heads indicate small punctuate structures, presumably TGN. Scale bars represent 10 µm.

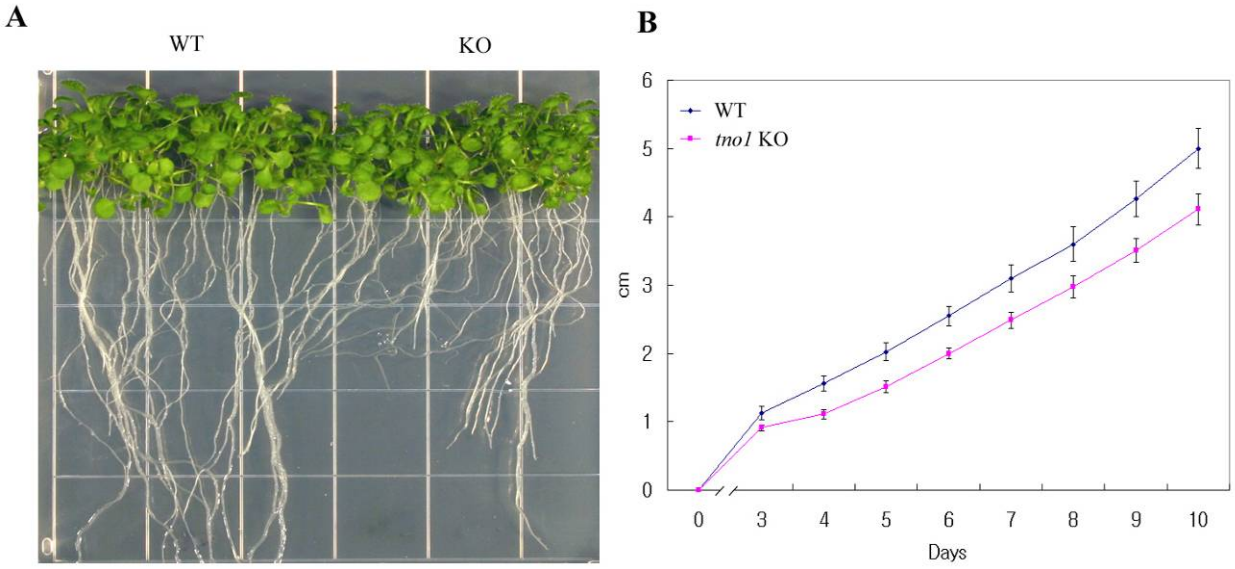

Figure 10. Root growth under BFA treatment

A-B. Inhibition of root growth of *tno1* KO mutant seedlings by BFA

WT and *tno1* KO seeds were germinated on MS plates containing 2.5 μM and grown for 10 days (A). Root length was measured for 10 days after germination (B). Error bars represent standard error. Results shown are an average of three independent experiments.

Table 1. Primer sequences. The restriction sites used for cloning are underlined.

Primer name	Direction	Sequence
TSI1 cDNA	Forward	5'-GGTTGGGATCGTATTTAGATAATG-3'
	Reverse	5'-GTAGTAGTTTCATGTGAGAGACC-3'
TSI1 internal	Forward	5'-TTGACCGACTTGCTGGGTACA-3'
	Reverse	5'-GCAATGACATCCACGTCTCTAAGG-3'
T-DNA left border-a1		5'-TGGTTCACGTAGTGGGCCATCG-3'
TSI1 promoter	Forward	5'–ATCAGTCGACAACAAATCAGTCAATT-3'
	Reverse	5'-GCGGCCGCTATCTAAATACGATCC-3'
genomic *TSI1*	Forward	5'-GCGGCCGCATGCACGAGAAGGATG-3'
	Reverse	5'-TTCTGGTACCGATTCTCAGTGGACAG-3'
SYP41	Forward	5'- GATCCTCATGGCGACGAGGAATCGTACGT-TGCTGTTT-3'
	Reverse	5'- GGATCCTCAGACAAGCAGGATGCGCA-3'
DREB2A	Forward	5'-GGAGATGGCAGTTTATGATC-3'
	Reverse	5'-TTAGTTCTCCAGATCCAAGTA-3'
SOS1	Forward	5'-ATGACGACTG TAATCGACGC GACGA-3'
	Reverse	5'-TGACAACACCACTGAGGATAAATAT-3'
RD29	Forward	5'-ATGGATCAAACAGAGGAACCACCAC-3'
	Reverse	5'-CCATTCCAGTTTCAGTCTTCATATC-3'
SYP61	Forward	5'-GGATCCTCATGTCTTCAGCTCAAGATCC-3'
	Reverse	5'-GGATCCTTATATCATCATCATTTGAC-3'

Supplementary Fig 1A. TNO1 DNA sequence

```
TAIR seq 1   ATGCACGAGAAGGATGATCTTCCGCAGGATTCTATAGCTGATGGAATTGAGAATGATGAC 60
TNO1     1   ATGCACGAGAAGGATGATCTTCCGCAGGATTCTATAGCTGATGGAATTGAGAATGATGAC 60
TAIR seq 61  GAGTCTAATGGGCAAGAAGAAGAAGAGCTTGATCCTGACCAGGGAACAGCTTTCGTTGAT 120
TNO1     61  GAGTCTAATGGGCAAGAAGAAGAAGAGCTTGATCCTGACCAGGGAACAGCTTTCGTTGAT 120
TAIR seq 121 AGTAAGGAAGATATGTTTGTTGATGCTCCTGAAGAGTTGAATTTTGATACACCTAGCAAG 180
TNO1     121 AGTAAGGAAGATATGTTTGTTGATGCTCCTGAAGAGTTGAATTTTGATACACCTAGCAAG 180
TAIR seq 181 GAAGCTCTTACCACAGATGACGATGATAATGATGACCTTGGAACTCATTTCAATATTGAG 240
TNO1     181 GAAGCTCTTACCACAGATGACGATGATAATGATGACCTTGGAACTCATTTCAATATTGAG 240
TAIR seq 241 AAGGGGGATTGGGAGAAGGAACTTGCAGGGCTTCAGGAGCAGTTTAAGCTGTTGACTGGT 300
TNO1     241 AAGGGGGATTGGGAGAAGGAACTTGCAGGGCTTCAGGAGCAGTTTAAGCTGTTGACTGGT 300
TAIR seq 301 GAGAATGATTTGACAGGTGAAGATGGGAACACTACTGTGGATATTGTCAGTCGCTTCTCG 360
TNO1     301 GAGAATGATTTGACAGGTGAAGATGGGAACACTACTGTGGATATTGTCAGTCGCTTCTCG 360
TAIR seq 361 AAGTTCTTAAAAACTGCCAAGGAAGAGCGGATTCAGCATGAGGTTGCACTCAAGGAGCTT 420
TNO1     361 AAGTTCTTAAAAACTGCCAAGGAAGAGCGGATTCAGCATGAGGTTGCACTCAAGGAGCTT 420
TAIR seq 421 CACGGGGTTATTAGTGGGAGGGACGATGAGATTGCTGATCTCACCACAAAAATCTCTGAG 480
TNO1     421 CACGGGGTTATTAGTGGGAGGGACGATGAGATTGCTGATCTCACCACAAAAATCTCTGAG 480
TAIR seq 481 CTTTCTTCGTCGCAGCCGGTTTCCGAAATGGGTGATCAGGCACAGAACTTGGAGCACCTT 540
TNO1     481 CTTTCTTCGTCGCAGCCGGTTTCCGAAATGGGTGATCAGGCACAGAACTTGGAGCACCTT 540
TAIR seq 541 GAGGCTGCAACGGATAGGATTATGGTTTCTCTTAGTAATGTATTTGGGGAAGGGGAGTTG 600
TNO1     541 GAGGCTGCAACGGATAGGATTATGGTTTCTCTTAGTAATGTATTTGGGGAAGGGGAGTTG 600
TAIR seq 601 CAGTATGGTTCTTCTATCTCTGAAAAGCTTGCTCATCTGGAGAACCGAGTTTCGTTTTTA 660
TNO1     601 CAGTATGGTTCTTCTATCTCTGAAAAGCTTGCTCATCTGGAGAACCGAGTTTCGTTTTTA 660
TAIR seq 661 GGTGCAAAGTATACTGAGTTTTACTATGGTGCTGATCAGTTAAGGAAGTGTTTGGCTAGT 720
TNO1     661 GGTGCAAAGTATACTGAGTTTTACTATGGTGCTGATCAGTTAAGGAAGTGTTTGGCTAGT 720
TAIR seq 721 GATGTGTTGGATCTTAGTTTCCAAGAGGATTTTGGTTCAGCTCTTGGTGCTGCTTGTTCT 780
TNO1     721 GATGTGTTGGATCTTAGTTTCCAAGAGGATTTTGGTTCAGCTCTTGGTGCTGCTTGTTCT 780
TAIR seq 781 GAGCTATTTGAGCTCAAACAGAAGGAAGCAGCCTTTTTTGAAAGACTTAGTCATCTAGAA 840
TNO1     781 GAGCTATTTGAGCTCAAACAGAAGGAAGCAGCCTTTTTTGAAGGACTTAGTCATCTAGAA 840
TAIR seq 841 GATGAGAATAGGAACTTTGTTGAACAAGTGAACAGAGAGAAAGAAATGTGTGAGTCAATG 900
TNO1     841 GATGAGAATAGGAACTTTGTTGAACAAGTGAACAGAGAGAAAGAAATGTGTGAGTCAATG 900
TAIR seq 901 AGAACAGAATTTGAAAAATTGAAGGCAGAGCTTGAGCTAGAAAAGACTAAGTGTACTAAC 960
TNO1     901 AGAACAGAATTTGAAAAATTGAAGGCAGAGCTTGAGCTAGAAAAGACTAAGTGTACTAAC 960
TAIR seq 961 ACAAAAGAAAAGCTCAGCATGGCCGTAACAAAGGGGAAGGCGTTAGTTCAGAACCGGGAT 1020
TNO1     961 ACAAAAGAAAAGCTCAGCATGGCCGTAACAAAGGGGAAGGCGTTAGTTCAGAACCGGGAT 1020
```

```
TAIR seq 1021 GCTCTGAAGCATCAATTGTCTGAAAAAACAACAGAGCTTGCGAATAGGTTGACTGAATTA 1080
TNO1     1021 GCTCTGAAGCATCAATTGTCTGAAAAAACAACAGAGCTTGCGAATAGGTTGACTGAATTA 1080
TAIR seq 1081 CAAGAGAAGGAGATTGCCCTTGAAAGTTCTGAAGTAATGAAGGGGCAGCTGGAACAATCG 1140
TNO1     1081 CAAGAGAAGGAGATTGCCCTTGAAAGTTCTGAAGTAATGAAGGGGCAGCTGGAACAATCG 1140
TAIR seq 1141 TTAACCGAAAAGACGGATGAACTTGAGAAATGCTATGCTGAATTGAATGATAGGTCCGTA 1200
TNO1     1141 TTAACCGAAAAGACGGATGAACTTGAGAAATGCTATGCTGAATTGAATGATAGGTCCGTA 1200
TAIR seq 1201 TCCCTGGAAGCATATGAGCTAACAAAGAAGGAGTTGGAACAGTCTCTGGCTGAAAAAACA 1260
TNO1     1201 TCCCTGGAAGCATATGAGCTAACAAAGAAGGAGTTGGAACAGTCTCTGGCTGAAAAAACA 1260
TAIR seq 1261 AAAGAACTTGAAGAGTGTTTGACGAAACTACAAGAGATGTCAACAGCATTGGATCAATCT 1320
TNO1     1261 AAAGAACTTGAAGAGTGTTTGACGAAACTACAAGAGATGTCAACAGCATTGGATCAATCT 1320
TAIR seq 1321 GAACTCGACAAAGGCGAGTTAGCAAAATCCGATGCTATGGTTGCATCATATCAGGAAATG 1380
TNO1     1321 GAACTCGACAAAGGCGAGTTAGCAAAATCCGATGCTATGGTTGCATCATATCAGGAAATG 1380
TAIR seq 1381 TTATCGGTGAGGAACTCTATCATTGAAAATATTGAAACTATCCTGTCAAACATATATACA 1440
TNO1     1381 TTATCGGTGAGGAACTCTATCATTGAAAATATTGAAACTATCCTGTCAAACATATATACA 1440
TAIR seq 1441 CCTGAAGAAGGTCACTCTTTTGATATCGTTGAAAAAGTAAGGTCACTTGCAGAAGAGAGG 1500
TNO1     1441 CCTGAAGAAGGTCACTCTTTTGATATCGTTGAAAAAGTAAGGTCACTTGCAGAAGAGAGG 1500
TAIR seq 1501 AAAGAGCTCACAAATGTTTCCCAGGAATACAACAGACTAAAAGATTTGATCGTTTCCATT 1560
TNO1     1501 AAAGAGCTCACAAATGTTTCCCAGGAATACAACAGACTAAAAGATTTGATCGTTTCCATT 1560
TAIR seq 1561 GACTTACCAGAGGAGATGTCCCAATCCAGCTTAGAAAGTCGCCTAGCTTGGCTTAGAGAA 1620
TNO1     1561 GACTTACCAGAGGAGATGTCCCAATCCAGCTTAGAAAGTCGCCTAGCTTGGCTTAGAGAA 1620
TAIR seq 1621 TCTTTTCTCCAGGGAAAAGATGAAGTTAATGCCTTGCAAAACCGGATTGAAAGTGTAAGC 1680
TNO1     1621 TCTTTTCTCCAGGGAAAAGATGAAGTTAATGCCTTGCAAAACCGGATTGAAAGTGTAAGC 1680
TAIR seq 1681 ATGTCTCTTTCAGCAGAAATGGAGGAGAAAAGTAACATTAGAAAGGAACTGGATGATTTA 1740
TNO1     1681 ATGTCTCTTTCAGCAGAAATGGAGGAGAAAAGTAACATTAGAAAGGAACTGGATGATTTA 1740
TAIR seq 1741 AGTTTCAGTTTGAAAAAAATGGAGGAAACTGCAGAGCGAGGTTCGTTGGAGAGGGAGGAA 1800
TNO1     1741 AGTTTCAGTTTGAAAAAAATGGAGGAAACTGCAGAGCGAGGTTCGTTGGAGAGGGAGGAA 1800
TAIR seq 1801 ATTGTGAGGAGACTTGTGGAAACCTCTGGCTTGATGACAGAAGGAGTCGAAGATCATACT 1860
TNO1     1801 ATTGTGAGGAGACTTGTGGAAACCTCTGGCTTGATGACAGAAGGAGTCGAAGATCATACT 1860
TAIR seq 1861 TCTTCAGATATCAATTTACTTGTTGATAGATCATTCGACAAGATAGAAAAGCAAATCAGG 1920
TNO1     1861 TCTTCAGATATCAATTTACTTGTTGATAGATCATTCGACAAGATAGAAAAGCAAATCAGG 1920
TAIR seq 1921 GATTCTAGTGATAGTTCTTATGGCAACGAAGAAATATTTGAAGCCTTTCAAAGTCTCCTT 1980
TNO1     1921 GATTCTAGTGATAGTTCTTATGGCAACGAAGAAATATTTGAAGCCTTTCAAAGTCTCCTT 1980
TAIR seq 1981 TATGTGAGAGATCTGGAGTTTTCACTTTGTAAGGAAATGCTAGGAGAGGGAGAGCTGATT 2040
TNO1     1981 TATGTGAGAGATCTGGAGTTTTCACTTTGTAAGGAAATGCTAGGAGAGGGAGAGCTGATT 2040
TAIR seq 2041 AGCTTTCAGGTAAGCAATCTCTCAGATGAGCTAAAGATCGCATCTCAAGAACTTGCTTTC 2100
```

```
TNO1      2041 AGCTTTCAGGTAAGCAATCTCTCAGATGAGCTAAAGATCGCATCTCAAGAACTTGCTTTC 2100
TAIR seq  2101 GTGAAAGAAGAAAAAATTGCTTTGGAGAAAGATCTAGAGCGATCAGAGGAGAAATCTGCT 2160
TNO1      2101 GTGAAAGAAGAAAAAATTGCTTTGGAGAAAGATCTAGAGCGATCAGAGGAGAAATCTGCT 2160
TAIR seq  2161 TTGCTCAGAGACAAACTTTCTATGGCTATCAAGAAAGGCAAGGGACTAGTCCAAGATAGG 2220
TNO1      2161 TTGCTCAGAGACAAACTTTCTATGGCTATCAAGAAAGGCAAGGGACTAGTCCAAGATAGG 2220
TAIR seq  2221 GAAAAGTTTAAAACTCAGTTGGATGAGAAAAAATCTGAAATCGAAAAGCTGATGCTCGAG 2280
TNO1      2221 GAAAAGTTTAAAACTCAGTTGGATGAGAAAAAATCTGAAATCGAAAAGCTGATGCTCGAG 2280
TAIR seq  2281 TTGCAGCAGCTAGGTGGTACGGTTGATGGCTACAAGAATCAGATAGATATGTTATCGAGA 2340
TNO1      2281 TTGCAGCAGCTAGGTGGTACGGTTGATGGCTACAAGAATCAGATAGATATGTTATCGAGA 2340
TAIR seq  2341 GACTTAGAGCGCACGAAAGAGCTAGAGACTGAGCTTGTTGCTACTAAAGAAGAAAGAGAT 2400
TNO1      2341 GACTTAGAGCGCACGAAAGAGCTAGAGACTGAGCTTGTTGCTACTAAAGAAGAAAGAGAT 2400
TAIR seq  2401 CAACTTCAGCAATCCTTATCTCTAATTGACACGTTGTTGCAGAAAGTGATGAAATCAGTT 2460
TNO1      2401 CAACTTCAGCAATCCTTATCTCTAATTGACACGTTGTTGCAGAAAGTGATGAAATCAGTT 2460
TAIR seq  2461 GAAATTATAGCTCTCCCTGTTGATCTAGCATCTGAAGATCCTTCAGAAAAGATTGACCGA 2520
TNO1      2461 GAAATTATAGCTCTCCCTGTTGATCTAGCATCTGAAGATCCTTCAGAAAAGATTGACCGA 2520
TAIR seq  2521 CTTGCTGGGTACATCCAAGAAGTGCAGCTGGCTAGAGTAGAGGAACAAGAAGAAATAGAA 2580
TNO1      2521 CTTGCTGGGTACATCCAAGAAGTGCAGCTGGCTAGAGTAGAGGAACAAGAAGAAATAGAA 2580
TAIR seq  2581 AAAGTAAAGTCAGAAGTTGATGCGTTAACCAGTAAATTAGCAGAAACCCAAACAGCCCTG 2640
TNO1      2581 AAAGTAAAGTCAGAAGTTGATGCGTTAACCAGTAAATTAGCAGAAACCCAAACAGCCCTG 2640
TAIR seq  2641 AAGTTGGTTGAGGATGCCTTGTCTACTGCAGAGGATAACATCAGTCGGCTTACTGAGGAG 2700
TNO1      2641 AAGTTGGTTGAGGATGCCTTGTCTACTGCAGAGGATAACATCAGTCGGCTTACTGAGGAG 2700
TAIR seq  2701 AATAGAAATGTCCAAGCTGCCAAGGAAAATGCTGAGCTTGAGCTGCAAAAAGCAGTTGCA 2760
TNO1      2701 AATAGAAATGTCCAAGCTGCCAAGGAAAATGCTGAGCTTGAGCTGCAAAAAGCAGTTGCA 2760
TAIR seq  2761 GATGCCTCCTCTGTAGCTAGCGAACTGGATGAAGTTCTTGCAACCAAAAGCACACTTGAA 2820
TNO1      2761 GATGCCTCCTCTGTAGCTAGCGAACTGGATGAAGTTCTTGCAACCAAAAGCACACTTGAA 2820
TAIR seq  2821 GCTGCACTCATGCAGGCTGAAAGAAATATATCTGATATTATTAGTGAAAAGGAAGAGGCT 2880
TNO1      2821 GCTGCACTCATGCAGGCTGAAAGAAATATATCTGATATTATTAGTGAAAAGGAAGAGGCT 2880
TAIR seq  2881 CAAGGCAGAACTGCTACTGCAGAGATGGAGCAAGAGATGCTGCAAAAAGAAGCTTCAATT 2940
TNO1      2881 CAAGGCAGAACTGCTACTGCAGAGATGGAGCATGAGATGCTGCAAAAAGAAGCTTCAATT 2940
TAIR seq  2941 CAGAAGAACAAATTAACAGAAGCACATAGCACCATAAATTCACTTGAAGAAACACTTGCT 3000
TNO1      2941 CAGAAGAACAAATTAACAGAAGCACATAGCACCATAAATTCACTTGAAGAAACACTTGCT 3000
TAIR seq  3001 CAGACAGAAAGCAACATGGATTCGCTGTCCAAACAAATTGAAGATGACAAAGTTCTTACT 3060
TNO1      3001 CAGACAGAAAGCAACATGGATTCGCTGTCCAAACAAATTGAAGATGACAAAGTTCTTACT 3060
TAIR seq  3061 ACAAGTTTAAAGAATGAGTTAGAGAAGCTTAAAATTGAGGCAGAATTTGAGCGTAACAAG 3120
TNO1      3061 ACAAGTTTAAAGAATGAGTTAGAGAAGCTTAAAATTGAGGCAGAATTTGAGCGTAACAAG 3120
```

```
TAIR seq 3121 ATGGCCGAAGCTTCCTTGACAATAGTATCCCATGAGGAGGCACTAATGAAGGCAGAGAAT 3180
TNO1     3121 ATGGCCGAAGCTTCCTTGACAATAGTATCCCATGAGGAGGCACTTATGAAKGCAGAGAAT 3180
TAIR seq 3181 AGTCTTTCTGCTTTACAAGGAGAAATGGTGAAAGCTGAAGGCGAGATATCAACTCTCAGT 3240
TNO1     3181 AGTCTTTCTGCTTTACAAGGAGAAATGGTGAAAGCTGAAGGCGAGATATCAACTCTCAGT 3240
TAIR seq 3241 AGTAAACTTAATGTATGCATGGAAGAGTTAGCTGGATCAAGCGGAAACTCACAGAGTAAA 3300
TNO1     3241 AGTAAACTTAATGTATGCATGGAAGAGTTAGCTGGATCAAGCGGAAACTCACAGAGTAAA 3300
TAIR seq 3301 TCTTTGGAGATTATTACTCATCTTGATAATCTCCAGATGCTACTGAAGGATGGAGGTCTA 3360
TNO1     3301 TCTTTGGAGATTATTACTCATCTTGATAATCTCCAGATGCTACTGAAGGATGGAGGKCTA 3360
TAIR seq 3361 ATTTCCAAGGTGAATGAATTCCTTCAAAGGAAGTTCAAGAGCCTTAGAGACGTGGATGTC 3420
TNO1     3361 ATTTCCAAGGTGAATGAATTCCTTCAAAGGAAGTTCAAGAGCCTTAGAGACGTGGATGTC 3420
TAIR seq 3421 ATTGCTAGAGATATCACACGAAATATTGGTGAGAATGGATTATTGGCAGGGGAAATGGGC 3480
TNO1     3421 ATTGCTAGAGATATCACACGAAATATTGGTGAGAATGGATTATTGGCAGGGGAAATGGGC 3480
TAIR seq 3481 AACGCTGAGGATGATTCGACTGAGGCAAAATCGTTGTTGAGTGACCTTGATAATTCAGTG 3540
TNO1     3481 AACGCTGAGGATGATTCGACTGAGGCAAAATCGTTGTTGAGTGACCTTGATAATTCAGTG 3540
TAIR seq 3541 AACACAGAGCCGGAGAATAGTCAAGGGAGTGCAGCTGATGAAGACGAAATTTCTTCATCC 3600
TNO1     3541 AACACAGAGCCGGAGAATAGTCAAGGGAGTGCAGCTGATGAAGACGAAATTTCTTCATCC 3600
TAIR seq 3601 CTTAGGAAGATGGCAGAGGGGGTCAGGCTGAGAAACAAAACCCTCGAGAATAACTTTGAG 3660
TNO1     3601 CTTAGGAAGATGGCAGAGGGGGTCAGGCTGAGAAACAAAACCCTCGAGAATAACTTTGAG 3660
TAIR seq 3661 GGTTTCTCAACTTCCATTGATACTCTCATAGCGACTTTGATGCAAAACATGACAGCAGCT 3720
TNO1     3661 GGTTTCTCAACTTCCATTGATACTCTCATAGCGACTTTGATGCAAAACATGACAGCAGCT 3720
TAIR seq 3721 AGGGCTGATGTGTTAAATATCGTGGGTCATAATTCATCCTTGGAAGAACAGGTGAGGAGT 3780
TNO1     3721 AGGGCTGATGTGTTAAATATCGTGGGTCATAATTCATCCTTGGAAGAACAGGTGAGGAGT 3780
TAIR seq 3781 GTGGAAAATATTGTTCGTGAACAGGAGAACACTATATCTGCATTACAAAAAGATTTGTCA 3840
TNO1     3781 GTGGAAAATATTGTTCGTGAACAGGAGAACACTATATCTGCATTACAAAAAGATTTGTCA 3840
TAIR seq 3841 TCTTTGATATCTGCATGTGGTGCGGCTGCCAGAGAACTGCAGTTGGAAGTGAAAAATAAC 3900
TNO1     3841 TCTTTGATATCTGCATGTGGTGCGGCTGCCAGAGAACTGCAGTTGGAAGTGAAAAATAAC 3900
TAIR seq 3901 CTCTTAGAGTTGGTTCAATTCCAAGAAAATGAAAACGGTGGTGAGATGGAATCAACTGAA 3960
TNO1     3901 CTCTTAGAGTTGGTTCAATTCCAAGAAAATGAAAACGGTGGTGAGATGGAATCAACTGAA 3960
TAIR seq 3961 GACCCACAGGAGCTTCATGTAAGTGAATGCGCCCAAAGGATAAAAGAATTATCTTCTGCC 4020
TNO1     3961 GACCCACAGGAGCTTCATGTAAGTGAATGCGCCCAAAGGATAAAAGAATTATCTTCTGCC 4020
TAIR seq 4021 GCAGAGAAGGCATGTGCTACTCTTAAACTCTTTGAGACAACAAATAATGCAGCTGCCACT 4080
TNO1     4021 GCAGAGAAGGCATGTGCTACTCTTAAACTCTTTGAGACAACAAATAATGCAGCTGCCACT 4080
TAIR seq 4081 GTAATCCGAGATATGGAGAACAGGCTAACAGAAGCATCTGTCGCTCTAGAAAAGGCTGTG 4140
TNO1     4081 GTAATCCGAGATATGGAGAACAGGCTAACAGAAGCATCTGTCGCTCTAGAAAAGGCTGTG 4140
```

```
TAIR seq 4141 TTAGAAAGAGATCTAAACCAAACTAAGGTTTCAAGTTCTGAGGCCAAGG~~~~~~~~~~~ 4200
TNO1     4141 TTAGAAAGAGATCTAAACCAAACTAAGGTTTCAAGTTCTGAGGCCAAGGTGGAATCTCTG 4200
TAIR seq 4201 ~~~~~~~~~~~~~~~~~~~~~~~~~~~~~~~~~~~~~~~~~~~~~~~~~~~~AAGAGAAA 4260
TNO1     4201 GAAGAGCTTCGCCAAGACCTGAAACTTCAGTTGGAAAATCTCAGAGTGAAGGAAGAGAAA 4260
TAIR seq 4261 TGGCATGAAAAAGAGGTGGAACTGTCTACGTTATATGATAAACTATTGGTGCAAGAGCAA 4320
TNO1     4261 TGGCATGAAAAAAAGGTGGAACTGTCTACGTTATATGATAAACTATTGGTGCAAGAGCAA 4320
TAIR seq 4321 GAGGCAAAGGAAAATCTAATTCCAGCTTCTGATATGCGAACCCTTTTTGACAAAATAAAT 4380
TNO1     4321 GAGGCAAAGGAACATCTAATTCCAGCTTCTGATATGCGAACCCTTTTTGACAAAATAAAT 4380
TAIR seq 4381 GGTATTGAAGTGCCATCAGTAGATCTAGTCAACGGATTAGATCCACAGAGTCCATATGAT 4440
TNO1     4381 GGTATTGAAGTGCCATCAGTAGATCTAGTCAACGGATTAGATCCACAGAGTCCATATGAT 4440
TAIR seq 4441 GTGAAGAAGCTATTCGCGATTGTTGATAGTGTTACTGAGATGCAGCATCAGATAGACATC 4500
TNO1     4441 GTGAAAAAGCTATTCGCGATTGTTGATAGTGTTACTGAGATGCAGCATCAGATAGACATC 4500
TAIR seq 4501 TTATCATATGGACAAAAAGAGCTCAATTCTACTTTGGCAGAAAAGGATCTTGAAATTCAA 4560
TNO1     4501 TTATCATATGGACAAAAAGAGCTCAATTCTACTTTGGCAGAAAAGGATCTTGAAATTCAA 4560
TAIR seq 4561 GGTCTAAAGAAGGCGACTGAAGCAGAGAGTACGACCGAGCTAGAGTTAGTGAAGGCAAAG 4620
TNO1     4561 GGTCTAAAGAAGGCGACTGAAGCAGAGAGTACGACCGAGCTAGAGTTAGTGAAGGCAAAG 4620
TAIR seq 4621 AATGAACTGTCCAAGCTAATATCTGGCTTGGAAAAACTGCTGGGTATATTGGCAAGCAAT 4680
TNO1     4621 AATGAACTGTCCAAGCTAATATCTGGCTTGGAAAAACTGCTGGGTATATTGGCAAGCAAT 4680
TAIR seq 4681 AATCCTGTTGTAGACCCAAACTTCTCCGAGTCATGGACACTCGTACAAGCACTAGAAAAA 4740
TNO1     4681 AATCCTGTTGTAGACCCAAACTTCTCCGAGTCATGGACACTCGTACAAGCACTAGAAAAA 4740
TAIR seq 4741 AAGATAACTTCCCTTCTCCTAGAATCAGAGAGTTCAAAATCAAGGGCCCAAGAACTTGGT 4800
TNO1     4741 AAGATAACTTCCCTTCTCCTAGAATCAGAGAGTTCAAAATCAAGGGCCCAAGAACTTGGT 4800
TAIR seq 4801 TTAAAGTTGGCCGGTAGCGAGAAACTTGTCGATAAACTATCATTAAGAGTCAAAGAGTTT 4860
TNO1     4801 TTAAAGTTGGCCGGTAGCGAGAAACTTGTCGATAAACTATCATTAAGAGTCAAAGAGTTT 4860
TAIR seq 4861 GAAGAGAAACTTCAAACCAAAGCAATTCAGCCTGATATTGTTCAAGAAAGAAGCATCTTC 4920
TNO1     4861 GAAGAGAAACTTCAAACCAAAGCAATTCAGCCTGATATTGTTCAAGAAAGAAGCATCTTC 4920
TAIR seq 4921 GAAACACCGAGAGCACCTTCTACCTCAGAGATATCCGAGATTGAGGACAAGGGAGCCTTG 4980
TNO1     4921 GAAACACCGAGAGCACCTTCTACCTCAGAGATATCCGAGATTGAGGACAAGGGAGCCTTG 4980
TAIR seq 4981 GGAATAAAATCAATATCACCGGTGCCTACAGCAGCACAAGTGAGAACAGTGAGGAAGGGA 5040
TNO1     4981 GGAATAAAATCAATATCACCGGTGCCTACAGCAGCACAAGTGAGAACAGTGAGGAAGGGA 5040
TAIR seq 5041 TCGACGGATCATCTTTCAATCAACATAGATTCAGAGTCCGAGCATCTGATGAACAACAAC 5100
TNO1     5041 TCGACGGATCATCTTTCAATCAACATAGATTCAGAGTCCGAGCATCTGATGAACAACAAC 5100
TAIR seq 5101 GAAACAGATGAAGATAAAGGACATGTTTTCAAGTCTCTCAACATGTCTGGTCTGATTCCA 5160
TNO1     5101 GAAACAGATGAAGATAAAGGACATGTTTTCAAGTCTCTCAACATGTCTGGTCTGATTCCA 5160
```

```
TAIR seq 5161 ACGCAAGGAAAGATAATAGCAGATCGGGTTGATGGAATATGGGTCTCAGGTGGAAGAGTA 5220
TNO1     5161 ACGCAAGGAAAGATAATAGCAGATCGGGTTGATGGAATATGGGTCTCAGGTGGAAGAGTA 5220
TAIR seq 5221 TTGATGAGCCGTCCTCAAGCAAGGCTTGGCGTTATGGTATACAGTCTCTTATTGCATCTG 5280
TNO1     5221 TTGATGAGCCGTCCTCAAGCAAGGCTTGGCGTTATGGTATACAGTCTCTTATTGCATCTG 5280
TAIR seq 5281 TGGCTCCTAGCCTCCATCTTGTAA 5304
TNO1     5281 TGGCTCCTAGCCTCCATCTTGTAA 5304
```

Supplementary Fig 1B. TNO1 amino acid sequence

```
TAIR seq 1   MHEKDDLPQDSIADGIENDDESNGQEEEELDPDQGTAFVDSKEDMFVDAPEELNFDTPSK 60
TNO1     1   MHEKDDLPQDSIADGIENDDESNGQEEEELDPDQGTAFVDSKEDMFVDAPEELNFDTPSK 60
TAIR seq 61  EALTTDDDDNDDLGTHFNIEKGDWEKELAGLQEQFKLLTGENDLTGEDGNTTVDIVSRFS 120
TNO1     61  EALTTDDDDNDDLGTHFNIEKGDWEKELAGLQEQFKLLTGENDLTGEDGNTTVDIVSRFS 120
TAIR seq 121 KFLKTAKEERIQHEVALKELHGVISGRDDEIADLTTKISELSSSQPVSEMGDQAQNLEHL 180
TNO1     121 KFLKTAKEERIQHEVALKELHGVISGRDDEIADLTTKISELSSSQPVSEMGDQAQNLEHL 180
TAIR seq 181 EAATDRIMVSLSNVFGEGELQYGSSISEKLAHLENRVSFLGAKYTEFYYGADQLRKCLAS 240
TNO1     181 EAATDRIMVSLSNVFGEGELQYGSSISEKLAHLENRVSFLGAKYTEFYYGADQLRKCLAS 240
TAIR seq 241 DVLDLSFQEDFGSALGAACSELFELKQKEAAFFERLSHLEDENRNFVEQVNREKEMCESM 300
TNO1     241 DVLDLSFQEDFGSALGAACSELFELKQKEAAFFEGLSHLEDENRNFVEQVNREKEMCESM 300
TAIR seq 301 RTEFEKLKAELELEKTKCTNTKEKLSMAVTKGKALVQNRDALKHQLSEKTTELANRLTEL 360
TNO1     301 RTEFEKLKAELELEKTKCTNTKEKLSMAVTKGKALVQNRDALKHQLSEKTTELANRLTEL 360
TAIR seq 361 QEKEIALESSEVMKGQLEQSLTEKTDELEKCYAELNDRSVSLEAYELTKKELEQSLAEKT 420
TNO1     361 QEKEIALESSEVMKGQLEQSLTEKTDELEKCYAELNDRSVSLEAYELTKKELEQSLAEKT 420
TAIR seq 421 KELEECLTKLQEMSTALDQSELDKGELAKSDAMVASYQEMLSVRNSIIENIETILSNIYT 480
TNO1     421 KELEECLTKLQEMSTALDQSELDKGELAKSDAMVASYQEMLSVRNSIIENIETILSNIYT 480
TAIR seq 481 PEEGHSFDIVEKVRSLAEERKELTNVSQEYNRLKDLIVSIDLPEEMSQSSLESRLAWLRE 540
TNO1     481 PEEGHSFDIVEKVRSLAEERKELTNVSQEYNRLKDLIVSIDLPEEMSQSSLESRLAWLRE 540
TAIR seq 541 SFLQGKDEVNALQNRIESVSMSLSAEMEEKSNIRKELDDLSFSLKKMEETAERGSLEREE 600
TNO1     541 SFLQGKDEVNALQNRIESVSMSLSAEMEEKSNIRKELDDLSFSLKKMEETAERGSLEREE 600
TAIR seq 601 IVRRLVETSGLMTEGVEDHTSSDINLLVDRSFDKIEKQIRDSSDSSYGNEEIFEAFQSLL 660
TNO1     601 IVRRLVETSGLMTEGVEDHTSSDINLLVDRSFDKIEKQIRDSSDSSYGNEEIFEAFQSLL 660
TAIR seq 661 YVRDLEFSLCKEMLGEGELISFQVSNLSDELKIASQELAFVKEEKIALEKDLERSEEKSA 720
TNO1     661 YVRDLEFSLCKEMLGEGELISFQVSNLSDELKIASQELAFVKEEKIALEKDLERSEEKSA 720
TAIR seq 721 LLRDKLSMAIKKGKGLVQDREKFKTQLDEKKSEIEKLMLELQQLGGTVDGYKNQIDMLSR 780
TNO1     721 LLRDKLSMAIKKGKGLVQDREKFKTQLDEKKSEIEKLMLELQQLGGTVDGYKNQIDMLSR 780
TAIR seq 781 DLERTKELETELVATKEERDQLQQSLSLIDTLLQKVMKSVEIIALPVDLASEDPSEKIDR 840
```

```
TNO1      781 DLERTKELETELVATKEERDQLQQSLSLIDTLLQKVMKSVEIIALPVDLASEDPSEKIDR 840
TAIR seq  841 LAGYIQEVQLAR VEEQEEIEKVKSEVDALTSKLAETQTALKLVEDALSTAEDNISRLTEE 900
TNO1      841 LAGYIQEVQLAR VEEQEEIEKVKSEVDALTSKLAETQTALKLVEDALSTAEDNISRLTEE 900
TAIR seq  901 NRNVQAAKENAELELQKAVADASSVASELDEVLATKSTLEAALMQAERNISDIISEKEEA 960
TNO1      901 NRNVQAAKENAELELQKAVADASSVASELDEVLATKSTLEAALMQAERNISDIISEKEEA 960
TAIR seq  961 QGRTATAEMEQEMLQKEASIQKNKLTEAHSTINSLEETLAQTESNMDSLSKQIEDDKVLT 1020
TNO1      961 QGRTATAEMEHEMLQKEASIQKNKLTEAHSTINSLEETLAQTESNMDSLSKQIEDDKVLT 1020
TAIR seq 1021 TSLKNELEKLKIEAEFERNKMAEASLTIVSHEEALMKAENSLSALQGEMVKAEGEISTLS 1080
TNO1     1021 TSLKNELEKLKIEAEFERNKMAEASLTIVSHEEALMKAENSLSALQGEMVKAEGEISTLS 1080
TAIR seq 1081 SKLNVCMEELAGSSGNSQSKSLEIITHLDNLQMLLKDGGLISKVNEFLQRKFKSLRDVDV 1140
TNO1     1081 SKLNVCMEELAGSSGNSQSKSLEIITHLDNLQMLLKDGGLISKVNEFLQRKFKSLRDVDV 1140
TAIR seq 1141 IARDITRNIGENGLLAGEMGNAEDDSTEAKSLLSDLDNSVNTEPENSQGSAADEDEISSS 1200
TNO1     1141 IARDITRNIGENGLLAGEMGNAEDDSTEAKSLLSDLDNSVNTEPENSQGSAADEDEISSS 1200
TAIR seq 1201 LRKMAEGVRLRNKTLENNFEGFSTSIDTLIATLMQNMTAARADVLNIVGHNSSLEEQVR S 1260
TNO1     1201 LRKMAEGVRLRNKTLENNFEGFSTSIDTLIATLMQNMTAARADVLNIVGHNSSLEEQVR S 1260
TAIR seq 1261 VENIVREQENTISALQKDLSSLISACGAAARELQLEVKNNLLELVQFQENENGGEMESTE 1320
TNO1     1261 VENIVREQENTISALQKDLSSLISACGAAARELQLEVKNNLLELVQFQENENGGEMESTE 1320
TAIR seq 1321 DPQELHVSECAQRIKELSSAAEKACATLKLFETTNNAAATVIRDMENRLTEASVALEKAV 1380
TNO1     1321 DPQELHVSECAQRIKELSSAAEKACATLKLFETTNNAAATVIRDMENRLTEASVALEKAV 1380
TAIR seq 1381 LERDLNQTKVSSSEA--------------------KEEKWHEKEVELSTLYDKLLVQEQ 1440
TNO1     1381 LERDLNQTKVSSSEAKVESLEELRQDLKLQLENLRVKEEKWHEKKVELSTLYDKLLVQEQ 1440
TAIR seq 1441 EAKENLIPASDMRTLFDKINGIEVPSVDLVNGLDPQSPYDVKKLFAIVDSVTEMQHQIDI 1500
TNO1     1441 EAKEHLIPASDMRTLFDKINGIEVPSVDLVNGLDPQSPYDVKKLFAIVDSVTEMQHQIDI 1500
TAIR seq 1501 LSYGQKELNSTLAEKDLEIQGLKKATEAESTTELELVKAKNELSKLISGLEKLLGILASN 1560
TNO1     1501 LSYGQKELNSTLAEKDLEIQGLKKATEAESTTELELVKAKNELSKLISGLEKLLGILASN 1560
TAIR seq 1561 NPVVDPNFSESWTLVQALEKKITSLLLESESSKSRAQELGLKLAGSEKLVDKLSLRVKEF 1620
TNO1     1561 NPVVDPNFSESWTLVQALEKKITSLLLESESSKSRAQELGLKLAGSEKLVDKLSLRVKEF 1620
TAIR seq 1621 EEKLQTKAIQPDIVQERSIFETPRAPSTSEISEIEDKGALGIKSISPVPTAAQVRTVRKG 1680
TNO1     1621 EEKLQTKAIQPDIVQERSIFETPRAPSTSEISEIEDKGALGIKSISPVPTAAQVRTVRKG 1680
TAIR seq 1681 STDHLSINIDSESEHLMNNNETDEDKGHVFKSLNMSGLIPTQGKIIADRVDGIWVSGGRV 1740
TNO1     1681 STDHLSINIDSESEHLMNNNETDEDKGHVFKSLNMSGLIPTQGKIIADRVDGIWVSGGRV 1740
TAIR seq 1741 LMSRPQARLGVMVYSLLLHLWLLASIL 1767
TNO1     1741 LMSRPQARLGVMVYSLLLHLWLLASIL 1767
```

Supplementary Fig 1. Sequence analysis of *TNO1*

A. Comparison of cDNA sequence of *TNO1* with database

A deletion of 63 nt was found in the TAIR sequence. The extra exon in *TNO1* sequence is marked in red.

B. Comparison of amino acid sequence of *TNO1* with database.

The extra amino acids predicted by our sequence are marked in red, and the predicted transmembrane domain is marked in green. Nine peptides identified by tandom mass spectrometry are marked in Blue.

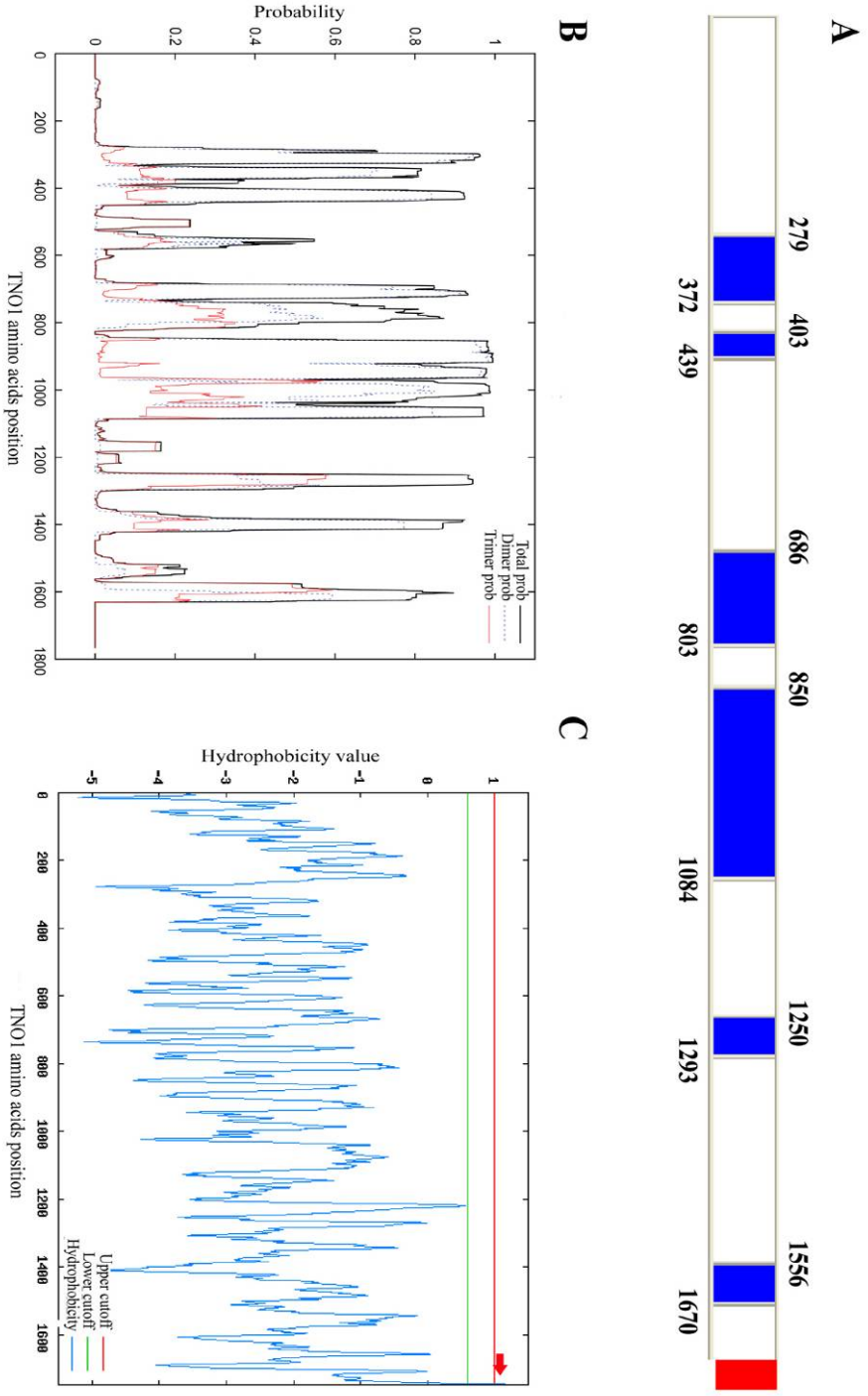

Supplementary Fig 2. TNO1 domain prediction

A. Position of coiled-coil domains and a *trans*-membrane domain

Positions are relative to the initiation amino acid. Blue boxes represent coiled-coil domains,

and the red box represents a transmembrane domain.

B. Probability of coiled-coil domain

Probability of coiled-coil domain is determined by Multicoil, coiled-coil domain prediction algorithm. Total probability, black solid line; dimer probability, black dotted line; trimer probability, red solid line.

C. Hydrophobicity value of TNO1

Hydrophobicity value of TNO1 is determined by Toppred, transmembrane topology prediction algorithm, and amino acids (1749-1767) are predicted to be a transmembrane domain.

Supplementary Fig 3A

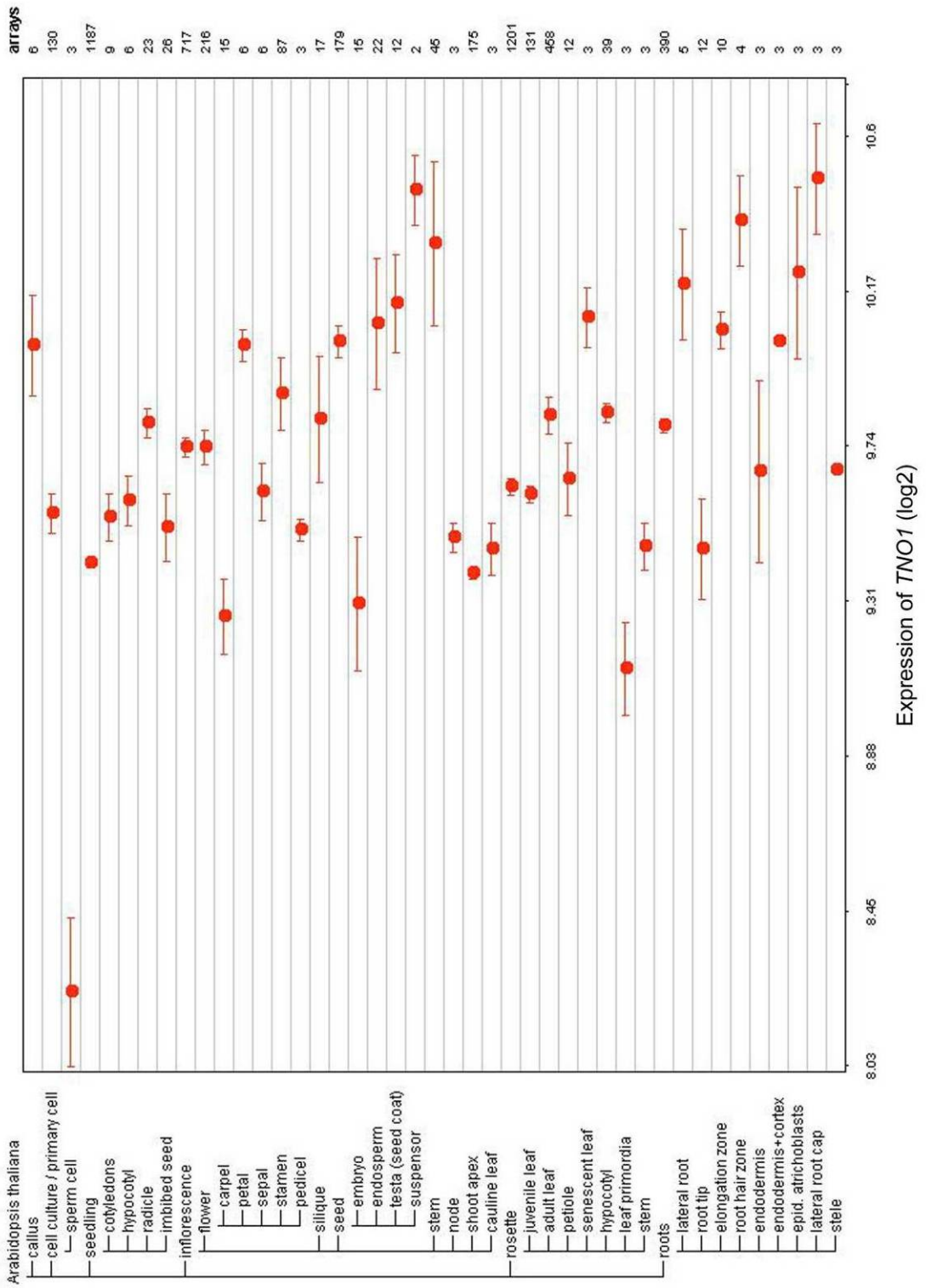

Supplementary Fig 3B

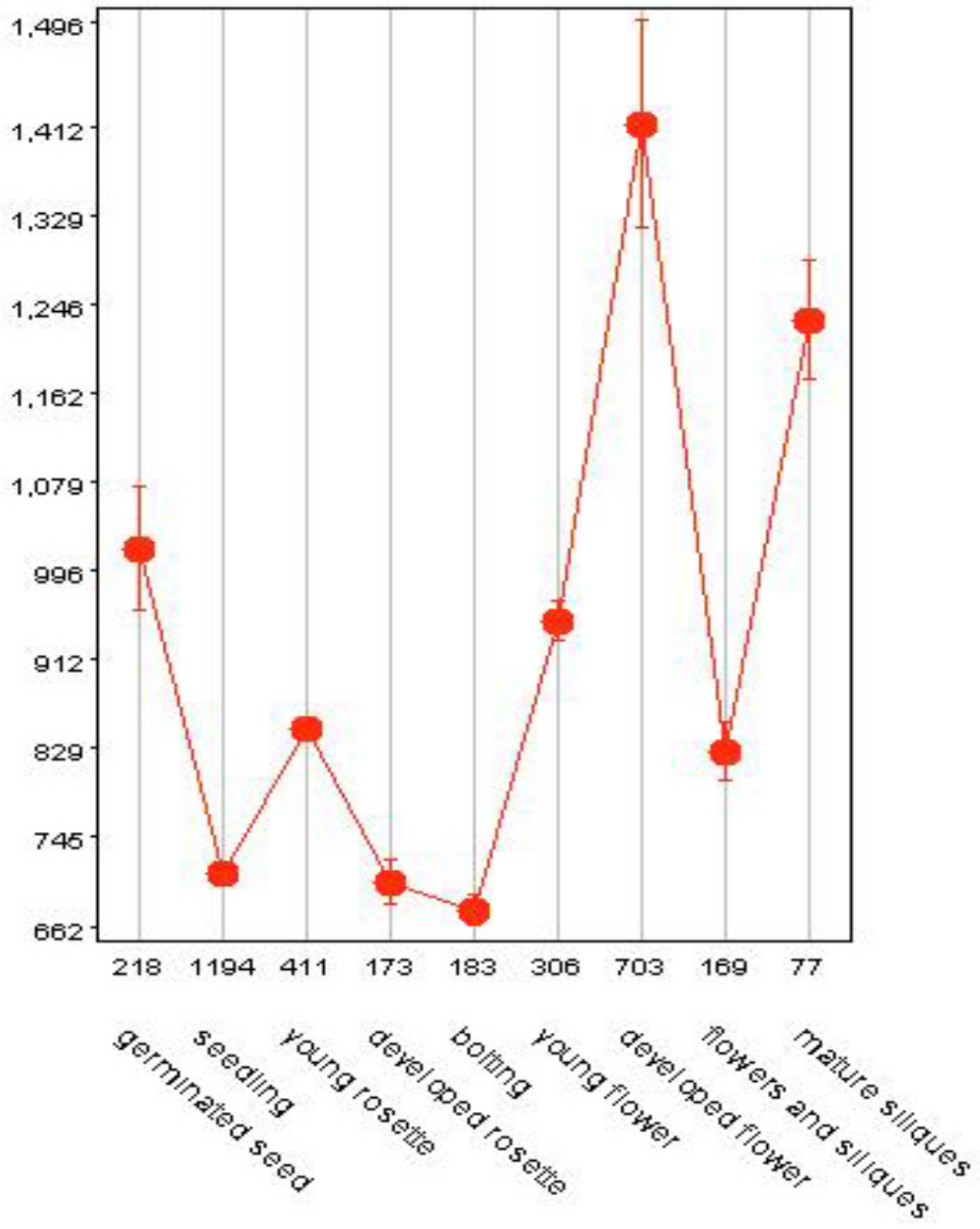

Supplementary Fig 3. Expression pattern of *TNO1* analyzed by microarray

A. Expression of TNO1 in diverse tissues in *Arabidopsis*

Expression of TNO1 in diverse tissues in Arabidopsis was determined by

GENEVESTIGATOR. The number of arrays used to determine the transcript level of *TNO1* is shown at right. The scale is logarithmic. Error bars indicate standard error.

B. Expression of TNO1 during development

Expression of TNO1 during development was determined by GENEVESTIGATOR. X-axis represents developmental stages and the number of arrays used to calculate the mean intensities are indicated. Y-axis represents the intensity of *TNO1* transcript. Error bars indicate standard error.

CHAPTER 3. CHARACTERIZATION OF SYP4 FAMILY PROTEINS IN VESICLE FUSION AND FUNCTIONAL REDUNDANCY OF VTI11 AND VTI12

A manuscript in preparation

Sang-Jin Kim[1,2] and Diane C Bassham[1,2,3]

[1]Department of Genetics, Development and Cell Biology, [2]Interdepartmental Genetics Program and [3]Plant Sciences Institute, Iowa State University, Ames, IA 50011, USA

Abstract

Vesicle fusion is an essential process for maintaining the structure and function of the endomembrane system. Fusion is mediated by t-SNARE fusion proteins on the target membrane and v-SNAREs on the vesicle membrane; v- and t-SNAREs interact with each other, driving vesicle fusion with the target membrane. The TGN resident SNAREs SYP41 and VTI12, along with YKT61/62, have been shown to function in vesicle fusion *in vitro*, consistent with immunoprecipitation results showing their interaction using *Arabidopsis* cell extract. Here we used a proteoliposome fusion assay to demonstrate that other proteins in the SYP4 and VTI1 families are also able to induce vesicle fusion. This result indicates that all members of the SYP4 family can also function with VTI12 in membrane fusion, and VTI11 can substitute for VTI12 in this reaction, explaining its partial functional redundancy *in vivo*. In addition, we have identified a role for an SM protein, AtVPS45, in membrane fusion. SM (Sec1/Munc18) proteins are known to regulate both the formation of SNARE complexes and

vesicle fusion. AtVPS45 interacts with SYP4 protein complexes via direct binding to SYP4 family proteins *in vitro*. Addition of AtVPS45 reduces the efficiency of membrane fusion between vesicles containing SYP4 and VTI1 family proteins, suggesting strong binding of AtVPS45 to SYP4 family proteins may inhibit membrane fusion between vesicles containing a SYP4 family protein and vesicles containing a VTI1 family protein. These results demonstrate that functional redundancy of VTI11 and regulation of vesicle fusion by VPS45 are mediated by interaction with SYP4 family SNAREs.

Introduction

The endomembrane system in plants has important roles throughout plant development, in responses to stress conditions and in defense responses (Zhu et al., 2002; Assaad et al., 2004; Leshem et al., 2006; Zhang et al., 2007). The endomembrane system consists of the endoplasmic reticulum, the Golgi apparatus, the *trans*-Golgi network (TGN), the prevacuolar compartment (PVC), the vacuole and endosomes. Transport between organelles of the endomembrane system is mediated by transport vesicles delivering appropriate proteins and lipids. The correct trafficking of vesicles requires a number of proteins that function in processes from vesicle budding to vesicle fusion (Sanderfoot and Raikhel, 1999).

N-ethylmaleimide-sensitive factor attachment protein receptor (SNARE) proteins have a central role in vesicle trafficking in the recognition of its target by a vesicle and fusion between vesicle and its target membranes (Sollner et al., 1993). SNAREs have a coiled-coil domain which interacts with other SNAREs and typically have a C-terminal integral membrane domain for anchoring into the membrane. There are two functional types

of SNAREs; v-SNAREs are inserted into the vesicular membrane, while t-SNAREs are located on the target membrane. SNAREs can be divided into 4 classes, Qa, Qb, Qc and R, depending on the presence of a conserved Q or R residue in their coiled-coil domain. Q-type SNAREs are usually located on the target membrane and R-type SNAREs are typically on the vesicular membrane (Bock et al., 2001). In general, three t-SNARE polypeptides form a *cis*-SNARE complex on the target membrane, which interacts with a v-SNARE on the vesicle via their coiled-coil domains, forming a four-helix *trans*-SNARE complex (Poirier et al., 1998). This *trans*-SNARE complex allows the vesicle to fuse with its target membrane and release its cargo. The *trans*-SNARE complex is formed only by the correct combination of v- and t-SNAREs, which provides fusion specificity (Paumet et al., 2004). The requirements for vesicle fusion have been studied extensively, and it has been demonstrated that SNARE complex formation is sufficient to drive membrane fusion in an *in vitro* proteoliposome fusion assay, suggesting that the SNAREs themselves form the core of the membrane fusion machinery (Weber et al., 1998; McNew et al., 2000; Chen et al., 2004; Chen et al., 2005).

The SYP4 family of SNAREs at the Arabidopsis TGN has 3 members, SYP41, SYP42 and SYP43. SYP41 and SYP42 were each found to interact with the t-SNARE SYP61 and v-SNARE VTI12 (Bassham et al., 2000). SYP41 and SYP42 are essential proteins in *Arabidopsis*, as *syp41* and *syp42* knockout single mutations are gametophyte lethal (Sanderfoot et al., 2001b). SYP43 has a high amino acid sequence identity to SYP41 and SYP42 (85% and 60%, respectively), but is not able to compensate for loss of SYP41 or SYP42 (Sanderfoot et al., 2001). Previously, YKT61/62, VTI12 and either SYP41 or SYP61 were found to be sufficient to drive liposome fusion *in vitro* (Chen et al., 2005). The

requirement for only three SNARE proteins in the fusion reaction also suggests that either a three-helix bundle may be formed at the Arabidopsis TGN or, more likely, two molecules of one component may be required to make four-helix bundle.

The *VTI1* family consists of four genes (*VTI11, VTI12, VTI13* and *VTI14*) in *Arabidopsis* (Zheng et al., 1999; Sanderfoot et al., 2000; Uemura et al., 2004). *VTI11* and *VTI12* are expressed, while *VTI13* is expressed at a lower level than *VTI11* and *VTI12*, and *VTI14* is only expressed in *Arabidopsis* suspension cell (Uemura et al., 2004). VTI11 and VTI12 have high amino acid sequence identity (60%), but they function in different trafficking pathways; VTI11 is involved in trafficking to the lytic vacuole, while VTI12 is involved in trafficking to the storage vacuole (Sanmartin et al., 2007). Mutant phenotypes of VTI11 and VTI12 are also distinct. A v*ti11* mutant shows defects in shoot gravitropism, whereas a *vti12* mutant is defective in the autophagy pathway and a *vti11/vti12* double mutant is lethal (Surpin et al., 2003; Yano et al., 2003). Although VTI11 and VTI12 have different functions in vacuolar trafficking, overexpressed VTI12 or a mutant of VTI12 that changes its specificity can substitute for VTI11 in the *vti11* mutant (Niihama et al., 2005), and VTI11 is also able to interact with SYP41 and SYP42 when VTI12 is not available (Surpin et al., 2003).

In addition, YKT61 and YKT62 have been identified as essential SNAREs involved in vesicle fusion *in vitro* (Chen et al., 2005). In yeast and mammalian cells, YKT6 is involved in vacuolar trafficking and recycling from endosomes to the TGN by interacting with Vti1p (Dilcher et al., 2001; Kweon et al., 2003; Fukasawa et al., 2004; Tai et al., 2004). In *Arabidopsis*, there are two proteins related to yeast Ykt6, and both of them are able to

drive membrane fusion with SYP41 and VTI12 *in vitro*, suggesting that they may be functionally redundant (Chen et al., 2005).

AtVPS45 is a Sec1/Munc18 type protein (SM protein) localized to the *Arabidopsis* TGN that interacts with SYP41 and SYP42 (Bassham et al., 2000). SM proteins regulate vesicle trafficking via binding to either the syntaxin-type SNAREs or to SNARE complexes (Carr et al., 1999; Dulubova et al., 1999; Misura et al., 2000; Bryant and James, 2001). A yeast homolog of AtVPS45 has been reported to positively regulate SNARE complex formation (Bryant and James, 2001; Dulubova et al., 2002; Carpp et al., 2007). In *Arabidopsis*, a decreased level of SYP41 was observed in a *siVPS45-1a* RNAi plant with reduced expression of AtVPS45, whereas there was no difference in transcript level compared with wild-type plants. This suggests that AtVPS45 could regulate vesicle fusion or SNARE complex formation mediated by SYP41 via stabilizing SYP41 at the TGN (Zouhar et al., 2009). Loss of AtVPS45 is lethal, and disruption of AtVPS45 expression by RNAi leads to defects in vacuolar trafficking and a dwarf phenotype caused by reduced cell size. A striking phenotype of the RNAi lines is the presence of multiple small vacuoles in hypocotyl and cotyledon cells instead of one large central vacuole, suggesting AtVPS45 may also be involved in vacuole biogenesis by affecting fusion between small vacuoles (Zouhar et al., 2009).

After *trans*-SNARE complex formation, the SNAREs are dissociated from the SNARE complex by *N*-ethylmaleimide sensitive factor (NSF) and soluble NSF attachment proteins (SNAP), and the v-SNARE is recycled back to its origin (Matveeva and Whiteheart, 1998). Yeast VPS45 has been reported to bind to *cis*-SNARE complexes after membrane fusion (Bryant and James, 2003). Then, the SNAREs are dissociated from the *cis*-SNARE

complex by NSF and SNAP, while VSP45 maintains its interaction with yeast SNARE Tlg2p. A SNARE complex containing the VPS45-bound Tlg2p forms again for the next round of vesicle fusion, and VPS45 dissociates either before or during *trans*-SNARE complex formation. This suggests it could be involved in disassembling the *cis*-SNARE complex consisting of three t-SNARE helices and one v-SNARE after vesicle fusion (Bryant and James, 2003). This disassembling of the *cis*-SNARE complex is an essential process to regenerate a three-helix t-SNARE bundle ready for fusion again. In addition, dissociation of VPS45 may also be required before completion of vesicle fusion.

Previously, we have shown that SYP41 and VTI12 along with YKT61/62 are able to drive liposome fusion (Chen et al., 2005). Here we show that SYP42 or SYP43 reconstituted into vesicles are also able to drive fusion with VTI12 containing vesicles. In addition, VTI11-containing vesicles are able to fuse with vesicles containing a SYP4 family member, indicating that functional redundancy between VTI11 and VTI12 is mediated by interaction with SYP4 family proteins. Addition of AtVPS45 to the liposome fusion assay containing reconstituted SYP4 and VTI1 family members partially inhibited the fusion process, suggesting AtVPS45 may inhibit efficient fusion, possibly due to its strong binding to SYP4 family proteins or inability to dissociate from *trans*-SNARE complexes.

Materials and Methods

Plasmid construction

Full-length SYP42, SYP43, VTI11, AtVPS45, MEMB11 and a soluble fragment of VTI11 (VTI11s, including amino acid sequence 1-200) were amplified by PCR using cDNAs generated from *Arabidopsis* seedlings and the following primers; SYP42 FP/RP,

SYP43 FP/RP, VTI11 FP/RP, AtVPS45 FP/RP, VTI11s FP/RP and MEMB11 FP/RP (Table 1). DNA fragments encoding SYP42 and SYP43 were digested using *NdeI* and *XhoI*. DNA fragments encoding VTI11, VPS45, VTI11s and MEMB11 were digested using *NdeI* and *HindIII*, *BamHI*, *BamHI* and *HindIII,* and *EcoRI* and *XhoI*, respectively, and ligated into pET28a expression vector (Novagen, Madison, WI) digested using the same restriction enzymes.

Protein expression and purification

Protein expression was performed as described in Chen et al. (2005) with minor changes. SYP41, SYP42, SYP43, VTI11, VTI12, VTI11s, VTI12s, YKT62, MEMB11 and AtVPS45 were expressed in *E. coli* strain BL21 (DE3) as N-terminal His_6-tagged proteins. Ten ml of an overnight culture were transferred to 500 ml Luria-Burtani media (LB broth) with 50 µg/ml kanamycin and 2 mg/ml glucose. Cells were grown at 37^{o}C until the OD600 reached 0.6. Isopropyl-ß-D-thiogalactopyranoside (IPTG) was added to 0.5 mM final concentration to induce expression, and cells were incubated for 5 h at 16^{o}C.

SYP41, VTI12s and YKT62 were purified according to Chen et al. (2005), and SYP42, SYP43, VTI11, VTI12, VTI11s, MEMB11 and AtVPS45 were purified with minor changes in the washing and elution steps. SYP42, SYP43 and VPS45 were eluted in elution buffer with 0.2% (v/v) Triton X-100 and VTI11s was purified in the same manner as VTI12s. VTI11, VTI12 and MEMB11 were washed sequentially using washing buffer I (50 mM NaH_2PO_4 (pH 8.0), 200 mM NaCl, 50 mM imidazole, 0.2% (v/v) Triton X-100), washing buffer II (50 mM Tris-HCl (pH 8.0), 300 mM NaCl, 50 mM imidazole, 0.2% (v/v) Triton X-100), washing buffer III (50 mM Tris-HCl (pH 8.0), 300 mM NaCl, 50 mM imidazole) and

washing buffer IV (50 mM Tris-HCl (pH 8.0), 300 mM NaCl, 50 mM imidazole, 0.8% (w/v) n-octylglucoside), followed by elution using elution buffer (50 mM Tris-HCl (pH 8.0), 300 mM NaCl, 300 mM imidazole, 0.8% (w/v) n-octylglucoside).

Immunoprecipitation

Ten μg each of the appropriate recombinant proteins were mixed in a total volume of 200 μl of phosphate-buffered saline containing 1 mM EDTA and 1% (v/v) Triton X-100 and incubated on ice for 1 h. The protein mixture was transferred to a pre-equilibrated 10 μl bed volume of protein A sepharose CL-4B (Amersham Pharmacia Biotech, Piscataway, NJ) with 5 μl of purified AtVPS45 antibody (Bassham and Raikhel, 1998), followed by incubation at 4^{o}C for 1 h with rocking. The resin was washed five times in the same buffer, and bound proteins were eluted using SDS-PAGE loading buffer. The immunoprecipitate was analyzed by SDS-PAGE and silver staining.

Preparation of lipid vesicles and membrane reconstitution

Preparation of lipid vesicles and reconstitution of proteins into vesicles were performed as described in Chen et al. (2005) except for proteins inserted into donor vesicles (VTI11, VTI12 and MEMB11). Donor vesicles containing fluorescent dyes were mixed with VTI11, VTI12 or MEMB11 at a 1:200 protein-to-lipid molar ratio and incubated at 4^{o}C for 30 minutes. The same volume of fusion assay buffer was added to the mixture, which was dialyzed overnight against fusion assay buffer with 4% (v/v) glycerol containing 1 g/l of Bio-beads SM-2 to remove the trace amount of detergent. The reconstitution efficiency was analyzed by SDS-PAGE and staining with Coomassie Blue (PageBlue, Fermentas, Glen

Burnie, MD). The amount of protein in vesicles was compared with a known concentration of protein before reconstitution using densitometry (GS-800 Calibrated Densitometer, Bio-Rad, Hercules, CA) and Quantity one software (Bio-Rad).

Removal of detergent from YKT62 and AtVPS45

The detergent in YKT62 and AtVPS45 samples was removed by adding 20 mg Bio-beads SM-2, followed by rocking at 4^{o}C for 30 min. Removal of detergent was repeated three times, followed by dialysis as described above.

Total lipid mixing assay

The donor and acceptor vesicles were mixed in a molar ratio of 1:9, and the same molar amount of YKT62 to SYP41, SYP42 or SYP43 was added to the mixture. The total lipid concentration was 0.5 mM and the total volume of the mixture was set to 100 µl. Fusion of donor vesicles with acceptor vesicles decreases quenching between rhodamine and NBD, measured as an increase in NBD fluorescence.

Fluorescence was measured at excitation and emission wavelengths of 465 and 530 nm, respectively. Fluorescence changes were recorded every 10 sec with a Varian Cary Eclipse model fluorescence spectrophotometer (Varian, Palo Alto, CA) with 2 mm path length at 25^{o}C for 10 min. The maximum fluorescence intensity (MFI) was achieved by adding 1 µl of 10% (v/v) Triton X-100.

Lipid mixing with VTI11s, VTI12s and AtVPS45

To inhibit fusion between donor and acceptor vesicles, a soluble version of VTI11 or VTI12 was added to the acceptor vesicles and incubated for 30 min at room temperature. The incubated acceptor vesicles were used for the lipid mixing assay as described above.

To investigate a role for AtVPS45 in membrane fusion, the same molar amounts of VPS45 and YKT62 to SYP41, SYP42 or SYP43 were added to acceptor vesicles and incubated for 1 h at 4^{o}C, followed by the lipid mixing assay with reconstituted donor vesicles.

Results

Expression of recombinant SNAREs and VPS45 in *Escherichia coli*

Recombinant proteins used in this study were expressed in *E. coli* and purified via their N-terminal His_6 tag using Ni-NTA resin. Purified proteins were separated by SDS-PAGE and stained with Coomassie Blue. The purified proteins migrated at their expected MW with the exception of SYP42 (Fig 1A). The predicted size of SYP42 is approximately 36 kDa, but recombinant SYP42 migrated at around 45 kDa, presumably due to structural hindrance during migration in the gel (Fig 1A, lane 2). This size difference was also observed in a previous study of epitope-tagged SYP42 in transgenic Arabidopsis plants (Bassham et al., 2000).

AtVPS45 interacts with SYP4 and VTI1 family SNAREs and YKT62

SM proteins are known to interact with the syntaxin-type SNAREs or with SNARE complexes (Carr et al., 1999; Dulubova et al., 1999; Misura et al., 2000; Bryant and James, 2001). The SM protein AtVPS45 could therefore also interact with an individual SNARE or a SNARE complex. Previously, we showed that AtVPS45, VTI12 and either SYP41 or

SYP42 co-precipitate from *Arabidopsis* extracts (Bassham et al., 2000) and that SYP41 interacts with VTI12 and YKT61/62 *in vitro* (Chen et al., 2005), suggesting AtVPS45 could interact with the SYP41 SNARE complex.

First, we tested whether AtVPS45 could interact with SNARE complexes containing SYP4 family members using *in vitro* binding assays. Ten μg each of AtVPS45, one SYP4 family member, VTI12 and YKT62 were mixed and immunoprecipitated using purified AtVPS45 antibody. Precipitated proteins were analyzed by SDS-PAGE and silver staining (Fig 1B). YKT62, SYP41 and VTI12 co-precipitated with AtVPS45, confirming our previous results (Fig 1B lane 3; Chen et al., 2005). YKT62, VTI12 and either SYP42 (Fig 1B and 1C lane 5) or SYP43 (Fig 1B lane 7) also co-precipitated with AtVPS45, suggesting that AtVPS45 could interact with SNARE complexes containing additional SYP4 family members. SYP43 is an uncharacterized protein in the SYP4 family with high sequence identity to SYP41 and SYP42, but non-redundant function (Sanderfoot et al., 2001). Co-precipitation of SYP43 with YKT62, AtVPS45 and VTI12 suggests that SYP43 forms similar protein complexes to SYP41.

Next, we examined whether AtVPS45 could interact with individual SYP4 family members. VPS45 in yeast is known to regulate vesicle fusion via direct interaction with the SYP41 homolog Tlg2p (Bryant and James, 2003). However, we cannot rule out the possibility that the results from *in vitro* binding assays were caused by direct interaction between AtVPS45 and other proteins used instead of SYP4 family members. Therefore, *in vitro* binding assays were performed using AtVPS45 with proteins in the SYP4 family, VTI12 and YKT62 individually and only with both YKT62 and VTI12. Fig 1D shows that only SYP4 family members were able to interact with AtVPS45 directly, suggesting that co-

precipitation of VTI12 and YKT62 with AtVPS45 in Fig 1B was bridged by SYP4 family members. This result demonstrates that AtVPS45 binds to single SNAREs of the SYP4 family in addition to SNARE complexes.

VTI11 and VTI12 are known to be partially functionally redundant (Surpin et al., 2003). Thus, we investigated whether VTI11 can substitute for VTI12 in SYP4 SNARE complexes. VTI11 also co-precipitated with one SYP4 family member, YKT62 and AtVPS45 in the *in vitro* binding assays, suggesting VTI11 could replace VTI12 (Fig 1B lane 2, 4 and 6). Although SYP42 co-precipitated with YKT62, VPS45 and both VTI11 and VTI12, the amount of SYP42 and VTI12 in the precipitate was different (Fig 1B and 1C lane 4 and 5). Less SYP42 and VTI12 compared with the SYP42 and VTI11 combination was detected in the AtVPS45 precipitate (Fig 1B and 1C lane 5), suggesting SYP42 may have a weaker interaction with VTI12 than VTI11 *in vitro.*

Overall, the *in vitro* binding assays demonstrated that SYP41, SYP42 and SYP43 can form complexes with VTI11 or VTI12 and YKT62, and AtVPS45 interacts *in vitro* with SYP4 family members individually or with SNARE complexes via binding to a SYP4 family member.

SYP42 and SYP43 can also drive liposome fusion

Previously, proteoliposome fusion assays using SYP41, VTI12 and YKT62 demonstrated that these proteins were sufficient to drive vesicle fusion (Fig 3A; Chen et al., 2005). This result led us to test whether other SYP4 family proteins are also able to drive membrane fusion in combination with VTI12 and YKT62. Recombinant SYP41, SYP42 or SYP43 was reconstituted into phospholipid vesicles (acceptor vesicles) containing 60 mol%

1,2-dioleoyl-sn-glycero-3-phosphocholine (DOPC), 20 mol% 1-palmitoyl-2-oleoylsn-glycero-3-(phospho-rac-(1-glycerol)) (POPG) and 20 mol% 1-palmitoyl-2-oleoyl-sn-glycero-3-phospho-ethanolamine (POPE) using a Bio-beads/dialysis method (Chen et al., 2004). VTI12 was reconstituted into separate vesicles (donor vesicles) of the same lipid composition, except for the addition of 1.5 mol% each of N-(7-nitro-2,1,3,benzoxadiazol-4-yl) (NBD) and rhodamine-labeled fluorescent lipids (NBD-PE and rhodamine-PE) replacing an equal amount of DOPC. The efficiency of reconstitution of proteins into liposomes was analyzed by SDS-PAGE and staining with Coomassie Blue, and the reconstitution efficiency as determined by densitometry was around 50~60% for each protein (Fig 2).

The basis for the *in vitro* liposome fusion assay is loss of fluorescence resonance energy transfer **(**FRET) due to dilution of the fluorescent lipids. Donor vesicles contain NBD and rhodamine-labeled fluorescent lipids, whereas acceptor vesicles are unlabeled. NBD fluorescence in donor vesicles is quenched by rhodamine resulting in very low initial fluorescence. When donor and acceptor vesicles fuse, dilution of the fluorescent lipids leads to a decrease in NBD fluorescence quenching, causing an increased NBD fluorescence which can be monitored by fluorescence spectrophotometry.

Acceptor vesicles containing SYP42 or SYP43 and donor vesicles containing VTI12 were mixed together with the soluble form of YKT62, which is normally present as a lipid-modified form for membrane association in yeast and lacks transmembrane domain. This led to a rapid increase in NBD fluorescence due to dilution of the fluorescent lipids caused by membrane fusion (Fig 3B and 3C). This result indicates that SYP41, SYP42 and SYP43 can all drive liposome fusion as predicted, and that SYP42 and SYP43 can also function with VTI12 and YKT62 in SNARE complexes *in vitro*, as previously suggested by their co-

immunoprecipitation. No fusion was observed when YKT62 was omitted from each fusion reaction, suggesting YKT62 is also required for membrane fusion with SYP4 and VTI1 family members and that liposome fusion is dependent on the presence of the SNAREs (Fig 3).

SYP4 family SNAREs and VTI11 can drive membrane fusion

In *Arabidopsis*, four genes (*VTI11, VTI12, VTI13* and *VTI14*) comprise the VTI1 family, and *VTI14* is only expressed in Arabidopsis suspension cells (Uemura et al., 2004). VTI11 and VTI12 are v-SNAREs localized to the PVC and TGN, respectively (Sanderfoot et al., 2001a). VTI11 and VTI12 were found to compensate for each other in each single knockout mutant, as a *vti11* and *vti12* double mutant is embryo lethal, suggesting they are at least partially functionally redundant (Surpin et al., 2003). Niihara et. al (2005) found that expression of *VTI12* was increased in a *vti11* mutant, and a single amino acid substitution in VTI12 which changes the cellular localization of VTI12 to the PVC suppressed the *vti11* mutant phenotype, providing evidence that VTI12 can function within the VTI11 SNARE complex. Therefore, we hypothesize that VTI11 is also able to mediate vesicle fusion in combination with members of the SYP4 family and that specificity of SNARE complex formation *in vivo* is due to the distinct localization of VTI11 and VTI12.

To test this hypothesis, VTI11 was reconstituted into donor vesicles containing fluorescent lipids, and proteoliposome fusion assays were performed with acceptor vesicles containing each SYP4 family member and donor vesicles containing VTI11, all in the presence of YKT62. As shown in Fig 4, all SYP4 family proteins were able to drive rapid vesicle fusion with donor vesicles containing VTI11, suggesting that the SYP4 family is also

able to form functional SNARE complexes with VTI11. When the maximum percentage of fusion of vesicles containing one SYP4 family member with vesicles containing either VTI11 or VTI12 was compared, SYP41 and SYP43 showed similar maximum fusion percentages. However, SYP42 showed more vesicle fusion with VTI11 than VTI12 by 5-10% of the maximum fusion percentage. This difference was found to be statistically significant (*t*-test, $p < 0.05$), suggesting that VTI11 functions with SYP42 better than VTI12 *in vitro* (Fig 4B and 4D). These fusion results are also consistent with the result of the *in vitro* binding assays shown in Fig 1C.

We have shown that both VTI11 and VTI12 interact with SYP4 family members individually through *in vitro* binding assays, and these interactions are sufficient to drive membrane fusion (Fig 1, 3 and 4). To test whether the membrane fusion is driven by the specific interaction between individual SYP4 and VTI1 family members rather than a general requirement that any SNARE can fulfill, MEMB11, a v-SNARE involved in ER to Golgi anterograde trafficking and fusion at the Arabidopsis *cis*-Golgi was synthesized and incorporated into donor vesicles (Chatre et al., 2005). Vesicles containing MEMB11 were not able to fuse with vesicles containing SYP4 family SNAREs in the presence of YKT62, presumably because of lack of interaction (Fig 4).

As a further confirmation that the observed membrane fusion is specifically dependent on the VTI1 family, soluble fragments of VTI11 and VTI12 (VTI11s and VTI12s) were synthesized lacking the transmembrane domain. These soluble VTI11 or VTI12 fragments were mixed with YKT62 and acceptor vesicles containing one SYP4 family member, followed by incubation for 30 min before adding reconstituted donor vesicles and measuring lipid mixing. The soluble VTI11 and VTI12 proteins inhibited the fusion of

vesicles containing their full length version. When cross inhibition (VTI11s with VTI12 and VTI12s with VTI11) was examined, the same inhibition was observed, presumably due to occupation of the entire available SYP4 family member by the soluble version of VTI11 or VTI12 proteins, thus preventing interaction with the full length version (Fig 5). Although SYP42 preferentially fuses with VTI11, VTI12s can still block VTI11 fusion. The disassembly of SNARE complexes requires NSF and SNAP (Matveeva and Whiteheart, 1998). Thus, the preformed SYP42 SNARE complex containing VTI12s and YKY62 cannot interact with VTI11, because the SYP42 SNARE complex is locked. These results suggest that the full-length proteins cannot displace the soluble fragments and membrane fusion is mediated by the interaction between SNAREs on the acceptor and donor vesicles.

These results demonstrate that individual SYP4 family members can interact with VTI11 during vesicle fusion in addition to VTI12. Inhibition by soluble VTI11 and VTI12 suggests that VTI11 and VTI12 could have similar abilities to drive membrane fusion. This implies that VTI11 can substitute for VTI12 in catalyzing membrane fusion via interaction with the same SYP4 family complexes to which VTI12 binds *in vivo*.

Inhibition of membrane fusion by AtVPS45

AtVPS45 belongs to the Sec1/Munc18 protein family (SM protein) and resides at the Arabidopsis TGN. SM proteins are known to regulate vesicle fusion by binding to the Qa SNARE or to the SNARE complex, and yeast VPS45 has been reported to positively regulate the formation of the SNARE complex consisting of Tlg2p and Vti1p, which are SYP4 and VTI1 family homologs (Carr et al., 1999; Dulubova et al., 1999; Misura et al., 2000; Bryant and James, 2001; Dulubova et al., 2002). Previously, VTI12 and either SYP41

or SYP42 was shown to co-immunoprecipitate with AtVPS45, suggesting AtVPS45 could regulate vesicle fusion mediated by SYP41 or SYP42 and VTI12 (Bassham et al., 2000). Therefore, AtVPS45 was hypothesized to affect the liposome fusion reaction driven by reconstituted SYP4 and VTI1 proteins in the presence of YKT62.

To test this hypothesis, acceptor vesicles incorporated with one SYP4 family member were incubated with the same molar amount of AtVPS45 and YKT62 as a SYP4 family member at 4^{o}C for 1 h. After incubation, the acceptor vesicles were mixed with vesicles reconstituted with VTI11 or VTI12, and the fusion efficiency of all the possible combinations was measured. Interestingly, AtVPS45 was found to partially inhibit all of the fusion reactions with no difference in inhibition efficiency between VTI11 and VTI12, with two exceptions, and the difference was statistically significant (*t*-test, $p < 0.05$; Fig 6). Fusion reactions between reconstituted SYP41 and reconstituted VTI11, and reconstituted SYP43 and reconstituted VTI12 showed reduction of membrane fusion in the presence of AtVPS45 in some experiments, but some replicates showed little difference between the presence or absence of AtVPS45, and overall the difference was not statistically significant (*t*-test, SYP41/VTI11, $p = 0.13$; SYP43/VTI12, $p = 0.19$). However, results from the fusion reactions taken together indicate that AtVPS45 negatively affects vesicle fusion *in vitro*. These results suggest that interaction of AtVPS45 with vesicles containing one SYP4 family member inhibits the fusion reaction with vesicles containing one VTI1 family member, possibly preventing efficient formation of the *trans*-SNARE complex.

Discussion

The *Arabidopsis* genome encodes three proteins that are members of the SYP4 family and three members of the VTI1 family. Previously, SYP41, VTI12 and YKT61/62 were found to be important components of the membrane fusion machinery at the Arabidopsis TGN (Bassham et al., 2000; Chen et al., 2005). Here, we demonstrate that other members of the SYP4 and VTI1 families are also able to drive rapid membrane fusion *in vitro*. AtVPS45, an SM protein at the Arabidopsis TGN, negatively affects membrane fusion when pre-incubated with reconstituted SYP4 family proteins into vesicles.

It has been shown that SYP41 and SYP42 interact with only one VTI1 family protein, VTI12, *in vivo*, suggesting SYP41 and SYP42 are involved in membrane fusion with vesicles containing VTI12 as a v-SNARE (Bassham et al., 2000). This was confirmed by an *in vitro* fusion assay using reconstituted SYP41 or SYP42 and VTI12 (Fig 3A and 3B). However, we found that each SYP4 family member was also able to interact with VTI11 in an *in vitro* binding assay, and less SYP42 and VTI12 were co-immunoprecipitated with AtVPS45 compared with the SYP42 and VTI11 combination (Fig 1B and 1C). Although AtVPS45 antibody was used for immunoprecipitation, yeast VPS45 and AtVPS45 are known to function through binding to the SYP41 homolog Tlg2p in yeast and SYP41 and SYP42 in *Arabidopsis* (Bassham et al., 2000; Carpp et al., 2007; Zouhar et al., 2009). When AtVPS45 and either VTI11 or VTI12 alone were immunoprecipitated using AtVPS45 antibody, no VTI11 or VTI12 was present in the AtVPS45 precipitate (Fig 1D), confirming that VTI11 and VTI12 in the precipitate was due to interaction with the SYP4 family proteins (Fig 1B). Similar amounts of each SYP4 family member co-immunoprecipitated with AtVPS45 antibodies in the absence of other SNAREs, indicating that there was no difference in binding specificity between AtVPS45 and SYP4 family members (Fig 1D).

Thus, the reduction in SYP42 and VTI12 in the AtVPS45 precipitate could be caused by weak interaction between AtVPS45 and SYP42/VTI12 *in vitro,* presumably due to structural changes after binding of VTI12 to SYP42.

It is possible, although speculative, that the difference between immunoprecipitation results using *Arabidopsis* cell extract and recombinant proteins could be caused by the distinct localization of VTI11 and VTI12 *in vivo*. VTI11 is hypothesized to function as a v-SNARE that targets vesicles containing VSR1 and ssVSD-containing cargo from the TGN to the PVC, and VTI12 is thought to be involved in trafficking to storage vacuoles via recycling of vesicle trafficking components from the PVC to the TGN (Zheng et al., 1999; Sanmartin et al., 2007). VTI11 localizes to the PVC and interacts with SYP21 and SYP51, while VTI12 localizes to the TGN (Sanderfoot et al., 2001a). The different localization of VTI11 versus VTI12 precludes the possibility of interaction of VTI11 with SYP4 family members at the TGN. In addition, VTI11 could have a higher binding affinity for SYP21 and SYP51 than SYP4 family proteins *in vivo*. It is also possible that SYP61 or other binding proteins could be required for strong interaction between SYP42 and VTI12, because SYP61 co-precipitated with SYP42 *in vivo* (Bassham et al., 2000). Thus, we cannot rule out a possible role for SYP61 or other proteins in the interaction between SYP42 and VTI12. This VTI11 preference for SYP42 was also observed in the *in vitro* fusion assay, further strengthening the evidence for strong binding of SYP42 to VTI11 (Fig 4B).

In addition to the results from the *in vitro* binding assay, the possible functional redundancy of VTI1 family members was also investigated using an *in vitro* fusion assay. Although VTI11 and VTI12 seem to be involved in distinct trafficking pathways, they can compensate for loss of the other protein in *vti11* and *vti12* single mutants (Surpin et al.,

2003). In addition, more VTI12 is expressed in a *vti11* mutant, presumably to make up for loss of VTI11, and a single amino acid substitution in VTI12 can suppress the zig phenotype of *vti11* mutants (Niihama et al., 2005). These results suggest that VTI1 family proteins can bind to the interacting partners of VTI11 and VTI12 when the other VTI1 family is not available. This possibility was tested using *in vitro* fusion assays with SYP4 family members, showing that VTI11 was able to mediate vesicle fusion by interacting with SYP4 family members. This result indicates that compensation by VTI11 in *vti12* mutants *in vivo* could be via ability to form a functional SNARE complex with the VTI12 binding partners. The inverse may also be true, that VTI12 may be able to interact with the normal VTI11 binding partners. *In vitro* fusion assays using recombinant SYP21 and SYP51 could provide further information about the redundant functions of VTI12 and VTI11.

SYP43 is a third member of the SYP4 family, and GFP-fused SYP43 was found to co-localize with SYP42, indicating its TGN localization (Uemura et al., 2004). SYP43 has very high amino acid sequence similarity to SYP41 and SYP42, but is not functionally redundant with either protein (Sanderfoot et al., 2001b). SYP43 is expressed ubiquitously in *Arabidopsis*, as are SYP41 and SYP42 (Schmid et al., 2005). These findings suggest that SYP43 is a component of a different vesicle trafficking machinery at the Arabidopsis TGN compared with SYP41 and SYP42. In this study, we showed that SYP43 can catalyze membrane fusion *in vitro* together with VTI11 or VTI12, as can SYP41 (Fig 1B, 3C and 4C). Although proteins interacting with SYP43 *in vivo* have not been identified, SYP43 may interact with VTI12 judging from its high similarity to SYP41 and the result from the *in vitro* binding assay. Further investigation of SYP43 using immunoprecipitation or *syp43* mutant analysis could provide valuable information about its function.

AtVPS45 is a peripheral protein at the Arabidopsis TGN that binds to SYP41 and SYP42 (Bassham et al., 2000). AtVPS45 is also known to regulate the cellular amount of SYP41, suggesting that it affects SYP41 stability (Zouhar et al., 2009). As an SM protein, AtVPS45 may function via binding to individual SNAREs or to entire SNARE complexes. VTI12 co-immunoprecipitated with AtVPS45 in the presence of a SYP4 family member, indicating that AtVPS45 may facilitate the interaction of SYP4 family members with VTI12 or alternatively may interact with SYP41 and VTI12 after SNARE complex formation. Yeast VPS45 associates with the *cis*-SNARE complex containing v- and t-SNAREs after membrane fusion and dissociates from the SNARE complex either before or during *trans*-SNARE complex formation (Bryant and James, 2003). Dissociation of VPS45 from the SNARE complex in yeast may require the Rab GTPase VPS21, which is a protein involved in the formation of *trans*-SNARE complex. (Lupashin and Waters, 1997; Bryant and James, 2003). In our study, addition of AtVPS45 to the *in vitro* fusion assay partially inhibited membrane fusion. This partial inhibition could be caused by hindering the completion of the fusion reaction between vesicles containing a SYP4 family member and a VTI1 family member by a strong interaction between SYP4 family members and AtVPS45, or alternatively by inhibiting *trans*-SNARE complex formation due to lack of proteins required for dissociation of AtVPS45 in this experiment.

In conclusion, we have demonstrated that each SYP4 family member at the TGN, together with VTI11 or VTI12, can drive proteoliposome fusion *in vitro*. All of the SNAREs tested in this study are likely to be involved in membrane fusion *in vivo*. The ability of VTI11 to interact with SYP4 family proteins and to catalyze membrane fusion together with a SYP4 family member extends our understanding of functional redundancy of VTI11 and

VTI12. Although the exact role of AtVPS45 during the fusion process is still unclear, AtVPS45 affects SNARE complex formation or membrane fusion processes at the TGN. Our *in vitro* experiments demonstrate the role of SYP4 family SNAREs at the TGN in membrane fusion and provide a detailed mechanism of functional redundancy mediated by VTI11 and VTI12.

Acknowledgements

We thank Drs Yeon-Kyun Shin, Zhengliu Su and Yong Chen for providing constructs, equipment and valuable assistance and expertise in *in vitro* fusion assay.

References

Assaad FF, Qiu JL, Youngs H, Ehrhardt D, Zimmerli L, Kalde M, Wanner G, Peck SC, Edwards H, Ramonell K, Somerville CR, Thordal-Christensen H (2004) The PEN1 syntaxin defines a novel cellular compartment upon fungal attack and is required for the timely assembly of papillae\. Molecular Biology of the Cell **15:** 5118-5129

Bassham DC, Raikhel NV (1998) An Arabidopsis VPS45p homolog implicated in protein transport to the vacuole. Plant Physiology **117:** 407-415

Bassham DC, Sanderfoot AA, Kovaleva V, Zheng HY, Raikhel NV (2000) AtVPS45 complex formation at the trans-Golgi network. Molecular Biology of the Cell **11:** 2251-2265

Bock JB, Matern HT, Peden AA, Scheller RH (2001) A genomic perspective on membrane compartment organization. Nature **409:** 839-841

Bryant NJ, James DE (2001) Vps45p stabilizes the syntaxin homologue Tlg2p and positively regulates SNARE complex formation. Embo Journal **20:** 3380-3388

Bryant NJ, James DE (2003) The Sec1p/Munc18 (SM) protein, Vps45p, cycles on and off membranes during vesicle transport. Journal of Cell Biology **161:** 691-696

Carpp LN, Shanks SG, Struthers MS, Bryant NJ (2007) Cellular levels of the syntaxin Tlg2p are regulated by a single mode of binding to Vps45p. Biochemical and Biophysical Research Communications **363:** 857-860

Carr CM, Grote E, Munson M, Hughson FM, Novick PJ (1999) Sec1p binds to SNARE complexes and concentrates at sites of secretion. Journal of Cell Biology **146:** 333-344

Chatre L, Brandizzi F, Hocquellet A, Hawes C, Moreau P (2005) Sec22 and Memb11 are v-SNAREs of the anterograde endoplasmic reticulum-Golgi pathway in tobacco leaf epidermal cells. Plant Physiology **139:** 1244-1254

Chen Y, Shin YK, Bassham DC (2005) YKT6 is a core constituent of membrane fusion machineries at the Arabidopsis trans-Golgi network. Journal of Molecular Biology **350:** 92-101

Chen Y, Xu YB, Zhang F, Shin YK (2004) Constitutive versus regulated SNARE assembly: a structural basis. Embo Journal **23:** 681-689

Dilcher M, Kohler B, von Mollard GF (2001) Genetic interactions with the yeast Q-SNARE VTI1 reveal novel functions for the R-SNARE YKT6. Journal of Biological Chemistry **276:** 34537-34544

Dulubova I, Sugita S, Hill S, Hosaka M, Fernandez I, Sudhof TC, Rizo J (1999) A conformational switch in syntaxin during exocytosis: role of munc18. Embo Journal **18:** 4372-4382

Dulubova I, Yamaguchi T, Gao Y, Min SW, Huryeva I, Sudhof TC, Rizo J (2002) How Tlg2p/syntaxin 16 'snares' Vps45. Embo Journal **21:** 3620-3631

Fukasawa M, Varlamov O, Eng WS, Sollner TH, Rothman JE (2004) Localization and activity of the SNARE Ykt6 determined by its regulatory domain and palmitoylation. Proceedings of the National Academy of Sciences of the United States of America **101:** 4815-4820

Kweon Y, Rothe A, Conibear E, Stevens TH (2003) Ykt6p is a multifunctional yeast R-SNARE that is required for multiple membrane transport pathways to the vacuole. Molecular Biology of the Cell **14:** 1868-1881

Leshem Y, Melamed-Book N, Cagnac O, Ronen G, Nishri Y, Solomon M, Cohen G, Levine A (2006) Suppression of Arabidopsis vesicle-SNARE expression inhibited

fusion of H2O2 containing vesicles with tonoplast and increased salt tolerance. Proceedings of the National Academy of Sciences of the United States of America **103:** 18008-18013

Lupashin VV, Waters MG (1997) t-SNARE activation through transient interaction with a Rab-like guanosine triphosphatase. Science **276:** 1255-1258

Matveeva E, Whiteheart SW (1998) The effects of SNAP/SNARE complexes on the ATPase of NSF. Febs Letters **435:** 211-214

McNew JA, Parlati F, Fukuda R, Johnston RJ, Paz K, Paumet F, Sollner TH, Rothman JE (2000) Compartmental specificity of cellular membrane fusion encoded in SNARE proteins. Nature **407:** 153-159

Misura KMS, Scheller RH, Weis WI (2000) Three-dimensional structure of the neuronal-Sec1-syntaxin 1a complex. Nature **404:** 355-362

Niihama M, Uemura T, Saito C, Nakano A, Sato MH, Tasaka M, Morita MT (2005) Conversion of functional specificity in Qb-SNARE VTI1 homologues of Arabidopsis. Current Biology **15:** 555-560

Paumet F, Rahimian V, Rothman JE (2004) The specificity of SNARE-dependent fusion is encoded in the SNARE motif. Proceedings of the National Academy of Sciences of the United States of America **101:** 3376-3380

Poirier MA, Xiao W, Macosko JC, Chan C, Shin YK, Bennett MK (1998) The synaptic SNARE complex: A parallel four-stranded helical bundle. Molecular Biology of the Cell **9:** 84A-84A

Sanderfoot AA, Assaad FF, Raikhel NV (2000) The Arabidopsis genome. An abundance of soluble N-ethylmaleimide-sensitive factor adaptor protein receptors. Plant Physiology **124:** 1558-1569

Sanderfoot AA, Kovaleva V, Bassham DC, Raikhel NV (2001a) Interactions between syntaxins identify at least five SNARE complexes within the golgi/prevacuolar system of the arabidopsis cell. Molecular Biology of the Cell **12:** 3733-3743

Sanderfoot AA, Pilgrim M, Adam L, Raikhel NV (2001) Disruption of individual members of arabidopsis syntaxin gene families indicates each has essential functions. Plant Cell **13:** 659-666

Sanderfoot AA, Pilgrim M, Adam L, Raikhel NV (2001b) Disruption of individual members of arabidopsis syntaxin gene families indicates each has essential functions. Plant Cell **13:** 659-666

Sanderfoot AA, Raikhel NV (1999) The specificity of vesicle trafficking: Coat proteins and SNAREs. Plant Cell **11:** 629-641

Sanmartin M, Ordonez A, Sohn EJ, Robert S, Sanchez-Serrano JJ, Surpin MA, Raikhel NV, Rojo E (2007) Divergent functions of VTI12 and VTI11 in trafficking to storage and lytic vacuoles in Arabidopsis. Proceedings of the National Academy of Sciences of the United States of America **104:** 3645-3650

Schmid M, Davison TS, Henz SR, Pape UJ, Demar M, Vingron M, Scholkopf B, Weigel D, Lohmann JU (2005) A gene expression map of Arabidopsis thaliana development. Nature Genetics **37:** 501-506

Sollner T, Whitehart SW, Brunner M, Erdjumentbromage H, Geromanos S, Tempst P, Rothman JE (1993) Snap Receptors Implicated in Vesicle Targeting and Fusion. Nature **362:** 318-324

Surpin M, Zheng HJ, Morita MT, Saito C, Avila E, Blakeslee JJ, Bandyopadhyay A, Kovaleva V, Carter D, Murphy A, Tasaka M, Raikhel N (2003) The VTI family of SNARE proteins is necessary for plant viability and mediates different protein transport pathways. Plant Cell **15:** 2885-2899

Tai GH, Lu L, Wang TL, Tang BL, Goud B, Johannes L, Hong WJ (2004) Participation of the syntaxin 5/Ykt6/GS28/GS15 SNARE complex in transport from the early/recycling endosome to the trans-Golgi network. Molecular Biology of the Cell **15:** 4011-4022

Uemura T, Ueda T, Ohniwa RL, Nakano A, Takeyasu K, Sato MH (2004) Systematic analysis of SNARE molecules in Arabidopsis: Dissection of the post-Golgi network in plant cells. Cell Structure and Function **29:** 49-65

Weber T, Zemelman BV, McNew JA, Westermann B, Gmachl M, Parlati F, Sollner TH, Rothman JE (1998) SNAREpins: Minimal machinery for membrane fusion. Cell **92:** 759-772

Yano D, Sato M, Saito C, Sato MH, Morita MT, Tasaka M (2003) A SNARE complex containing SGR3/AtVAM3 and ZIG/VTI11 in gravity-sensing cells is important for

Arabidopsis shoot gravitropism. Proceedings of the National Academy of Sciences of the United States of America **100:** 8589-8594

Zhang ZG, Feechan A, Pedersen C, Newman MA, Qiu JL, Olesen KL, Thordal-Christensen H (2007) A SNARE-protein has opposing functions in penetration resistance and defence signalling pathways. Plant Journal **49:** 302-312

Zheng HY, von Mollard GF, Kovaleva V, Stevens TH, Raikhel NV (1999) The plant vesicle-associated SNARE AtVTI1a likely mediates vesicle transport from the trans-Golgi network to the prevacuolar compartment. Molecular Biology of the Cell **10:** 2251-2264

Zhu JH, Gong ZZ, Zhang CQ, Song CP, Damsz B, Inan G, Koiwa H, Zhu JK, Hasegawa PM, Bressan RA (2002) OSM1/SYP61: A syntaxin protein in Arabidopsis controls abscisic acid-mediated and non-abscisic acid-mediated responses to abiotic stress. Plant Cell **14:** 3009-3028

Zouhar J, Rojo E, Bassham DC (2009) AtVPS45 Is a Positive Regulator of the SYP41/SYP61/VTI12 SNARE Complex Involved in Trafficking of Vacuolar Cargo. Plant Physiology **149:** 1668-1678

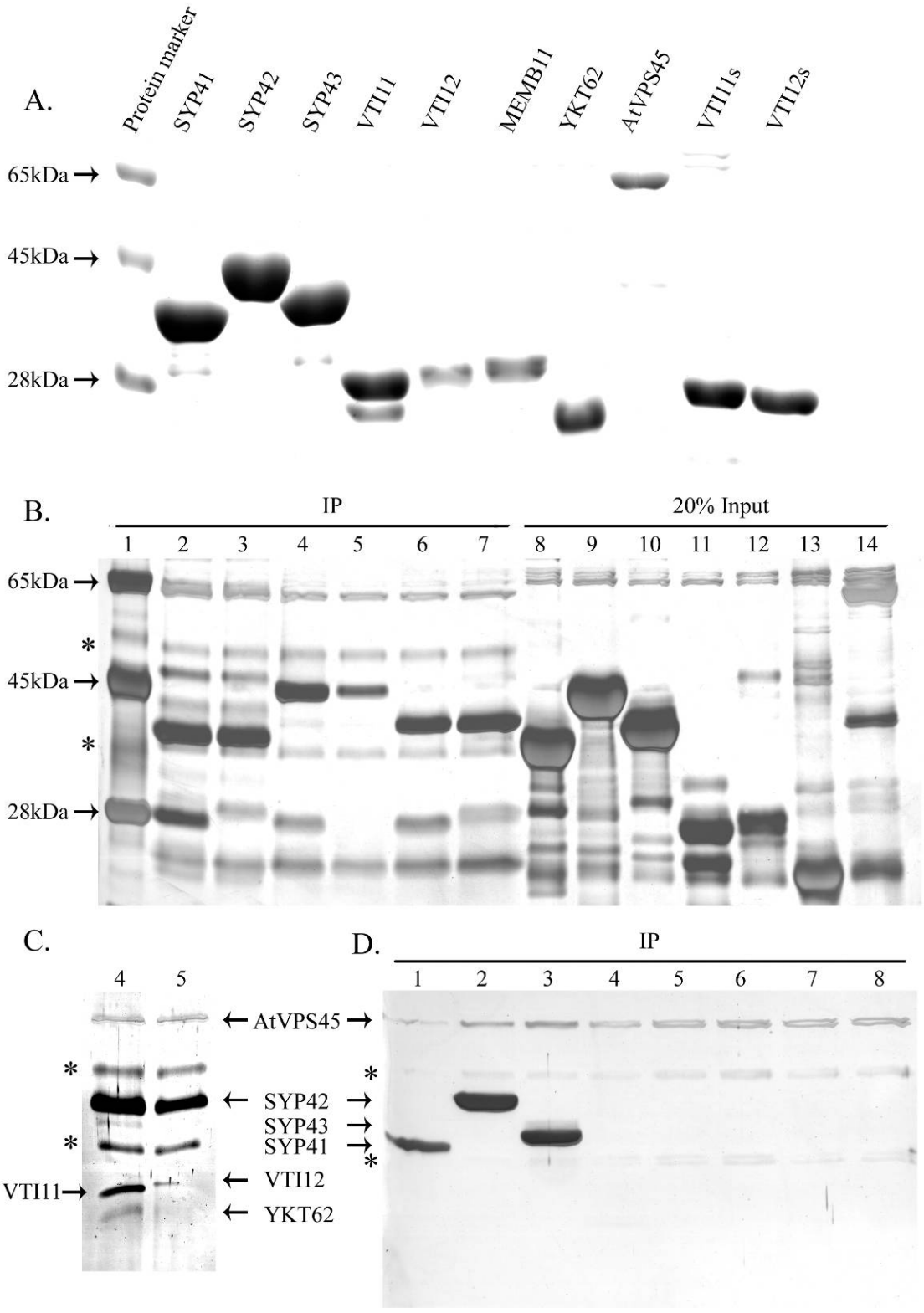
A.
Protein marker
SYP41
SYP42
SYP43
VTI11
VTI12
MEMB11
YKT62
AtVPS45
VTI11s
VTI12s
65kDa
45kDa
28kDa
B.
IP
20% Input
1 2 3 4 5 6 7 8 9 10 11 12 13 14
65kDa
45kDa
28kDa
C.
4 5
AtVPS45
SYP42
SYP43
SYP41
VTI12
YKT62
VTI11
D.
IP
1 2 3 4 5 6 7 8

Figure 1. Expression of recombinant proteins and *in vitro* binding assay using AtVPS45 antibody

A. Expression of purified proteins

His-tagged recombinant proteins as indicated were expressed in *E.coli* and purified using Ni-NTA resin. Ten μg each of the purified proteins were separated by SDS-PAGE and stained using Coomassie Blue. MW markers are indicated at left.

B-D. *In vitro* binding assay

Purified proteins were mixed and incubated on ice for 1 h, followed by the addition of protein A sepharose and AtVPS45 antibody. After additional incubation for 1 h, samples were washed 5 times. Proteins were eluted using SDS-PAGE sample buffer. Eluted proteins (lanes 2-7) and 20% of the input (lanes 8-14) were analyzed by SDS-PAGE and silver staining. Lanes contained the following proteins: protein marker (lane 1), SYP41, YKT62, AtVPS45 and either VTI11 or VTI12 (lanes 2 and 3, respectively), SYP42, YKT62, AtVPS45 and either VTI11 or VTI12 (lanes 4 and 5, respectively), SYP43, YKT62, AtVPS45 and either VTI11 or VTI12 (lanes 6 and 7, respectively), SYP41, SYP42, SYP43, VTI11, VTI12, YKT62, VPS45 (lanes 8-14, respectively) (B). The same precipitates from lanes 4 and 5 were over-stained to detect VTI12 (C). AtVPS45 was mixed with either SYP41 (lane 1), SYP42 (lane 2), SYP43 (lane 3), VTI11 (lane 4), VTI12 (lane 5), YKT62 (lane 6) or YKT62 with either VTI11 (lane 7) or VTI12 (lane 8), followed by immunoprecipitation as described above (D). Antibody bands are indicated with asterisks.

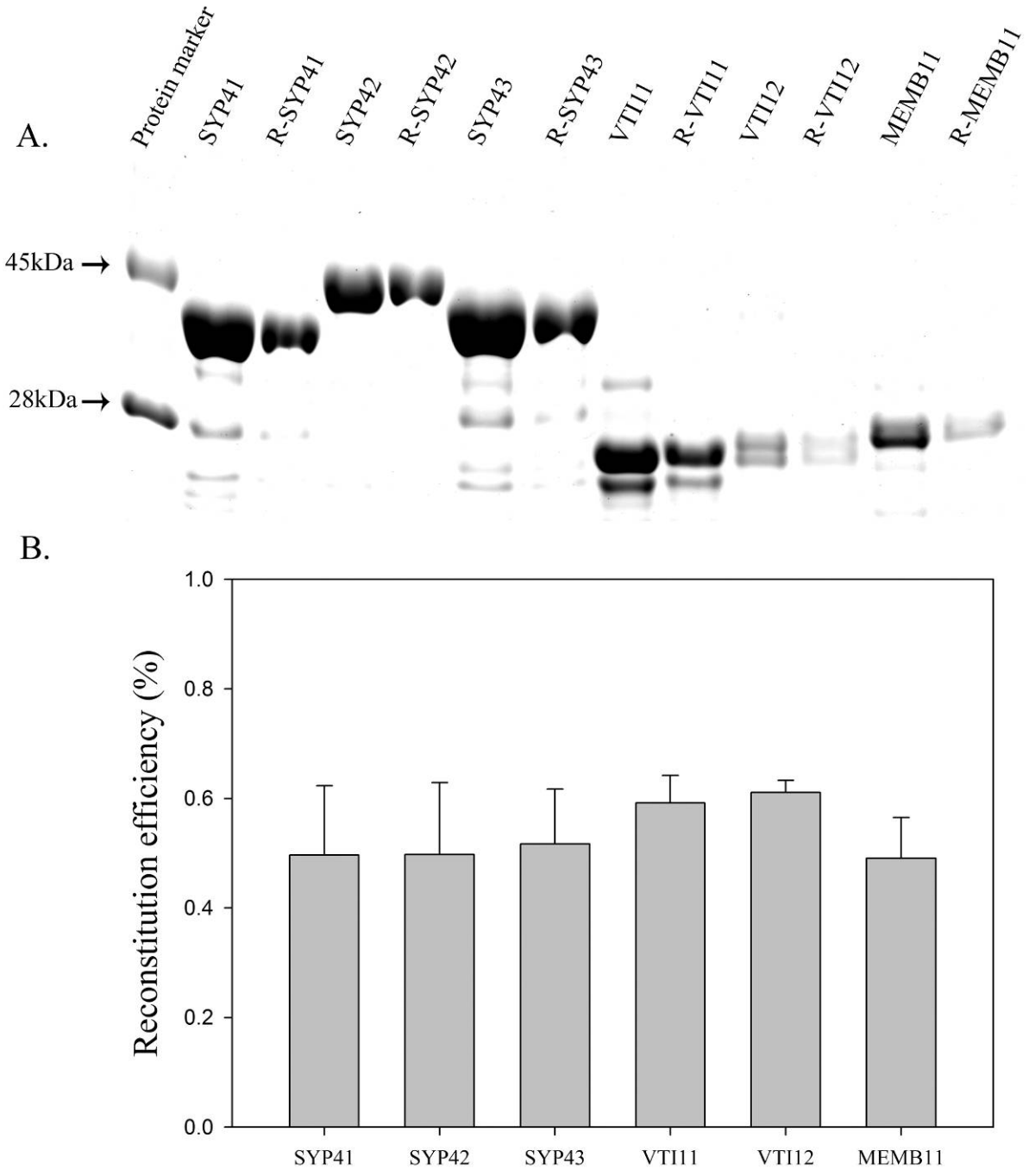

Figure 2. Reconstitution of recombinant proteins into liposomes

A. Recombinant proteins were reconstituted into liposomes in the presence of detergent (Triton X-100 or n-octylglucoside), followed by dialysis to remove detergents after

reconstitution. The reconstitution efficiency was analyzed by SDS-PAGE and Coomassie Blue staining. The amount of proteins before and after reconstitution was analyzed. Prefix R- stands for reconstituted proteins.

B. The average reconstitution efficiency was obtained from three independent experiments by densitometry of gels. The average reconstitution efficiency was ~50% for all proteins. Error bars represent standard deviation (n=3).

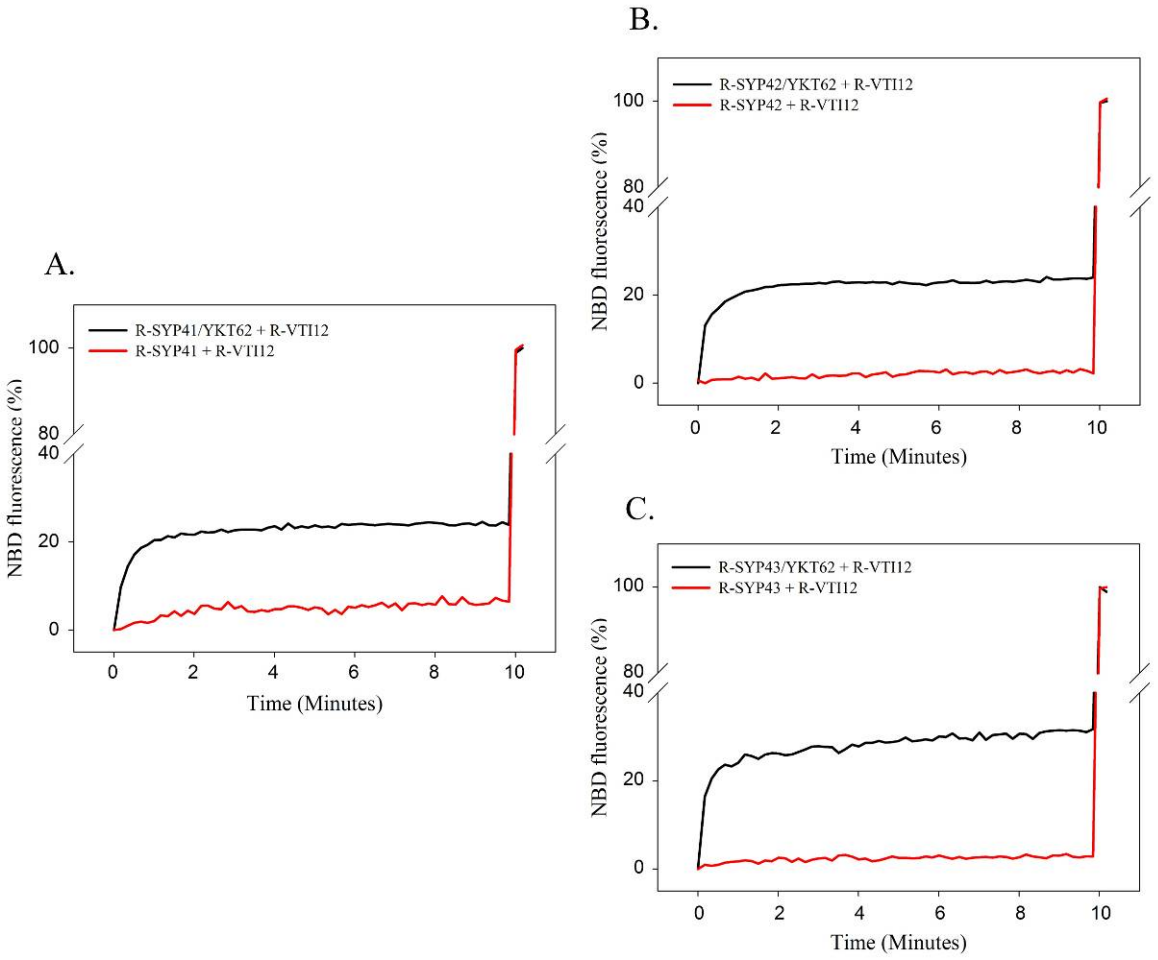

Figure 3. SYP42 and SYP43 can drive liposome fusion

Purified SYP41 (A), SYP42 (B), or SYP43 (C) was incorporated into acceptor vesicles (non-fluorescent vesicles), and VTI12 was reconstituted into donor vesicles containing fluorescent lipids. Membrane fusion with (black) or without (red) YKT62 was measured by monitoring NBD fluorescence with excitation wavelength of 460 ηm and emission wavelength of 530 ηm. The fluorescence was recorded every ten seconds for 10 min. The maximal fluorescence intensity (MFI) was obtained by adding 1 µl of 10% (v/v) Triton X-100, and recorded fluorescence measurements were normalized to the MFI.

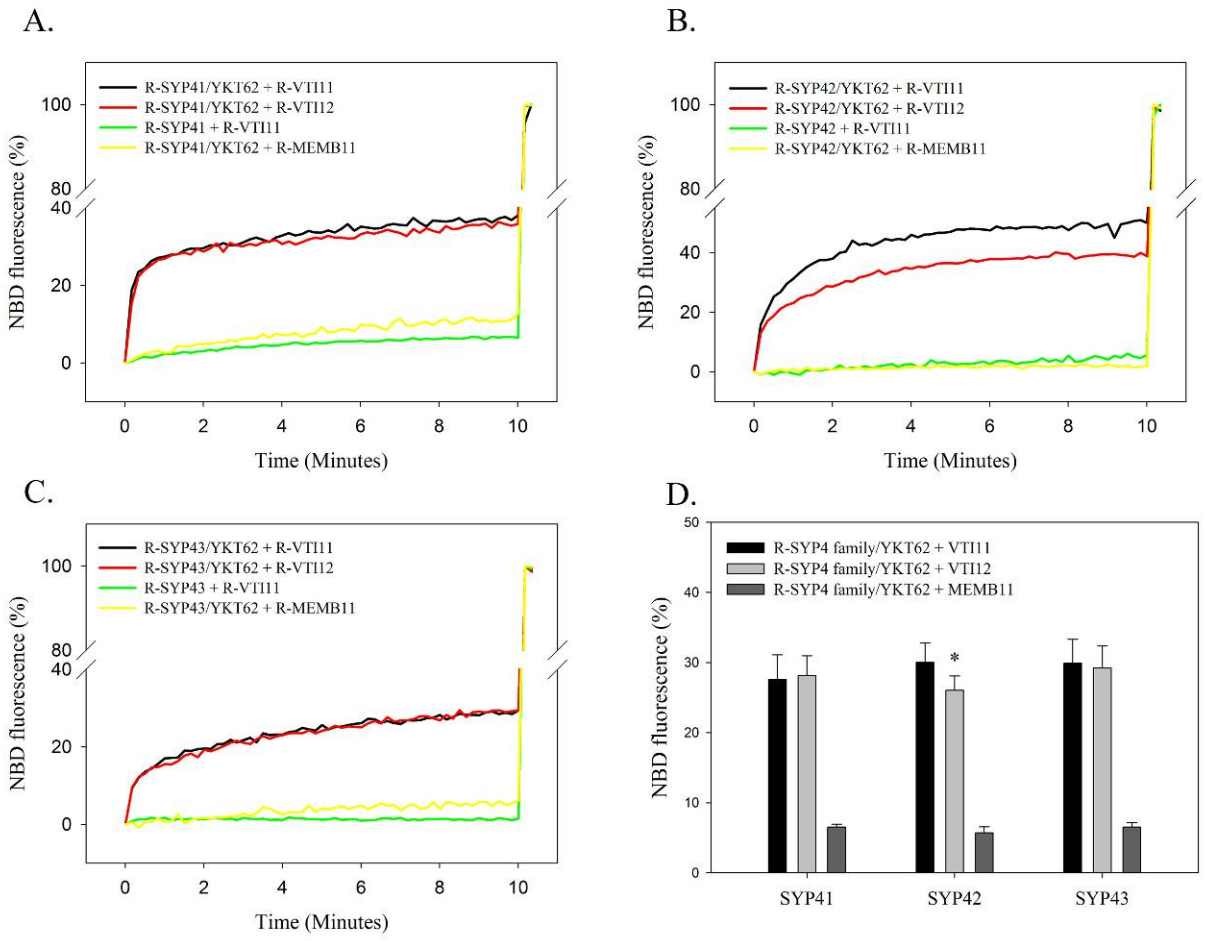

Figure 4. SYP4 family members and VTI11 can function together in membrane fusion

A-C. Purified SYP41 (A), SYP42 (B) or SYP43 (C) were incorporated into acceptor vesicles, and VTI11, VTI12 or MEMB11 were reconstituted into donor vesicles. Mixing of acceptor vesicles and donor vesicles was measured as in Fig 3. The change in NBD fluorescence was monitored after mixing each R-SYP4 family and R-VTI11 either in the presence (black line) or absence of YKT62 (green line) and mixing each R-SYP4 family and either R-MEMB11 (yellow line) or R-VTI12 (red line) in the presence of YKT62.

D. Maximum percentages of fusion of donor vesicles containing R-VTI11, R-VTI12 or R-MEMB11 with vesicles reconstituted with a SYP4 family protein were analyzed statistically

and compared. Maximum percentage of fusion between R-SYP42 and either R-VTI11 or R-VTI12 showed a significant difference by *t*-test (p=0.006, labeled with asterisk). Error bars represent standard deviation (n=7)

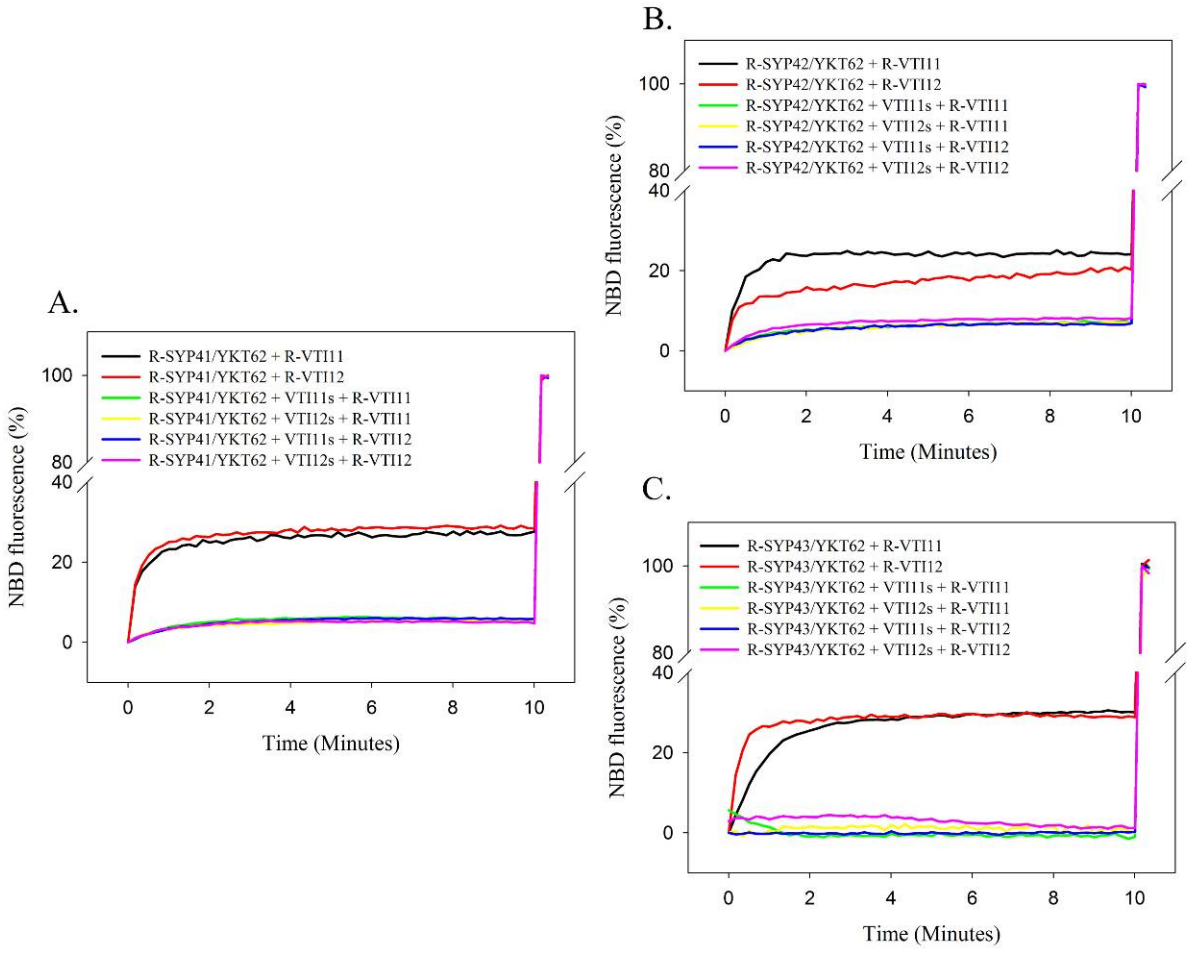

Figure 5. SYP4 and VTI1 family-mediated fusion can be inhibited by soluble VTI11 or soluble VTI12

Reconstituted vesicles containing either SYP41 (A), SYP42 (B) or SYP43 (C) were mixed with YKT62 and either soluble VTI11 or soluble VTI12 for 30 min, followed by addition of either R-VTI11 or R-VTI12. The fluorescence did not increase significantly (less than 4%), indicating inhibition of the fusion reaction in the presence of soluble VTI11 or soluble VTI12.

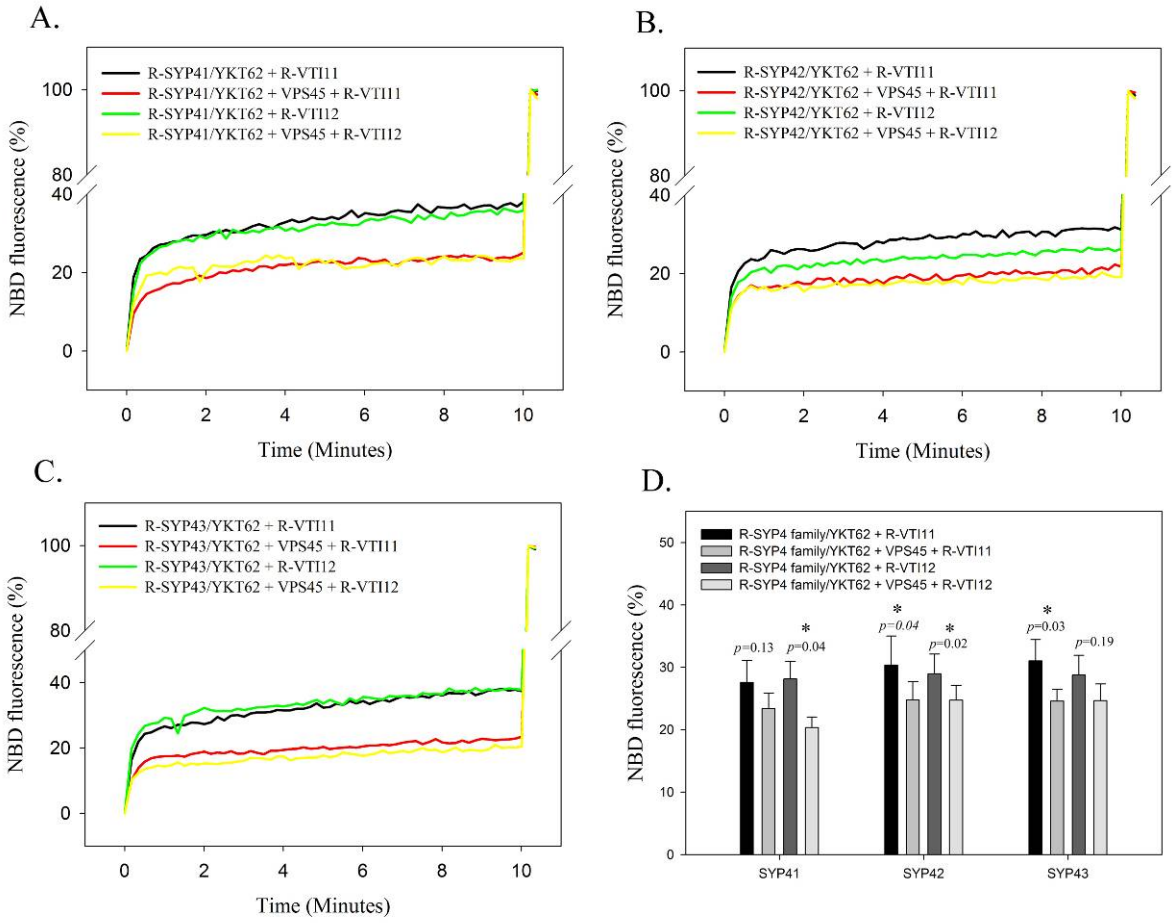

Figure 6. AtVPS45 inhibits fusion mediated by SYP4 and VTI1 families

A-C. Reconstituted vesicles containing either SYP41 (A), SYP42 (B) or SYP43 (C) were mixed with YKT62 and AtVPS45 for 1 h, followed by addition of either R-VTI11 or R-VTI12. The fluorescence from lipid mixing in the presence of AtVPS45 was approximately 5 to 10% lower than without AtVPS45, indicating inhibition of the fusion reactions by AtVPS45.

D. Maximal percentage of membrane fusion in the presence and absence of AtVPS45 was compared. Results of a *t*-test are shown above the bars, and reactions showing a significant difference ($p < 0.05$) are labeled with asterisks. Error bars represent standard deviation (n=7)

Table 1. Primer sequences. The restriction sites used for cloning are underlined.

Gene	Direction	Sequence
SYP42	Forward	5'-GGAATTCCATATGGCGACGAGGAATCGAACGACGGTG-3'
	Reverse	5'-CGCCTCGAGCTAAAACAAAATATTCTTAAGAATTAA-3'
SYP43	Forward	5'-GGAATTCCATATGGCGACTAGGAATCGTACGCTGTTG-3'
	Reverse	5'-CGCCTCGAGTCACAACAGAATCTCCTTGAGGATTAAGA-3'
VTI11	Forward	5'-GGAATTCCATATGAGTGACGTGTTTGATGGATATGAG-3'
	Reverse	5'-CCCAAGCTTTTACTTGGTGAGTTTGAAGTACAAGATG-3'
AtVPS45	Forward	5'-GGATCCATGGTTTTGGTTACGTCTGT-3'
	Reverse	5'-GGATCCTCACACCATATGGCTACCTG-3'
VTI11s	Forward	5'-GGATCCATGAGTGACGTGTTTGATGG-3'
	Reverse	5'-AAGCTTTTAGGTCCATTTGTTCTTGT-3'
MEMB11	Forward	5'-GAATTCATGGCGTCTGGTATCGTCGA-3'
	Reverse	5'- CTCGAGGGTTAGCGTGTCCATCTTATGA-3'

CHAPTER 4. GENERAL CONCLUSIONS

Overview

Several SNAREs (SYP41, SYP42, SYP61, VTI12 and YKT61/62) and an SM protein (AtVPS45) involved in vesicle fusion at the TGN have been studied previously. They were found to interact with each other *in vivo* and or *in vitro* and comprise the core components required for vesicle fusion (Bassham et al., 2000; Chen et al., 2005). Mutant analysis of each gene has shown that SYP41, SYP42 and VPS45 are essential for viability in *Arabidopsis,* and are probably important for vesicle trafficking at the TGN (Sanderfoot et al., 2001b; Zouhar et al., 2009). Here, I demonstrate a role for another protein, TNO1, in the SYP41 complex at the TGN.

In this dissertation, chapter one presents a general introduction on the vacuolar trafficking pathway, components required for vesicle fusion and useful tools in the investigation of vesicle transport pathways. In chapter two, I demonstrate a role of TNO1 under salt, ionic and osmotic stress, and the role of TNO1 in vacuolar trafficking, along with a putative role as a matrix protein and component for membrane fusion at the Arabidopsis TGN. In chapter three, fusion between vesicles containing a SYP4 family protein and vesicles containing a VTI1 family protein is demonstrated along with a role for AtVPS45 in the fusion reaction.

Role of TNO1 at the Arabidopsis *trans*-Golgi Network

Chapter two focused on the identification and characterization of the Arabidopsis TNO1 protein. TNO1 is a protein containing long coiled-coil domains that resides at the TGN. Analysis of a *tno1* knockout mutant indicates that TNO1 is involved in the response to salt stress and in the transport of vacuolar proteins. In the *tno1* mutant, a change in the localization pattern of SYP61 was observed. As SYP61 is also involved in the salt stress response, this presents one possible reason for the salt sensitive phenotype in the *tno1* knockout mutant. Application of the vesicle trafficking inhibitor BFA to wild-type and *tno1* mutant plants produced two interesting phenotypes. In wild-type plants, TNO1 was not present in the BFA compartment upon BFA treatment. In the cotyledons of the *tno1* mutant, delayed formation of BFA compartments compared with wild-type seedlings was observed upon BFA treatment. These results suggest that lack of TNO1 leads to less efficient vesicle trafficking in the *tno1* mutant, and that TNO1 may be involved in maintaining TGN structure in *Arabidopsis*. This chapter presents TNO1 as a protein functioning in vesicle trafficking and membrane fusion at the TGN.

Vesicle fusion machineries and functional redundancy of VTI11 and VTI12 at the Arabidopsis TGN.

In chapter three, members of the SYP4 and VTI1 families were shown to mediate membrane fusion. Previously, VTI12 and either SYP41 or SYP61 were shown to be required for liposome fusion (Chen et al., 2005). Further investigation using SYP42 and SYP43 showed that these two SYP4 family members were also able to drive membrane fusion by interacting with VTI12. VTI11, which localizes to the PVC *in vivo*, was found to interact with each member of SYP4 family during vesicle fusion *in vitro.* This result suggests that functional redundancy between VTI11 and VTI12 could be achieved by interaction of VTI11

with SYP4 family proteins, with which VTI12 normally interacts *in vivo*. AtVPS45, an SM protein known to interact with SYP41 and SYP42, partially inhibited membrane fusion between vesicles containing a SYP4 family member and a VTI1 family member. This indicates that AtVPS45 negatively affects membrane fusion between vesicles containing SYP4 and VTI1 family proteins.

Impact of Dissertation Study

Both studies presented in my dissertation have contributed new knowledge in understanding the function of the SYP41 complex at the Arabidopsis TGN. I provide evidence that TNO1 is important for salt and osmotic stress tolerance and also for the proper transport of vacuolar proteins. These two features are important factors that determine agricultural crop quality. Salt stress is a major problem for agriculture. Excessive salts in the soil inhibit growth of most plants, because salt stress usually causes dehydration, ionic stress and production of reactive oxygen species (Zhu, 2001). Genes involved in sensing salt stress or in compartmentalizing sodium ions to vacuoles have been major targets of agricultural research (Qiu et al., 2002; Qiu et al., 2004; Brini et al., 2005; Zorb et al., 2005). Increasing evidence that trafficking components are involved in salt tolerance suggests that endomembrane trafficking also has an important role in the response to salt stress (Leshem et al., 2007; Hamaji et al., 2009; Hernandez et al., 2009). Some of the trafficking components known as SNARE proteins have been shown to have a role in vacuolar trafficking. Thus, salt tolerance and vacuolar trafficking are likely to be closely connected. Vacuoles in plants are multifunctional organelles that maintain homeostasis by storing ions, metabolites, proteins and pigments (Marty, 1999). In the *tno1* knockout mutant, a change of the localization

pattern of SYP61 was observed, suggesting a possible inhibition of vesicle trafficking dependant on SYP61. This suggests that salt sensitivity in the *tno1* mutant is closely related to the function of trafficking component. Therefore, manipulating trafficking components will contribute to improve agricultural crop yield and quality by providing abiotic stress resistance and improving nutrition in crop.

Functional redundancy between VTI11 and VTI12 has been studied *in vivo,* and I demonstrate how it is mediated *in vitro* (Surpin et al., 2003). Thus, our *in vitro* results, along with *in vivo* studies, enlarge our understanding of functional redundancy between VTI11 and VTI12. In *Arabidopsis*, there are a number of SNARE families. Functional redundancy between members in a SNARE family has been reported *in vivo*. Thus, application of an *in vitro* fusion assay will help to understand how functional redundancy is mediated.

Future directions

How TNO1 affects salt stress resistance

A t-SNARE, SYP61/OSM1, that interacts with SYP41 has been reported to be involved in a general salt/osmotic stress response (Zhu et al., 2002). TNO1 interacts with SYP41, and the *tno1* knockout mutant also showed a salt-sensitive phenotype, suggesting that TNO1 and SYP61 may function in the same pathway. Investigation of the localization of SYP41 and SYP61 in a *tno1* KO mutant showed a change in the localization pattern of SYP61, while no difference was observed in SYP41, suggesting that TNO1 is required for correct localization of SYP61. It will be interesting to determine whether the salt sensitive phenotype of the *tno1* KO mutant is due to mis-localization of SYP61 using genetic

approaches. To test this possibility, a *syp61/tno1* double mutant will be generated by crossing *syp61* and *tno1* mutants. If the *syp61/tno1* double mutant shows the same degree of salt sensitivity shown in the *osm1/syp61* mutant, TNO1 and SYP61 could be in the same pathway. If the *syp61/tno1* double mutant shows more severe salt sensitivity, TNO1 and SYP61 may be in different pathways. Alternatively, a SYP61 overexpression line and *tno1* mutant will be crossed. Excessive expression of SYP61 in the transgenic mutant may compensate for mis-localization of SYP61 in the *tno1* KO mutant, resulting in similar salt sensitivity to wild type.

Another approach is identification of proteins that interact with TNO1 and with SYP61. Immunoprecipitation using SYP41 antibody identified TNO1 and SYP61 in the SYP41 precipitate (Bassham et al., 2000). However, *syp41, syp61* and *tno1* mutants show different phenotypes, and either SYP41 or SYP61, but not both, are required for membrane fusion, suggesting these proteins have different functions in trafficking pathways. Thus, immunoprecipitation using SYP61 and TNO1 antibodies could precipitate other proteins involved in salt resistance such as v-SNAREs on vesicles containing cargo receptors which bind to and pack salt stress responsive protein into the transport vesicles. These genetic and molecular approaches will provide information on how TNO1 affects salt sensitivity in *Arabidopsis* and help us to understand the role of this TGN-localized complex in abiotic stress conditions.

Is TNO1 really a TGN matrix protein?

Under normal conditions, TNO1 co-localizes with VHAa1-GFP at the TGN. However, unlike VHAa1-GFP, TNO1 did not accumulate in the BFA compartment upon

BFA treatment. This characteristic was also observed for the mammalian golgin GM130, which functions as a Golgi matrix protein (Seemann et al., 2000). Upon BFA treatment, lumenal proteins in the Golgi were transported back to the ER, while GM130 remained in the remnant of the Golgi. golgin-97 is a tethering factor at the TGN in mammals and has extensive coiled-coil domains and a conserved C-terminal GRIP (Golgin-97, RanBP2a, Imh1p and p230) domain which is important for the TGN localization (Munro and Nichols, 1999; Yoshino et al., 2003). Overexpression of golgin-97 affects the structure and function of the TGN as well as localization of TGN resident proteins (Yoshino et al., 2003). Electron microscopy of HeLa cells overexpressing golgin-97 showed disruption of Golgi/ TGN structure and an increased number of enlarged late endosomes. Thus, golgin-97 is proposed to function in the maintenance of TGN integrity as a matrix protein, although a proteinaceous skeleton has not yet been identified at the TGN. Therefore, the structural similarity of TNO1 to mammalian golgins and its localization upon BFA treatment suggests that it could serve as a matrix protein in *Arabidopsis*. To address this question, one strategy that would determine whether TNO1 is a matrix protein is electron microscopy (EM). Firstly, BFA or control treated VHAa1-GFP transgenic plants would be fixed and labeled using TNO1 and GFP antibodies. EM images will provide greater resolution to identify the cellular behavior of TNO1 upon BFA treatment. Then, wild-type, *tno1* KO mutants and TNO1 overexpressing transgenic plants can be used to observe structural differences in the TGN. In *tno1* mutant, TGN may show different morphology compared with TGN in wild-type due to lack of its integrity that is normally maintained by TNO1, and plants overexpressing TNO1 may show disruption of Golgi/ TGN structure as golgin-97-overexpressing HeLa cells. Analysis of TGN structure and BFA response of TNO1 using these two sets of electron

microscopy will enhance our understanding of structural maintenance of the TGN and indicate whether TNO1 is a TGN matrix protein.

Putative role of TNO1 as a tethering factor.

This study suggests that TNO1 is involved in vacuolar trafficking. Delayed formation of the BFA compartment in the *tno1* mutant may indicate that TNO1 is involved in vesicle trafficking or vesicle fusion. Although we do not know the exact mechanism of TNO1 function in vacuolar trafficking, a putative role for TNO1 in vesicle fusion could explain the secretion of vacuolar proteins in the *tno1* KO mutant. TNO1 has long coiled-coil domains and interacts with SNARE proteins. In addition, its similarity to the yeast tethering factor USO1 suggests TNO1 could be involved in tethering vesicles before *trans*-SNARE complex formation and complete fusion via interaction with vesicle membrane as shown in USO1 (Noda et al., 2007). Another role of tethering factors is in SNARE complex formation, and p115 in mammalian cells and USO1 in yeast are essential for the formation of SNARE complexes (Sapperstein et al., 1996; Shorter et al., 2002). TNO1 may also be involved in SNARE complex formation, considering the mis-localization of SYP61 in the *tno1* mutant. To address whether TNO1 is involved in vesicle tethering and SNARE complex formation, *in vitro* liposome fusion assays could be used with several different versions of TNO1. Full length recombinant TNO1 will be reconstituted into acceptor vesicles containing SYP41 and the kinetics of membrane fusion between the donor vesicles containing VTI12 and acceptor vesicles in the presence and absence of TNO1 would be compared. TNO1 on the acceptor vesicle may bind to membrane of donor vesicle to pull the vesicle close to the target membrane, and then SNARE proteins on both membranes interact and drive membrane

fusion. Therefore, the presence of a tethering factor could increase the kinetics of membrane fusion. In addition, different versions of TNO1 produced by deleting one of six coiled-coil domains within TNO1, which may be required for interaction with SNARE proteins or with membrane, will indicate which coiled-coil domain is important to tether vesicles and to form a SNARE complex. Deletion of the coiled-coil domain for membrane binding is expected to show similar kinetics of membrane fusion to the fusion reaction in the absence of TNO1. Using *in vitro* binding assays, we can determine which coiled-coil domain is essential for the interaction with SNAREs. The results from *in vitro* fusion and *in vitro* binding assays using SNARE proteins found at the TGN and several truncated versions of TNO1 will increase our understanding of TNO1 as a putative tethering factor at Arabidopsis TGN.

Redundant function of VTI11 and VTI12

VTI11 has a greater affinity for SNAREs at the PVC than at the TGN *in vivo* (Sanderfoot et al., 2001a). VTI11 is thought to compensate for the loss of VTI12 in the *vti12* mutant, and we have shown that VTI11 is able to interact with SYP4 family proteins at the TGN and drive membrane fusion *in vitro*. VTI12 is also able to substitute for VTI11 *in vivo*. Therefore, it will be interesting to determine how VTI12 functions in the *vti11* mutant. To address this question, the same approach used for VTI11 would be employed. An *in vitro* fusion assay will be performed to determine whether VTI12 is able to drive membrane fusion with SYP21 and SYP51. This in vitro fusion result should indicate the extent to which functional redundancy between VTI11 and VTI12 is due to substitution of v-SNAREs in the respective SNARE complexes. This experiment would provide information on the functional

redundancy of VTI11 and VTI12 and increase our understanding of the function of the VTI1 family in *Arabidopsis*.

References

Bassham DC, Sanderfoot AA, Kovaleva V, Zheng HY, Raikhel NV (2000) AtVPS45 complex formation at the trans-Golgi network. Molecular Biology of the Cell **11:** 2251-2265

Brini F, Gaxiola RA, Berkowitz GA, Masmoudi K (2005) Cloning and characterization of a wheat vacuolar cation/proton antiporter and pyrophosphatase proton pump. Plant Physiology and Biochemistry **43:** 347-354

Chen Y, Shin YK, Bassham DC (2005) YKT6 is a core constituent of membrane fusion machineries at the Arabidopsis trans-Golgi network. Journal of Molecular Biology **350:** 92-101

Diao J, Su Z, Lu X, Yoon T, Shin Y, Ha T (2010) Single-Vesicle Fusion Assay Reveals Munc18-1 Binding to the SNARE Core Is Sufficient for Stimulating Membrane Fusion. ACS Chem Neurosci **1:** 168–174

Hamaji K, Nagira M, Yoshida K, Ohnishi M, Oda Y, Uemura T, Goh T, Sato MH, Morita MT, Tasaka M, Hasezawa S, Nakano A, Hara-Nishimura I, Maeshima M, Fukaki H, Mimura T (2009) Dynamic Aspects of Ion Accumulation by Vesicle Traffic Under Salt Stress in Arabidopsis. Plant and Cell Physiology **50:** 2023-2033

Hernandez A, Jiang XY, Cubero B, Nieto PM, Bressan RA, Hasegawa PM, Pardo JM (2009) Mutants of the Arabidopsis thaliana Cation/H+ Antiporter AtNHX1 Conferring Increased Salt Tolerance in Yeast THE ENDOSOME/PREVACUOLAR COMPARTMENT IS A TARGET FOR SALT TOXICITY. Journal of Biological Chemistry **284:** 14276-14285

Leshem Y, Seri L, Levine A (2007) Induction of phosphatidylinositol 3-kinase-mediated endocytosis by salt stress leads to intracellular production of reactive oxygen species and salt tolerance. Plant Journal **51:** 185-197

Marty F (1999) Plant vacuoles. Plant Cell **11:** 587-599

Munro S, Nichols BJ (1999) The GRIP domain - a novel Golgi-targeting domain found in several coiled-coil proteins. Curr Biol **9:** 377-380

Noda Y, Yamagishi T, Yoda K (2007) Specific membrane recruitment of Uso1 protein, the essential endoplasmic reticulum-to-Golgi tethering factor in yeast vesicular transport. J Cell Biochem **101:** 686-694

Poirier MA, Xiao W, Macosko JC, Chan C, Shin YK, Bennett MK (1998) The synaptic SNARE complex: A parallel four-stranded helical bundle. Molecular Biology of the Cell **9:** 84A-84A

Qiu QS, Guo Y, Dietrich MA, Schumaker KS, Zhu JK (2002) Regulation of SOS1, a plasma membrane Na+/H+ exchanger in Arabidopsis thaliana, by SOS2 and SOS3. Proceedings of the National Academy of Sciences of the United States of America **99:** 8436-8441

Qiu QS, Guo Y, Quintero FJ, Pardo JM, Schumaker KS, Zhu JK (2004) Regulation of vacuolar Na+/H+ exchange in Arabidopsis thaliana by the salt-overly-sensitive (SOS) pathway. Journal of Biological Chemistry **279:** 207-215

Sanderfoot AA, Kovaleva V, Bassham DC, Raikhel NV (2001a) Interactions between syntaxins identify at least five SNARE complexes within the golgi/prevacuolar system of the arabidopsis cell. Molecular Biology of the Cell **12:** 3733-3743

Sanderfoot AA, Pilgrim M, Adam L, Raikhel NV (2001b) Disruption of individual members of arabidopsis syntaxin gene families indicates each has essential functions. Plant Cell **13:** 659-666

Sapperstein SK, Lupashin VV, Schmitt HD, Waters MG (1996) Assembly of the ER to Golgi SNARE complex requires Uso1p. Journal of Cell Biology **132:** 755-767

Seemann J, Jokitalo E, Pypaert M, Warren G (2000) Matrix proteins can generate the higher order architecture of the Golgi apparatus. Nature **407:** 1022-1026

Shen JS, Tareste DC, Paumet F, Rothman JE, Melia TJ (2007) Selective activation of cognate SNAREpins by Sec1/Munc18 proteins. Cell **128:** 183-195

Shorter J, Beard MB, Seemann J, Dirac-Svejstrup AB, Warren G (2002) Sequential tethering of Golgins and catalysis of SNAREpin assembly by the vesicle-tethering protein p115. Journal of Cell Biology **157:** 45-62

Surpin M, Zheng HJ, Morita MT, Saito C, Avila E, Blakeslee JJ, Bandyopadhyay A, Kovaleva V, Carter D, Murphy A, Tasaka M, Raikhel N (2003) The VTI family of SNARE proteins is necessary for plant viability and mediates different protein transport pathways. Plant Cell **15:** 2885-2899

Sutton RB, Fasshauer D, Jahn R, Brunger AT (1998) Crystal structure of a SNARE complex involved in synaptic exocytosis at 2.4 angstrom resolution. Nature **395:** 347-353

Tareste D, Shen J, Melia TJ, Rothman JE (2008) SNAREpin/Munc18 promotes adhesion and fusion of large vesicles to giant membranes. Proceedings of the National Academy of Sciences of the United States of America **105:** 2380-2385

Yoshino A, Bieler BM, Harper DC, Cowan DA, Sutterwala S, Gay DM, Cole NB, McCaffery JM, Marks MS (2003) A role for GRIP domain proteins and/or their ligands in structure and function of the trans Golgi network. J Cell Sci **116:** 4441-4454

Zhu JH, Gong ZZ, Zhang CQ, Song CP, Damsz B, Inan G, Koiwa H, Zhu JK, Hasegawa PM, Bressan RA (2002) OSM1/SYP61: A syntaxin protein in Arabidopsis controls abscisic acid-mediated and non-abscisic acid-mediated responses to abiotic stress. Plant Cell **14:** 3009-3028

Zhu JK (2001) Plant salt tolerance. Trends in Plant Science **6:** 66-71

Zorb C, Noll A, Karl S, Leib K, Yan F, Schubert S (2005) Molecular characterization of Na+/H+ antiporters (ZmNHX) of maize (Zea mays L.) and their expression under salt stress. Journal of Plant Physiology **162:** 55-66

Zouhar J, Rojo E, Bassham DC (2009) AtVPS45 Is a Positive Regulator of the SYP41/SYP61/VTI12 SNARE Complex Involved in Trafficking of Vacuolar Cargo. Plant Physiology **149:** 1668-1678

APPENDIX A. TRANSCRIPTOME PROFILING OF THE RESPONSE OF *ARABIDOPSIS THALIANA* SUSPENSION CULTURE CELLS TO SUCROSE STARVATION

A paper published in Plant physiology

Anthony L. Contento[1,3], Sang-Jin Kim[1,2] and Diane C. Bassham[1,2,3]

[1]Department of Genetics, Development and Cell Biology, [2]Interdepartmental Genetics Program and [3]Plant Sciences Institute, Iowa State University, Ames, IA 50011, USA

ABSTRACT

Upon encountering nutrient stress conditions, plant cells undergo extensive metabolic changes and induce nutrient recycling pathways for their continued survival. The role of nutrient mobilization in the response of *Arabidopsis thaliana* suspension cells to sucrose starvation was examined. Vacuolar autophagy was induced within 24 hrs of starvation, with increased expression of vacuolar proteases that are likely to be required for degradation of cytoplasmic components delivered to the vacuole, and thus for nutrient recycling. After 48 hrs of starvation, culture viability began to decrease, and substantial cell death was evident by 72 hrs. To provide further insight into the pathways required for survival during sucrose deficit, transcriptional profiling during sucrose starvation was performed using the ATH1 GeneChip array containing 22,810 probe sets. A significant increase in transcript levels was observed for 343 genes within 48 hours of starvation, indicating a response to nutrient stress that utilizes the recycling of cellular components and nutrient scavenging for maintaining cell function, the protection of the cell from death through activation of various defense and

stress response pathways, and regulation of these processes by specific protein kinases and transcription factors. These physiological and molecular data support a model in which plant cells initiate a coordinated response of nutrient mobilization at the onset of sucrose depletion that is able to maintain cell viability for up to 48 hours. After this point, genes potentially involved in cell death increase in expression, whereas those functioning in translation and replication decrease, leading to a decrease in culture viability and activation of cell death programs.

INTRODUCTION

All organisms are dependent on nutrients from the environment for their continued viability and growth. In plants, the availability of nitrogen in the soil and the presence of adequate light are necessary for proper synthesis of proteins, lipids and polysaccharides. Plants have evolved both general and specific systems for survival during periods of nutrient stress that may be brought on by extended darkness. These systems utilize stored polysaccharides and recycled cellular components to replace missing nutrients, in order to prevent severe decreases in the amount of respiratory substrates and maintain important biochemical pathways during sucrose starvation (Aubert et al., 1996).

Major responses to carbon limitation include directed release of stored nutrients, and degradation of proteins, starch and fatty acids (Journet et al., 1986; Koch, 1996). Journet et al. performed a comprehensive study of the biochemical changes occurring in sycamore cells during starvation, and observed a decrease in the amount of sucrose, starch, protein and phospho- and galactolipids, suggesting an induction of degradative pathways for these components. This large-scale degradation was accompanied by decreases in the activity of

glycolytic enzymes and a loss in respiratory capacity. Vacuole-specific proteolysis during carbon starvation was induced by extended periods of darkness in maize roots and young leaves (Brouquisse et al., 1991; James et al., 1993; Brouquisse et al., 1998), with increased expression of a specific vacuolar serine endopeptidase (RSIP), leading to an increase in free amino acids. Fatty acid catabolism was also found to increase during glucose starvation in maize root tips (Dieuaide et al., 1992 and 1993). Through mobilization of the breakdown products of these metabolic processes, the cell is able to maintain those pathways and systems most essential for its survival for an extended period of time.

One of the key degradative processes for survival of eukaryotic cells during periods of nutrient starvation is vacuolar autophagy. During autophagy, portions of cytoplasm are transported to the vacuole or lysosome for degradation (see Huang and Klionsky, 2002 for a review), and this process is initiated by nutrient starvation in fungi, plants and animals. Carbon-starvation, and autophagy induced by carbon starvation, has been characterized in maize root tips (Brouquisse et al., 1991; James et al., 1993) and whole maize plants (Brouquisse et al., 1998), and rice (Chen et al., 1994), sycamore (Aubert et al., 1996), tobacco (Moriyasu and Ohsumi, 1996) and *Arabidopsis* (Bassham, 2002) suspension cell cultures during sucrose starvation. Changes observed in the starving cells include an increase in the size of the vacuole, a decrease in amount of cytoplasm and an increase in the activity of vacuolar enzymes (Moriyasu and Ohsumi, 1996). Large portions of cytoplasm, including organelles, are enveloped by membrane-bound vesicles to form autophagosomes, and transported to the vacuole for degradation, releasing nutrients for use in other pathways. The loss of oxidation potential seen in starving plant cells may also stem from the breakdown of mitochondria during this process (Journet et al., 1986). Studies in sycamore cells, using

electron microscopy and the accumulation of phosphorylcholine as a marker for an increase in autophagy, suggest that decrease in the supply of respiratory substrates is responsible for the onset of autophagy (Aubert et al., 1996).

Genetic studies of autophagy in yeast have revealed a group of mutants that are sensitive to nitrogen starvation. Autophagy in yeast requires a unique conjugation system, involving a number of proteins, which drives the initiation of macroautophagy, the formation of autophagosomes and the control of autophagosome size (Mizushima et al., 1998a and 1998b; Klionsky and Ohsumi, 1999; Ichimura et al., 2000). In *Arabidopsis,* genes encoding potential homologs for many of these yeast autophagy proteins have been found. *Arabidopsis* knockout mutants of the homologs of the yeast autophagy genes *APG9, APG7* and *VTI1* showed increased sensitivity to nitrogen deficiency and an early senescence phenotype (Hanaoka et al., 2002; Doelling et al., 2002; Surpin et al., 2003).

Starvation has been shown to induce the expression of a number of genes in various plant systems (Koch, 1996; Yu, 1999), including genes involved in transport and degradation of nutrients. Sucrose starvation in cucumber suspension cells increased the expression of glyoxylate cycle genes encoding malate synthase and isocitrate lyase (Graham et al., 1994), and carbohydrate depletion of the roots of a *Citrus reticulata* hybrid led to the induction of genes involved in sucrose transport and carbohydrate metabolism (Li et al., 2003). Genes encoding various vacuolar enzymes are specifically up regulated by sucrose starvation in suspension cells (Bassham, 2002), including invertase (Tymowska-Lalanne and Kreis, 1998), vacuolar processing enzyme-γ (Kinoshita et al., 1999) and aleurain (Ahmed et al., 2000), emphasizing the importance of this organelle in the degradation of macromolecules. One of the best-studied examples of sucrose starvation-regulated gene expression is the increase of

α-amylases during sucrose starvation of cultured rice cells (Chen et al., 1994), concomitant with the degradation of amyloplasts, suggesting an increase in starch breakdown. A TATCCA element present in the rice α-amylase promoters is recognized by three novel MYB transcription factors that are also upregulated by starvation (Lu et al., 2002). The promoters of the dark-inducible branched-chain-α-keto acid dehydrogenase subunits are activated during sugar starvation (Fujiki et al., 2000); however, they do not contain the TATCCA cis-element, suggesting that other cis-acting transcriptional elements are also involved in gene expression changes during sucrose starvation in plants.

While a significant amount of information is now available on the biochemical responses of plants to sucrose depletion, in many cases the genes responsible for these responses and their regulation remain unknown. Here, we characterize the physiological and morphological changes that occur in Arabidopsis suspension cells during sucrose starvation, and use Affymetrix GeneChip analysis to determine the changes in gene expression that may be responsible for these characteristic effects. We have identified transcripts encoding degradative enzymes and putative membrane transporters whose levels increase dramatically during sucrose starvation, and therefore are likely to function in starvation responses. mRNA levels for a number of genes predicted to encode transcription factors and signal transduction components also increased, and these genes are potentially involved in regulation of the observed responses. Genes known to be upregulated during other stress conditions were also identified, suggesting that, in addition to specific responses, general stress response pathways are induced during starvation. In contrast, genes encoding components of the translational apparatus and proteins functioning in cell division decreased in expression

during starvation, suggesting that these processes are specifically down-regulated during sucrose starvation.

MATERIALS AND METHODS

Growth of Arabidopsis suspension cell cultures

An *Arabidopsis thaliana* Columbia-0 suspension cell culture was obtained from Dr. SB Gelvin and maintained by subculturing weekly into 50-mL of medium (Murashige-Skoog Minimal Organics Medium (Gibco BRL, Gaithersburg, MD), 2% (w/v) sucrose, 1 μg/mL naphthalene acetic acid (Sigma, St. Louis, MO), 50ng/mL kinetin (Sigma, St. Louis, MO)). Cultures were grown in Erlenmeyer flasks at room temperature, under ambient light, with constant shaking (115-rpm rotation).

Sucrose starvation treatment of suspension cell cultures

All starvation time-courses were begun using suspension cells three days after subculturing, at an approximate cell density 2 x 10^5 cells/mL. Cultures were washed three times with either sucrose-containing medium for control samples, medium lacking sucrose for starvation samples, or medium containing 0.058M polyethylene glycol (PEG 4000) for osmoticum-replaced samples. After the third wash, 50-mL of the appropriate medium was added and the cells were grown for up to 72 hrs on a rotational shaker using the conditions described above. Samples (2-mL) were removed for morphological analysis and RNA extraction after 0, 6, 24, 48 and 72 hrs.

Measurement of respiration rate

One milliliter samples from suspension cultures starved for 0, 24, 48 and 72 hours, and control cultures grown in sucrose-containing medium, were pelleted and the fresh weight determined. Cells were then resuspended in the appropriate fresh medium (1 mL). Oxygen consumption was measured using an O_2 electrode (Rank Brothers, Bottisham, Cambridge, UK) at 25^{o}C and recorded by a Houston Instrument Chart Recorder (GTCO CalComp, Columbia, MD). Data were converted into nmol O_2 consumed/minute and standardized by total fresh weight. Each experiment was repeated three times.

Fluorescein cell viability assay

For fluorescein staining (Chaves et al., 2002), 5-mL samples of sucrose-starvation and control cultures were taken after 0, 24, 48 and 72 hrs. The medium was removed from each sample and replaced with 5-mL of phosphate-buffered saline. Fluorescein diacetate in ethanol was added to each sample to a concentration of 2.5μg/mL, followed by incubation at room temperature for 3 minutes. The samples were then placed on ice and three hundred cells from each sample were analyzed using UV-fluorescence microscopy. Fluorescing cells were counted as living.

Culture viability assay

After sucrose starvation of suspension cultures for 0, 24, 48 and 72 hrs, as described above, the starvation medium was replaced with sucrose-containing medium and growth continued. 5-mL samples were taken every 48 hrs for 12 days and cell volume and fresh cell mass was measured for each time point.

Total RNA isolation and northern blot analyses

Suspension cell samples were collected, the medium was removed and the cells were stored at –80^{o} C until RNA extractions were performed. Total RNA for northern blot analysis, RT-PCR and GeneChip microarray analysis was isolated using a TRIzol extraction method (http://www.science.siu.edu/plantbiology/PLB420/DNA.Techniques/TRIzol.method.html) followed by the RNeasy Clean-up protocol (Qiagen, Valencia, CA), as recommended by the University of Iowa DNA Core Facility, to obtain the best results for use with Affymetrix's GeneChip Expression Analysis system. Northern blot analyses were performed using probes consisting of radiolabeled cDNA fragments corresponding to At5g60360 (*AALP*; Ahmed et al., 2000), At4g32940 (*VPE-γ*; Kinoshita et al., 1999), At3g30775 (*PRODH*; Nakashima et al., 1998) and At5g17290 (*APG5/ATG5*). All primers used in this study are listed in Table IV. Hybridization was performed using the manufacturer's protocol for UltraHyb solution (Ambion, Austin, TX).

GeneChip analysis and expression data processing

RNA was isolated from suspension cells starved for 0, 24 or 48 hrs, from cells grown for 48 hrs in the presence of sucrose, and from 48 hr starved cultures containing 0.058M PEG 4000 as an osmotic control. In each case, RNA was pooled from three independent experiments and used to synthesize cRNA, which was hybridized to an ATH1 Arabidopsis GeneChip microarray (Affymetrix, Santa Clara, CA) containing 22,810 probe sets. Two independent biological replicate microarray hybridizations were performed for all samples except for the 48 hr no sucrose plus PEG 4000 sample. Each replicate was from an

independent starvation time course, started from different subcultures and performed at different times. Synthesis of cRNA, hybridization to the ATH1 GeneChips, chip scanning and data accumulation was performed at the University of Iowa DNA Core Facility, using the Affymetrix-recommended protocol. Data was accumulated using Affymetrix's MicroArray Suite version 5.0. Relative expression intensities were generated in the form of average difference values. GeneSpring (Silicon Genetics, Redwood, CA) was used for data normalization, data visualization and cluster analysis. Using GeneSpring, the median expression level of each chip was normalized to a value of one by dividing each measurement for each probe set by the 50^{th} percentile of all measurements on that chip. MAS 5.0 calculated the 50th percentile using the average difference of all probe sets labeled "present" in at least one sample. Normalized values less than 0 were set to 0. Fold change was calculated by dividing the average difference for each experimental starvation sample by the average difference for the untreated 0 hr sample. Probe sets with a four-fold (rounded up) or greater change in expression levels in either of the sucrose starvation samples compared with the 0 and 48 hr controls were identified. A normalized intensity value of 0.8 was used as a cutoff for reliable detection, and also removed a negative bias in lower intensity values when comparing scatter plots of replicate samples from different hybridizations. Probe sets that did not also show a change in transcript level of at least two-fold (rounded up) in the starvation samples containing PEG 4000, as compared to the 0 and 48 hr controls, were discarded, as potentially being due to osmotic differences. Using these criteria, transcript levels for 343 unique genes were found to increase during starvation, whereas 263 genes showed a decrease in transcript level. The probe sets for the upregulated genes were used to perform k-means cluster analysis, using 5 clusters, with 100 iterations, comparing

similarity by Pearson Correlation. Individual Pearson correlations were also performed using a 0.95 minimum correlation based on the characteristic expression patterns of the following probe sets: At3g48360 (set1), At1g66280 (set 2) and At1g20620 (set 3). Four of the five clusters were combined into two separate clusters, based on the similarity in their expression patterns and comparison with the Pearson correlations for the individual probe sets.

Verification of GeneChip data by northern blot hybridization and reverse transcriptase-polymerase chain reaction

Oligonucleotide primers were designed for eight gene transcripts (At1g13260, At1g20620, At1g21920, At1g78290, At2g33830, At4g36670, At5g10030 and At5g61590) that showed an increase in expression in the starvation samples, according to the GeneChip data. First-strand cDNA was synthesized from 2μg of DNase-treated total RNA from suspension cells using Superscript II Reverse Transcriptase (Invitrogen, Carlsbad, CA), followed by PCR amplification. The products were ligated into the pGEM-Teasy vector system (Promega, Madison, WI) and gene identity was verified by DNA sequencing performed at the Iowa State University DNA Sequencing and Synthesis Facility. RT-PCR samples were used to semi-quantitatively determine the relative amount of product by visualization using DNA agarose electrophoresis. The products were also used as probes for northern blot hybridization analysis, as described above.

Upon request, all novel materials described in this publication will be made available in a timely manner for non-commercial research purposes.

RESULTS

Changes in cellular morphology and growth during sucrose starvation of Arabidopsis suspension cell cultures

An *Arabidopsis thaliana* ecotype Columbia suspension cell culture was chosen for initial studies on sucrose starvation because the cells lack mature plastids and are incapable of photosynthesis. The cells are therefore dependent on the sucrose in the growth medium for their sole source of carbon. Suspension cell cultures also allow for homogeneity in the type of tissue used for the experiment, thus synchronizing the onset of starvation responses. To analyze the effect of sucrose depletion on cell morphology and growth, suspension cultures were grown for three days in the presence or absence of sucrose. Samples were taken at 0, 6, 24, 48 and 72 hrs and used for microscopy and RNA extraction.

Light microscopy of the cells at various time-points during starvation revealed similar morphology to that seen in previous studies in tobacco (Moriyasu and Ohsumi, 1996) and *Arabidopsis* (Bassham, 2002). The size of the vacuole began to increase and the cytoplasmic volume was reduced after 24 hrs of sucrose starvation (Figure 1). After 48 hrs of starvation, much of the cytoplasm, including its organelles, was gone, and the vacuolar compartment took up most of the cellular volume, whereas after 72 hrs, the incidence of cell death increased. Autophagosome formation was observed in the cells after 24 hrs and 48 hrs of starvation (A.L. Contento, Y. Xiong and D.C. Bassham, manuscript in preparation), and an increase in expression of the autophagy marker *APG8* occurred at these time points (see Figure 7). These cytological changes indicate that autophagy is induced by 24 hrs after transfer to sucrose-free medium, and continues for at least another 24 hrs.

To correlate these morphological changes with physiological activity of the cultures, respiration rate was measured during starvation. Compared with the 0 hr time point, the rate of respiration was reduced by approximately 70% after 24 hrs of starvation, and still further after 48 hrs starvation to approximately 20% of the control (Figure 2A). By 72 hrs, respiration decreased almost to zero, potentially reflecting a loss in culture viability and cell death. In contrast, a small increase was seen after 24 hrs in control (plus sucrose) time courses (Figure 2B), possibly due to the transfer to fresh medium. Even after 72 hrs, only a 30% decrease in respiration rate was observed, indicating that control cultures are active throughout the study. In addition, the total RNA level in the cells remained constant for the first 48 hrs of starvation, whereas after 72 hrs, total RNA levels decreased dramatically (data not shown), also suggesting that cell death is occurring by this time point.

To determine the viability of the culture during starvation, suspension cells were grown in the absence of sucrose for up to 2 days, after which the medium was replaced with medium containing sucrose and growth continued. The fresh weight of the cells was measured during the rescue period to evaluate recovery of the cultures (Figure 2C). Cultures starved for 24 hrs were able to recover in a manner similar to non-starved cultures, but by 48 hrs a decrease in the viability of the culture was observed. The cultures starved for 48 and 72 hrs never resumed growth, even after several weeks, indicating that starvation is irreversible by 48 hrs. The small increase in fresh weight of 48 and 72 hr cultures during the time course in figure 2C may be due to an increase in water content, rather than growth of the cells. A similar result was observed in starved maize root tips, where water content increased steadily during starvation, leading to an increase in fresh weight, even though dry weight decreased (Brouquisse et al., 1991). To determine the percentage of living cells, cells were stained with

fluorescein diacetate at each time-point after initiation of starvation, and the percentage of viable cells calculated (Figure 2D). Control samples, washed with sucrose-containing medium, consistently demonstrated approximately 80% living cells. Viability was maintained after 24 hrs starvation, while the number of living cells dropped sharply afterwards, to less than 50% after 72 hrs of starvation. When the vital staining data is taken together with the cell rescue data, it is evident that while more than half of the cells are still living by 48 hrs of starvation, and respiration is maintained at similar rates to cultures starved for 24 hrs, the culture is not able to recover. This suggests that a change in the physiology of the cell culture is taking place between 24 and 48 hrs of starvation, leading to a loss of reversibility of starvation.

Increase in expression of genes encoding vacuolar proteases during starvation

A number of sugar-responsive genes have previously been identified (e.g. Koch 1996; Fujiki et al., 2000; Sheen, 1990), and typically increase in expression rapidly after removal of sucrose. However, our focus is on nutrient mobilization processes during starvation, rather than direct sugar regulation, and these processes occur at much later time points after sugar removal. Expression of genes encoding the vacuolar proteases aleurain-like protein (AALP; Ahmed et al., 2000) and vacuolar processing enzyme-γ (VPE-γ; Kinoshita et al., 1999) are known to increase under conditions of stress, including sucrose starvation, potentially to breakdown and recycle damaged and non-essential proteins (Bassham, 2002). The increase in the expression of these vacuolar genes was therefore used as a marker to determine when nutrient remobilization occurred, using the stably expressed *autophagy 5* gene (*APG5*/*ATG5*) as a control (Figure 3). *AALP* and *VPE-γ* transcript levels were found to

increase as the starvation time-course progressed, with maximum transcript levels observed after 48 hrs of starvation, whereas no increase in expression was seen in non-starved control cultures. These data suggest that an increase in vacuolar function and autophagy occurs within 48 hrs of starvation in Arabidopsis suspension cultures, as a component of the nutrient stress response.

Gene expression profiles in response to sucrose starvation

From the above data, most of the morphological and molecular responses of Arabidopsis suspension cells to starvation occur by 48 hrs in sucrose-free medium. We therefore examined the changes in gene expression that occur between 0 and 48 hrs of sucrose starvation. RNA was extracted from cultures grown for 0, 24 or 48 hrs after transfer to starvation medium, or 48 hrs in sucrose-containing medium as a control. As an additional control for osmotic differences in the growth media, in one sample sucrose was replaced with polyethylene glycol (PEG) to maintain iso-osmotic conditions. These total RNA samples were used as templates for labeled cRNA synthesis and hybridized to *Arabidopsis* ATH1 Genome GeneChip microarrays (Affymetrix, Santa Clara, CA), which contain probe sets representing 22,810 unique genes. Microarray Suite 5.0 (Affymetrix, Santa Clara, CA) and GeneSpring (Silicon Graphics, Redwood, CA) were used to normalize the data from each experiment, and probe sets showing changes in transcript levels in the starved cells, as compared to the non-starvation controls, were identified.

Scatter plots comparing expression data between biological replicates of control samples (0 hrs; Figure 4A) demonstrated that the majority (99%) of the genes varied in expression by less than 4-fold. It was therefore decided that a 4-fold cutoff would be used to

identify expression changes between samples, as this would allow identification of differentially expressed genes with a high confidence. Genes that fell outside of this cutoff when comparing replicate samples were excluded from further analysis. Probe sets showing normalized signal intensities of less than 0.8 in all samples were considered to be below the limit of detection, and were not analyzed further. Figures 4B and C show scatter plots of signal intensities from 24 and 48 hr starved samples against the control 0 hr sample. RNA levels corresponding to many different genes can be seen to increase or decrease dramatically during sucrose starvation. Genes showing a 4-fold increase or decrease in transcript levels in at least one of the starvation samples, compared to the 0 hr and 48 hr control samples, were identified as being significantly induced. In addition, any transcripts whose expression did not change in the PEG osmotic control as compared with non-starved controls were discarded. Using these criteria, a total of 343 genes were found to have increased mRNA levels when subjected to sucrose starvation, whereas the mRNA level of 263 genes decreased (see supplemental data). The genes were assigned a functional classification based on the Munich Information Center for Protein Sequencing (MIPS) database (Figure 5; Schoof et al., 2002). Approximately 40% of the genes identified are not yet classified based on known function and/or sequence or structure homology.

Genes upregulated during starvation

Nine of the genes that increase in expression during starvation are classified as being involved in energy production, including two light-harvesting chlorophyll a/b binding proteins and five photosystem I and II component proteins. A number of photosynthetic genes have been found to be induced by sugar starvation in maize (Sheen, 1990) and the

increase in transcript levels of these genes in our samples could be considered a response designed to increase the level of photosynthesis, even though the suspension culture used is non-photosynthetic.

Over 15% of the identified genes are involved in metabolic processes including carbohydrate metabolism, tyrosine, isoleucine and valine amino acid metabolism, protein and lipid degradation, and trehalose metabolism. Numerous members of various glycosyl hydrolase families are represented in the data and may be involved in carbohydrate degradation. Two forms of branched-chain-α-keto acid dehydrogenase may be involved in amino acid metabolism and have been documented as expressed during darkness-induced starvation (Fujiki et al., 2000 and 2002). A group of putative lipases may be involved in lipid degradation during starvation. Twenty-four of the genes identified encode proteins potentially involved in transport facilitation, including a number of carbohydrate and ion transporters, presumably for the scavenging of nutrients. These metabolic and transport proteins are most likely involved in a cellular response to compensate for the sucrose starvation by seeking out new sources of nutrients and initiating the use of other metabolic substrate pathways.

Three of the eleven trehalose-6-phosphate synthases (Figure 6A) and one of the ten trehalose 6-phosphate phosphatases (Figure 6B) found in *Arabidopsis* are significantly upregulated upon sucrose starvation. Trehalose 6-phosphate (T6P) levels have been shown to regulate carbohydrate utilization and growth, through regulation of glycolysis (Schluepmann et al., 2003). Schluepman et al. have shown in *Arabidopsis* that supplied sugar leads to a reduction in T6P levels, which leads to decreased carbohydrate metabolism and growth. An increase in T6P levels, via increased levels of trehalose phosphate synthases, should cause an

increase in carbohydrate utilization. A knockout mutant in the *TPS1* gene is embryo-lethal, indicating that this gene is required for embryo development (Eastmond et al., 2002). Interestingly, the mutant embryos arrest at the time when deposition of storage reserves is initiated, and a dramatic increase in the sugar supply to the embryo occurs in wild-type seeds, again indicating a correlation between sugar metabolism and T6P level. The physiological function of the remaining *TPS* genes is as yet unknown, but the increase in expression of three of these genes during sucrose starvation may also lead to an increase in T6P, and therefore to enhanced carbohydrate metabolism.

Two TPP genes also change in expression during starvation, one increasing and the other decreasing in mRNA level (Figure 6B). TPP breaks down T6P to trehalose, thus having an opposing effect on T6P levels when compared with TPS. When TPS and TPP were expressed in rice as a gene fusion, an increase in trehalose levels were observed, and the transgenic plants showed an increased tolerance to various abiotic stresses (Garg et al., 2002). We also observed that two of the TPP genes were responsive to changes in osmotic potential (At5g10100 and At5g51460 in Figure 6B). Clearly, much additional work is needed before the precise function of T6P and trehalose in starvation and other stress conditions, and the role of each of the TPS and TPP isoforms, can be determined. Morphological analysis of suspension cells during sucrose starvation (Figure 1) indicated that vacuolar autophagy occurred by 24 hrs of starvation. In agreement with this, a transcript encoding a homolog of the yeast APG8/ATG8 protein displayed increased transcript levels under these conditions (Figure 7). APG8/ATG8 in yeast is thought to be required for lipid recruitment and regulation of the size of autophagosomes during autophagy (Kirisako et al., 1999 and 2000; Ichimura et al., 2000). An increase in the amount of Arabidopsis

APG8/ATG8 therefore suggests an increase in autophagy. There are nine homologs of the yeast *APG8/ATG8* gene in Arabidopsis, but only one of them (At2g45170) increased significantly in expression due to starvation of the suspension cells (Figure 7), possibly indicating a functional specialization of members of the gene family. A second *APG8/ATG8* gene (At3g06420) increased during starvation only under osmotic stress conditions, suggesting that members of this family may be involved in response to diverse environmental stresses.

Thirty-nine genes with increased expression during starvation are predicted to be involved in transcription, including a group of 4 *bZIP* transcription factors, 6 *myb* transcription factors, 2 WRKY transcription factors and a RAV1 DNA-binding element (Table I). The basic region/leucine zipper motif (bZIP) transcription factor family has 75 members that have been shown to regulate processes including pathogen defense, light and stress signaling, seed maturation and flower development (see Jakoby et al., 2002 for a review). The RAV1 DNA-binding protein has been cloned from *Arabidopsis* and contains amino acid sequence domains that are unique to plants (Kagaya et al., 1999). No specific physiological function or target genes are currently known for these proteins, but the promoters of a 2-Cys peroxiredoxin gene and an auxin binding protein gene have been shown contain binding regions for RAV1. However, neither of these genes shows increased expression in our experiment. Three *myb* proteins have recently been found to mediate α-amylase expression during periods of sugar starvation in rice (Lu et al., 2002). It is possible that the six *myb* family proteins found during this study could have similar regulatory control in *Arabidopsis* during nutrient stress. The WRKY transcription factor family has 74 members in *Arabidopsis* and they have been suggested to be involved in responses to biotic

and abiotic stresses, defense responses and regulation of senescence (see Eulgem et al., 2000 for a review).

Thirty of the genes are known or predicted to function in cell rescue, defense and virulence. These genes included reactive oxygen scavenging enzymes and several disease resistance proteins, and are most likely involved in the non-specific response to the stress of sucrose starvation in *Arabidopsis* cells. Catalase-3 was found to have a large increase in expression. Of the three Arabidopsis catalase proteins, catalase-3, a Class III catalase, is commonly found in glyoxysomes and may be involved in removal of the H_2O_2 created during β-oxidation (Willekens et al., 1995; Dat et al., 2000). Three genes for DnaJ proteins also show an increase in transcript levels. The J-domain family of proteins has 89 members in *Arabidopsis* and DnaJ-like proteins can act independently or in conjugation with DnaK and GrpE as molecular chaperones during environmental stresses, such as heat shock (Miernyk, 2001). Interestingly, the three genes showing an increase in transcript levels during sucrose starvation all lie within the same subgroup of J-domain proteins, and have all been predicted to be localized within the plastid. It is possible that these proteins could be involved in proper chloroplast assembly during periods of nutrient stress. Five potential disease resistance Toll/interleukin-1 receptor (TIR) class proteins (R genes) were also found during this study. Many R genes are involved in the local hypersensitive defense response to pathogen attack (Meyers et al., 2002), although the specific function of the genes that we identified is not yet known.

Nineteen of the genes are predicted to function in cellular communication and signal transduction (Table II), including seven protein kinases. The transcript levels of three of these genes, ethylene responsive binding element factor 5, a putative phosphatidylinositol-4-

phosphate-5-kinase and an auxin regulated protein, are all found to increase during phosphate starvation as well (Wu et al., 2003). It is possible that these genes may be involved in a general starvation response, although, in contrast to sucrose starvation, phosphate starvation involves a decrease in photosynthesis and carbon metabolism. However, it may be suggested that a lack of different nutrients induce the expression of similar genes and thus activate the same signal transduction pathway.

Genes downregulated during starvation

Our main focus is on genes that increase in expression during starvation, as these are likely to function in the stress response. However, an examination of genes that decrease in mRNA level during sucrose starvation reveals a striking number of genes involved in translation (Figure 5B). These include 19 ribosomal proteins and two translation initiation factors, eIF4A and eIF2γ (Table III). This indicates that a general decrease in protein synthesis may occur, particularly at later time points during starvation, as the mRNA levels continue to decrease throughout the time course. It is known that in yeast and animal cells, translational activity is tightly linked to nutritional status, and is controlled by the TOR kinase pathway (Barbet et al., 1996; Proud, 2004). A TOR homolog is present in Arabidopsis (Menand et al., 2002), and it is likely that translation is also regulated by TOR during starvation in plant cells.

Genes involved in cell division also decrease in expression during sucrose starvation (Figure 5B), as might be expected with growth arrest of the culture. These include the Arabidopsis homologs of the DNA replication factors RPA1 (Van der Knaap et al., 1997) and MCM3 (Stevens et al., 2002), two B-type cyclins (Ito et al., 1998) and the cytokinesis-

specific syntaxin KNOLLE (Lukowitz et al., 1996; Lauber et al., 1997). Each of these genes is known to be under cell cycle control, either in Arabidopsis or in other species, and the decrease in expression during starvation may therefore be due to a cessation in cell division. In addition, 7 genes encoding putative histone proteins were identified. As histones are synthesized preferentially during S-phase (Callard and Mazzolini, 1997), although lower amounts are synthesized throughout the cell cycle, the reduced expression during starvation could again be linked to cell division arrest.

Analyses of expression profiles of up-regulated genes

The expression patterns of the 343 starvation-induced transcripts were classified into three groups using k-means cluster analysis and Pearson correlations, corresponding to (1) an increase in RNA level from 24 to 48 hrs; (2) a decrease from 24 to 48 hrs; and (3) no change between 24 and 48 hrs of starvation (Figure 8). As might be expected, genes involved in metabolism and transcription, the two categories containing the highest number of genes, were spread throughout the three groups. In contrast, most of the genes classified as functioning in membrane transport and those in stress responses and defense were found in groups 1 and 3, with very few genes showing a decrease in expression at the later time points. These gene products therefore appear to be required throughout the time course, indicating that nutrient scavenging and general stress responses continue even during extreme starvation conditions. Strikingly, a large number of the genes predicted to function in disease resistance or pathogen response increased in expression throughout the time course. A characteristic feature of plant-pathogen responses is cell death, and one possibility is that the increase in expression of these genes plays a role in the loss of culture viability seen after 48

hrs of starvation. Several potential plasma membrane aquaporins also increase at 48 hrs, and it is possible that these proteins cause changes in membrane permeability leading to cell death. Brouquisse et al. (1991) measured the intracellular osmolarity in excised maize root tips during sucrose starvation, and saw a sharp decrease in osmolarity concomitant with loss of reversibility of the starvation responses. They proposed that this is likely to be due to a rapid increase in permeability of the plasma membrane and tonoplast, eventually causing cell death, and a similar process may be occurring in our suspension cultures. Genes involved in signal transduction showed perhaps the most interesting trend, with subsets of transcripts increasing or decreasing between 24 and 48 hrs of starvation, but very few remaining constant in expression between these times. This suggests that distinct signaling pathways are activated at different starvation time points, and the kinetics of activation of these pathways may hint as to their role in the nutrient stress response.

The promoter regions (1000 nucleotides upstream of the start codon) of genes in each of the three groups were examined for the presence of common regulatory elements using the AlignAce program (Hughes et al., 2000). However, no clear candidates for *cis*-acting motifs were obtained. In addition, promoters were analyzed for known motifs in the PLACE database (Higo et al., 1999) using the Signal Scan program (Prestridge, 1991). Several of the genes in group 1 had a large number (up to 11) of WRKY transcription factor binding motifs in their upstream regions, and two WRKY transcription factors are also in this group, suggesting that they may be involved in the regulation of these genes. However, these motifs are commonly found within the genome, and the significance of this finding remains to be determined experimentally.

Verification of GeneChip Expression Data

Northern blot analysis was used to verify the increased transcript levels of eight genes identified by the GeneChip analysis: RAV1 DNA-binding protein (*RAV1*), catalase-3 (*CAT3*), a putative phosphotidylinositol-4-phosphate-5-kinase-like protein (*PI4P-5K*), a serine/threonine protein kinase (*STPK*), a potential auxin-regulated protein kinase (*AUX*), a sugar transporter (*SUG*), a bZIP family transcription factor (*OBF4*) and an ethylene-responsive binding factor element (*ERF5*). These genes were chosen to represent diverse functional categories, and various overall transcript levels. In each case, the trend in transcript level was the same for the northern blot hybridizations and GeneChip analysis (Figure 9A).

As several of these genes are members of gene families that could potential cross-hybridize with the above probes, the results were confirmed by Reverse Transcriptase-PCR using transcript-specific primers (Figure 9B). The identity of the RT-PCR products was confirmed by DNA sequencing. In each case, a good correlation was observed between the RNA blots, RT-PCR and GeneChip analysis (Figure 9B), confirming that the GeneChip analysis has reliably identified specific genes whose transcript levels increase during carbon starvation.

DISCUSSION

Sucrose starvation in Arabidopsis suspension cells induces increases in the transcript levels of 343 genes

In this study, we report increases in the transcript levels of 343 distinct genes that we hypothesize are involved in the response to sucrose starvation in *Arabidopsis thaliana*

suspension cells. Zero, 24 and 48 hr starvation time points were chosen for GeneChip analysis, based on the observation that most of the morphological changes of the suspension cultures occurred between 24 and 48 hrs after transfer to sucrose-free medium, and that the increase in expression of vacuolar enzymes showed similar kinetics. Cluster analysis revealed that the genes showing an increase in mRNA level during starvation showed three possible expression patterns. Twenty-two genes showed a significant decrease in transcript levels between 24 and 48 hrs of starvation and 84 genes showed a significant increase. The transcripts showing a decrease in expression after 24 hrs may potentially be involved with the initiation and regulation of the nutrient mobilization and recycling responses that occur at this time. These transcripts encode proteins with a wide variety of potential functions, including the SUC1 sucrose transporter, a bZIP transcription factor, a homeodomain protein, and trehalose 6-phosphate phosphatase. After 24 hrs of sucrose starvation, they may be down regulated during a shift to a response for the increasing severity of the nutrient stress. Processes that respond to these increasing levels of nutrient stress or that are involved in cell death may regulate the genes that showed an increase in expression after 24 hrs. Examples of these genes include three of the cytochrome p450 family genes, a putative heat shock transcription factor and RAV1. These proteins could be required for a rising metabolic response to nutrient starvation or the activation of proteins designed to deal with the increasing level of stress. Surprisingly, expression of most of the genes did not change between 24 and 48 hrs, suggesting that many of the processes involved in the plant response to sucrose starvation are maintained between 24 and 48 hrs.

One point that needs to be considered is the transition, occurring between 24 and 48 hrs of starvation, from a survival response to cell death, evident in the loss of culture and cell

viability (Figure 2). Autophagy is induced in the starved cultures by 24 hrs (Figures 1 and 7), presumably to recycle nutrients for cell survival, and continues throughout the time course. In mammalian cells, autophagic or type II programmed cell death has been characterized as showing the morphological hallmarks of autophagy (Bursch et al., 2000), although the relationship between the mechanism of autophagy as a survival response and autophagic cell death has been the subject of some debate. Recently, two proteins involved in autophagy, ATG7 and Beclin1, identified originally in yeast as being required for survival during starvation (Kametaka et al., 1998; Mizushima et al., 1998), have also been shown to function during autophagic cell death in mammals (Yu et al., 2004). This indicates that starvation-induced autophagy and autophagic cell death share at least some of the same machinery. In plants, cell death with morphological characteristics of autophagic cell death has been observed (Lam, 2004), and it is possible that a similar mechanism is responsible for cell death at later time points during sucrose starvation.

Sucrose starvation may induce changes to carbohydrate metabolism, and degradation of proteins and fatty acids as alternate sources of respiratory substrates

With sucrose as the sole carbon source and an inability to perform photosynthesis, the cells used in this study were forced to seek out alternative sources of metabolic substrates to maintain cellular respiration. α-galactosidases and β-galactosidases, as well as a number of other glycosyl hydrolases, showed increased transcript levels. This may suggest an attempt to switch to other types of carbohydrate metabolism, as an alternative source of metabolic substrates, by the suspension cells. Transcripts encoding enzymes involved in tyrosine (homogentisate 1,2-dioxygenase), isoleucine, leucine, valine, (α-ketoacid

dehydrogenase), lysine (lysine-ketoglutarate reductase), and arginine catabolism (ornithine aminotransferase) also increase during starvation. Increases in proteolysis have already been witnessed in starving maize root tips (James et al., 1993). This, coupled with the observed increase in the transcript levels of carboxypeptidases, suggests an increase in proteolysis and possible utilization of amino acids from unnecessary proteins as another source of carbon and/or energy to maintain vital functions in the starving cells. This protein degradation is likely to occur at least in part in the vacuole, as vacuolar autophagy increases during starvation by both morphological criteria (Figure 1) and increase in expression of the autophagy-specific gene *APG8/ATG8* (Figure 7).

Increases in the transcript levels of a phospholipase, a triacylglycerol lipase, a putative lipase, and transcripts for genes involved in fatty acid oxidation suggest a possible increase in the breakdown of fatty acids as well. It has been reported that β-oxidation increases in plants during carbon starvation (Dieuaide et al., 1992 and 1993), and transcript levels for a peroxisomal acyl-CoA synthase and a peroxisomal acyl-CoA oxidase (ACX4), shown to be unique to plants and involved in short-chain acyl CoA oxidation (Hayashi et al., 1999), increase under our experimental conditions. Acyl CoA oxidase is a hydrogen peroxide- generating enzyme, and the increase in transcript for the peroxisomal catalase-3 may be in response to excess hydrogen peroxide produced by an increase in β-oxidation. A potential increase in isoleucine, leucine and valine degradation is suggested by induction of two mitochondrial α-ketoacid dehydrogenase (BCKDH) transcripts. Products from this degradation must feed into β-oxidation in order to be completely catabolized (Graham and Eastmond, 2002). An increase in transcript levels of an α-dioxygenase-peroxidase suggests that α-oxidation also increases. Hamburg et al. have suggested that α-oxidation is involved in

the induction of the plant response to pathogens (Hamburg et al., 1999), and the products of α-oxidation may also act as signals for the response to nutrient stress. Overall, these results indicate an apparent switch towards the degradation and oxidation of fatty acids in carbon starved cells.

Like sucrose starvation responses, senescence also involves the breakdown of macromolecules and mobilization of nutrients, in this case to different parts of the plant. Parallels may therefore be drawn between these two processes, and it has been suggested that senescence may be induced by sugar depletion in some species (Yoshida, 2003). Four senescence-associated genes showed altered expression levels during starvation, two increasing and two decreasing (see supplementary data tables; Oh et al., 1996; Panavas et al., 1999; Quirino et al., 1999), suggesting that these genes may in fact be responding to changes in sucrose concentration. A comparison of gene expression profiles during starvation with expression profiles during senescence of leaves or flowers reveals some similarities, such as an increase in catalase-3 (Swidzinski et al., 2002), several transcription factors (At2g23340, At5g10030, At5g65210; Chen et al., 2002), and genes potentially involved in lipid metabolism and protein degradation (Bhalerao et al., 2003; van Doorn et al., 2003). However, the majority of genes studied do not show similar trends during senescence and starvation, indicating that while senescence and starvation responses share some common pathways, these processes also have unique features and requirements, as might be expected due to their distinct physiological roles in stress and development.

Increased levels of transcription factors and proteins involved in signal transduction may activate and regulate the responses to sucrose starvation in Arabidopsis

suspension cells

A recent microarray study of *Arabidopsis* transcription factors has determined that many of the factors found in this species are multifunctional for responses to environmental stresses and hormones (Chen et al., 2002), and in concurrence with these results, thirty-nine potential transcription factor genes displayed increased transcript levels in our study. These include several genes of the bZIP (basic region/leucine zipper) family, members of which have been shown to be involved in light and stress signaling and seed maturation (see Jakoby et al., 2002 for a review). One of the bZIP factors is from a group of proteins that may regulate seed storage protein production and responses to environmental or pathogen stresses. Another three of the bZIP proteins are from a group linked to defense against pathogens and development. Two WRKY transcription factors were also identified. WRKY proteins bind to the (T)(T)TGAC(C/T) W-box motif (de Pater et al., 1996), and members of the protein family have been shown to be expressed during plant wounding (Hara et al., 2000), and as early regulators of plant defense (Eulgem et al., 1999). Of the two genes identified, WRKY45 is also upregulated in response to pathogen infection and salicylic acid (Dong et al., 2003), implicating this factor in regulation of diverse stress responses, whereas the expression pattern of WRKY65 is unknown. Considering that the WRKY family has 74 members in Arabidopsis, it is likely that these two WRKY proteins are involved in the regulation of gene expression during carbon nutrient stresses. These transcription factors may be involved in the regulation of the many metabolic and stress-related proteins that were induced during starvation.

One well-characterized system of transcriptional regulation during starvation is the expression of amylase genes in rice. The amylase3 promoter contains a TATCCA element

that has been shown to serve as an enhancer for sugar starvation-induced expression (Lu et al., 2002). Variants of the TATCCA element are found upstream of 18 amylase genes isolated from various plant species (Yu, 1999) and other sugar-starvation induced genes, such as the cucumber malate synthase and isocitrate lyase genes (Graham et al., 1994) and the maize sucrose synthase gene (Koch, 1996). These findings suggest that the TATCCA element could be a common cis-regulatory element used during sugar starvation. Three novel rice *myb* transcription factors were shown to bind to the TATCCA region and mediate α-amylase expression (Lu et al., 2002). None of the starvation-induced genes above increased substantially in expression under our experimental conditions; however, several potential *myb* transcription factors showed an increase, and may function in the up-regulation of a subset of the identified starvation-induced genes; future study of these transcription factors should lead to a better understanding of their targets and the pathways that they regulate.

Regulation of starvation responses is likely to involve signaling cascades, typically involving a series of protein kinases. While these pathways are often not transcriptionally controlled, a number of genes predicted to function in cellular communication and signal transduction increase in expression during sucrose starvation. These genes include a large group of protein kinases, a phosphatidylinositol-4-phosphate 5-kinase-like protein, and several proteins known to play a role in hormone signaling pathways. The precise function of these proteins, and whether some of the observed starvation responses are hormonally controlled, remains to be determined.

Genes functioning in translation, metabolism and cell division are down-regulated during starvation

A number of ribosomal protein genes show significant decreases in mRNA level during starvation. In addition, two putative translation initiation factors also decrease in expression, together suggesting that translation activity declines over the starvation time course. In all eukaryotes, the TOR kinase is thought to act as a master regulator of multiple nutrient starvation responses, including autophagy, protein synthesis, ribosome biosynthesis, and some transcriptional responses (Raught et al., 2001). During starvation, TOR is inactivated, leading to inhibition of translation both by direct inactivation of translation initiation factors, and by the inhibition of transcription of ribosomal protein and translation initiation factor genes (Powers and Walter, 1999; Cardenas et al., 1999). TOR is present in Arabidopsis; however, a T-DNA knockout mutation in the TOR gene is embryo-lethal (Menand et al., 2002), and its function in nutrient stress responses is therefore difficult to assess. We hypothesize that the observed decrease in expression of a large number of ribosomal protein genes, concomitant with the induction of autophagy, may be due to the action of the Arabidopsis TOR protein, as seen in yeast and animal cells.

A second notable group of down-regulated genes is those that are known or expected to be cell cycle-regulated. Two mitotic B-type cyclins that probably function in cell cycle progression (John et al., 2001) are included, as is the syntaxin homolog KNOLLE (Lukowitz et al., 1996), required for the fusion of transport vesicles to form the cell plate during cytokinesis. Genes encoding two proteins involved in DNA replication also decrease in expression. RPA1 is required for DNA repair as well as replication in yeast (Umezu et al., 1998) and thus plays a role in both stress responses and cell division. A rice homolog has been implicated in DNA replication, and is highly expressed in proliferating cells (van der Knaap et al., 1997), suggesting a similar function in plants. The MCM3 protein functions in

yeast at the G1/S transition in the initiation of DNA replication (Tye, 1999), and Arabidopsis *MCM3* is transcriptionally regulated in a cell cycle-dependent manner (Stevens et al., 2002). In addition, several histone proteins show a decrease in mRNA level after sucrose starvation; histones are known to be more highly expressed during DNA replication (Callard and Mazzolini, 1997). It is likely that the change in expression for these genes is due to the inhibition of growth of the cell cultures in the absence of sucrose (Figure 2).

As might be expected during a period of sucrose limitation, genes involved in some aspects of metabolism also decrease in expression, including those potentially involved in glycolysis, the pentose phosphate pathway, and nucleotide, amino acid and fatty acid biosynthesis. This suggests that certain metabolic pathways are suppressed to conserve resources during nutrient starvation. This resembles the suppression of metabolism observed in situations of dormancy, where unnecessary metabolic pathways are shut down to allow survival until environmental conditions are encountered that are favorable for resumption of growth (Bewley, 1997; Shimizu and Mori, 1998; Pnueli et al., 2002). The extent of this similarity at the level of gene expression remains to be determined.

It should be noted that, while a number of genes that have previously been reported to be regulated by sucrose starvation were also identified in our analysis (e.g. several *din* genes (Fujiki et al., 2000) and glycosyl hydrolases (Lee et al., 2004)), others did not show a significant change in our experiments. This may be due partially to differences in experimental design; our aim was to identify genes involved in starvation responses, and in particular nutrient mobilization, rather than sugar-regulated genes, and thus an extended starvation period was used. In addition, differences between plant species are evident; for example, the glyoxylate cycle genes malate synthase and isocitrate lyase are upregulated

during starvation of cucumber cultured cells (Graham et al., 1994), but show no increase during starvation of Arabidopsis. Finally, we excluded genes that appeared to be regulated by osmotic conditions from our analysis. Several of the genes identified by Lee et al. (2004) were excluded in this manner, and may in fact respond to osmotic changes, or, most likely from our data, a combination of osmotic and starvation stresses.

In conclusion, we have identified a group of genes showing significant changes in transcript level during a 48 hr period of sucrose starvation in Arabidopsis suspension cells. Many of the genes that increase in expression appear to be involved in nutrient mobilization and scavenging, responses apparently intended to allow survival under nutrient limiting conditions. Some of the predicted transcription factors and signaling molecules identified are expected to function in the regulation of these responses. In addition, a number of genes previously shown to be regulated by biotic or abiotic stress conditions were upregulated, suggesting that general stress response pathways are induced as well as those specific to sucrose starvation. In contrast, genes that function in translation and replication decreased in expression during starvation. The amount and activities of the encoded proteins will now have to be determined to confirm the significance of the transcriptional regulation. However, in yeast, polysome microarray analysis of Tor-regulated responses has indicated a surprisingly strong correlation between increases in gene transcription and translation, providing an amplification of responses termed potentiation (Preiss et al., 2003), and validating the use of transcriptional analysis to identify pathways induced under specific conditions. The challenge now will be to determine the physiological and biochemical functions of the identified genes and pathways, both at the cellular level and in the context of a whole plant. The characterization of the phenotypes of knockout mutants in genes

upregulated by starvation, both in terms of the whole plant response when grown under nutrient stress conditions, and the biochemical and molecular changes that result from the mutation, should allow the elucidation of the role of the gene in the starvation response. In the case of putative transcription factors, identification of the subset of genes that are regulated by each factor, either by transcriptional profiling of knockout mutants or transgenic plants overexpressing the factor, transient expression analysis, or in vitro DNA-binding analysis, will be critical in determining it's function in survival during starvation. Analysis of the contribution of the induced pathways to the tolerance of nutrient stress will lead to a clearer understanding of the global response to starvation in plants.

ACKNOWLEDGMENTS

We thank Drs Steven Whitham and Ron Mittler for critical reading of the manuscript, Dr Carol Foster for helpful suggestions on data analysis and Dr Dan Voytas for providing the Arabidopsis suspension culture.

References

Amed SU*, Rojo E, Kovaleva V, Venkataraman S, Dombrowski JE, Matsuoka K, Raikhel NV (2000)* The plant vacuolar sorting receptor AtELP is involved in transport of NH_2-terminal propeptide-containing vacuolar proteins in Arabidopsis thaliana. J Cell Biol 149: 1335-1344

Aubert S, Gout E, Bligny R, Marty-Mazars D, Barrieu F, Alabouvette J, Marty F, Douce R (1996) Ultrastructural and biochemical characterization of autophagy in higher plant cells subjected to carbon deprivation: control by the supply of mitochondria with respiratory substrates. J Cell Biol 133: 1251-1263

Barbet NC, Schneider U, Helliwell SB, Stansfield I, Tuite MF, Hall MN (1996) TOR controls translation initiation and early G1 progression in yeast. Mol Biol Cell 7: 25-42

Bassham DC (2002) Golgi-independent trafficking of macromolecules to the plant vacuole. Adv Bot Res 38: 65-92

Bewley JD (1997) Seed germination and dormancy. Plant Cell 9: 1055-1066

Bhalerao R, Keskitalo J, Sterky F, Erlandsson R, Bjorkbacka H, Birve SJ, Karlsson J, Gardestrom P, Gustafsson P, Lundeberg J, Jansson S (2003) Gene expression in autumn leaves. Plant Physiol 131: 430-442

Brouquisse R, Gaudillere JP, Raymond P (1998) Induction of a carbon-starvation-related proteolysis in whole maize plants submitted to light/dark cycles and to extended darkness. Plant Physiol 117:1281-1291

Brouquisse R, James F, Raymond P, Pradet A (1991) Study of glucose starvation in excised maize root tips. Plant Physiol 96: 619-626

Bursch W, Ellinger A, Gerner CH, Frohwein U, Schulte-Hermann R (2000) Programmed cell death (PCD). Apoptosis, autophagic PCD, or others? Ann N Y Acad Sci 926: 1-12

Callard D, Mazzolini L (1997) Identification of proliferation-induced genes in Arabidopsis thaliana. Characterization of a new member of the highly evolutionarily conserved histone H2A.F/Z variant subfamily. Plant Physiol 115: 1385-1395

Cardenas ME, Cutler NS, Lorenz MC, Di Como CJ, Heitman, J (1999) The TOR signaling cascade regulates gene expression in response to nutrients. Genes Dev 13: 3271-3279

Chaves I, Regalado AP, Chen M, Ricardo CP, Showalter AM (2002) Programmed cell death induced by $(\beta\text{-D-galactosyl})_3$ Yariv reagent in *Nicotiana tabacum* BY-2 suspension-cultured cells. Physiol Plant 116: 548-553

Chen M-H, Liu L-F, Chen Y-R, Wu HK, Yu S-M (1994) Expression of α-amylases, carbohydrate metabolism, and autophagy in cultured rise cells is coordinately regulated by sugar nutrient. Plant J 6: 625-636

Chen W, Provart NJ, Glazebrook J, Katagiri F, Chang HS, Eulgem T, Mauch F, Luan S, Zou G, Whitham SA, Budworth PR, Tao Y, Xie Z, Chen X, Lam S, Kreps JA,

Harper JF, Si-Ammour A, Mauch-Mani B, Heinlein M, Kobayashi K, Hohn T, Dangl JL, Wang X, Zhu T (2002) Expression profile matrix of *Arabidopsis* transcription factor genes suggests their putative functions in response to environmental stresses. Plant Cell 14: 559-574

Dat J, Vandenabeele S, Vranova E, Van Montagu M, Inze D, Van Breusegem F (2000) Dual action of the active oxygen species during plant stress responses. Cell Mol Life Sci 57: 779-795

de Pater S, Greco V, Pham K, Memelink J, Kijne J (1996) Characterization of a zinc-dependent transcriptional activator from *Arabidopsis*. Nucleic Acids Res 24: 4624-4631

Dieuaide M, Brouquisse R, Pradet A, Raymond P (1992) Increased fatty acid β-oxidation after glucose starvation in maize root tips. Plant Physiol 99:595-600

Dieuaide M, Couee I, Pradet A, Raymond P (1993) Effects of glucose starvation on the oxidation of fatty acids by maize root tip mitochondria and peroxisomes: evidence for fatty acid β-oxidation and acyl-coA dehydrogenase activity in higher plants. Biochem J 296: 199-207

Doelling JH, Walker JM, Friedman EM, Thompson AR, Vierstra RD (2002) The APG8/12-activating enzyme APG7 is required for proper nutrient recycling and senescence in *Arabidopsis thaliana*. J Biol Chem 277: 33105-33114

Dong J, Chen C, Chen Z (2003) Expression profiles of the *Arabidopsis* WRKY gene superfamily during plant defense response. Plant Mol Biol 51: 21-37

Eastmond PJ, van Dijken AJ, Spielman M, Kerr A, Tissier AF, Dickinson HG, Jones JD, Smeekens SC, Graham IA (2002) Trehalose-6-phosphate synthase 1, which catalyses the first step in trehalose synthesis, is essential for Arabidopsis embryo maturation. Plant J 29: 225-235

Eulgem T, Rushton PJ, Robatzek S, Sommssich IE (2000) The WRKY superfamily of plant transcription factors. Trends Plant Sci 5: 199-206

Eulgem T, Rushton PJ, Schmelzer E, Hahlbrock K, Somssich IE (1999) Early nuclear events in plant defense signaling: rapid gene activation by WRKY transcription factors. EMBO J 18: 4689-4699

Fujiki Y, Ito M, Nishida I, Watanabe A (2000) Multiple signaling pathways in gene expression during sugar starvation. Pharmacological analysis of din gene expression in suspension-cultured cells of *Arabidopsis*. Plant Physiol 124: 1139-1147

Fujiki Y, Masaki I, Takashi I, Ikou N, Watanabe A (2002) Activation of the promoters of *Arabidopsis* genes for the branched-chain-α-keto acid dehydrogenase complex in transgenic tobacco BY-2 cells under sucrose starvation. Plant Cell Physiol 43: 275-280

Garg AK, Kim JK, Owens TG, Ranwala AP, Choi YD, Kochian LV, Wu RJ (2002) Trehalose accumulation in rice plants confers high tolerance levels to different abiotic stresses. Proc Natl Acad Sci USA 99: 15898-15903

Graham IA, Denby KJ, Leaver CJ (1994) Carbon catabolite repression regulates glyoxylate cycle gene expression in cucumber. Plant Cell 6: 761-772

Graham IA, Eastmond PJ (2002) Pathways of straight and branched chain fatty acid catabolism in higher plants. Prog Lipid Res 41: 156-181

Hamburg M, Sanz A, Castresana C (1999) α-oxidation of fatty acids in higher plants. Identification of a pathogen-inducible oxygenase (piox) as an α-dioxygenase and biosynthesis of 2-hydroperoxylinolenic acid. J Biol Chem 274: 24503-24513

Hanaoka H, Noda T, Shirano Y, Kato T, Hayashi H, Shibata D, Tabata S, Ohsumi Y (2002) Leaf senescence and starvation-induced chlorosis are accelerated by the disruption of an *Arabidopsis* autophagy gene. Plant Physiol 129: 1181-1193

Hara K, Yagi M, Kusano T, Sano H (2000) Rapid systemic accumulation of transcripts encoding a tobacco WRKY transcription factor upon wounding. Mol Gen Genet 263: 30-37

Hayashi H, De Bellis L, Ciurli A, Kondo M, Hayashi M, Nishimura M (1999) A novel acyl-CoA oxidase that can oxidize short-chain acyl-CoA in plant peroxisomes. J Biol Chem 273: 8301-8307

Higo K, Ugawa Y, Iwamoto M, Korenaga T (1999) Plant *cis*-acting regulatory DNA elements (PLACE) database:1999. Nucl Acids Res 27: 297-300

Huang WP and Klionsky DJ (2002) Autophagy in yeast: a review of the molecular machinery. Cell Struct Funct 27: 409-20

Hughes JD, Estep PW, Tavazoie S, Church GM (2000) Computational identification of *cis*-regulatory elements associated with groups of functionally related genes in *Saccharomyces cerevisiae*. J Mol Biol 296: 1205-1214

Ichimura Y, Kirisako T, Takao T, Satomi Y, Shimonishi Y, Ishihara N, Mizushima N, Tanida I, Kominami E, Ohsumi M, Noda T, Ohsumi Y (2000) A ubiquitin-like system mediates protein lipidation. Nature 408: 488-492

Ito M, Iwase M, Kodama H, Lavisse P, Komamine A, Nishihama R, Machida Y, Watanabe A (1998) A novel cis-acting element in promoters of plant B-type cyclin genes activates M phase-specific transcription. Plant Cell 10: 331-341

Jakoby M, Weisshaar B, Droge-Laser W, Vicente-Carbajosa J, Tiedemann J, Kroj T, Parcy F (2002) bZIP transcription factors in *Arabidopsis*. Trends Plant Sci 7:106-111

James F, Brouquisse R, Pradet A, Raymond P (1993) Changes in proteolytic activities in glucose-starved maize root tips: regulation by sugars. Plant Physiol Biochem 31: 845-856

John PC, Mews M, Moore R (2001) Cyclin/Cdk complexes: their involvement in cell cycle progression and mitotic division. Protoplasma 216: 119-142

Journet EP, Bligny R, Douce R (1986) Biochemical changes during sucrose deprivation in higher plant cells. J Biol Chem 261:3193-3199

Kagaya Y, Ohmiya K, Hattori T (1999) RAV1, a novel DNA-binding protein, binds to bipartite recognition sequence through two distinct DNA-binding domains uniquely found in plants. Nucleic Acids Res 27: 470-478

Kametaka S, Okano T, Ohsumi M, Ohsumi Y (1998) Apg14p and Apg6/Vps30p form a protein complex essential for autophagy in the yeast, Saccharomyces cerevisiae. J Biol Chem 273: 22284-22291

Kinoshita T, Yamada K, Hiraiwa N, Kondo M, Nishimura M, Hara-Nishimura, I (1999) Vacuolar processing enzyme is up-regulated in the lytic vacuoles of vegetable tissues during senescence and various stressed conditions. Plant J 19: 43-53

Kirisako T, Baba M, Ishihara N, Miyazawa K, Ohsumi M, Yoshimori T, Noda T, Ohsumi Y (1999) Formation process of autophagosome is traced with Apg8/Aut7p in yeast. J Cell Biol 147: 435-46

Kirisako T, Ichimura Y, Okada H, Kabeya Y, Mizushima N, Yoshimori T, Ohsumi M, Takao T, Noda T, Ohsumi Y (2000) The reversible modification regulates the membrane-binding state of Apg8/Aut7 essential for autophagy and the cytoplasm to vacuole targeting pathway. J Cell Biol 151: 263-76

Klionsky DJ, Ohsumi Y (1999) Vacuolar import of proteins and organelles from the cytoplasm. Annu Rev Cell Dev Biol 15: 1-32

Koch KE (1996) Carbohydrate modulated gene expression in plants. Annu Rev Plant Physiol Plant Mol Biol 47: 509-540

Lam E (2004) Controlled cell death, plant survival and development. Nature Rev Mol Cell Biol 5: 305-315

Lauber MH, Waizenegger I, Steinmann T, Schwarz H, Mayer U, Hwang I, Lukowitz W, Jurgens G (1997) The Arabidopsis KNOLLE protein is a cytokinesis-specific syntaxin. J Cell Biol 139: 1485-1493

Lee EJ, Koizumi N, Sano H (2004) Identification of genes that are up-regulated in concert during sugar depletion in Arabidopsis. Plant Cell Env 27: 337-345

Li CY, Weiss D, Goldschmidt EE (2003) Effects of carbohydrate starvation on gene expression in citrus root. Planta 217: 11–20

Lu C-A, Ho, T-H, Ho S-L, Yu S-M (2002) Three novel MYB proteins with one DNA binding repeat mediate sugar and hormone regulation of α-amylase gene expression. Plant Cell 14: 1963-1980

Lukowitz W, Mayer U, Jurgens G (1996) Cytokinesis in the Arabidopsis embryo involves the syntaxin-related KNOLLE gene product. Cell 84: 61-71

Menand B, Desnos T, Nussaume L, Berger F, Bouchez D, Meyer C, Robaglia C (2002) Expression and disruption of the Arabidopsis TOR (target of rapamycin) gene. Proc Natl Acad Sci USA 99: 6422-6427

Meyers BC, Morgante M, Michelmore RW (2002) TIR-X and TIR-NBS proteins: two new families related to disease resistance TIR-NBS-LRR proteins encoded in *Arabidopsis* and other plant genomes. Plant J 32: 77-92

Miernyk JA (2001) The J-domain proteins of *Arabidopsis thaliana*: an unexpectedly large and diverse family of chaperones. Cell Stress Chaperones 6: 209-218

Mizushima N, Sugita H, Yoshimori T, Ohsumi Y (1998a) A new protein conjugation system in human. The counterpart of the yeast Apg12p conjugation system essential for autophagy. J Biol Chem 273: 33889-33892

Mizushima N, Sugita H, Yoshimori T, Tanaka Y, Ishii T, George MD, Klionsky DJ, Ohsumi M, Ohsumi Y (1998b) A protein conjugation system essential for autophagy. Nature 395: 395-398

Moriyasu Y, Ohsumi Y (1996) Autophagy in tobacco suspension-cultured cell in response to sucrose starvation. Plant Physiol 111:1233-1241

Nakashima K, Satoh R, Kiyosue T, Yamaguchi-Shinozaki K, Shinozaki K (1998) A gene encoding proline dehydrogenase is not only induced by proline and hypoosmolarity, but is also developmentally regulated in the reproductive organs of *Arabidopsis*. Plant Physiol 118: 1233-1241

Oh SA, Lee SY, Chung LK, Lee CH, Nam HG (1996) A senescence-associated gene of Arabidopsis thaliana is distinctively regulated during natural and artificially induced leaf senescence. Plant Mol Biol 30: 739-754

Panavas T, Pikula A, Reid PD, Rubinstein B, Walker EL (1999) Identification of senescence-associated genes from daylily petals. Plant Mol Biol 40: 237-248

Pnueli L, Hallak-Herr E, Rozenberg M, Cohen M, Goloubinoff P, Kaplan A, Mittler R (2002) Molecular and biochemical mechanisms associated with dormancy and drought tolerance in the desert legume Retama raetam. Plant J 31: 319-330

Powers T, Walter P (1999) Regulation of ribosome biogenesis by the rapamycin-sensitive TOR-signaling pathway in Saccharomyces cerevisiae. Mol Biol Cell 10: 987-1000

Preiss T, Baron-Benhamou J, Ansorge W, Hentze MW (2003) Homodirectional changes in transcriptome composition and mRNA translation induced by rapamycin and heat shock. Nat Struct Biol 10: 1039-1047

Prestridge, DS (1991) SIGNAL SCAN: A computer program that scans DNA sequences for eukaryotic transcriptional elements. CABIOS 7: 203-206

Proud CG (2004) Role of mTOR signaling in the control of translation initiation and elongation by nutrients. Curr Top Microbiol Immunol 279: 215-244

Quirino BF, Normanly J, Amasino RM (1999) Diverse range of gene activity during Arabidopsis thaliana leaf senescence includes pathogen-independent induciton of defense-related genes. Plant Mol Biol 40: 267-278

Raught B, Gingras AC, Sonenberg N (2001) The target of rapamycin (TOR) proteins. Proc Natl Acad Sci USA 98: 7037-7044

Schluepmann H, Pellny T, van Dijken A, Smeekens S, Paul M (2003) Trehalose 6-phosphate is indispensable for carbohydrate utilization and growth in *Arabidopsis thaliana*. Proc Natl Acad Sci USA 100: 6849-6854

Schoof H, Zaccaria P, Gundlach H, Lemcke K, Rudd S, Kolesov G, Arnold R, Mewes HW, Mayer KF (2002) MIPS Arabidopsis thaliana Database (MAtDB): an integrated biological knowledge resource based on the first complete plant genome. Nucleic Acids Res 30: 91-3

Sheen J (1990) Metabolic repression of transcription in higher plants. Plant Cell 2: 1027-1038

Shimizu S, Mori H (1998) Analysis of cycles of dormancy and growth in pea axillary buds based on mRNA accumulation patterns of cell cycle-related genes. Plant Cell Physiol 39: 255-262

Stevens R, Mariconti L, Rossignol P, Perennes C, Cella R, Bergounioux C (2002) Two E2F sites in the Arabidopsis MCM3 promoter have different roles in cell cycle activation and meristematic expression. J Biol Chem 277: 32978-32984

Surpin M, Zheng H, Morita MT, Saito C, Avila E, Blakeslee JJ, Bandyopadhyay A, Kovaleva V, Carter D, Murphy A, Tasaka M, Raikhel NV (2003) The VTI family of SNARE proteins is necessary for plant viability and mediates different protein transport pathways. Plant Cell 15: 2885-2899

Swidzinski JA, Sweetlove LJ, Leaver CJ (2002) A custom microarray analysis of gene expression during programmed cell death in Arabidopsis thaliana. Plant J 30: 431-446

Tye BK (1999) MCM proteins in DNA replication. Annu Rev Biochem 68: 649-686

Tymowska-Lalanne Z, Kreis M (1998) Expression of the *Arabidopsis thaliana* invertase gene family. Planta 207: 259-265

Umezu K, Sugawara N, Chen C, Haber JE, Kolodner RD (1998) Genetic analysis of yeast RPA1 reveals its multiple functions in DNA metabolism. Genetics 148: 989-1005

Van der Knaap E, Jagoueix S, Kende H (1997) Expression of an ortholog of replication protein A1 (RPA1) is induced by gibberellin in deepwater rice. Proc Natl Acad Sci USA 94: 9979-9983

Van Doorn WG, Balk PA, van Houwelingen AM, Hoeberichts FA, Hall RD, Vorst O, van der Schoot C, van Wordragen MF (2003) Gene expression during anthesis and senescence in Iris flowers. Plant Mol Biol 53: 845-863

Willekens H, Inze D, Van Montagu M, Van Camp W (1995) Catalases in plants. Mol Breed 1: 207-228

Wu P, Ma L, Hou X, Wang M, Wu Y, Liu F, Deng XW (2003) Phosphate starvation triggers distinct alterations of genome expression in *Arabidopsis* roots and leaves. Plant Physiol 132: 1260-1271

Yoshida S (2003) Molecular regulation of leaf senescence. Curr Opin Plant Biol 6: 79-84

Yu L, Alva A, Su H, Dutt P, Freundt E, Welsh S, Baehrecke EH, Lenardo MJ (2004) Regulation of an *ATG7-beclin 1* program of autophagic cell death by caspase-8. Science 304: 1500-1502

Yu S-M (1999) Cellular and genetic responses of plants to sugar starvation. Plant Physiol 121:687-693

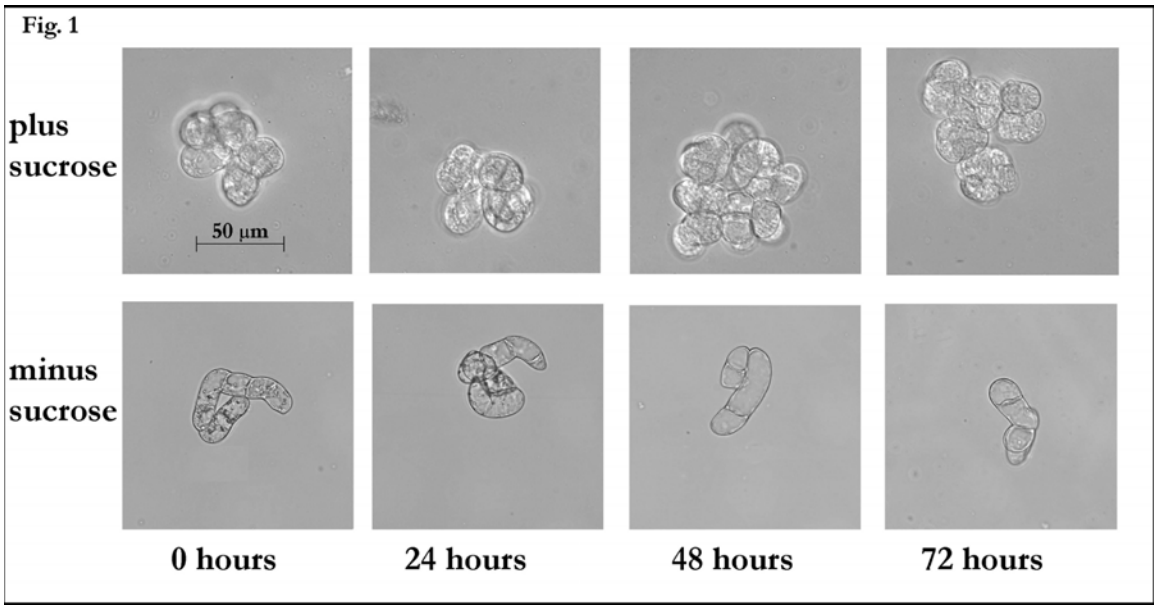

Figure 1. **Cellular morphology changes during sucrose starvation**.

Arabidopsis suspension cell cultures were transferred to sucrose-free medium and subcellular structure analyzed after 0, 24, 48 and 72 hours, compared with control cultures. Scale bar is equal to 50 µm.

Fig. 2

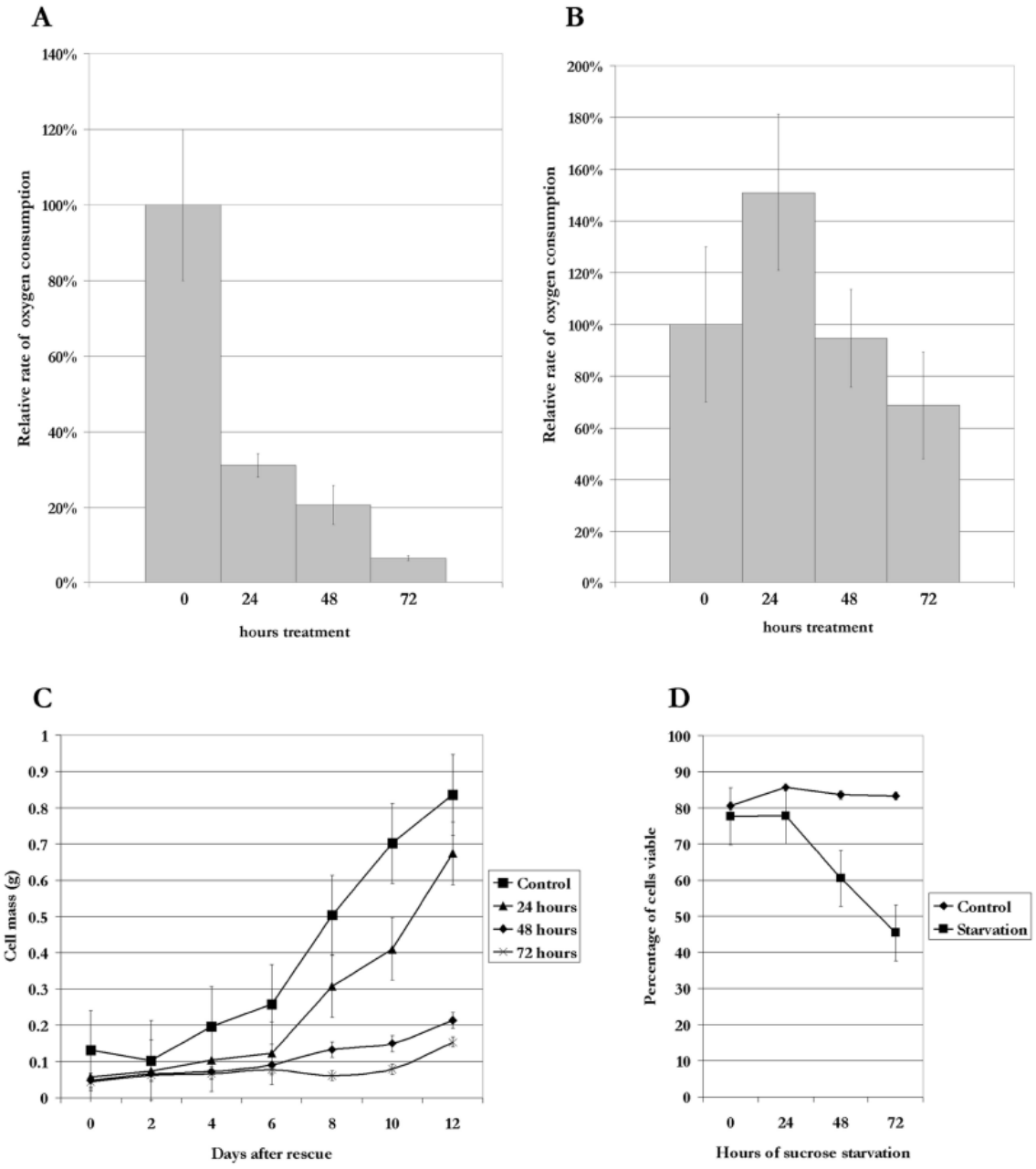

Figure 2. **Analysis of oxygen consumption and culture viability during sucrose starvation**.

A-D. Suspension cultures were grown with or without sucrose for 0, 24, 48 or 72-hours. The rate of respiration per gram of cells was determined for starved cells (A) and for control cells

(B). Oxygen consumption rate is represented as a percentage of the 0-hour control sample. (C) Suspension cultures were starved of sucrose for 0, 24, 48 or 72-hours, after which they were rescued by replacing the starvation medium with sucrose-containing medium. Samples (5 mL) were taken every 48 hrs after rescue for 12 days and the fresh weight of cells was measured for each sample. (D) Suspension cell cultures were starved for three days, with 5 mL samples taken every 24 hrs. The cells were stained with fluorescein diacetate and viewed under a UV-fluorescence microscope to determine the percentage of viable cells. Error bars indicate standard error.

Fig. 3

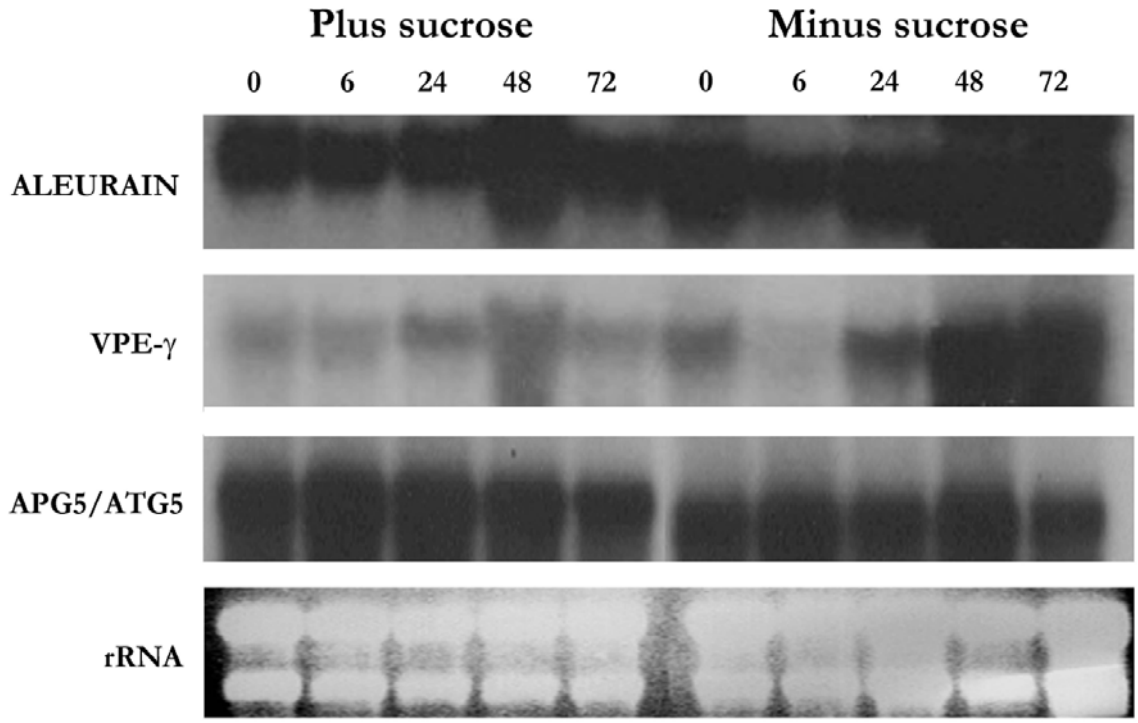

Figure 3. **Transcript levels of vacuolar enzymes increase during sucrose starvation**. Total RNA was extracted from suspension cells after 0, 6, 24, 48 or 72 hours of sucrose starvation, or control cells grown in the presence of sucrose. RNA gel blots were probed with labeled cDNAs for the vacuole-specific proteases aleurain-like protein (At5g60360) and vacuolar-processing enzyme-γ (At4g32940) An APG5/ATG5 (At5g17290) probe and ethidium bromide-stained rRNA were used as controls for equal loading.

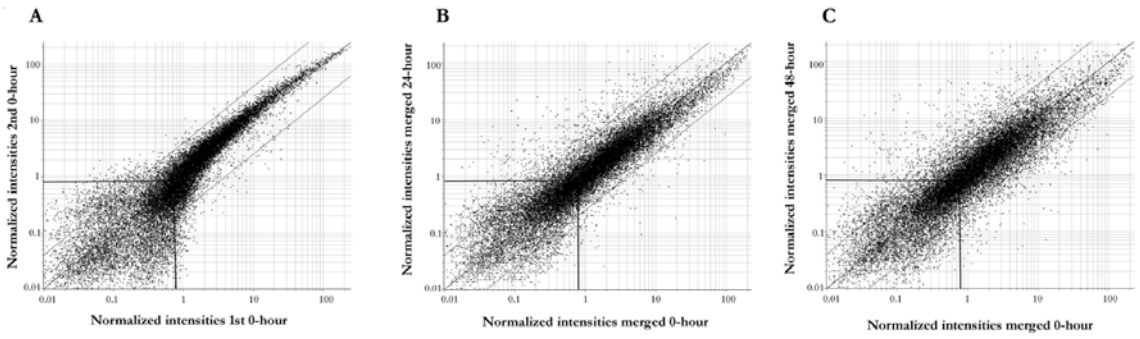

Figure 4. **Scatter plots of Arabidopsis ATH1 GeneChip data**.

A-C. Normalized signal intensities are plotted, with guide lines on each graph representing a four-fold change, increasing or decreasing, in signal, and indicating a signal intensity of 0.8, used as the lower limit of detection. (A) Two biological replicates are compared for the 0-hour time-point. (B) Comparison of 0 hr and 24 hr starvation samples. (C) Comparison of 0 hr and 48 hr starvation samples. For (B) and (C), signal intensities are the average of two biological replicates.

Fig. 5

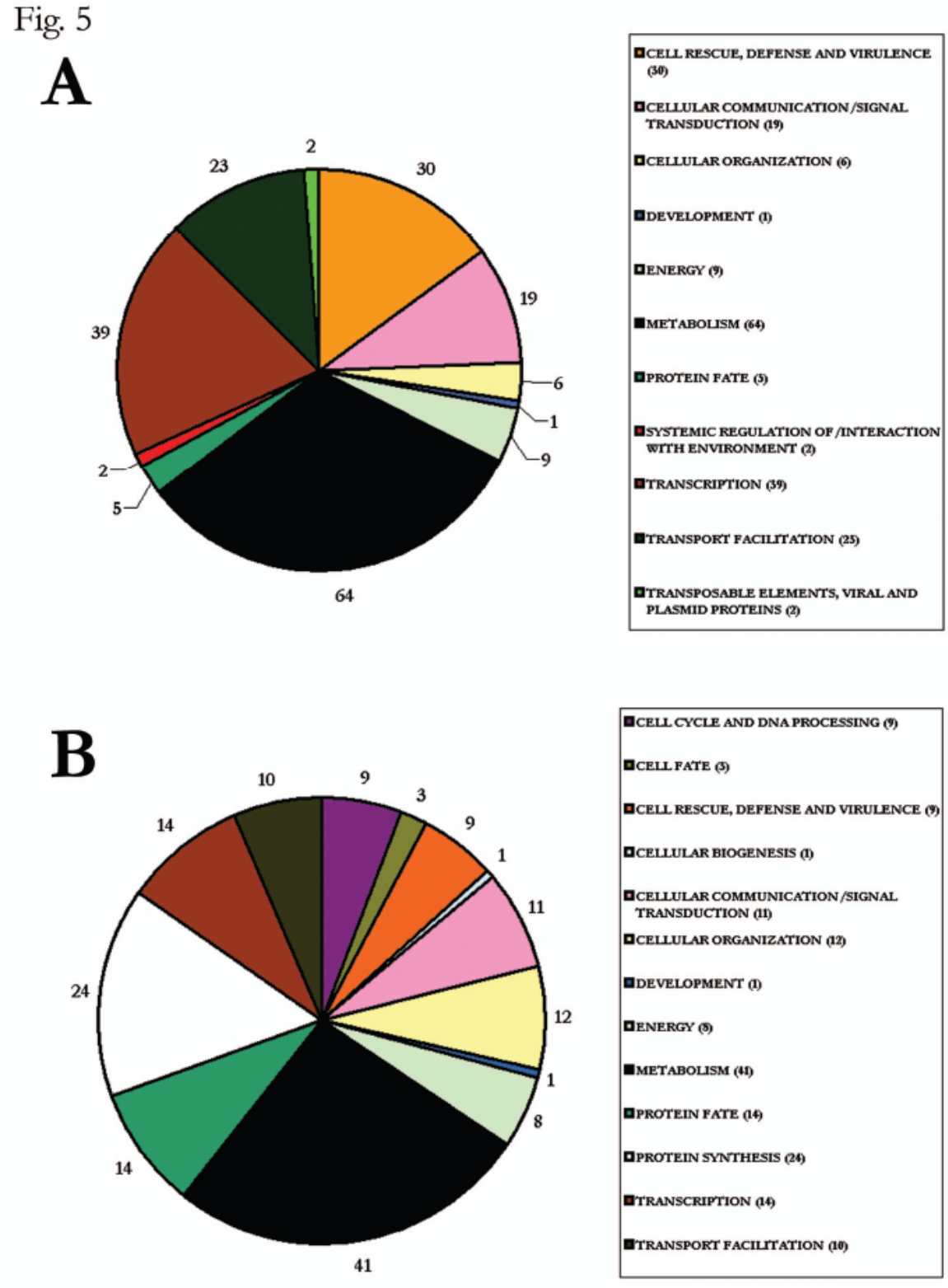

Figure 5. Functional categories of genes.

Each gene was assigned a functional category based on the known or putative function of its protein, according to the MIPS (Munich Information Center for Protein Sequencing) Functional Category database. Pie charts show the number of probe sets identified in each category that show at least a 4-fold increase (A) or decrease (B) in transcript level during starvation. Those categorized as ‘unclassified’, 143 probe sets for (A) and 104 probe sets for (B), are excluded from the pie charts for clarity.

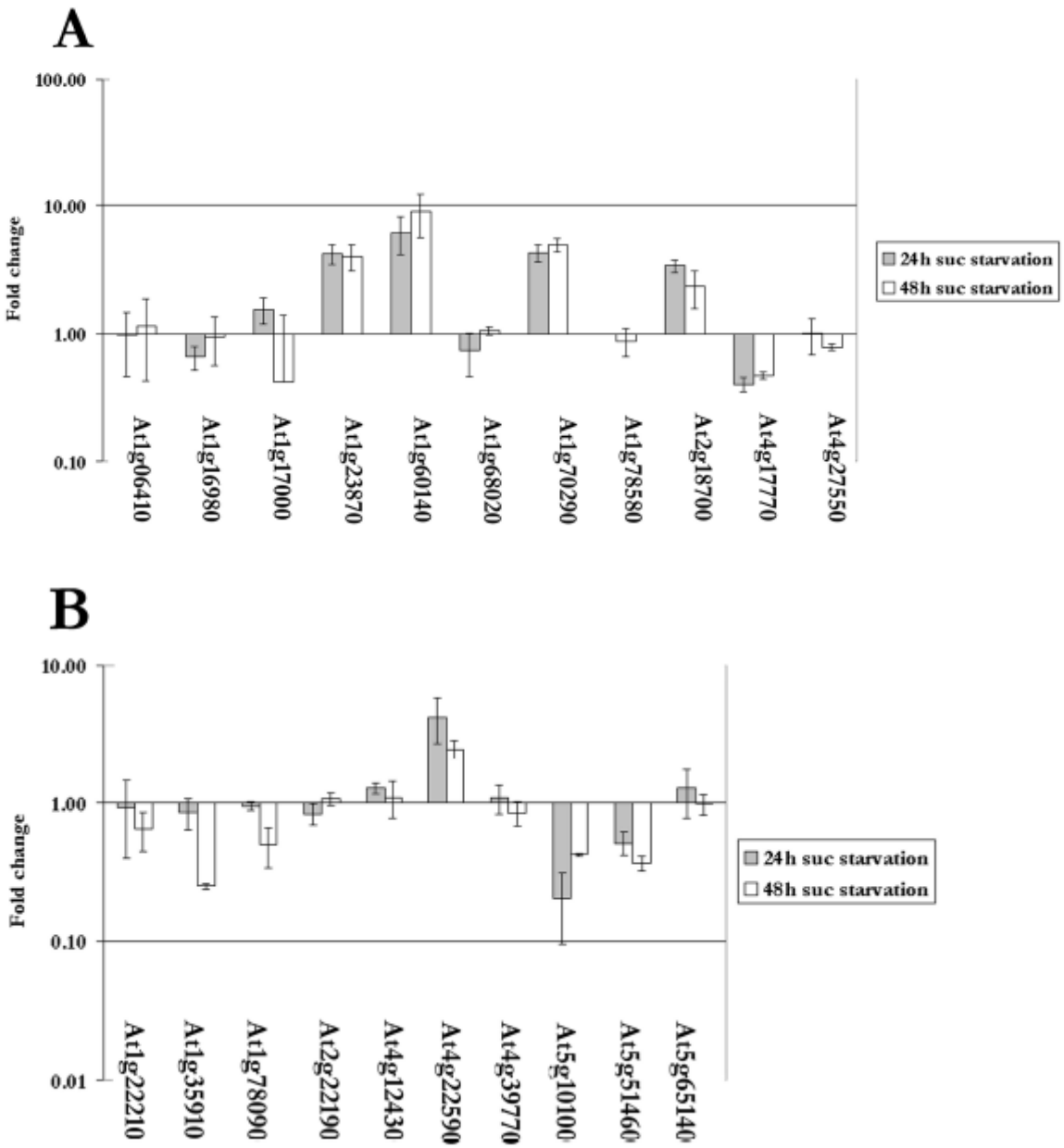

Figure 6. **Genes encoding trehalose metabolic enzymes change in expression during starvation.**

The fold change in transcript level of trehalose 6-phosphate synthase genes (A) and trehalose 6-phosphate phosphatase genes (B) after 24 hrs (gray bars) and 48 hrs (white bars) was

calculated from the mean intensities of two sets of biological replicates. Error bars indicate standard error. The scale is logarithmic.

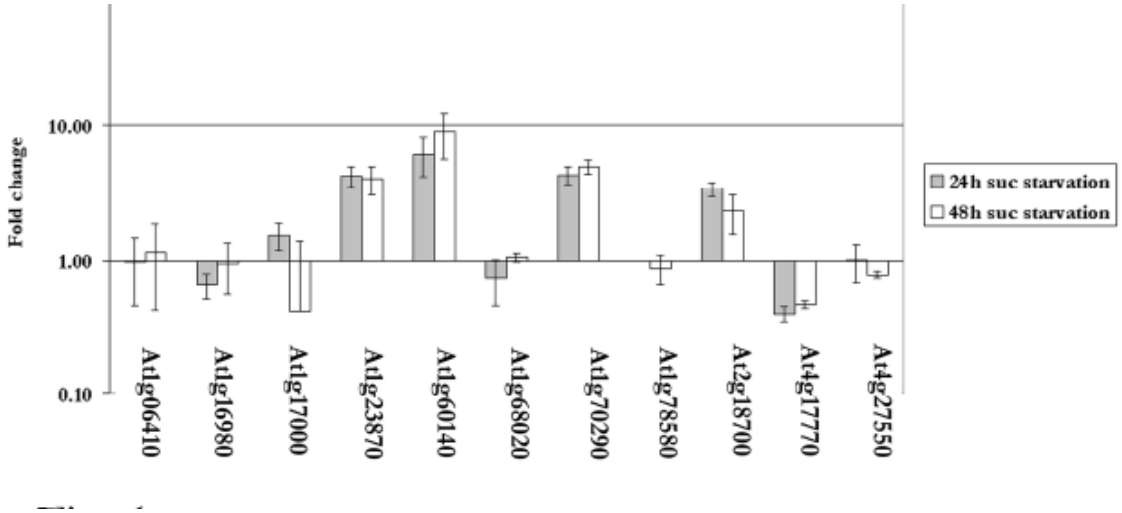

Figure 7. **Changes in transcript levels of putative *APG8/ATG8* genes in *Arabidopsis* suspension cells during sucrose starvation.**

The fold change in transcript level after 24 hrs (gray bars) and 48 hrs (white bars) was calculated from the mean intensities of two sets of biological replicates. Error bars indicate standard error. The scale is logarithmic.

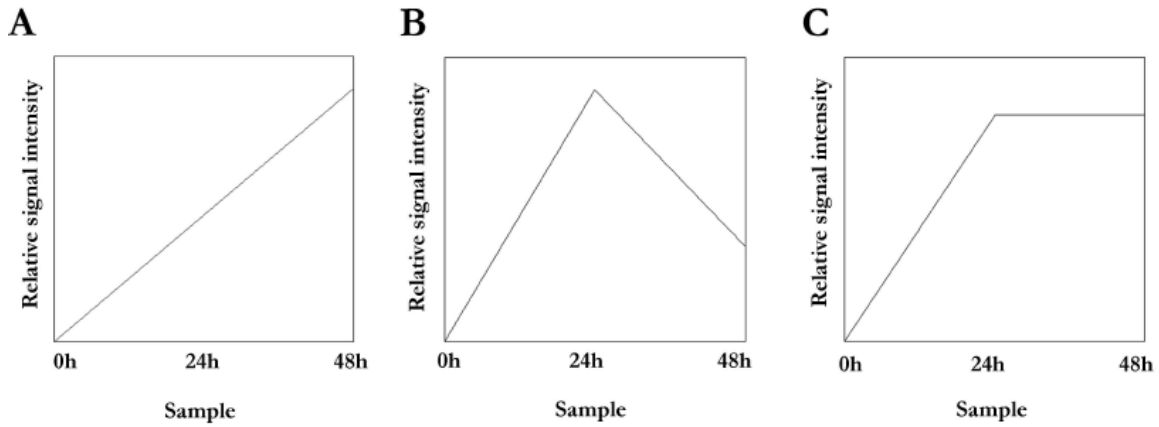

Figure 8. **Expression patterns observed over a 48 hour sucrose starvation time course**. **A-C.** Three distinct patterns of gene expression were identified in the subset of genes that were upregulated by sucrose starvation, illustrated by plotting relative signal intensity for 0 hour control and 24 and 48 hour sucrose starvation samples. (A) A significant increase in signal intensity from 24 to 48 hrs is observed. This pattern correlates with k-Means cluster group 1. (B) A decrease in relative signal intensity is seen between the 24 hour and the 48 hour starvation samples. This pattern correlates with k-Means cluster group 2. (C) No significant change in signal intensities is seen between the 24 and 48 hour starvation samples. This pattern correlates with k-Means cluster group 3.

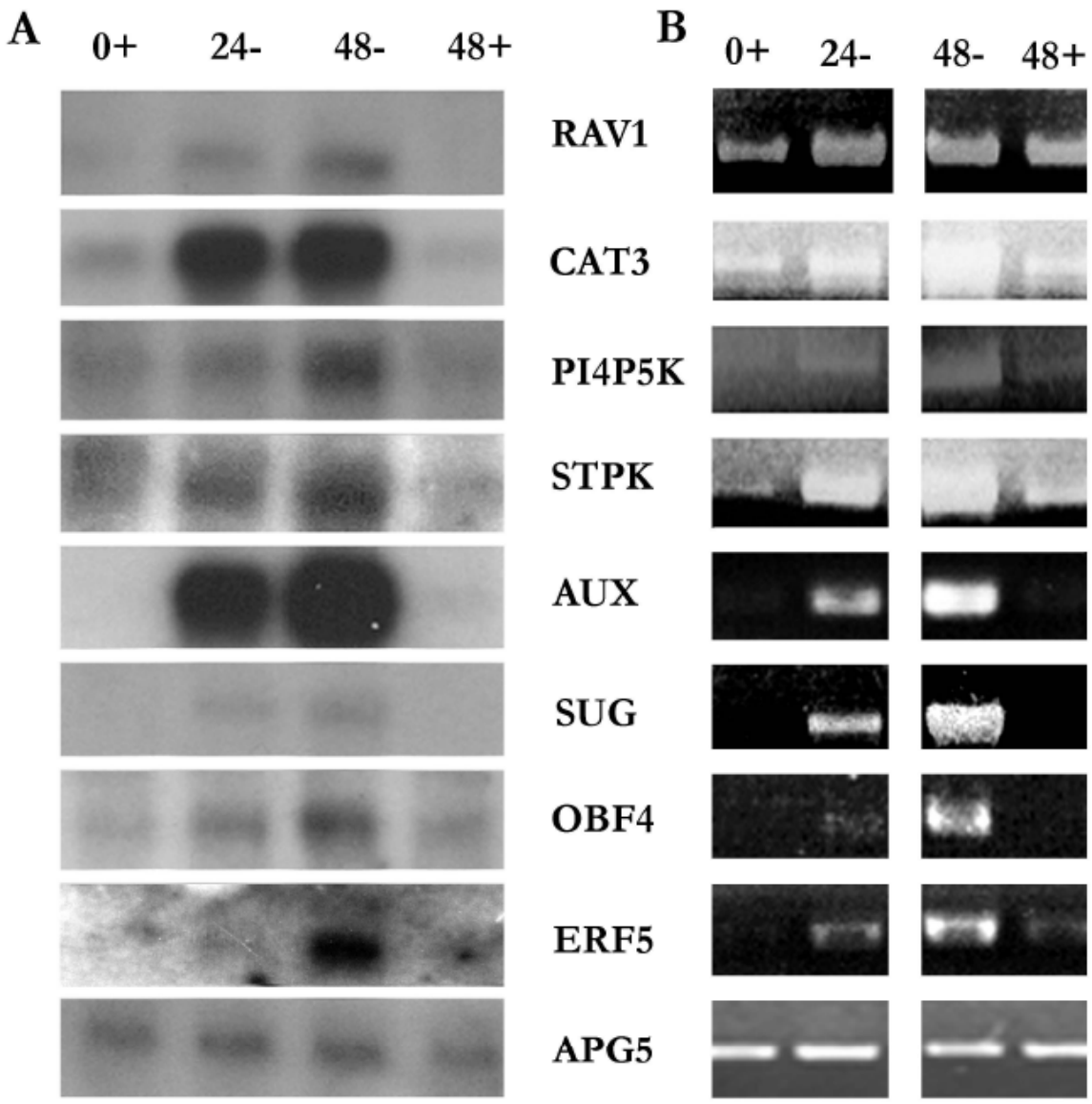

Figure 9. Verification of GeneChip expression data by RNA blot analysis and RT-PCR. Total RNA from Arabidopsis suspension cell cultures after 24 and 48-hour sucrose starvation (24 and 48), and 0 and 48 hour non-starved controls (0+ and 48+) was used for RNA blot hybridizations (A) and for RT-PCR reactions (B) for eight genes identified by the GeneChip analysis as induced during starvation. The genes chosen were: At1g13260 (*RAV1*), a DNA-binding protein; At1g20620 (*CAT3*), catalase-3; At1g21920 (*PI4P5K*), a

phosphoinositol-4-phosphate-5-kinase; At1g78290 (*STK*), a ser/thr kinase; At2g33830 (*AUX*), a putative auxin-regulated protein kinase; At4g36670 (*SUGT*), a sugar transporter; At5g10030 (*OBF4*), a bZIP transcription factor; and At5g61590 (*EREBF*), an ethylene-responsive element binding factor. The Arabidopsis *APG5/ATG5* gene (At5g17290) was used as a loading control in both experiments.

Table I. Transcription-related genes that show a significant increase in transcript level in *Arabidopsis* suspension cells during sucrose starvation. The fold change values reported were calculated using the mean intensities of two sets of biological replicates.

Probe Set[a]	**AGI**[b]	**24**[c]	**48**[d]	**Description**
260999_at	At1g26580	2.15	3.68	hypothetical protein; similar to putative MYB family transcription factor
260887_at	At1g29160	2.31	3.54	Dof zinc finger protein; similar to ascorbate oxidase promoter-binding protein
260882_at	At1g29280	4.92	6.55	WRKY family transcription factor
262552_at	At1g31350	3.65	4.36	F-box protein family
260632_at	At1g62360	5.89	3.79	homeobox protein, putative
264942_at	At1g67340	3.89	4.36	F-box protein family
260220_at	At1g74650	1.91	3.68	Myb family transcription factor
259982_at	At1g76410	30.63	29.54	putative RING zinc finger protein
261395_at	At1g79700	25.56	31.83	ovule development protein, putative; similar to AINTEGUMENTA
265321_at	At2g18280	3.93	8.09	F-box containing tubby family protein
266695_at	At2g19810	3.96	4.54	putative CCCH-type zinc finger protein
245078_at	At2g23340	16.13	25.39	putative AP2 domain transcription factor
265989_at	At2g24260	2.35	4.09	bHLH protein
266656_at	At2g25900	7.85	9.86	putative CCCH-type zinc finger protein
258975_at	At3g01970	3.30	4.18	WRKY family transcription factor
258795_at	At3g04570	2.48	4.05	expressed protein; similar to putative DNA-binding proteins
258890_at	At3g05690	6.32	4.08	putative transcription factor
256255_at	At3g11280	10.14	9.51	MYB-family transcription factor, putative
257265_at	At3g14980	6.53	8.35	PHD-finger protein, putative
256914_at	At3g23880	8.02	13.46	F-box protein family
252751_at	At3g43430	5.50	7.12	putative protein; RING-H2 zinc finger protein ATL4
252340_at	At3g48920	47.63	52.86	Myb family transcription factor
252081_at	At3g51910	3.98	5.94	heat shock transcription factor HSF30

254919_at	At4g11360	3.76	3.22	RING-H2 finger protein RHA1b
245331_at	At4g14410	4.06	4.28	bHLH protein
254681_at	At4g18140	2.80	3.86	putative protein; HYA22 protein
253872_at	At4g27410	4.68	9.62	putative protein
253061_at	At4g37610	9.86	10.66	putative protein; SPOP
251066_at	At5g01880	31.26	34.96	putative protein; RING-H2 finger protein RHA3a
250463_at	At5g10030	5.55	3.40	bZIP transcription factor, OBF4
246432_at	At5g17490	5.21	5.20	RGA-like protein; putative member of the VHIID domain transcription factor family RGAL
246755_at	At5g27920	3.48	5.16	F-box protein family
245925_at	At5g28770	8.42	9.33	bZIP family transcription factor; similar to seed storage protein opaque-2(bZIP family)
248606_at	At5g49450	13.82	12.58	bZIP family transcription factor
248618_at	At5g49620	2.61	3.74	Myb family transcription factor
247868_at	At5g57620	3.80	5.96	myb family transcription factor
247696_at	At5g59780	3.19	4.72	myb family transcription factor
247199_at	At5g65210	3.97	4.36	bZIP transcription factor, TGA1
247052_at	At5g66700	3.76	2.32	homeodomain transcription factor-like

[a] Affymetrix Probe Set

[b] *Arabidopsis* Genome Initiative number

[c] Fold-change between the normalized intensities of 0 hr sucrose control sample and 24 hr sucrose starvation sample

[d] Fold-change between the normalized intensities of 0 hr sucrose control sample and 48 hr sucrose starvation sample

Table II. Cellular communication and signal transduction-related genes that show a significant increase in transcript level in *Arabidopsis* suspension cells during sucrose starvation. The fold change values reported were calculated using the mean intensities of two sets of biological replicates.

Probe Set[a]	**AGI**[b]	**24**[c]	**48**[d]	**Description**
263657_at	At1g04440	4.89	6.48	putative casein kinase I
262531_at	At1g17230	2.42	7.05	putative leucine-rich receptor protein kinase
260855_at	At1g21920	3.15	4.71	phosphatidylinositol-4-phosphate 5-kinase, putative
260974_at	At1g53440	3.57	4.56	receptor-like serine/threonine kinase, putative
260774_at	At1g78290	10.00	12.97	serine-threonine protein kinase, putative
267477_at	At2g02710	6.21	7.64	putative receptor-like protein kinase
266019_at	At2g18750	3.24	4.93	calmodulin-binding protein
267254_at	At2g23030	7.74	13.16	putative protein kinase
266324_at	At2g46710	4.89	4.09	putative rac GTPase activating protein
257892_at	At3g17020	2.52	4.10	expressed protein; similar to ER6 protein
251665_at	At3g57040	3.53	5.37	response reactor 4
254901_at	At4g11530	6.30	4.79	serine/threonine kinase-like protein (fragment); receptor-like protein kinase RLK3
250981_at	At5g03140	4.32	7.35	receptor like protein kinase
250697_at	At5g06800	1.87	3.55	putative protein; contains similarity to transfactor
246028_at	At5g21170	6.50	5.47	AKIN beta1
249550_at	At5g38210	3.22	3.67	wall-associated kinase 4 (wak4)
249361_at	At5g40540	2.70	3.63	protein kinase ATN1
247790_at	At5g58720	2.71	3.80	putative PRL1 associated protein
247540_at	At5g61590	15.19	17.63	ethylene responsive element binding factor - like ERF5_ARATH

[a] Affymetrix Probe Set

[b] *Arabidopsis* Genome Initiative number

[c] Fold-change between the normalized intensities of 0 hr sucrose control sample and 24 hr sucrose starvation sample

[d] Fold-change between the normalized intensities of 0 hr sucrose control sample and 48 hr sucrose starvation sample

Table III. Genes involved in protein synthesis showing a significant decrease in transcript level in *Arabidopsis* suspension cells during sucrose starvation. The fold change values reported were calculated using the mean intensities of two sets of biological replicates.

Probe Set[a]	AGI[b]	24[c]	48[d]	Description
256065_at	At1g07070	-2.48	-4.99	ribosomal protein, putative; similar to ribosomal protein L35a GI:57118 from (Rattus norvegicus); supported by full-length cDNA: Ceres: 2778.
263691_at	At1g26880	-2.57	-4.86	60s ribosomal protein L34; identical to GB:Q42351, location of EST 105E2T7, gb|T22624;supported by full-length cDNA: Ceres:7182.
265147_at	At1g51380	-2.08	-5.76	eukaryotic translation initiation factor 4A (eIF-4A), putative; contains DEAD/DEAH box helicase; similar to PIR:S71280 from (Arabidopsis thaliana)
259678_at	At1g77750	-2.64	-3.80	putative 30S ribosomal protein S13; similar to putative 30S ribosomal protein S13, chloroplast precursor GB:P42732 (Arabidopsis thaliana)
266061_at	At2g18720	-1.29	-4.98	translation initiation factor eIF-2 gamma subunit, putative
266980_at	At2g39390	-2.26	-4.43	60S ribosomal protein L35; supported by full-length cDNA: Ceres:11583.
266822_at	At2g44860	-2.17	-3.59	60S ribosomal protein L30; supported by full-length cDNA: Ceres:34564.
259130_at	At3g02190	-2.28	-3.61	putative ribosomal protein L39; similar to ribosomal protein L39 GB:P51424 (Arabidopsis thaliana);supported by full-length cDNA: Ceres:946.
258521_at	At3g06680	-2.83	-6.50	ribosomal protein L29, putative; similar to 60S ribosomal protein L29 GB:P25886

				from (Rattus norvegicus)
258532_at	At3g06700	-2.72	-5.88	ribosomal protein L29, putative; similar to ribosomal protein L29 GI:7959366 (Panax ginseng);supported by full-length cDNA: Ceres:315.
258296_at	At3g23390	-2.10	-3.89	putative ribosomal protein; similar to ribosomal protein L41 GB:AAA34366 from (Candida maltosa); supported by full-length cDNA: Ceres: 13557.
252643_at	At3g44590	-2.94	-5.13	acidic ribosomal protein P2 -like; acidic ribosomal protein P2, maize, PIR:S54179
252287_at	At3g49080	-2.29	-4.38	30S ribosomal protein S9 -like; similar to 30S ribosomal proteins
251538_at	At3g58660	-2.91	-5.45	putative protein; PBK1 protein, Homo sapiens, EMBL:HSA7398; supported by cDNA: gi_17979348
255657_at	At4g00810	-2.67	-4.32	acidic ribosomal protein p1; similar to acidic ribosomal protein p1;supported by full-length cDNA: Ceres:26442.
255455_at	At4g02930	-2.09	-3.89	mitochondrial elongation factor Tu
254981_at	At4g10480	-2.61	-4.77	putative alpha NAC; stung similarity to Nascent polypeptide associated complex alpha chain - human, PIR2:S49326; supported by cDNA: gi_15027908_gb_AY045811.1_
254763_at	At4g13170	-2.76	-5.52	ribosomal protein L13a like protein; ribosomal protein L13a -Lupinus luteus,PID:e1237871; supported by cDNA: gi_15529277_gb_AY052263.1_
245311_at	At4g14320	-1.85	-3.59	ribosomal protein; supported by full-length cDNA: Ceres: 18153.
254355_at	At4g22380	-2.29	-5.76	Ribosomal protein L7Ae - like; NHP2/RS6 FAMILY PROTEIN, Homo sapiens, PID:g4826860; supported by cDNA: 2673.

253598_at	At4g30800	-3.79	-7.85	ribosomal protein S11 - like; ribosomal protein S11, Arabidopsis thaliana,PIR2:C35542; supported by cDNA: gi_15028244_gb_AY046037.1_
247900_at	At5g57290	-1.91	-3.55	60S acidic ribosomal protein P3; supported by full-length cDNA: Ceres: 8695.
247739_at	At5g59240	-3.49	-7.28	40S ribosomal protein S8 - like; 40S ribosomal protein S8, Prunus armeniaca, EMBL:AF071889
247566_at	At5g61170	-2.33	-3.93	40S ribosomal protein S19 - like; 40S ribosomal protein S19, Oryza sativa, SWISSPROT:RS19_ORYSA

[a] Affymetrix Probe Set

[b] *Arabidopsis* Genome Initiative number

[c] Fold-change between the normalized intensities of 0 hr sucrose control sample and 24 hr sucrose starvation sample

[d] Fold-change between the normalized intensities of 0 hr sucrose control sample and 48 hr sucrose starvation sample

Table IV. Primers used.

AGI[a]	Product	Sequence
At5g60360	AALP	FOR 5' ACCATCAGGCATTTGGAAAA 3'
		REV 5' TCTTCCCCATCTCCATCTTG 3'
At4g32940	VPE-γ	FOR 5' CGGATCTAGCGGATATTGGA 3'
		REV 5' TCAGGAAGAAGCCCTTCAAA 3'
At3g30774	PRODH	FOR 5' ATGGCAACCCGTCTTCTCCGAACAA 3'
		REV 5' TTACGCAATCCCGGCGATTAATCTC 3'
At5g17290	APG5/ATG5	FOR 5' CGAAGGAAGCGGTCAAGTAT 3'
		REV 5' ATCACCGTTCATGACAGAGG 3'
At1g13260	RAV1	FOR 5' GTCGACATGGAATCGAGTAGCGTTGAT 3'
		REV 5' CCTAGGTTACGAGGCGTCAAAGATGCG 3'
At1g20620	CAT3	FOR 5' GTCGACATGGATCCTTACAAGTATCGTCCTTCAAGC 3'
		REV 5' GCGGCCGCCTAGATGCTTGGCCTCACGTTCAGACGGCT 3'
At1g21920	PI4P-5K	FOR 5' GTCGACATGGAAAAACAGGCGAAGCTA 3'
		REV 5' CCTAGGTCAACTTTGACAAAATTTACC 3'
At1g78290	STPK	FOR 5' GTCGACATGGAGAGGTACGAAATAGTC 3'
		REV 5' CCTAGGTCACAAAGGGGAAAGGAGATC 3'
At2g33830	AUX	FOR 5' GTCGACATGTGGGATGAAACTGTAGCC 3'
		REV 5' CCTAGGTCAACGGTGCTTGCTCCTAGT 3'
At4g36670	SUG	FOR 5' GTCGACATGGCCGATCAAATCTCCGGC 3'
		REV 5' CCTAGGCTAAGCTGCACCGTTTTCGCC 3'
At5g10030	OBF4	FOR 5' GTCGACATGAATACAACCTCGACACAT 3'
		REV 5' CCTAGGTTACGTTGGTTCACGTTGCCT 3'
At5g61590	ERF5	FOR 5' GTCGACATGGAGACTTTTGAGGAAACG 3'
		REV 5' TCTAGATTAGTTTGATGACGATGATGA 3'

[a] *Arabidopsis* Genome Initiative number

APPENDIX B. OVEREXPRESSION OF *ARABIDOPSIS* SORTING NEXIN ATSNX2B INHIBITS ENDOCYTIC TRAFFICKING TO THE VACUOLE.

A paper published in Molecular plant

Nguyen Q Phan[1,2], Sang-Jin Kim[1,2] and Diane C Bassham[1,2,3]

[1]Department of Genetics, Development and Cell Biology, [2]Interdepartmental Genetics Program and [3]Plant Sciences Institute, Iowa State University, Ames, IA 50011, USA

Abstract

Sorting nexins are conserved proteins that function in vesicular trafficking and contain a characteristic phox homology (PX) domain. Here we characterize the ubiquitously-expressed *Arabidopsis thaliana* sorting nexin AtSNX2b. Subcellular fractionation studies indicate that AtSNX2b is peripherally associated with membranes. The AtSNX2b PX domain binds to phosphatidylinositol 3-phosphate *in vitro* and this association is required for the localization of GFP-AtSNX2b to punctate structures *in vivo,* identified as the *trans*-Golgi network, prevacuolar compartment and endosomes. Overexpression of GFP-tagged AtSNX2b produces enlarged GFP-labeled compartments that can also be labeled by the endocytic tracer FM4-64. Endocytic trafficking of FM4-64 to the vacuole is arrested in these GFP-AtSNX2b compartments, and similar FM4-64-accumulating compartments are seen upon overexpression of untagged AtSNX2b. This suggests that exit of membrane components from these enlarged or aggregated endosomes is inhibited. Vacuolar proteins containing an N-terminal propeptide, but not those with a C-terminal propeptide, are also

present in these enlarged compartments. We hypothesize that AtSNX2b is involved in vesicular trafficking from endosomes to the vacuole.

INTRODUCTION

The structure and function of cellular organelles is maintained by a network of pathways for protein synthesis, sorting, recycling, regulation and degradation. In the endomembrane system, new proteins are synthesized on membrane-bound ribosomes at the endoplasmic reticulum (ER). These proteins are folded and glycosylated before being transported to the Golgi where they can be further modified as they move from the *cis* to the *trans* cisternae. At the *trans* face of the Golgi resides the *trans*-Golgi network (TGN), where critical sorting events take place to target proteins either to the cell surface or to the vacuole. Transport to the plasma membrane may occur via a default pathway (Batoko et al., 2000; Mitsuhashi et al., 2000), while vacuolar proteins bind to specific receptors for sorting to their final destinations (Kirsch et al., 1994; Ahmed et al., 2000; Shimada et al., 2003; Park et al., 2005). However, some secreted material, for example cell wall components, is deposited in a polarized manner (Freshour et al., 2003; Lee et al., 2005), and some proteins show a polarized distribution in the plasma membrane (Dhonukshe et al., 2005), suggesting that the default secretion hypothesis is an oversimplification.

In plants, the vacuole is a multifunctional organelle that is essential for plant survival. Vacuolar functions include storage, degradation, sequestration of xenobiotics, maintenance of turgor and protoplasmic homeostasis (Marty, 1999). Whereas some cell types appear to contain a single central vacuole that performs all of these functions, other cell types may contain multiple functionally distinct vacuoles that can be distinguished by their unique

protein composition (Paris et al., 1996; Di Sansebastiano et al., 2001; Olbrich et al., 2007). Delivery of proteins to the vacuole in plants involves two general pathways: [1] the biosynthetic route via ER and Golgi compartments and [2] the endocytic route via endocytosis from the cell surface (Chrispeels and Raikhel, 1992; Marty, 1999; Matsuoka and Neuhaus, 1999; Hanton and Brandizzi, 2006). Three types of signal have been identified for targeting proteins to the plant vacuole via the biosynthetic route, a C-terminal propeptide (CTPP), a sequence-specific vacuolar sorting signal, usually in the form of an N-terminal propeptide (NTPP), and an internal signal (Marty, 1999). These signals are recognized at the TGN by vacuolar sorting receptors for correct targeting to the lytic or storage vacuole (Ahmed et al., 2000; Paris and Neuhaus, 2002; Shimada et al., 2003; Jolliffe et al., 2005). Distinct pathways, and possibly different receptors, exist for transport to different vacuole types, and some storage proteins are even transported directly from the ER to the vacuole, bypassing the Golgi apparatus entirely (Hillmer et al., 2001; Shimada et al., 2003; Park et al., 2005).

Endocytic trafficking to the plant vacuole begins at the plasma membrane, where membrane and extracellular cargo are internalized either by clathrin-coated vesicles or via a clathrin-independent pathway (Grebe et al., 2003; Baluska et al., 2004; Holstein and Oliviusson, 2005). These vesicles probably fuse with endosomes, organelles that function in sorting, recycling and further transport of cargo and membrane (Samaj et al., 2005; Muller et al., 2007). They can be classified into several distinct types based both on their protein content and by functional criteria (Ueda et al., 2004; Yamada et al., 2005; Dettmer et al., 2006; Haas et al., 2007; Lam et al., 2007; Jaillais et al., 2008). The biosynthetic and endocytic transport pathways probably merge at late endosomes, which may be equivalent to

the prevacuolar compartment (PVC), from which point both pathways utilize similar trafficking components to aid routing of cargos to the vacuole (Samaj et al., 2005; Yamada et al., 2005; Muller et al., 2007; Jaillais et al., 2008).

Increasing evidence indicates a role for the sorting nexin family of lipid-binding proteins in protein trafficking and sorting. Sorting nexins (SNXs) are membrane-associated proteins that are involved in endocytosis and protein trafficking through phosphatidylinositol lipid-containing organelles and are conserved in eukaryotes (Worby and Dixon, 2002; Carlton et al., 2005). SNXs are part of a large family of proteins that are defined by the presence of a phox homology domain (Teasdale et al., 2001), a 100-130 amino acid domain that binds phosphatidylinositol (PI) phosphates and targets the proteins to specific cellular membranes enriched in that phospholipid. In mammals, SNX functions include recycling or degradation of receptors (Kurten et al., 1996), control of endosome morphology (Barr et al., 2000), and regulation of endosomal function (Xu et al., 2001; Rojas et al., 2007). Several lines of evidence have implicated SNXs in an endosome-to-Golgi retrograde trafficking pathway. Genetics screens in yeast have identified a pentameric retromer complex required for the transport of proteins, including the sorting receptor Vps10p, from the PVC to the Golgi complex (Seaman et al., 1997; Seaman et al., 1998). Vps5p and Vps17p are SNXs that dimerize (Horazdovsky et al., 1997) to mechanically aid in vesicle budding while Vps35p and Vps29p act as cargo selectors (Seaman et al., 1998; Reddy and Seaman, 2001). Lastly Vps26p binds the complex together (Reddy and Seaman, 2001). Recent work from several laboratories has provided evidence of retromers in other model organisms and identified homologs of the yeast genes *VPS29*, *VPS30* and *VPS35* in Arabidopsis and mammals (Haft et al., 2000; Oliviusson et al., 2006; Shimada et al., 2006; Jaillais et al., 2007; Yamazaki et

al., 2008). These homologs show similarity to the yeast counterparts and assemble into a macromolecular complex that is presumed to similarly function in endosome-to-Golgi transport/recycling. Among the better characterized SNXs, mammalian SNX1 and 2, orthologs of Vps5p, have been shown to play a role in the mammalian retromer complex (Haft et al., 2000; Rojas et al., 2007). Other mammalian SNXs are involved in endocytic trafficking and endocytosis of plasma membrane receptors (Parks et al., 2001; Xu et al., 2001; Leprince et al., 2003; Lundmark and Carlsson, 2003; Merino-Trigo et al., 2004).

Initial evidence for a function of SNXs in plants came from a yeast-two hybrid assay demonstrating that the *Brassica oleracea* S locus receptor kinase intracellular domain interacts with a SNX (*Brassica oleracea* SNX1, BoSNX1) during the self-incompatibility response in pollen recognition (Vanoosthuyse et al., 2003). The closest *BoSNX1* homolog in Arabidopsis is the gene At5g06140 (named *AtSNX1*). AtSNX1 is involved in trafficking of the auxin transport component PIN2 through an AtSNX1-containing PVC via a novel transport pathway (Jaillais et al., 2006; Jaillais et al., 2008) and is probably a component of the Arabidopsis retromer complex (Jaillais et al., 2007). Two additional SNX genes are present in the Arabidopsis genome, designated *AtSNX2a* (At5g58440) and *AtSNX2b* (At5g07120) (Vanoosthuyse et al., 2003). We demonstrate here that the AtSNX2b protein can bind to phosphatidylinositol 3-phosphate (PI3P) and that this interaction is required for its localization to endosomes. Overexpression of AtSNX2b leads to enlargement or aggregation of the AtSNX2b-containing endosomes and interferes with efficient transport to the vacuole. These data implicate AtSNX2b in trafficking of cargo and membrane through an endosomal compartment.

METHODS

Plant materials and growth conditions

Arabidopsis thaliana seeds were surface-sterilized in 33% (v/v) bleach and 0.1% (v/v) triton X-100 solution for 20 min followed by cold treatment of at least 2 d at 4^{o}C. Plants were grown on soil or MS solid medium [Murashige–Skoog Vitamin and Salt Mixture (Caisson Lab, Inc., North Logan, UT), 1% (w/v) sucrose (Sigma-Aldrich, St. Louis, MO), 2.4 mM 2-morphinolino-ethanesulfonic acid (MES; Sigma-Aldrich, St. Louis, MO) and 0.8% (w/v) phytoblend agar (Caisson Lab, Inc., North Logan, UT)] under long-day conditions with ambient light (16 h light; 100μmol $m^{-2}s^{-1}$) at 22°C. *Arabidopsis thaliana* suspension cell cultures were maintained as described by Contento et al. (2005).

A homozygous *Atsnx2b* knockout (GABI_105E07) mutant line was received from the GABI-Kat mutant collection at the Max-Planck-Institute for Plant Breeding Research (Rosso et al., 2003). The T-DNA insertion site was verified by GABI_Kat personnel by sequencing the junction between the T-DNA left border and the *AtSNX2b* first exon. Additional verification of the mutant allele was done by analysis of segregation of the sulfadiazine resistance marker encoded by the T-DNA insertion by growing seedlings on MS medium containing 12 mg/L (4-amino-*N*-[2-pyrimidinyl]benzene-sulfonamide-Na).

RT-PCR analysis of *AtSNX2b* and *AtSNX2a*

Total RNA was extracted from Arabidopsis organs (3-week-old roots grown in liquid culture, and 6-week-old mature plants grown in soil for aerial organs) using the TRIzol RNA isolation method

(http://www.arabidopsis.org/info/2010_projects/comp_proj/AFGC/RevisedAFGC/site2RnaL

.htm#isolation) with DNase I treatment. cDNAs were generated using Superscript III reverse transcriptase (Invitrogen, Carlsbad, CA, USA) using an oligo dT primer. Gene-specific primers were used to amplify a 1.7 kb fragment containing the complete open reading frame of *AtSNX2b* (At5g07120); (forward) 5'-GGATCCAAAGAAGAGATGGAGAAAC-3' and (reverse) 5'-GGATCCAATTACACTGTGCTCTCATG-3' or 1.8 kb fragment containing the complete open reading frame of *AtSNX2a* (At5g58440); (forward) 5'-ACTCCAGAGAAGTCGAAATG-3' and (reverse) 5'-CCAAAATGAACATCGTTCAC-3'. Introduced restriction sites are underlined. For each sample, 0.25μg of cDNA was amplified for 29 (*AtSNX2b*) or 31 (*AtSNX2a*) cycles, with an annealing temperature of 54^{o}C.

Plasmid Construction

A GFP-AtSNX2b fusion was constructed using a pJ4GFP-XB vector (Igarashi et al., 2001) with modifications as described in Contento et al. (2005). A *Bam*HI-*Bam*HI fragment consisting of the coding region of the *AtSNX2b* cDNA (At5g07120) was amplified as above. The *Bam*HI-digested fragment was then subcloned into the modified pJ4GFP-XB digested with *Bgl*II. Similarly, a GFP-AtSNX2b-1 mutant fusion construct was made using a three step PCR mutagenesis (Li and Shapiro, 1993) amplifying a 233RR→LG amino acid mutation using mutation primers 5'-GTGGAGCAGCTAGGAGTTGCATTGG-3' (forward) and 5'-CCAATGCAACTCCTAGCTGCTCCAC-3' (reverse) in the first 2 steps followed by amplification of the full *AtSNX2b-1* mutant using *AtSNX2b* specific primers (above) and finally subcloning into the modified pJ4GFP-XB at the same *Bgl*II digested site.

GFP-PX and GFP-PX mutant fusion constructs were made using a similar procedure. A digested *Bam*HI-*Bam*HI fragment of the PX domain of AtSNX2b (amino acids

142-257) was subcloned into a *Bgl*II-digested pJ4GFP-XB to generate GFP-PX construct. The mutant PX domain (PX-1, amino acid 233RR→LG) was generated using the mutation primers (above) using the three step PCR mutagenesis. A second PX domain mutant (PX-2, amino acid 211PP→AA) was generated through the same three step PCR mutagenesis using primers 5'-CTGCATTGCAGCGAGGCCAGATAA-3' (forward) and 5'-CTTATCTGGCCTCGCTGCCAATGCAG-3' (reverse). PX primers used were 5'-GGATCCCCGAATTCCCGGGTCGA-3' (forward) and 5'-GGATCCTCAGTCACTCAAAGCGGTAACTTCCC-3' (reverse) for PX, PX-1 and PX-2 constructs. Restriction sites are underlined. The digested *Bam*HI-*Bam*HI PX fragment was then cloned into *Bgl*II-digested pJ4GFP-XB.

Antibody Production and Purification

The *AtSNX2b* coding region flanked by *Sal*I-*Not*I restriction sites was generated by RT-PCR from total *Arabidopsis* RNA using the following primers: (forward) 5'-GTCGACTCCCATCTCCACTCATCC-3' and (reverse) 5'-GCGGCCGCATTACACTGTGCTCTC-3' and subcloned into pET28b (Novagen, Madison WI) to produce HIS-AtSNX2b fusion plasmid. The fusion protein was synthesized in *Escherichia coli* according to the Novagen protocol, where it accumulated in inclusion bodies.

HIS-fusions were purified following the manufacturers protocol using HIS·bind resin (Novagen, CAT# 70666). Cells were broken by sonication, and insoluble material was pelleted at 24,000*g*. The pellet was resuspended in 6M urea in HIS binding buffer for 1 h at 4°C and pelleted again by centrifugation at 24,000*g*. After centrifugation, the supernatant was incubated with HIS·bind resin for 30 min and eluted with 100mM imidazole elution buffer.

The eluted protein was separated by SDS-PAGE (200 µg), cut from the gel and used to immunize rabbits.

For affinity purification of antibodies, purified HIS-AtSNX2b protein was separated by SDS-PAGE, transferred to nitrocellulose, and the strip containing the fusion protein was cut out after staining with Ponceau S. After blocking in 3% (w/v) dried nonfat milk in PBS, serum was incubated with the strip for 2 h at 4°C to allow binding of the antibodies. The strip was washed with PBS and specific antibodies were eluted using 100 mM glycine, pH 2.5. The eluate was adjusted to pH 7.0 using 2M Tris-HCl, pH 8. These affinity-purified antibodies were used in all further experiments.

Lipid Overlay Assay

Wild-type PX domain and the mutant PX domain PX-1 were generated by PCR using the primers 5'-GTCGACCGCTCTGATTACATCAAGATC-3' (forward) and 5'-GCGGCCGCTCAAAGCGGTAACTTCCCTTGCG-3' (reverse) from either GFP-PX or GFP-PX-1. *Sal*I-*Not*I fragments of PX and PX-1 were subcloned into pGEX-5X-1 (Amersham Bioscience, Piscataway, NJ) to yield GST-PX and GST-PX-1. GST-PX and GST-PX-1 fusion proteins were synthesized in *E. coli* according to the Novagen protocol. GST-fusions were purified using GST·bind resin (Novagen, CAT# 70541) following the manufacturer's protocol.

Lipid overlay assays were performed according to Dowler et al. (2002). In brief, purified GST-fusions were allowed to bind to PIP^{TM} lipid strips (Echelon Biosciences Inc., Salt Lake, UT) followed by immunoblotting using GST antibodies (Invitrogen, Carlsbad, CA) to detect bound GST-fusions.

Transient transformation of Arabidopsis protoplasts

For suspension cells, protoplasts were prepared and transformed according to Contento et al. (2005). For leaf tissue, protoplasts were prepared and transformed according to Sheen (2002). Protoplasts were transformed with 30µg of DNA per transformation. Images were obtained using fluorescence and confocal laser microscopy.

Immunofluorescence

Three-d-old Arabidopsis seedlings grown on MS solid medium were fixed following Sivaguru et al. (1999). Plants were transferred into 5 mL of MTSB buffer (50 mM PIPES-KOH [pH 6.9], 5 mM EGTA, and 5 mM $MgSO_4$) containing 5% (v/v) dimethyl sulfoxide for 15 min at room temperature. Afterward, they were fixed with 4% (w/v) paraformaldehyde in the above buffer containing 10% (v/v) dimethyl sulfoxide for 60 min at 20°C with the initial 10 min under vacuum. Plants were then washed with MTSB prior to immunostaining. Immunofluorescence staining of treated Arabidopsis seedlings was performed according to Müller et al. (Muller et al., 1998). Treated seedlings were incubated with primary antibodies in a humid chamber for 15-18 h at 4ºC, washed three times for 5 min in MTSB and further incubated for 45 min – 2 h at room temperature with conjugated secondary anti-rabbit or anti-mouse IgG antibodies in 3% (w/v) bovine serum albumin in MTSB. Seedlings were washed five times with MTSB and mounted with a coverslip in 50% (v/v) glycerol in phosphate-buffered saline (PBS, pH 7.4). Primary antibodies used were T7·tag monoclonal antibodies (Novagen/EMD Biosciences, Inc, La Jolla, CA; 1:100), anti-AtSNX2b antibodies (1:200) and preimmune antibodies (for AtSNX2b; 1:200). Secondary antibodies used were

Alexa Fluor® 594-conjugated goat anti-rabbit IgG, Alexa Fluor® 488-conjugated goat anti-mouse IgG and Alexa Fluor® 488-conjugated goat anti-rabbit IgG or Alexa Fluor® 594-conjugated goat anti-rabbit IgG (Molecular Probes, Eugene, OR, USA; 1:250).

For protoplasts, transformed protoplasts were fixed in 4% (w/v) paraformaldehyde in MTSB buffer for 20 min followed by 3 washes with MTSBS (MTSB containing 0.4M sorbitol) prior to immunostaining. Protoplast were permeabilized using permeabilization solution (3% (v/v) Triton X-100, 10% (v/v) dimethyl sulfoxide in MTSB) for 20 min. Immunofluorescence staining of fixed protoplasts was performed according to Kang et al. (2001). Cells were washed five times with MTSB and mounted with a coverslip in 50% (v/v) glycerol in PBS. Antibodies used were anti-AtSNX2b antibodies (1:200) , anti-SYP41 antibodies (1:200; Bassham et al., 2000) and anti-SYP21 antibodies (1:200; Conceicao et al., 1997) for primary antibodies and Alexa Fluor® 488-conjugated goat anti-rabbit IgG or Alexa Fluor® 594-conjugated goat anti-rabbit IgG as secondary antibodies.

Fluorescent signal detection and documentation was performed using a confocal laser scanning microscope (Leica TCS/NT, Leica Microsystems, Exton, PA, USA). The confocal laser microscope utilizes a Krypton 568nm and Argon 488nm laser for excitation. Filters for emission were RST588 BP525±25 (FITC-specific detection) and LP590 (TRITC-specific detection). Images were further processed for graphic presentation using Adobe Photoshop (Adobe Systems, Mountain View, CA, USA).

For all experiments, controls were performed consisting of omission of both primary antibodies (to control for nonspecific staining), omission of only one primary antibody (to confirm that no fluorescence bleed-through between filters was visible in double labeling), and omission of secondary antibodies or all immunochemicals (to control for fixative-

induced autofluorescence). The controls confirmed the absence of nonspecific fluorescence. All experiments were carried out at least three times with cells from independent preparations.

Immunoblot analysis

Arabidopsis plants or suspension cells were homogenized in PBS, 1mM EDTA, 0.1 mM phenylmethylsulfonyl fluoride. The homogenate was centrifuged at 1,000*g* for 10 min at 4°C to remove cell debris and large organelles. The pellet was discarded and the supernatant was incubated in SDS reducing sample buffer (Biorad, Hercules, CA) for 5 min at 65°C, and separated by electrophoresis on 10% SDS–PAGE gels. Proteins were electrotransferred to nitrocellulose membranes; blots were blocked with PBS/4% low fat milk powder for at least 1 h and incubated with anti-AtSNX2b antibodies for 15-18 h at 4°C. Signal detection was achieved using peroxidase-conjugated secondary antibodies and chemiluminescence reaction followed by X-ray film exposure. For differential centrifugation, the 1,000*g* supernatant from suspension cells was centrifuged sequentially to produce 12,000*g*, 39,000*g* and 125,000*g* pellets and a 125,000*g* supernatant which were analyzed by immunoblot with AtSNX2b antibodies or GFP antibodies (Invitrogen, Carlsbad, CA).

Extraction of AtSNX2b from membranes

A 1,000*g* supernatant from suspension cells was centrifuged at 125,000*g* to produce a total membrane pellet (P125). The supernatant fraction was discarded and membrane pellets were resuspended in 200 µL of extraction buffer (PBS, 1mM EDTA, 0.1 mM phenylmethylsulfonyl fluoride) or extraction buffer containing 0.1M Na_2CO_3, 1M NaCl, 2M

urea, or 1% (v/v) triton X-100, and incubated for 2 h on ice. Insoluble material was pelleted at 125,000*g* and pellets were resuspended in SDS sample buffer. Supernatants were precipitated using TCA, and protein pellets were washed in acetone and resuspended in SDS sample buffer. Samples were analyzed by SDS-PAGE and immunoblotting using AtSNX2b antibodies, or SYP41 antibodies as a control (Bassham et al., 2000).

Sucrose gradients

Five-d-old *Arabidopsis* suspension cultures were homogenized in HKE buffer (50 mM Hepes-KOH, pH 7.5, 10 mM potassium acetate, and 1 mM EDTA) containing 400 mM Suc, 1 mM dithiothreitol, and 0.1 mM phenylmethylsulfonyl fluoride, and centrifuged at 1,000*g* for 5 min to generate a postnuclear supernatant. The supernatant was loaded onto a sucrose step gradient as described in Sanderfoot et al. (1998). Gradients were centrifuged at 150,000*g* in a swinging-bucket rotor at 4°C for 18 h. Fractions (1 mL) were collected from the top of the gradient. Protein in each fraction was analyzed by SDS-PAGE and immunoblotting. Blots were probed using antibodies against aleurain (1:2000; Ahmed et al., 2000), γTIP (1:500; Hicks et al., 2004), FUM1 (fumarase; 1:500; Behal and Oliver, 1997), SYP21 (1:1000; Sanderfoot et al., 2001b), AtSNX2b (1:1500) and VTI12 (1:500; Bassham et al., 2000) followed by secondary antibodies conjugated to horseradish peroxidase.

FM4-64 staining of protoplasts

Protoplasts were stained with FM4-64 according to Ueda et al. (2001) by incubation for 10 min at 4°C with 50 μM FM4-64 in MS medium containing 0.4M mannitol. They were washed three times with the same medium, followed by incubation at room temperature for

30 min to 12 h. Confocal microscopy was performed with a Leica TCS/NT confocal microscope (Leica Microsystems, Exton, PA, USA) as described above.

Viability assays

Protoplasts were incubated in 50μg/mL fluorescein diacetate for 30 minutes followed by visualization by fluorescence microscopy using a FITC filter. Counts for viable (fluorescent) and nonviable (unstained) cells were performed and recorded. Four replicates of at least 700 cells per treatment were analyzed.

RESULTS

Three putative SNXs have been identified in the model plant Arabidopsis (Vanoosthuyse et al., 2003). Here we focus on AtSNX2b, a potential SNX based on amino acid similarity (40-50%) with yeast and human SNXs, with the majority of the similarity residing in the region of the PX domain. Of the Arabidopsis sorting nexins, AtSNX2b is most similar to AtSNX2a (86% amino acid similarity) and shows much lower similarity to AtSNX1 (47% amino acid similarity). AtSNX2b has two major domains: (1) an N-terminal conserved PX domain which defines a SNX (Worby and Dixon, 2002; Carlton et al., 2004; Carlton et al., 2005) and (2) a C-terminal coiled-coil region potentially important for protein-protein interactions (Zhong et al., 2002; Leprince et al., 2003; Merino-Trigo et al., 2004; Carlton et al., 2005; Gallop and McMahon, 2005; Figure 1A).

AtSNX2b is a ubiquitously-expressed membrane-associated protein

To determine the expression pattern of *AtSNX2b*, RNA was extracted from different *Arabidopsis* plant organs and RT-PCR was performed using *AtSNX2b* gene-specific primers. Figure 1B shows that *AtSNX2b* expression can be detected in all of the plant organs tested, including roots, rosette leaves, cauline leaves, stem, flowers and siliques, suggesting that its function is important throughout the plant. For comparison, the expression pattern of *AtSNX2a* was also determined (Figure 1C). *AtSNX2a* mRNA was also detected throughout the plant, although at lower levels in flowers, siliques and senescing leaves. The overlapping expression patterns of *AtSNX2b* and *AtSNX2a* raises the possibility that the two genes may also have overlapping functions.

To analyze the AtSNX2b protein, antibodies were raised against recombinant AtSNX2b. Full-length AtSNX2b protein was synthesized in *E. coli* as a His-tagged fusion protein and purified by affinity chromatography. The protein was injected into rabbits and the generated antibodies were affinity-purified against the recombinant protein prior to use. Immunoreactivity of the affinity-purified antibodies (Figure 2A) was compared with that of the crude serum (Figure 2C) and preimmune serum (Figure 2B) by immunoblotting against the recombinant protein antigen and a protein preparation from Arabidopsis. The purified anti-AtSNX2b antibodies recognized the recombinant protein and a band of similar molecular weight (approximately 67 kDa) in a total protein preparation from Arabidopsis (Figure 2A), which was not recognized by the pre-immune serum (Figure 2B). Cross-reacting bands were present in the crude serum blots (Figure 2C) that were mostly absent after affinity purification.

It was observed that in addition to a prominent band of the expected molecular mass, a second, weak band of slightly lower mobility on SDS-PAGE (approximately 70 kDa) was

sometimes recognized by the AtSNX2b antibodies. We hypothesized that this band may either correspond to a modified form of AtSNX2b, or, because of the sequence similarity between AtSNX2a and AtSNX2b, may correspond to AtSNX2a. To investigate this further, an Arabidopsis knockout mutant was isolated from the GABI-Kat flanking sequence tag database (Rosso et al., 2003) in which the *AtSNX2b* gene was disrupted by a T-DNA insertion (Figure 2D). Loss of gene expression was confirmed by RT-PCR using gene-specific primers. No phenotype has yet been observed for the *Atsnx2b* mutant, either at a morphological level after examination throughout its life cycle, in protein trafficking pathways to the vacuole, or in hormone-related responses such as gravitropism (data not shown). As the AtSNX2a protein is closely related in sequence and *AtSNX2a* and *AtSNX2b* have overlapping expression patterns (Figure 1B and C), we hypothesize that the two genes may perform redundant functions. Comparison of protein extracts from the *Atsnx2b* mutant with those from wild-type plants by immunoblotting demonstrated that the major, lower band of the doublet recognized by the AtSNX2b antibodies was absent in the mutant, confirming that it corresponds to AtSNX2b itself. The higher, much weaker band was still present in the mutant, suggesting that this is most likely AtSNX2a, rather than a modified version of AtSNX2b.

The distribution of AtSNX2b protein in aerial organs of Arabidopsis mature plants was analyzed (Figure 2E) and compared with the RT-PCR analysis of mRNA level (Figure 1B). High protein levels were seen in flowers, inflorescence stems and cauline leaves, and lower but detectable levels in siliques and rosette leaves (Figure 2E), as well as a significant amount in roots and young seedlings (see also Figure 6). These results are consistent with the

RT-PCR analysis, although much greater variation is seen in protein level than mRNA level, possibly suggesting that post-translational regulation may occur.

Because SNXs are typically associated with membranes, a total protein extract was separated into membrane and soluble fractions by centrifugation at 125,000*g* and analyzed by immunoblotting using AtSNX2b antibodies. AtSNX2b was detected in both the pellet and soluble fractions, indicating that AtSNX2b is partially membrane-associated (Figure 2A). To analyze further this membrane association, differential centrifugation was performed at 12,000*g*, 39,000*g* and 125,000*g* and fractions were probed for the presence of AtSNX2b. AtSNX2b was detected in all three membrane fractions and the soluble fraction, confirming that AtSNX2b is partially membrane-associated (Figure 2F). The upper weak band, potentially AtSNX2a, also appeared to be membrane-associated, although the weak and variable cross-reactivity made it difficult to draw definitive conclusions about this protein.

To determine how AtSNX2b protein associates with the membrane, total membrane pellets were resuspended in either extraction buffer alone, or extraction buffer containing 2M NaCl, 0.1M Na_2CO_3, 2M urea or 1% (v/v) triton X-100. After incubation for 2 h, membranes were repelleted and pellet and supernatant fractions analyzed by immunoblotting with AtSNX2b antibodies (Figure 2G). Each of the treatments was able to extract AtSNX2b from the membrane, indicating that AtSNX2b is peripherally associated with membranes. As a control, SYP41, an integral membrane protein (Bassham et al., 2000), was only extracted from the membrane by the detergent triton X-100 (Figure 2G).

AtSNX2b can bind PI3P

SNXs are defined by the presence of a PX domain and its ability to bind phosphoinositol lipids (Worby and Dixon, 2002).To determine if the AtSNX2b PX domain can associate with PI lipids, or phospholipids in general, the PX domain fragment of AtSNX2b was fused with GST (glutathione-S-transferase) to generate GST-PX. As a control, point mutations were introduced into the PX domain to create an amino acid 233RR→LG change that has been shown previously to prevent PI binding in human SNXs (Zhong et al., 2002). GST fusions with the wild-type or mutant PX domains were synthesized in *E.coli*, purified over a glutathione resin (Figure 3A) and allowed to bind to PIP^{TM} strips (Echelon Inc.) containing various phospholipids. Binding was detected using antibodies against GST. The PX domain of AtSNX2b (GST-PX) specifically bound to PI3P while the PX domain mutant (GST-PX-1) and GST alone were not able to bind to any lipid (Figure 3B).

Localization of AtSNX2b

To gain insight into AtSNX2b function, its subcellular localization was examined *in vivo*. A GFP fusion was generated with full length AtSNX2b (GFP-AtSNX2b) and transiently expressed in Arabidopsis protoplasts derived from suspension cultured cells. In addition, immunofluorescence using anti-AtSNX2b antibodies was used to assess AtSNX2b subcellular localization in *Arabidopsis* protoplasts. Both immunofluorescence and GFP-fusion localization show that AtSNX2b localizes to punctate spots in the cytoplasm (Figure 4A and 4B). To verify that a full-length GFP-AtSNX2b fusion is produced and correctly associates with membranes, membrane and soluble fractions were prepared from protoplasts expressing GFP-AtSNX2b, or GFP as a control. The proteins were expressed for 20 h to allow the proteins to accumulate to high enough levels for detection by immunoblotting

using GFP antibodies. A GFP-AtSNX2b fusion of the expected size was detected predominantly in the membrane fraction (Figure 4D).

To analyze the role of the PX domain in localization of AtSNX2b to these structures, a fusion between the full length AtSNX2b protein containing the PX domain mutation described above and GFP was generated (GFP-AtSNX2b-1). In contrast to the wild-type protein, the GFP-AtSNX2b-1 mutant did not localize to discrete structures but rather showed a diffuse fluorescence pattern throughout the cell (Figure 4C), suggesting that the PX domain is required for correct localization *in vivo*. To determine whether the PX domain alone is sufficient for localization to punctate spots, GFP was fused with the PX domain or mutant PX domain alone and the localization analyzed by fluorescence microscopy. GFP-PX and GFP-PX-1 fusions showed diffuse GFP patterns similar to the GFP-AtSNX2b-1 mutant (Figure 4E). To confirm this result, an additional PX domain mutant was generated (PX-2; 211PP→AA). Unfortunately, the full length GFP-AtSNX2b-2 fusion protein was not expressed in protoplasts, based on GFP fluorescence. The fusion of GFP with the PX-2 mutant PX domain also showed diffuse cytoplasmic localization, as for the wild-type and PX-1 fusions. Our results suggest that the PX domain is necessary but not sufficient for the localization of AtSNX2b to punctate compartments.

As an initial approach to determine the identity of the AtSNX2b-labeled structures, the distribution of AtSNX2b and several known intracellular markers in a sucrose density gradient (13-55%) was examined. Fractions from the gradient were analyzed by immunoblotting using antibodies against aleurain (ALEU; vacuolar soluble protein), γTIP (vacuolar membrane protein), fumarase (FUM1; mitochondria), SYP21 (PVC t-SNARE), VTI12 (TGN-localized v-SNARE) and AtSNX2b. Both the AtSNX2b band (67kDa) and the

cross-reacting 70 kDa band were visible in these fractions. Figure 5 shows that AtSNX2b has a bipartite distribution with a small part soluble (fractions 2-5) and the majority membrane-bound (fractions 7-12), as predicted from the differential centrifugation (Figure 2F). The 70 kDa band was present in the same fractions as AtSNX2b, but showed a greater percentage present in the soluble fractions compared with membrane-bound. The distribution of the membrane-associated portion of AtSNX2b on the sucrose gradient overlapped extensively with that of VTI12 and with the upper band of SYP21. The SYP21 antibodies recognize a triplet of proteins, all of which correspond to the SYP21 protein (Conceicao et al., 1997); the nature of these three isoforms is unclear but may be due to post-translational modifications. These results suggest a possible localization to an organelle with similar density to the TGN and/or PVC, and distinct from the vacuole and mitochondria.

To determine more precisely the localization of AtSNX2b, roots of transgenic Arabidopsis lines expressing markers for the TGN (T7-SYP42; Bassham et al., 2000), PVC (T7-SYP21 and T7-SYP22; Sanderfoot et al., 1999), late endosomes (YFP-Rha1; Preuss et al., 2004) or Golgi apparatus (sialyl transferase (ST)-GFP; Wee et al., 1998) were analyzed by double immunofluorescence-labeling using AtSNX2b and T7 antibodies or comparison with YFP or GFP fluorescence as appropriate. As in protoplasts, AtSNX2b antibodies recognized punctate structures in root cells that were not labeled with preimmune serum (Figure 6A). To assess the specificity of AtSNX2b labeling, immunofluorescence was also performed under identical conditions on roots from the *Atsnx2b* knockout mutant. No specific signal was seen, indicating that the immunofluorescence staining observed corresponds only to AtSNX2b. White spots in merged images show that some of the AtSNX2b-labeled organelles also contained T7-SYP42, T7-SYP21 (data not shown), T7-

SYP22 or YFP-Rha1 (Figure 6B). By contrast, no overlap was seen between ST-GFP and AtSNX2b, suggesting that AtSNX2b does not reside in the Golgi apparatus.

Percent co-localization was determined by counting the number of AtSNX2b-labeled structures that co-localized with each of the markers. Partial colocalization of AtSNX2b with T7-SYP42, T7-SYP21, T7-SYP22, and YFP-Rha1 was observed (Figure 6B and C). The PVC and late endosomal markers T7-SYP21, T7-SYP22 and YFP-Rha1 show extensive overlap in their localization (Lee et al., 2004), leading to the conclusion that a large portion of AtSNX2b (60 - 80%) does not co-localize with any of the markers tested. As our antibodies are specific for AtSNX2b under these experimental conditions (Figure 6A), this localization pattern suggests that AtSNX2b might localize to or cycle between PVC/late endosomal compartments, the TGN, which has been suggested also to be an early endosome (Dettmer et al., 2006; Lam et al., 2007), and possibly an additional unidentified compartment.

Over-expression of AtSNX2b affects trafficking

It is known that Arabidopsis cells contain multiple endosome types (Ueda et al., 2004), and we therefore hypothesized that the unidentified compartment with which AtSNX2b associates could be an additional type of endosome. To test this hypothesis, we analyzed the localization of GFP-AtSNX2b in transiently transformed protoplasts compared with the fluorescent marker FM4-64. FM4-64 is widely used as an endocytic tracer in live cells (Vida and Emr, 1995; Betz et al., 1996; Bolte et al., 2004). The cell cultures used contain cells of varying sizes; no differences were seen between large and small cells in any experiment. FM4-64 binds to the plasma membrane, is internalized by endocytosis, traffics through the endosomal system and reaches the vacuolar membrane after 3-4 h in Arabidopsis

(Bolte et al., 2004). Arabidopsis protoplasts were transiently transformed with GFP-AtSNX2b and incubated for 12 h to allow expression of the protein. They were then labeled with FM4-64 and uptake of the dye was observed over a time course of up to 4 h (Figure 7). After 0.5 h of uptake, FM4-64 staining was seen mainly at the plasma membrane, with a few puncta in the cytoplasm; no colocalization of FM4-64 with GFP-AtSNX2b was seen at this early time point. Between 1 h and 3 h of uptake, FM4-64 was found in punctate structures that have been shown previously to correspond to Golgi/TGN, PVC and endosomes (Betz et al., 1996; Bolte et al., 2004; Dettmer et al., 2006). Almost complete colocalization of FM4-64 and GFP-AtSNX2b was seen at these times, suggesting that AtSNX2b is predominantly localized to organelles on the endocytic pathway.

By the 4 h time point, FM4-64 reached the vacuolar membrane in control protoplasts transformed with GFP alone, while in GFP-AtSNX2b transformed protoplasts FM4-64 was not present on the vacuolar membrane, instead being trapped in cytoplasmic structures containing GFP-AtSNX2b. FM4-64 was not able to exit the GFP-labeled compartments even after 12 h. In addition, the appearance of the GFP-AtSNX2b structures varied over time. At early time points the GFP-AtSNX2b localized to structures similar in appearance, although apparently somewhat larger than the structures in which endogenous AtSNX2b resides; the size of these organelles is difficult to assess by fluorescence microscopy. At later time points these structures became enlarged and/or aggregated, and by 4 h of FM4-64 labeling the protoplasts contained just a few large GFP-AtSNX2b-labeled structures (Figure 7). This is not related to the presence of FM4-64, as similar effects are seen in the absence of FM4-64 staining, with a gradual increase in the size of the labeled structures over time. The GFP-AtSNX2b in the enlarged structures is most likely membrane-associated, as it pellets with a

membrane fraction after lysis of protoplasts (see Figure 4D) and it co-localizes with FM4-64, which is a membrane-bound dye. These results suggest that over-expression of AtSNX2b causes inhibition of FM4-64 trafficking to the vacuole, possibly by blocking the exit of material from endosomes.

To confirm that the inhibition of transport of FM4-64 to the vacuole was caused by an effect on trafficking, rather than a loss of cell viability, protoplasts were transiently transformed with the GFP-AtSNX2b construct and expression allowed to proceed for up to 24 h. Fluorescence microscopy confirmed the formation of enlarged structures as above, and protoplasts were stained with the vital stain fluorescein diacetate to assay for cell viability. No difference was seen between untransformed and transformed protoplasts, and in both cases almost all protoplasts survived, indicating very little loss of viability (Figure 8).

To verify that over-expression of AtSNX2b alone affects FM4-64 trafficking to the vacuolar membrane, rather than the presence of the GFP tag, an untagged AtSNX2b overexpression construct was introduced into protoplasts, followed by FM4-64 labeling as above. Similar to the effect of GFP-AtSNX2b expression, enlarged FM4-64 structures were observed in the cytoplasm, and most of the FM4-64 failed to reach the vacuolar membrane (Figure 7), even at later time points. This confirms that over-expression of AtSNX2b affects trafficking along the endocytic pathway to the vacuole.

Biosynthetic protein trafficking to the plant vacuole occurs through at least two major pathways, and markers are available for each pathway consisting of GFP fused to an N-terminal vacuolar sorting signal (NTPP-GFP; Ahmed et al., 2000) or a C-terminal vacuolar sorting signal (GFP-CTPP; Fluckiger et al., 2003; Sanmartin et al., 2007). To determine whether the over-expression of AtSNX2b inhibits either of these biosynthetic pathways in

addition to endocytic trafficking, AtSNX2b was co-expressed in protoplasts with either NTPP-GFP or GFP-CTPP. At 15 h after transformation, punctate motile GFP spots were seen (Figure 9A, arrows) along with a clear vacuolar NTPP-GFP or GFP-CTPP signal. By 30 h after transformation, motile GFP spots diminished and vacuolar labeling of GFP became very dominant (Figure 9A). In protoplasts transformed with NTPP-GFP or GFP-CTPP alone, only vacuolar GFP signal was observed after 30 h. In double transformants expressing NTPP-GFP plus 35S::AtSNX2b, non-motile GFP spots accumulated in addition to vacuolar GFP labeling after 30 h (Figure 9A, arrowheads); in contrast, double transformed GFP-CTPP protoplasts did not accumulate GFP spots and only vacuolar GFP labeling was evident at the 30 h time point. These results indicate that overexpression of AtSNX2b causes accumulation of NTPP-GFP in punctate structures in addition to the vacuole, whereas no effect is seen on GFP-CTPP trafficking.

To determine whether the structures accumulating NTPP-GFP upon overexpression of AtSNX2b are the same structures in which FM4-64 accumulates, protoplasts overexpressing AtSNX2b and NTPP-GFP were labeled with FM4-64. At 3 h after FM4-64 uptake, FM4-64 labeling co-localized with non-vacuolar NTPP-GFP signal; these colocalized structures persisted up to 12 h after FM4-64 uptake (Figure 9B). This demonstrates that the NTPP-GFP-containing bodies which are the result of over-expression of AtSNX2b are endosomes. While most of the NTPP-GFP still reaches the vacuole upon AtSNX2b overexpression, these results suggest that over-expression of AtSNX2b partially interferes with the normal trafficking of NTPP-GFP (Figure 9B).

Endogenous AtSNX2b co-localizes with TGN and endosomal markers (Figures 6 and 7). To determine whether these markers are also present in the enlarged structures produced

upon AtSNX2b overexpression, protoplasts overexpressing GFP-AtSNX2b were probed with antibodies against the TGN marker SYP41 (Bassham et al., 2000) or the PVC marker SYP21 (Conceicao et al., 1997) followed by immunofluorescence confocal microscopy. Both SYP41 and SYP21 were present in the enlarged, GFP-AtSNX2b-containing structures and the typical punctate organelles labeled by these antibodies in wild-type cells (Ueda et al., 2004; Dettmer et al., 2006; Tamura et al., 2007) are largely absent. This indicates that these enlarged structures are likely to be aberrant membrane structures or aggregates containing markers proteins from multiple organelles (Figure 9C and 9D).

DISCUSSION

The sorting nexin family in Arabidopsis

Arabidopsis has three sorting nexins named AtSNX1, AtSNX2a and AtSNX2b (Vanoosthuyse et al., 2003; Jaillais et al., 2006). AtSNX1 is most similar to *Brassica oleracea* SNX1 and yeast Vps5p and has been suggested to function as Vps5p in the plant retromer complex (Jaillais et al., 2007). Vps17p, an additional SNX that partners with Vps5p in the retromer complex, does not have an easily identifiable homolog in *Arabidopsis* but one of the other SNXs may perform this function (Vanoosthuyse et al., 2003; Oliviusson et al., 2006). AtSNX1 functions in the trafficking of the auxin transport component PIN2 through a novel pathway independent from that of PIN1/GNOM (Jaillais et al., 2006). In addition it has been implicated as a component of the retromer complex in *Arabidopsis* (Jaillais et al., 2007; Oliviusson et al., 2006). AtSNX2a and AtSNX2b are highly similar and have been suggested to be encoded by duplicate genes with redundant functions (Vanoosthuyse et al., 2003;

Jaillais et al., 2006). This study presents the characterization of AtSNX2b as a SNX involved in trafficking in the Arabidopsis endosomal system.

Typical of SNXs, AtSNX2b is present in a soluble and membrane-bound state, with the membrane-bound form most likely to be the active form in trafficking. Consistent with common motifs in SNXs, AtSNX2b has a PX domain in the N-terminal region of the protein and a C-terminal coiled-coil region which is likely to be a BAR domain. BAR domains form curved structures that can sense membrane curvature (Habermann, 2004; Peter et al., 2004; Ren et al., 2006) and, together with the PX domain, they target the SNX to specific phosphatidylinositol-lipid-rich organelles. The characteristic PX domain of AtSNX2b selectively binds to PI3P *in vitro*, although it is not sufficient for correct localization of GFP *in vivo*, suggesting that other factors or regions of the protein are also required for membrane targeting. PI3P lipids are reported in various species to be most abundant in endosomes (Gillooly et al., 2000; Gruenberg, 2003; Lemmon, 2003; Vermeer et al., 2006), Golgi (Gillooly et al., 2001; Vermeer et al., 2006), TGN (Kim et al., 2001), PVC (Vermeer et al., 2006) and the vacuole (Kim et al., 2001; Vermeer et al., 2006). Using a GFP-fused endosomal binding domain in Arabidopsis, Kim et al. (2001) localized PI3P to the TGN, PVC, tonoplast, and vesicles. In addition they proposed PI3Ps to be synthesized at the TGN and transported from the TGN through the PVC to the central vacuole presumably for degradation by vacuolar hydrolases. Consistent with these results, AtSNX2b is localized to endosomes, TGN and the PVC, as determined by colocalization with markers for these compartments and with the fluorescent endocytic marker FM4-64. This localization to multiple compartments suggests that AtSNX2b may cycle between the TGN, PVC and endosomes, and may function in trafficking between or through these organelles.

To further analyze the function of AtSNX2b, we have isolated a T-DNA knockout mutant in the *AtSNX2b* gene. Expression of the *AtSNX2b* mRNA and protein is lost in this mutant, demonstrating that it is a null mutant and is expected to have completely lost AtSNX2b function. As the AtSNX2a protein shows a high degree of sequence similarity to AtSNX2b (86% amino acid similarity), and both genes are expressed ubiquitously throughout the plant (Figure 1 and www.genevestigator.ethz.ch; Zimmermann et al., 2004), we hypothesize that these two proteins may perform redundant functions. One possibility is that AtSNX2a and/or AtSNX2b may function as the Vps17 constituent in Arabidopsis retromer, as a component of the subcomplex also containing AtSNX1. However, no obvious phenotype is evident for the *Atsnx2b* mutant, either at a morphological level, in protein trafficking pathways, or in auxin-related responses such as gravitropism (data not shown). In addition, we have been unable to detect an interaction between AtSNX2b and AtSNX1 in pull-down assays after transient expression. An *Atsnx2a/Atsnx2b* double mutant will help to clarify this issue.

Overexpression of AtSNX2b inhibits vesicle trafficking

Overexpression of trafficking components can lead to inhibition of trafficking by disruption of the dynamics of the trafficking process as a result of sequestration of receptors or other factors involved in trafficking (Barr et al., 2000). Expression of high levels of GFP-tagged AtSNX2b leads to the formation of large, GFP-AtSNX2b-containing compartments in the cell. These compartments are most likely enlarged or aggregated endosomes as they accumulate FM4-64, which becomes trapped in these compartments and can no longer reach the vacuolar membrane. They may also contain membrane and cargo derived from multiple

sources, as TGN and PVC markers accumulate within them. Overexpression of untagged AtSNX2b gave a similar phenotype in that FM4-64-labeled enlarged compartments are present and FM4-64 in these compartments does not reach the vacuolar membrane. AtSNX2b overexpression also resulted in partial accumulation of the vacuolar marker NTPP-GFP in endosomes, although most of the NTPP-GFP still reached the vacuole. In a small but consistent number of cells, a portion of the NTPP-GFP was arrested in the enlarged FM4-64-labeled endosomes. This relatively minor effect on biosynthetic cargo compared with endocytic cargo may suggest that the effect on NTPP-GFP is a secondary effect of disrupting the structure of the endomembrane system, rather than indicating a direct role for AtSNX2b in vacuolar trafficking.

Based on the localization of AtSNX2b on endosomes, the TGN and PVC, and the overexpression phenotype of enlarged endosomes or endosomal aggregates and inhibition of transport through these endosomes, we hypothesize that AtSNX2b is involved in exit from endosomes. However, there are several possible explanations for the phenotype caused by AtSNX2b overexpression. First, the overexpression of AtSNX2b may interfere with the function of endogenous AtSNX2b. Second, overexpression could interfere with functions of other SNXs by sequestering components common to multiple pathways. In this case, the phenotype observed could be a result of the disruption of several trafficking pathways involving different SNXs. Finally, sequestration of PI3P due to AtSNX2b binding may prevent recognition of PI3P-rich lipid membranes by other proteins. The phenotype would therefore be a result of blocking multiple PI3P-dependent transport pathways. In this study, we have shown that AtSNX2b overexpression disrupts vacuolar protein trafficking through biosynthetic and endocytic pathways, suggesting that the AtSNX2b sorting nexin may be

involved in protein trafficking. Additional experiments are now underway to define a more precise function of AtSNX2b in vesicle trafficking pathways.

ACKNOWLEDGEMENTS

We thank Drs Chris Hawes, Erik Nielsen, David Oliver, Natasha Raikhel and Tony Sanderfoot for antibodies, constructs and transgenic lines, Margie Carter (ISU Confocal Microscopy and Image Analysis Facility) and Tracey Pepper (ISU Microscopy and Nanoimaging Facility) for valuable assistance and expertise in microscopy and Tony Contento for helpful comments on the manuscript.

REFERENCES

Ahmed SU, et al. The plant vacuolar sorting receptor AtELP is involved in transport of NH(2)-terminal propeptide-containing vacuolar proteins in Arabidopsis thaliana. J Cell Biol (2000) 149:1335-1344.

Baluska F, Samaj J, Hlavacka A, Kendrick-Jones J, Volkmann D. Actin-dependent fluid-phase endocytosis in inner cortex cells of maize root apices. J Exp Bot (2004) 55:463-473.

Barr VA, Phillips SA, Taylor SI, Haft CR. Overexpression of a novel sorting nexin, SNX15, affects endosome morphology and protein trafficking. Traffic (2000) 1:904-916.

Bassham DC, Sanderfoot AA, Kovaleva V, Zheng H, Raikhel NV. AtVPS45 complex formation at the trans-Golgi network. Mol Biol Cell (2000) 11:2251-2265.

Batoko H, Zheng HQ, Hawes C, Moore I. A rab1 GTPase is required for transport between the endoplasmic reticulum and golgi apparatus and for normal golgi movement in plants. Plant Cell (2000) 12:2201-2218.

Behal RH, Oliver DJ. Biochemical and molecular characterization of fumarase from plants: purification and characterization of the enzyme--cloning, sequencing, and expression of the gene. Arch Biochem Biophys (1997) 348:65-74.

Betz WJ, Mao F, Smith CB. Imaging exocytosis and endocytosis. Curr Opin Neurobiol (1996) 6:365-371.

Bolte S, Talbot C, Boutte Y, Catrice O, Read ND, Satiat-Jeunemaitre B. FM-dyes as experimental probes for dissecting vesicle trafficking in living plant cells. J Microsc (2004) 214:159-173.

Carlton J, et al. Sorting nexin-1 mediates tubular endosome-to-TGN transport through coincidence sensing of high- curvature membranes and 3-phosphoinositides. Curr Biol (2004) 14:1791-1800.

Carlton J, Bujny M, Rutherford A, Cullen P. Sorting nexins - Unifying trends and new perspectives. Traffic (2005) 6:75-82.

Chrispeels MJ, Raikhel NV. Short peptide domains target proteins to plant vacuoles. Cell (1992) 68:613-616.

Conceicao A, Marty-Mazars D, Bassham DC, Sanderfoot AA, Marty F, Raikhel NV. The syntaxin homolog AtPEP12p resides on a late post-Golgi compartment in plants. Plant Cell (1997) 9:571-582.

Contento AL, Xiong Y, Bassham DC. Visualization of autophagy in Arabidopsis using the fluorescent dye monodansylcadaverine and a GFP-AtATG8e fusion protein. Plant J (2005) 42:598-608.

Dettmer J, Hong-Hermesdorf A, Stierhof YD, Schumacher K. Vacuolar H+-ATPase activity is required for endocytic and secretory trafficking in Arabidopsis. Plant Cell (2006) 18:715-730.

Dhonukshe P, Kleine-Vehn J, Friml J. Cell polarity, auxin transport, and cytoskeleton-mediated division planes: who comes first? Protoplasma (2005) 226:67-73.

Di Sansebastiano GP, Paris N, Marc-Martin S, Neuhaus JM. Regeneration of a lytic central vacuole and of neutral peripheral vacuoles can be visualized by green fluorescent proteins targeted to either type of vacuoles. Plant Physiol (2001) 126:78-86.

Dowler S, Kular G, Alessi DR. Protein lipid overlay assay. Sci STKE (2002) 2002:PL6.

Fluckiger R, De Caroli M, Piro G, Dalessandro G, Neuhaus JM, Di Sansebastiano GP. Vacuolar system distribution in Arabidopsis tissues, visualized using GFP fusion proteins. J Exp Bot (2003) 54:1577-1584.

Freshour G, Bonin CP, Reiter WD, Albersheim P, Darvill AG, Hahn MG. Distribution of fucose-containing xyloglucans in cell walls of the mur1 mutant of Arabidopsis. Plant Physiol (2003) 131:1602-1612.

Gallop JL, McMahon HT. BAR domains and membrane curvature: bringing your curves to the BAR. Biochem Soc Symp (2005):223-231.

Gillooly DJ, et al. Localization of phosphatidylinositol 3-phosphate in yeast and mammalian cells. EMBO J (2000) 19:4577-4588.

Gillooly DJ, Simonsen A, Stenmark H. Cellular functions of phosphatidylinositol 3-phosphate and FYVE domain proteins. Biochem J (2001) 355:249-258.

Grebe M, et al. Arabidopsis sterol endocytosis involves actin-mediated trafficking via ARA6-positive early endosomes. Curr Biol (2003) 13:1378-1387.

Gruenberg J. Lipids in endocytic membrane transport and sorting. Curr Opin Cell Biol (2003) 15:382-388.

Haas TJ, et al. The Arabidopsis AAA ATPase SKD1 is involved in multivesicular endosome function and interacts with its positive regulator LYST-INTERACTING PROTEIN5. Plant Cell (2007) 19:1295-1312.

Habermann B. The BAR-domain family of proteins: a case of bending and binding? EMBO Rep (2004) 5:250-255.

Haft CR, de la Luz Sierra M, Bafford R, Lesniak MA, Barr VA, Taylor SI. Human orthologs of yeast vacuolar protein sorting proteins Vps26, 29, and 35: assembly into multimeric complexes. Mol Biol Cell (2000) 11:4105-4116.

Hanton SL, Brandizzi F. Protein transport in the plant secretory pathway. Canadian J Bot (2006) 84:523-530.

Hicks GR, Rojo E, Hong S, Carter DG, Raikhel NV. Geminating pollen has tubular vacuoles, displays highly dynamic vacuole biogenesis, and requires VACUOLESS1 for proper function. Plant Physiol (2004) 134:1227-1239.

Hillmer S, Movafeghi A, Robinson DG, Hinz G. Vacuolar storage proteins are sorted in the cis-cisternae of the pea cotyledon Golgi apparatus. J Cell Biol (2001) 152:41-50.

Holstein SE, Oliviusson P. Sequence analysis of Arabidopsis thaliana E/ANTH-domain-containing proteins: membrane tethers of the clathrin-dependent vesicle budding machinery. Protoplasma (2005) 226:13-21.

Horazdovsky BF, Davies BA, Seaman MN, McLaughlin SA, Yoon S, Emr SD. A sorting nexin-1 homologue, Vps5p, forms a complex with Vps17p and is required for recycling the vacuolar protein-sorting receptor. Mol Biol Cell (1997) 8:1529-1541.

Igarashi D, Ishida S, Fukazawa J, Takahashi Y. 14-3-3 proteins regulate intracellular localization of the bZIP transcriptional activator RSG. Plant Cell (2001) 13:2483-2497.

Jaillais Y, Fobis-Loisy I, Miege C, Gaude T. Evidence for a sorting endosome in Arabidopsis root cells. Plant J (2008) 53:237-247.

Jaillais Y, Fobis-Loisy I, Miege C, Rollin C, Gaude T. AtSNX1 defines an endosome for auxin-carrier trafficking in Arabidopsis. Nature (2006) 443:106-109.

Jaillais Y, Santambrogio M, Rozier F, Fobis-Loisy I, Miege C, Gaude T. The retromer protein VPS29 links cell polarity and organ initiation in plants. Cell (2007) 130:1057-1070.

Jolliffe NA, Craddock CP, Frigerio L. Pathways for protein transport to seed storage vacuoles. Biochem Soc Trans (2005) 33:1016-1018.

Kang BH, Busse JS, Dickey C, Rancour DM, Bednarek SY. The arabidopsis cell plate-associated dynamin-like protein, ADL1Ap, is required for multiple stages of plant growth and development. Plant Physiol (2001) 126:47-68.

Kim DH, et al. Trafficking of phosphatidylinositol 3-phosphate from the trans-Golgi network to the lumen of the central vacuole in plant cells. Plant Cell (2001) 13:287-301.

Kirsch T, Paris N, Butler JM, Beevers L, Rogers JC. Purification and initial characterization of a potential plant vacuolar targeting receptor. Proc Natl Acad Sci USA (1994) 91:3403-3407.

Kurten RC, Cadena DL, Gill GN. Enhanced degradation of EGF receptors by a sorting nexin, SNX1. Science (1996) 272:1008-1010.

Lam SK, et al. Rice SCAMP1 defines clathrin-coated, *trans*-golgi-located tubular-vesicular structures as an early endosome in tobacco BY-2 cells. Plant Cell (2007) 19:296-319.

Lee GJ, Sohn EJ, Lee MH, Hwang I. The Arabidopsis rab5 homologs rha1 and ara7 localize to the prevacuolar compartment. Plant Cell Physiol (2004) 45:1211-1220.

Lee KJ, et al. Arabinogalactan proteins are required for apical cell extension in the moss Physcomitrella patens. Plant Cell (2005) 17:3051-3065.

Lemmon MA. Phosphoinositide recognition domains. Traffic (2003) 4:201-213.

Leprince C, et al. Sorting nexin 4 and amphiphysin 2, a new partnership between endocytosis and intracellular trafficking. J Cell Sci (2003) 116:1937-1948.

Li XM, Shapiro LJ. Three-step PCR mutagenesis for 'linker scanning'. Nucleic Acids Res (1993) 21:3745-3748.

Lundmark R, Carlsson SR. Sorting nexin 9 participates in clathrin-mediated endocytosis through interactions with the core components. J Biol Chem (2003) 278:46772-46781.

Marty F. Plant vacuoles. Plant Cell (1999) 11:587-600.

Matsuoka K, Neuhaus J. Cis-elements of protein transport to the plant vacuoles. J Exp Bot (1999) 50:165-174.

Merino-Trigo A, et al. Sorting nexin 5 is localized to a subdomain of the early endosomes and is recruited to the plasma membrane following EGF stimulation. J Cell Sci (2004) 117:6413-6424.

Mitsuhashi N, Shimada T, Mano S, Nishimura M, Hara-Nishimura I. Characterization of organelles in the vacuolar-sorting pathway by visualization with GFP in tobacco BY-2 cells. Plant Cell Physiol (2000) 41:993-1001.

Muller A, et al. AtPIN2 defines a locus of Arabidopsis for root gravitropism control. EMBO J (1998) 17:6903-6911.

Muller J, Mettbach U, Menzel D, Samaj J. Molecular dissection of endosomal compartments in plants. Plant Physiol (2007) 145:293-304.

Olbrich A, Hillmer S, Hinz G, Oliviusson P, Robinson DG. Newly formed vacuoles in root meristems of barley and pea seedlings have characteristics of both protein storage and lytic vacuoles. Plant Physiol (2007) 145:1383-1394.

Oliviusson P, et al. Plant retromer, localized to the prevacuolar compartment and microvesicles in Arabidopsis, may interact with vacuolar sorting receptors. Plant Cell (2006) 18:1239-1252.

Paris N, Neuhaus JM. BP-80 as a vacuolar sorting receptor. Plant Mol Biol (2002) 50:903-914.

Paris N, Stanley CM, Jones RL, Rogers JC. Plant cells contain two functionally distinct vacuolar compartments. Cell (1996) 85:563-572.

Park M, Lee D, Lee GJ, Hwang I. AtRMR1 functions as a cargo receptor for protein trafficking to the protein storage vacuole. J Cell Biol (2005) 170:757-767.

Parks WT, et al. Sorting nexin 6, a novel SNX, interacts with the transforming growth factor-beta family of receptor serine-threonine kinases. J Biol Chem (2001) 276:19332-19339.

Peter BJ, et al. BAR domains as sensors of membrane curvature: the amphiphysin BAR structure. Science (2004) 303:495-499.

Preuss ML, Serna J, Falbel TG, Bednarek SY, Nielsen E. The Arabidopsis Rab GTPase RabA4b localizes to the tips of growing root hair cells. Plant Cell (2004) 16:1589-1603.

Reddy JV, Seaman MN. Vps26p, a component of retromer, directs the interactions of Vps35p in endosome-to-Golgi retrieval. Mol Biol Cell (2001) 12:3242-3256.

Ren G, Vajjhala P, Lee JS, Winsor B, Munn AL. The BAR domain proteins: molding membranes in fission, fusion, and phagy. Microbiol Mol Biol Rev (2006) 70:37-120.

Rojas R, Kametaka S, Haft CR, Bonifacino JS. Interchangeable but essential functions of SNX1 and SNX2 in the association of retromer with endosomes and the trafficking of mannose 6-phosphate receptors. Mol Cell Biol (2007) 27:1112-1124.

Rosso MG, Li Y, Strizhov N, Reiss B, Dekker K, Weisshaar B. An Arabidopsis thaliana T-DNA mutagenized population (GABI-Kat) for flanking sequence tag-based reverse genetics. Plant Mol Biol (2003) 53:247-259.

Samaj J, Read ND, Volkmann D, Menzel D, Baluska F. The endocytic network in plants. Trends Cell Biol (2005) 15:425-433.

Sanderfoot AA, et al. A putative vacuolar cargo receptor partially colocalizes with AtPEP12p on a prevacuolar compartment in Arabidopsis roots. Proc Natl Acad Sci USA (1998) 95:9920-9925.

Sanderfoot AA, Kovaleva V, Zheng H, Raikhel NV. The t-SNARE AtVAM3p resides on the prevacuolar compartment in Arabidopsis root cells. Plant Physiol (1999) 121:929-938.

Sanderfoot AA, Pilgrim M, Adam L, Raikhel NV. Disruption of individual members of Arabidopsis syntaxin gene families indicates each has essential functions. Plant Cell (2001) 13:659-666.

Sanmartin M, et al. Divergent functions of VTI12 and VTI11 in trafficking to storage and lytic vacuoles in Arabidopsis. Proc Natl Acad Sci USA (2007) 104:3645-3650.

Seaman MN, Marcusson EG, Cereghino JL, Emr SD. Endosome to Golgi retrieval of the vacuolar protein sorting receptor, Vps10p, requires the function of the VPS29, VPS30, and VPS35 gene products. J Cell Biol (1997) 137:79-92.

Seaman MN, McCaffery JM, Emr SD. A membrane coat complex essential for endosome-to-Golgi retrograde transport in yeast. J Cell Biol (1998) 142:665-681.

Sheen J. A transient expression assay using Arabidopsis mesophyll protoplasts. In: http://genetics.mgh.harvard.edu/sheenweb/ (2002).

Shimada T, Fuji K, Tamura K, Kondo M, Nishimura M, Hara-Nishimura I. Vacuolar sorting receptor for seed storage proteins in Arabidopsis thaliana. Proc Natl Acad Sci USA (2003) 100:16095-16100.

Shimada T, et al. AtVPS29, a putative component of a retromer complex, is required for the efficient sorting of seed storage proteins. Plant Cell Physiol (2006) 47:1187-1194.

Sivaguru M, Baluska F, Volkmann D, Felle HH, Horst WJ. Impacts of aluminum on the cytoskeleton of the maize root apex. short-term effects on the distal part of the transition zone. Plant Physiol (1999) 119:1073-1082.

Tamura K, Takahashi H, Kunieda T, Fuji K, Shimada T, Hara-Nishimura I. Arabidopsis KAM2/GRV2 is required for proper endosome formation and functions in vacuolar sorting and determination of the embryo growth axis. Plant Cell (2007) 19:320-332.

Teasdale RD, Loci D, Houghton F, Karlsson L, Gleeson PA. A large family of endosome-localized proteins related to sorting nexin 1. Biochem J (2001) 358:7-16.

Ueda T, Uemura T, Sato MH, Nakano A. Functional differentiation of endosomes in Arabidopsis cells. Plant J (2004) 40:783-789.

Ueda T, Yamaguchi M, Uchimiya H, Nakano A. Ara6, a plant-unique novel type Rab GTPase, functions in the endocytic pathway of Arabidopsis thaliana. EMBO J (2001) 20:4730-4741.

Vanoosthuyse V, Tichtinsky G, Dumas C, Gaude T, Cock JM. Interaction of calmodulin, a sorting nexin and kinase-associated protein phosphatase with the Brassica oleracea S locus receptor kinase. Plant Physiol (2003) 133:919-929.

Vermeer JE, et al. Visualization of PtdIns3P dynamics in living plant cells. Plant J (2006) 47:687-700.

Vida TA, Emr SD. A new vital stain for visualizing vacuolar membrane dynamics and endocytosis in yeast. J Cell Biol (1995) 128:779-792.

Wee EG, Sherrier DJ, Prime TA, Dupree P. Targeting of active sialyltransferase to the plant Golgi apparatus. Plant Cell (1998) 10:1759-1768.

Worby CA, Dixon JE. Sorting out the cellular functions of sorting nexins. Nat Rev Mol Cell Biol (2002) 3:919-931.

Xu Y, Hortsman H, Seet L, Wong SH, Hong W. SNX3 regulates endosomal function through its PX-domain-mediated interaction with PtdIns(3)P. Nat Cell Biol (2001) 3:658-666.

Yamada K, Fuji K, Shimada T, Nishimura M, Hara-Nishimura I. Endosomal proteases facilitate the fusion of endosomes with vacuoles at the final step of the endocytotic pathway. Plant J (2005) 41:888-898.

Yamazaki M, et al. Arabidopsis VPS35, a retromer component, is required for vacuolar protein sorting and involved in plant growth and leaf senescence. Plant Cell Physiol (2008) 49:142-156.

Zhong Q, et al. Endosomal localization and function of sorting nexin 1. Proc Natl Acad Sci USA (2002) 99:6767-6772.

Zimmermann P, Hirsch-Hoffmann M, Hennig L, Gruissem W. GENEVESTIGATOR. Arabidopsis microarray database and analysis toolbox. Plant Physiol (2004) 136:2621-2632.

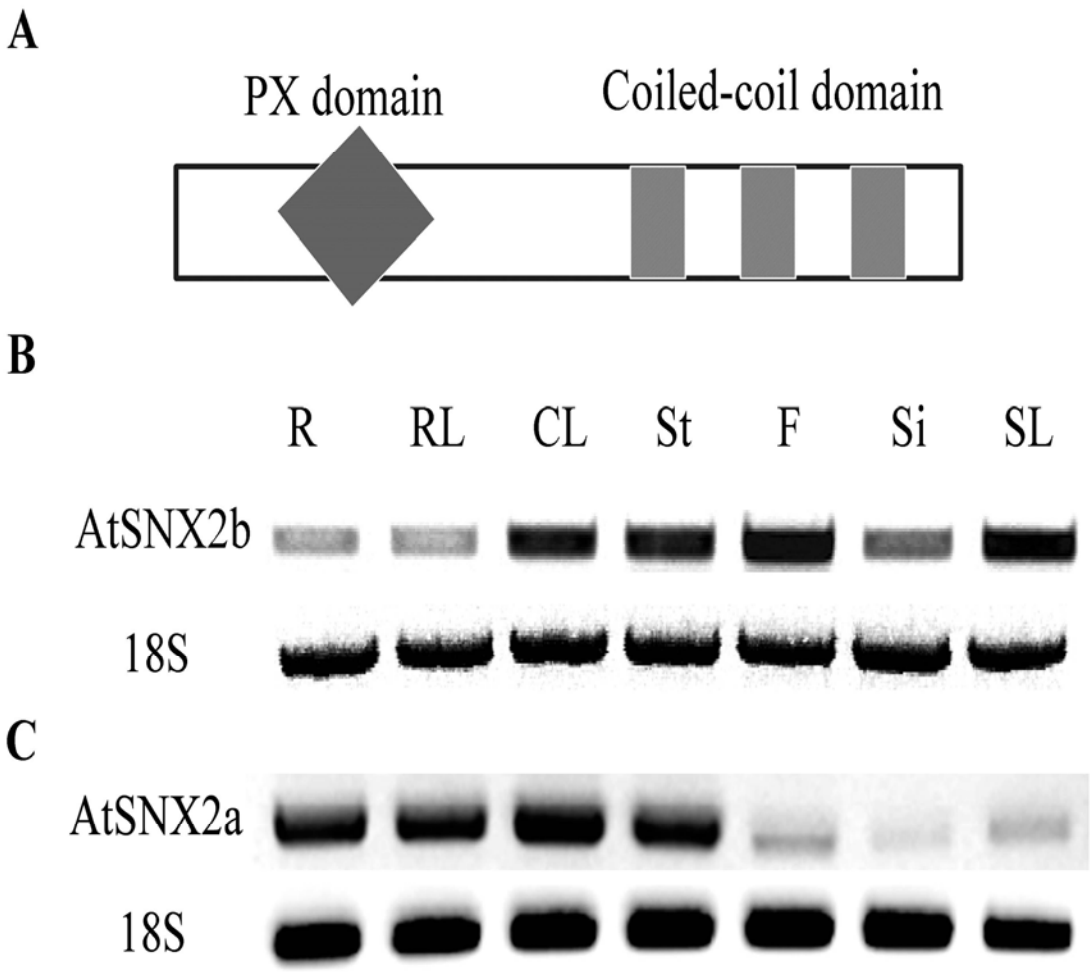

Figure 1. **Structural features of AtSNX2b**.

A-C. The AtSNX2b protein contains a PX domain near the N-terminus and a C-terminal coiled-coil region. B, Expression of *AtSNX2b* mRNA throughout the Arabidopsis plant. RT-PCR analysis using *AtSNX2b*-specific primers shows *AtSNX2b* is ubiquitously expressed in roots (R), rosette leaves (RL), cauline leaves (CL), inflorescence stem (St), flowers (F), siliques (Si) and senescing leaves (SL). 18S RNA is present as a loading control. C, Expression of *AtSNX2a* mRNA throughout the Arabidopsis plant. RT-PCR analysis was performed as in B, except using primers specific to *AtSNX2a*. 18S RNA is used as a loading control.

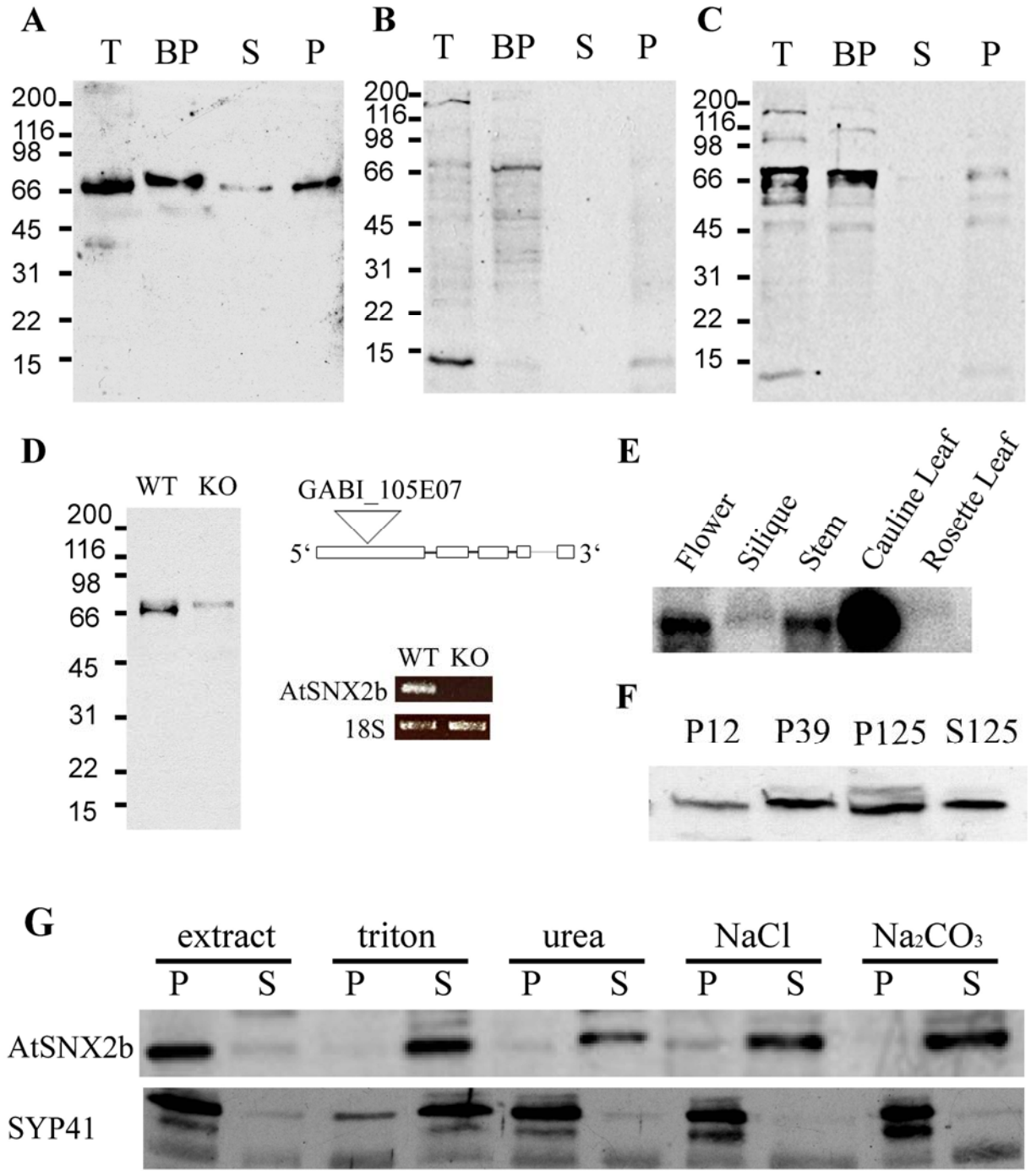

Figure 2. **Characterization of AtSNX2b protein in Arabidopsis**.

A-D. Detection of AtSNX2b in protein extracts using A, affinity-purified AtSNX2b antibodies; B, preimmune serum; or C, crude immune serum. Lanes show total Arabidopsis

protein (T), *E. coli*-expressed purified protein (BP), total plant soluble (S) and total plant membrane (P) proteins. Molecular mass markers are shown at left (kDa). D, Affinity purified antibodies detect a strong lower and a weak upper band in a total protein extract from wild–type Arabidopsis plants. Only the weak upper band is present in an extract from the *Atsnx2b* TDNA knockout line GABI_105E07. RT-PCR analysis using *AtSNX2b*-specific primers indicates that no *AtSNX2b* RNA can be detected in the GABI_105E07 line. Primers against 18S rRNA are used as a control.

E. Distribution of AtSNX2b protein throughout the plant

Total protein extracts from the indicated structures were analyzed by immunoblotting using AtSNX2b antibodies.

F. Differential centrifugation

Differential centrifugation of an Arabidopsis extract to generate 12,000*g* (P12), 39,000*g* (P39) and 125,000*g* (P125) pellets and a 125,000*g* supernatant (S125). Fractions were probed with antibodies against AtSNX2b. G, AtSNX2b membrane association test. Proteins were extracted from a total membrane pellet using extraction buffer alone or containing Na_2CO_3, NaCl, urea, or Triton X-100. Proteins extracted to the soluble phase (S) or remaining in the insoluble pellet (P) were analyzed by immunoblotting using AtSNX2b antibodies, or SYP41 antibodies as a control.

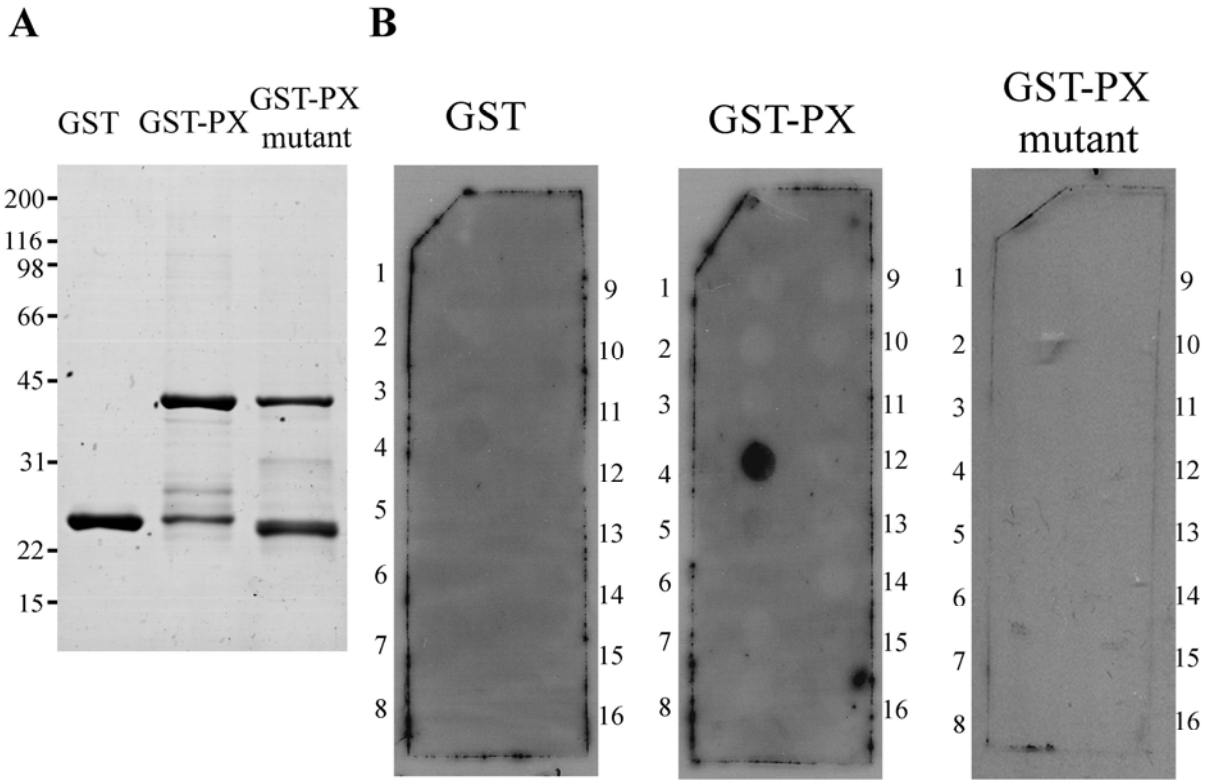

Figure 3. **The PX domain of AtSNX2b binds to phospholipids**.

A. Expression of GST fused PX domain

Coomassie-stained gel showing purified GST-fused PX domain and PX-1 mutant, or GST alone as a control, synthesized in *E. coli*.

B. **Lipid overlay assay for binding to various phospholipids**

The purified GST-fusion proteins were allowed to bind to phospholipids immobilized on a membrane (PIP^{TM} strips) and lipid binding was detected using GST antibodies (Invitrogen, Carlsbad, CA). Phospholipids are spotted as follows (1) Lysophosphatidic acid; (2) Lysophosphocholine; (3) Phosphatidylinositol (PtdIns); (4) PtdIns(3)P; (5) PtdIns(4)P; (6) PtdIns(5)P; (7) Phosphatidylethanolamine; (8) Phosphatidylcholine; (9) Sphingosine-1-

phosphate; (10) PtdIns(3,4)P; (11) PtdIns(3,5)P; (12) PtdIns(4,5)P; (13) PtdIns(3,4,5)P; (14) Phosphatidic acid; (15) Phosphatidylserine; and (16) no lipid.

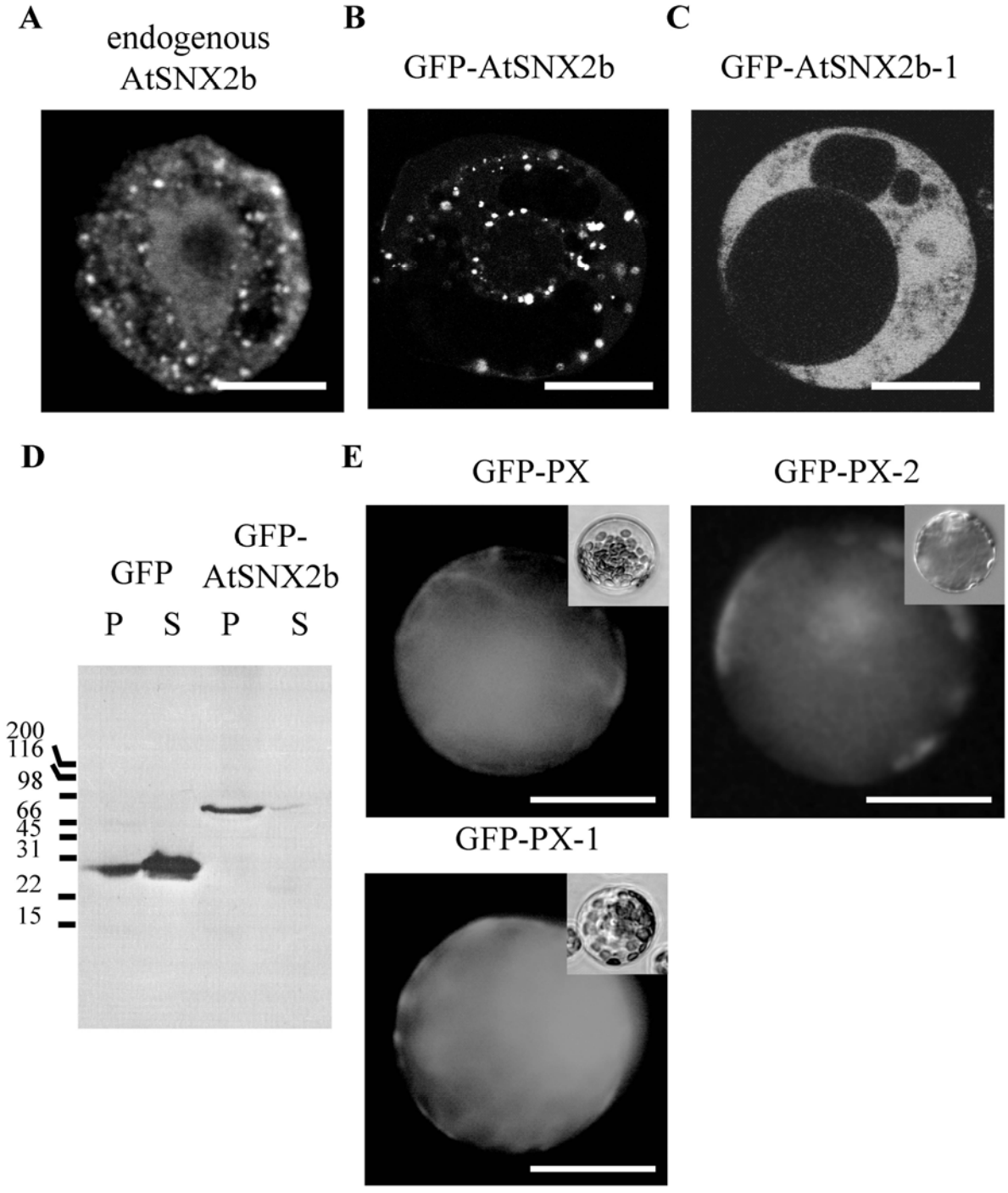

Figure 4. **Transient expression of GFP-tagged AtSNX2b and PX domains**.

A. Immunofluorescence labeling of endogenous AtSNX2b in Arabidopsis protoplasts.

B. Expression of GFP-tagged AtSNX2b in Arabidopsis protoplasts. Punctate GFP structures are seen, similar to the endogenous protein labeling.

C. Expression of the GFP-AtSNX2b-1 PX domain mutant in Arabidopsis protoplasts shows diffuse cytoplasmic GFP labeling.

D. Immunoblot of GFP-AtSNX2b expression in protoplasts. Extracts from protoplasts transiently expressing GFP-AtSNX2b were fractionated by centrifugation at 125,000*g* yielding soluble (S) and membrane pellet (P) fractions. GFP-fused AtSNX2b is membrane-associated while GFP is mostly soluble. Molecular mass markers are shown at left (kDa).

E. Fluorescence images of GFP-tagged PX domain (GFP-PX) and GFP-tagged PX domain mutants (GFP-PX-1 and GFP-PX-2) showing diffuse cytoplasmic GFP labeling. Insets show brightfield images. Scale bars for all figures are 10μm.

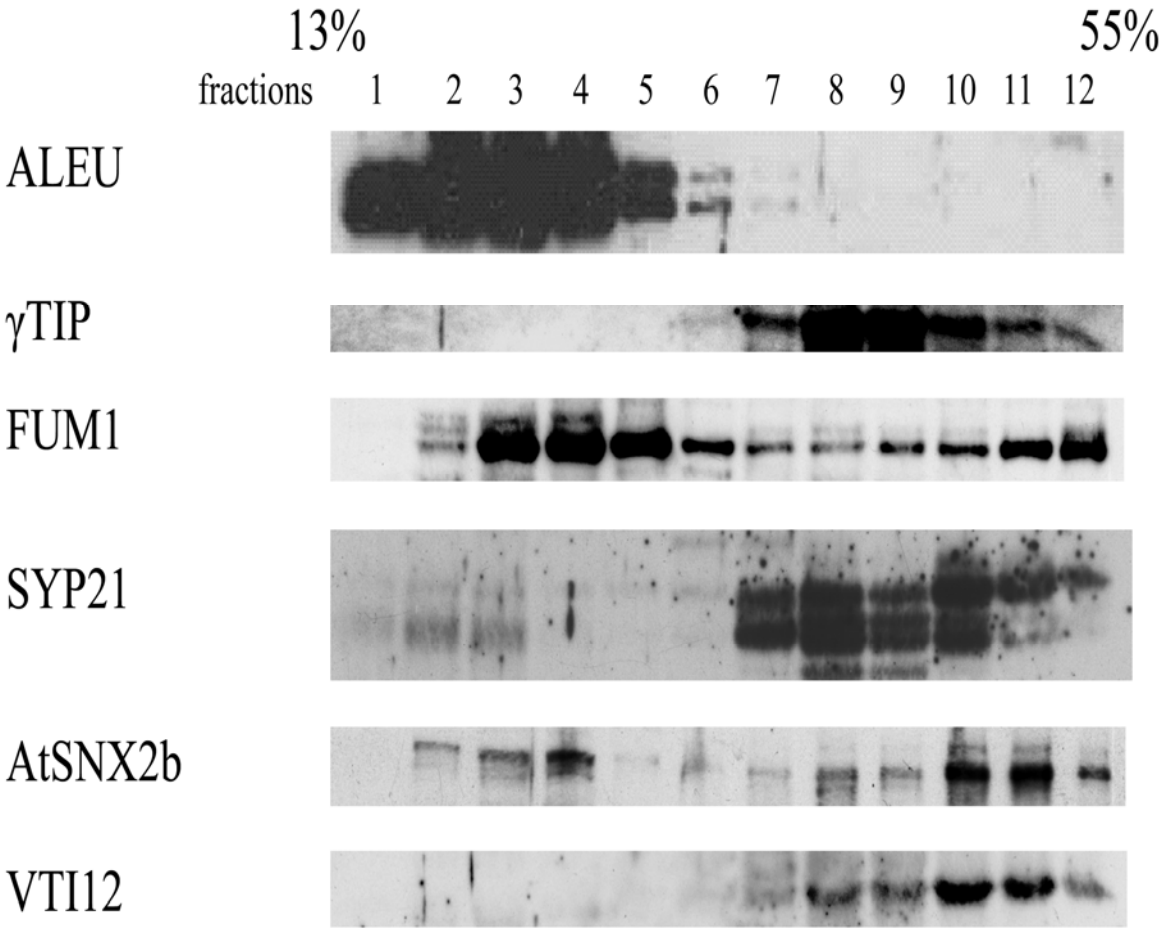

Figure 5. **Sucrose gradient profiles of AtSNX2b and various subcellular markers.**

An Arabidopsis protein extract was fractionated on a 13% to 55% sucrose density gradient and analyzed by immunoblotting with antibodies against aleurain (ALEU), fumarase (FUM1), γ-tonoplast intrinsic protein (γTIP), the t-SNARE SYP21, the v-SNARE VTI12 and AtSNX2b.

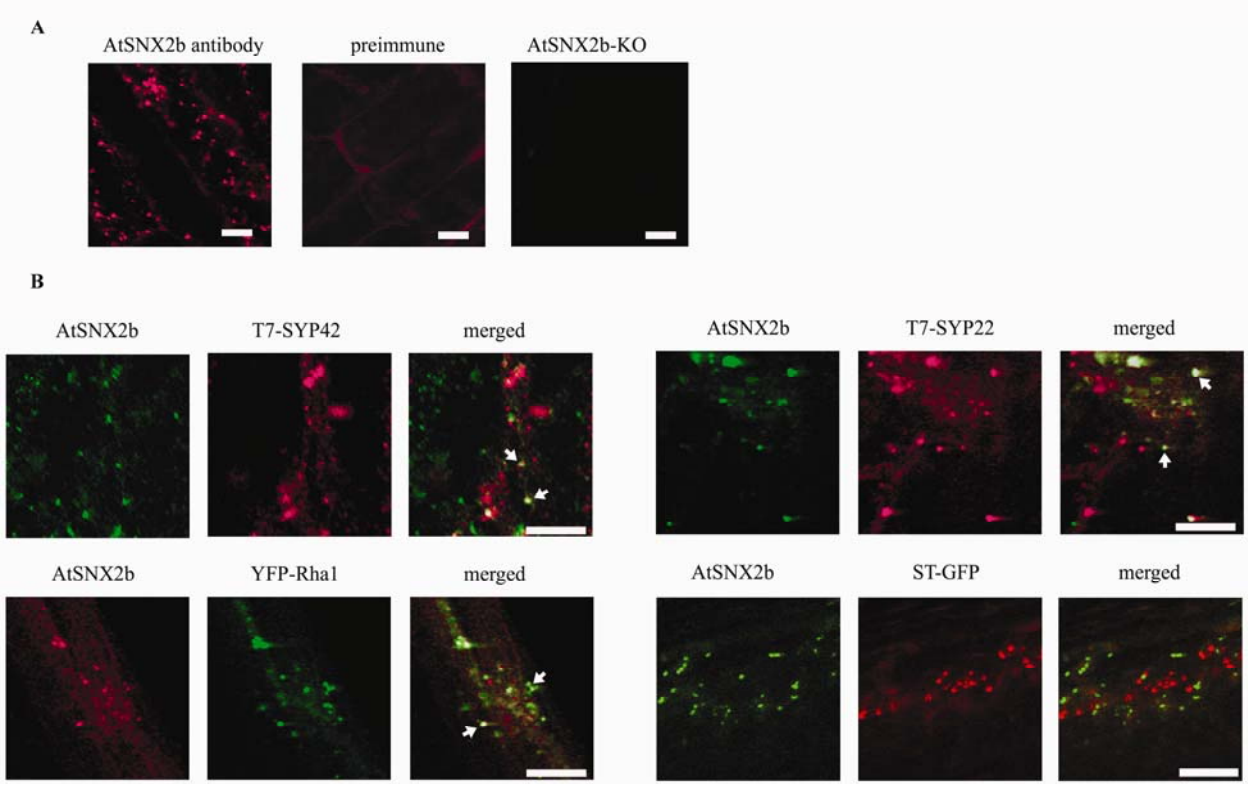

C

Markers	Percentage Colocalization
T7-SYP42	11.78±0.57
T7-SYP22	24.41±3.04
T7-SYP21	18.50±0.98
YFP-Rha1	19.35±2.40
ST-GFP	0

Figure 6. **Immunofluorescence showing colocalization of AtSNX2b with various subcellular markers in Arabidopsis.**

Arabidopsis roots were fixed and analyzed by single or double immunofluorescence labeling using T7 and purified AtSNX2b antibodies.

A. immunofluorescence using affinity-purified AtSNX2b antibodies detects punctate spots in root cells. Preimmune serum does not produce any specific signal. No signal is seen upon staining with affinity-purified AtSNX2b antibodies under identical conditions in the *Atsnx2b* knockout mutant (AtSNX2b-KO).

B. Immunofluorescence images showing double labeling of AtSNX2b with T7-SYP42, T7-SYP22, YFP-Rha1, and ST-GFP in transgenic plants expressing the appropriate tagged protein. Merged images show partial colocalization of AtSNX2b with each of the tested markers except for ST-GFP. Scale bars represent 10μm. Arrows indicate examples of co-localization.

C, Percentage colocalization of AtSNX2b with various subcellular markers. Ten independent images were counted for each marker.

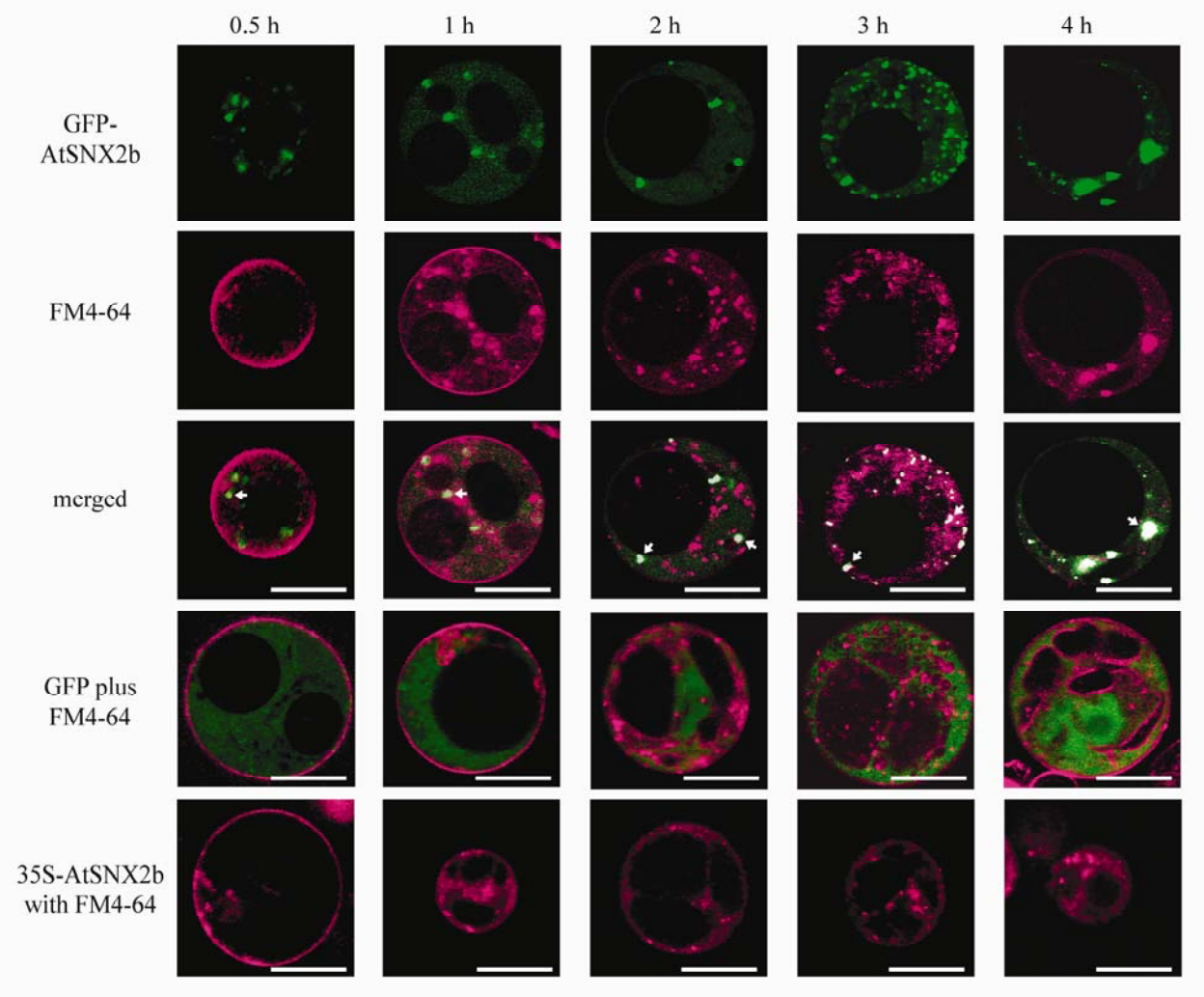

Figure 7. **Timecourse of FM4-64 uptake in protoplasts overexpressing AtSNX2b**. Arabidopsis protoplasts were transformed with a GFP vector control, GFP-AtSNX2b or 35S::AtSNX2b plus the GFP vector control to tag transformed protoplasts, followed by labeling with the fluorescent dye FM4-64 and incubation for up to 4 h to allow FM4-64 uptake by endocytosis. Scale bars are 10μm. Arrows indicate examples of co-localization.

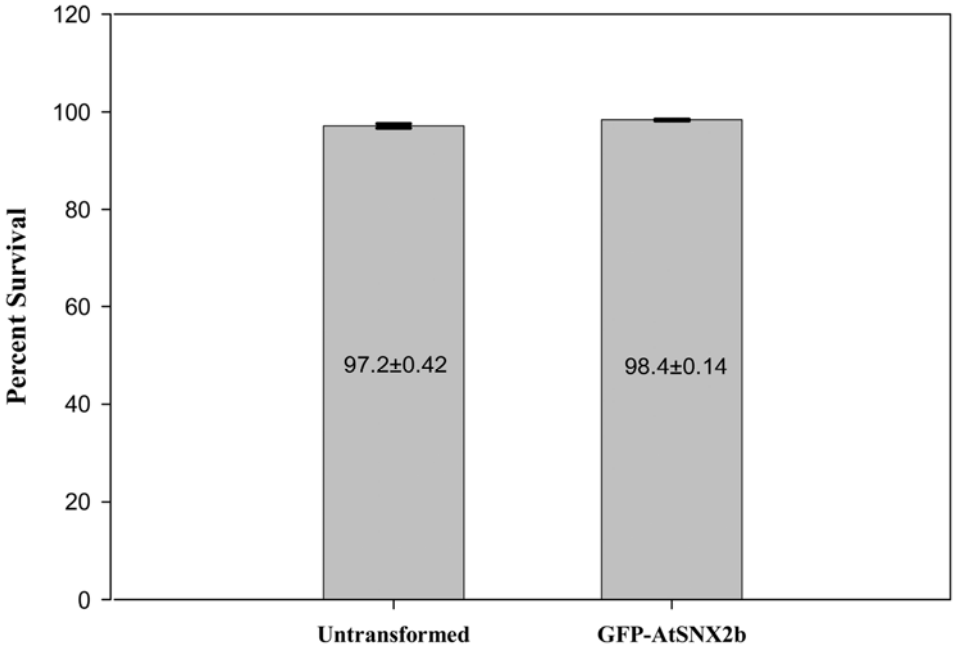

Figure 8. Viability of Arabidopsis protoplasts.

Arabidopsis protoplast viability was determined in control (untransformed) and GFP-AtSNX2b-transformed Arabidopsis protoplasts using fluorescein diacetate, 24 h after transformation.

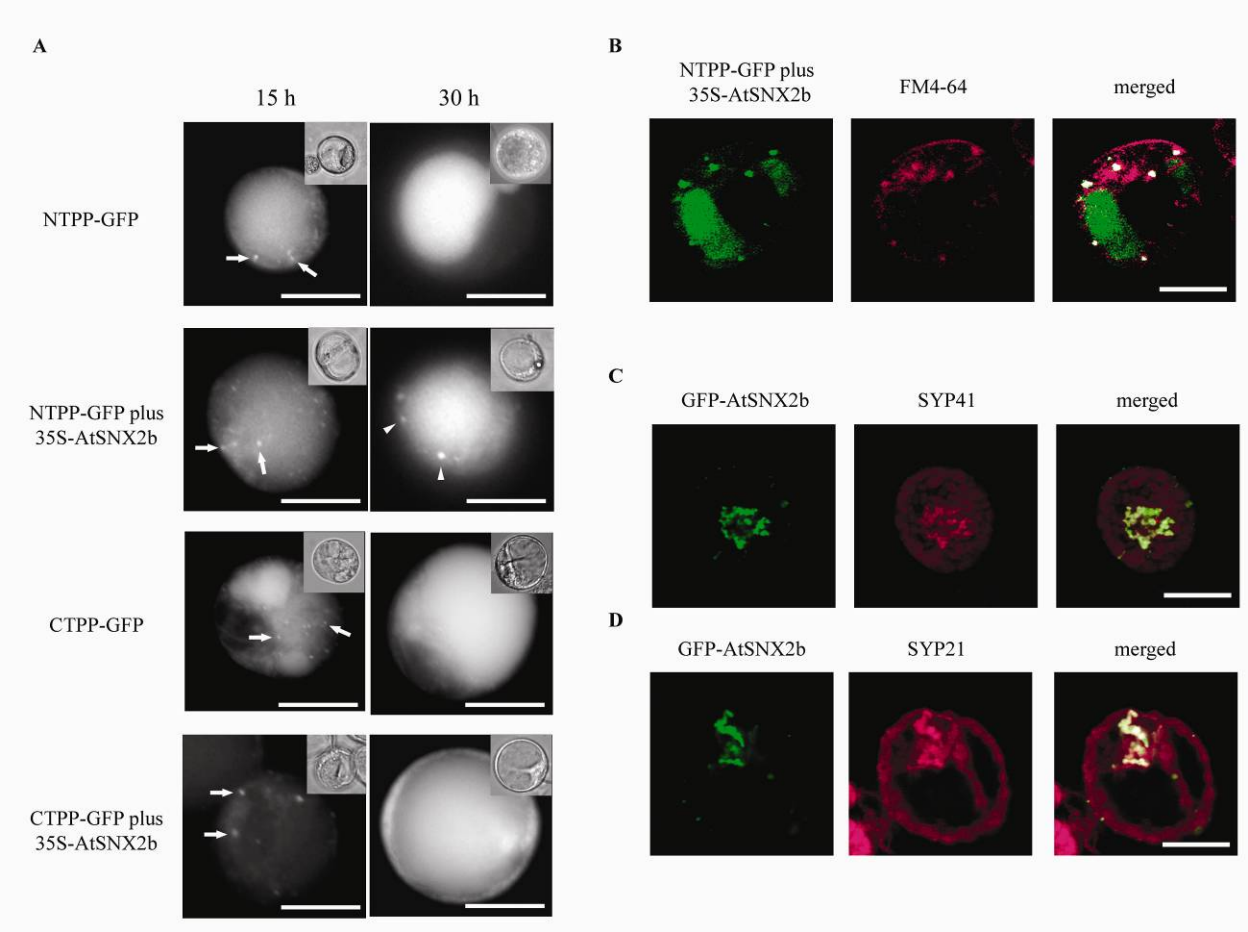

Figure 9. **Overexpression of AtSNX2b affects vacuolar trafficking.**

A. Arabidopsis protoplasts were transfected with the vacuolar markers NTPP-GFP or GFP-CTPP, both +/- 35S::AtSNX2b. At 15 h after transformation, motile GFP spots (arrows) can be seen in all cases and vacuolar labeling of GFP is clear. At 30 h post-transformation, motile GFP spots are absent and vacuolar GFP labeling is more dominant. In protoplasts transfected with NTPP-GFP plus 35S::AtSNX2b, some nonmotile GFP spots accumulate (arrowheads).

B. Confocal images of FM4-64 uptake indicate that these GFP-labeled structures are endosomes.

C. Immunofluorescence labeling of protoplasts expressing GFP-AtSNX2b with antibodies against the TGN marker SYP41. **D.** Immunofluorescence labeling of protoplasts expressing GFP-AtSNX2b with antibodies against the PVC marker SYP21. Scale bars are 10μm.